Table of Contents

Table of Contents (cont'd)

Table of Contents (cont'd)

Section ***Page***

Table of Contents (cont'd)

Table of Contents (cont'd)

Appendix

Table of Contents (cont'd)

Appendix

List of Tables

Page

Section IV

Section V

Section VI

List of Tables (cont'd)

List of Figures*

(* Figures are located at the end of each section)

Section III

Section IV

Section V

List of Figures* (cont'd)

Section V

Section VI

Section VII

List of Figures* (cont'd)

Section VII

Section VIII

Section IX

I. Executive Summary

DB Environmental Laboratories, Inc. (DBEL) was awarded a contract on February 12, 1998, to demonstrate the phosphorus (P) removal effectiveness of the Submerged Aquatic Macrophyte/Limerock Technology. This candidate "Supplemental Technology" consists of a wetland dominated by submerged aquatic vegetation (SAV), followed by a limerock (LR) bed. This project entailed optimization and demonstration of SAV/LR system performance in experimental mesocosms located at the Everglades Nutrient Removal (ENR) Project North and South Supplemental Technology Sites.

Experiments with SAV/LR technology at the North Project Site focused on documenting the effects of hydraulic retention time and loading rates (HRT and HLR), water depth, plant harvest regime, and limerock characteristics on P removal from Post-BMP waters (maximum total P (TP) concentration of 183 μg/L). Experiments at the South Project Site addressed the ability of three different SAV/LR configurations to treat Post-STA waters (maximum TP concentration of 34 μg/L). The SAV configurations evaluated included low velocity/shallow, low velocity/deep and high velocity/shallow systems.

Selected SAV/LR mesocosm configurations successfully treated Post-BMP and Post-STA waters to sub-10 μg/L TP levels, the first time a constructed wetland-based treatment technology has attained such low TP effluent concentrations at the outdoor mesocosm scale. The findings in this report represent results collected during an eight month study, encompassing both summer and winter performance periods. Many of these experiments are being continued into a second phase to assess SAV/LR performance over long-term, steady-state conditions.

Pertinent technical findings on Post-BMP waters are as follows:

- The SAV systems operated at HRTs ranging from 7.0 to 1.5 days (HLRs of 11-53 cm/day) removed P at 3.3 to 11.8 g P/m^2-yr, mass removal rates that were much higher than those documented for emergent macrophyte wetlands.
- Phosphorus removal performance was related to HRT. At a fixed water depth (0.8 m), SAV unit processes operating at 1.5 day (53 cm/day HLR), 3.5 day (23 cm/day) and 7.0 day (11

cm/day) HRTs produced average effluent TP levels of 39, 23 and 18 µg/L, respectively. Phosphorus settling rates (k) for these treatments, based on eight months of influent and effluent data, were 182, 123 and 69 m/year, respectively.

- The SAV unit process provided effective TP removal over the range of water depths tested (a range of 0.4 to 1.2 m) at a constant HLR of 10 cm/day. The shallowest (0.4 m deep) systems provided a significantly lower effluent total P level (average of 13 µg /L over 33 weeks), despite having a shorter HRT than the deeper systems.
- Vertical water column gradients (concentration differences with depth) for soluble reactive P (SRP), calcium (Ca) and alkalinity were less prominent in the shallow (0.4 m deep) SAV mesocosms than in the deeper (0.8 m and 1.2 m) systems. Additionally, hydraulic tracer studies demonstrated reduced short-circuiting in the shallow compared to the deeper SAV mesocosms. These observations may account for the superior performance of the shallow systems, and are likely related to the water column being fully occupied by submerged macrophyte biomass.
- The SAV unit process was very effective at removing the SRP (typically 61% of TP) of the influent Post-BMP water. At a 7.0 day HRT (HLR = 11 cm/day), essentially 100% of the SRP was removed by the SAV mesocosms.
- Characteristics and performance of full-scale SAV systems in the Everglades Nutrient Removal Project (ENR) substantiate our mesocosm findings. Sampling in ENR Cell 1 demonstrated that SRP and dissolved organic P levels in the water column of SAV beds were lower by 10 and 2-fold, respectively, than concentrations of these constituents in emergent macrophyte (*Typha*) stands.
- Despite large day - night fluctuations in pH and dissolved oxygen in the SAV water column, the TP removal performance of the SAV/LR system was consistent on a diel basis.
- Phosphorus removed from the mesocosm influent waters was stored in plant tissues and sediments. Because of the short duration of our studies, SAV tissues were the dominant storage compartment, containing 1.5 times greater mass of P than newly deposited sediments.
- The newly- deposited sediments in the SAV systems contained high levels of Ca (16%) and moderate P concentrations (503 mg/kg). Sequential extractions of the sediments revealed that the bulk of the P (74-92%) was in non-labile forms (Ca-mineral and residual P). The stability of

the remaining "labile" P fractions (e.g., $CaCO_3$-P, Fe & Al-P, biogenic P) to environmental perturbations (e.g., low pH, anoxia, dessication) is unknown.

- Phosphorus stored in the vegetation and newly deposited sediments only accounted for an average of 37% of the P removed from the water column. We attribute our inability to account for the all the P that entered the system to the difficulty in obtaining an accurate sediment accumulation depth due to the short duration of this study.
- Because SAV communities are so effective at SRP removal, the challenge to achieving low effluent total P levels (ca. 10 µg /L) is to reduce export of particulate P (PP) and dissolved organic P (DOP). These constituents occur in the Post-BMP waters, and can be generated internally within STAs and SAV/LR systems.
- The limerock unit process served principally as a physical filter, removing particulate P. Neither the chemical composition of the rock, nor the physical size of the rock (in a nominal size range of 1.3-5.0 cm in diameter) affected P removal efficiency. Under low P loadings, such as the effluent of a SAV system, a LR bed may be effective for removing PP prior to effluent discharge. Under high loadings, for example near the system influent or mid-point, LR may serve as an efficient transformer of water column PP to SRP.
- Fish (bannerfin shiner), zooplankton (water flea), and a unicellular green alga (*Selenastrum*) exposed to SAV influent, SAV effluent, and LR effluent waters showed variable chronic toxicity effects. Although the SAV effluent sample slightly reduced fish survival in a statistically significant manner, it was not "biologically" significant. A 50% mortality for the water flea (*Ceriodaphnia*) exposed to the LR effluent was deemed "biologically" significant, but no obvious toxic constituents were found in the water.
- The algal growth potential was reduced 5x-12x in the effluent waters compared to the influent, indicating the effectiveness of the SAV/LR system at reducing nutrient levels.

Pertinent technical findings on Post-STA waters are as follows:

- From July 1998 - February 1999, a shallow (9 cm deep), low velocity periphyton/LR raceway with an HRT of 0.8 days provided a mean effluent TP concentration of 10 µg/L, the tentative "target" concentration for the Supplemental Technology program. Influent TP concentrations during this period were low, however, averaging 17 µg/L. The P settling rate (k) of the shallow

system was 21 m/yr, and the mass removal rate was 0.29 g P/m^2-yr. A limerock bed with a 1 hr HRT situated at the effluent of the periphyton raceway removed additional P, providing a mean effluent TP concentration of 8 µg/L.

- A deeper (0.65 m) mesocosm system dominated by SAV species and having an HRT of 3.3 days provided a mean effluent TP concentration of only 14 µg /L. Mass P removal for this system was 0.15 g P/m^2-yr, and the P settling rate was 10 m/yr. A limerock bed with a 1 hr HRT situated at the effluent of the deep SAV system removed additional PP and DOP, reducing TP effluent levels to 11 µg /L.
- Mass balance calculations revealed that nearly all (93 - 102%) of the P removed from the influent water to the low velocity raceway was in the periphyton standing crop. A mass balance could not be performed for the deep SAV system because we could not quantitatively sample the sparse sediments.
- A shallow, high velocity periphyton raceway system (HRT = 6.5-13 minutes) reduced influent TP levels from 17 to 14 µg/L. Mass P removal, based on biomass accumulation of P, averaged 1.4 g P/m^2-yr. Productivity and P removal in this routinely harvested system appeared to be limited by low SRP concentrations in the influent waters.
- Neither SAV influent, SAV effluent, nor LR effluent waters caused chronic toxicity effects to fish (bannerfin shiner), zooplankton (water flea), or a unicellular green alga (*Selenastrum*).
- Algal growth potential was reduced in the effluent waters compared to the influent.

The SAV/LR technology has many favorable attributes. It is a passive, environmentally-acceptable technology, that should produce a marsh-ready effluent. It is compatible with current STA designs, and indeed, it appears capable of providing near-10 µg TP/L effluent quality on an operational-scale.

We performed an economic assessment of the SAV/LR technology using our most successful Post-BMP mesocosm configuration as a model. This system was established in October 1998, and consisted of a 0.8 m deep SAV mesocosm operated at a 3.6 day HRT, followed by a 0.4 m deep SAV mesocosm operated at a 1.8 day HRT. A limerock bed with 1 hr retention time completed the treatment train. During January and February 1999, this system reduced the TP of

influent Post-BMP waters from 130 µg/L to 9 µg/L. We based subsequent economic analyses on this deep – shallow concept, using Post-BMP drainage as the feed water.

We modeled a conceptual SAV/LR system using the STA-2 data set (flows and total P concentrations, 10 year period-of-record). Due to the rainfall-event driven nature of the EAA Post-BMP flows, a full-scale SAV/LR system, like an STA, will be subject to wide variations in flow and stage. Our data suggest, however, that it is desirable to maintain a constant stage, at least in the effluent region of a SAV/LR system. Stage fluctuations can be reduced by incorporating one or more of the following practices:

- bypass a portion of high storm flows
- utilize the front portion of the STA as a flow equalization basin (FEB)
- utilize more land for the treatment system

As a range-finding exercise, we assessed the cost-sensitivity of a SAV/LR system, designed to produce an effluent TP of 10 µg/L, to the three design variables described above. The design goals in sizing the SAV cells were to maintain constant water elevations with specified HRTs. A FEB was incorporated to control fluctuating runoff events and store water in order to achieve constant water elevations in the SAV cells. The most cost-effective SAV/LR designs bypassed a portion of large flow events, eliminating the need for additional land purchase.

Our initial assessment demonstrates there are many "compromise" design scenarios for a full-scale SAV/LR system. For example, if both bypass of peak flows and additional land purchase are unacceptable, then flow equalization coupled with increased event-based throughput (and likely, temporary reduction in treatment efficiency) is a viable alternative to achieving cost-effective P removal with an SAV/LR system in the existing STA-2 footprint.

Our mesocosm results and observations of ENR Cells 1 and 4 suggest that large-scale deployment of SAV/LR systems is a cost-effective approach for improving STA performance. A number of mechanistic, ecological and engineering issues remain to be addressed, however, before the SAV/LR technology is fully understood and optimized.

II. Introduction, Objectives and Background

Introduction and Objectives

On February 12, 1998, the District contracted with DB Environmental Laboratories, Inc. (DBEL) to design, construct, operate, and evaluate a 13-month, tank-scale (i.e., "mesocosm") demonstration of Submerged Aquatic Vegetation/Limerock (SAV/LR) Treatment System Technology for reducing phosphorus (P) discharge from Everglades Agricultural Area (EAA) waters. The objectives of this project were twofold. First, obtain the performance data and operational experience necessary to evaluate the technical, economic, and environmental feasibility of using SAV/LR technology for P removal at either the watershed-, basin- or farm-scale. Second, guide the design and operation of a larger, field-scale SAV/LR demonstration project should the District choose to investigate this technology further. The U.S. Environmental Protection Agency (USEPA), through the Florida Department of Environmental Protection (FDEP), provided 45% of the funding for this demonstration through a Section 319 Nonpoint Source Management Program grant. Because our initial findings were promising, the District amended our contract in March 1999 with additional funds and a 90-day time extension to provide for more intensive "close-out" experiments. This final report summarizes DB Environmental Laboratories, Inc.'s (DBEL) findings on the SAV/LR demonstration project for both the main contract and contract extension periods.

Background of Submerged Aquatic Vegetation and SAV/LR Phosphorus Removal Technologies

Phosphorus can be reduced in the water column of treatment wetlands to concentrations two-orders of magnitude lower than either nitrogen (N) or carbon (C) (Kadlec and Knight, 1996). Cost-effective P removal, however, has proven to be a challenge for most treatment wetlands, because the area requirement for P removal is exceptionally high (Kadlec and Knight, 1996). As an example, the Stormwater Treatment Areas (STAs), the wetlands being constructed to filter P from agricultural runoff prior to discharge to the Everglades, are projected to provide a very low mass P removal rate, with a P settling coefficient of only 10.2 m/yr (Walker, 1995). Moreover,

despite their large size, STAs dominated by emergent plants are not anticipated to produce effluent P concentrations below 30 - 50 µg/L, levels significantly higher than the anticipated effluent target (i.e., "threshold level") for protection of the Everglades (10 µg/L).

Investigators in Florida in the mid- to late- 1980s first recognized the P removal potential of submerged aquatic vegetation. Reddy et al. (1987) cultured the submerged macrophyte egeria (*Elodea densa*) at several nutrient loading rates in outdoor mesocosms maintained at a 1.5 day hydraulic retention time (HRT). At a high (4 mg N/L and 0.8 mg P/L) concentration range and loading rate, the system P removal rate was 129 mg P/m^2-day, with plant uptake accounting for 14% of the P removed. At a low (1 mg N/L and 0.2 mg P/L) loading rate, the mass P removal rate was lower (50 mg P/m^2-day), but plant uptake accounted for a greater percentage (54%) of the P removed from the water. These investigators suggested that P coprecipitation with $CaCO_3$ may have accounted for much of the removed P that was not recovered in plant biomass.

In a study conducted from November 1988 - May 1989 by DeBusk et al. (1989), *Ceratophyllum demersum* was cultured in dairy lagoon effluent and removed P at a rate 2.5-fold higher than the floating macrophytes *Lemna*, *Eichhornia* and *Pistia*. The mass P removal rate by this submerged plant averaged 109 mg P/m^2-day, providing mean system influent and effluent total P levels of 7.1 and 1.4 mg/L, respectively. The *Ceratophyllum* standing crop declined during the 7-month study (while tissue P levels remained fairly constant), so plant storage of P in this system was estimated to account for little of the P removed from the dairy wastewater. These investigators observed a decline in calcium and alkalinity levels within the *Ceratophyllum* mesocosms, and proposed that the most likely P removal mechanism involved coprecipitation with calcium compounds and accretion of this material into the bottom sediments.

In 1992, DBEL scientists began testing the removal of P from sugarcane field runoff (i.e., Post-BMP waters) using a sequential system of a SAV-dominated mesocosm followed by a bed of limerock (nominal rock diameter of 1.2 cm) contained in upflow columns. DBEL scientists incorporated the limerock to buffer the high daytime pH of the SAV effluent to more acceptable levels for receiving waters, and to provide additional P removal. DBEL's experiments suggested that the limerock may be acting as a nucleation site for precipitation of P from the high pH SAV effluent. These investigators hypothesized that this P removal mechanism could be permanent, since a stable precipitate was thermodynamically-favored to form in the limerock bed microenvironment.

DBELs initial experiments with SAV/LR showed that this technology could reduce Post-BMP water total P concentrations to below 15 µg/L, at a mass removal rate substantially higher than that projected for the emergent macrophyte-dominated Stormwater Treatment Areas (STAs) (Dierberg and DeBusk, unpublished data). The demonstration project described herein is a follow-on study to DBEL's initial research on the SAV/LR technology.

III. Planning and Quality Assurance: Tasks 1 - 3

Task 1. Preliminary Project Work Plan

The initial project kickoff meeting was held in West Palm Beach on March 5, 1998. DBEL scientists submitted the Preliminary Project Work Plan to District and FDEP staff on March 10, 1998.

Task 2. Final Project Work Plan

The final work plan was submitted to the District and FDEP on March 24, 1998. A copy of this work plan is appended (Appendix A). The project team for this work consisted of DB Environmental Laboratories, Inc. (Rockledge, FL) and Wetland Studies and Solutions, Inc. (Chantilly, VA). A subcontract laboratory (PPB Environmental Laboratories, Inc.) performed some of the non-P related water analyses. Dr. Michael Chimney was the SAV/LR Project Manager for the District, and Dr. Taufiqul Aziz was the Project Manager for FDEP (Fig. 3.1).

Task 3. Project Quality Assurance Project Plan

DBEL scientists submitted the Quality Assurance Project Plan (QAPP) to FDEP on March 23, 1998. Two revisions (March 31 and April 2, 1998) were made before final approval was granted by FDEP on May 1, 1998. A copy of the final plan is provided in Appendix B. It details the parameters analyzed during the study, their sampling frequencies and limits of detection (MDLs), turn-around-times (TAT), analytical methods, field procedures, and field and laboratory quality control samples. The QAPP also describes the project organization, site plan and sampling locations,.

DBEL participated in one FDEP-sponsored total P "Round-Robin" analysis (number VIII) during the project period. Results of these analyses of five "unknown" Everglades water samples are provided in Appendix B.

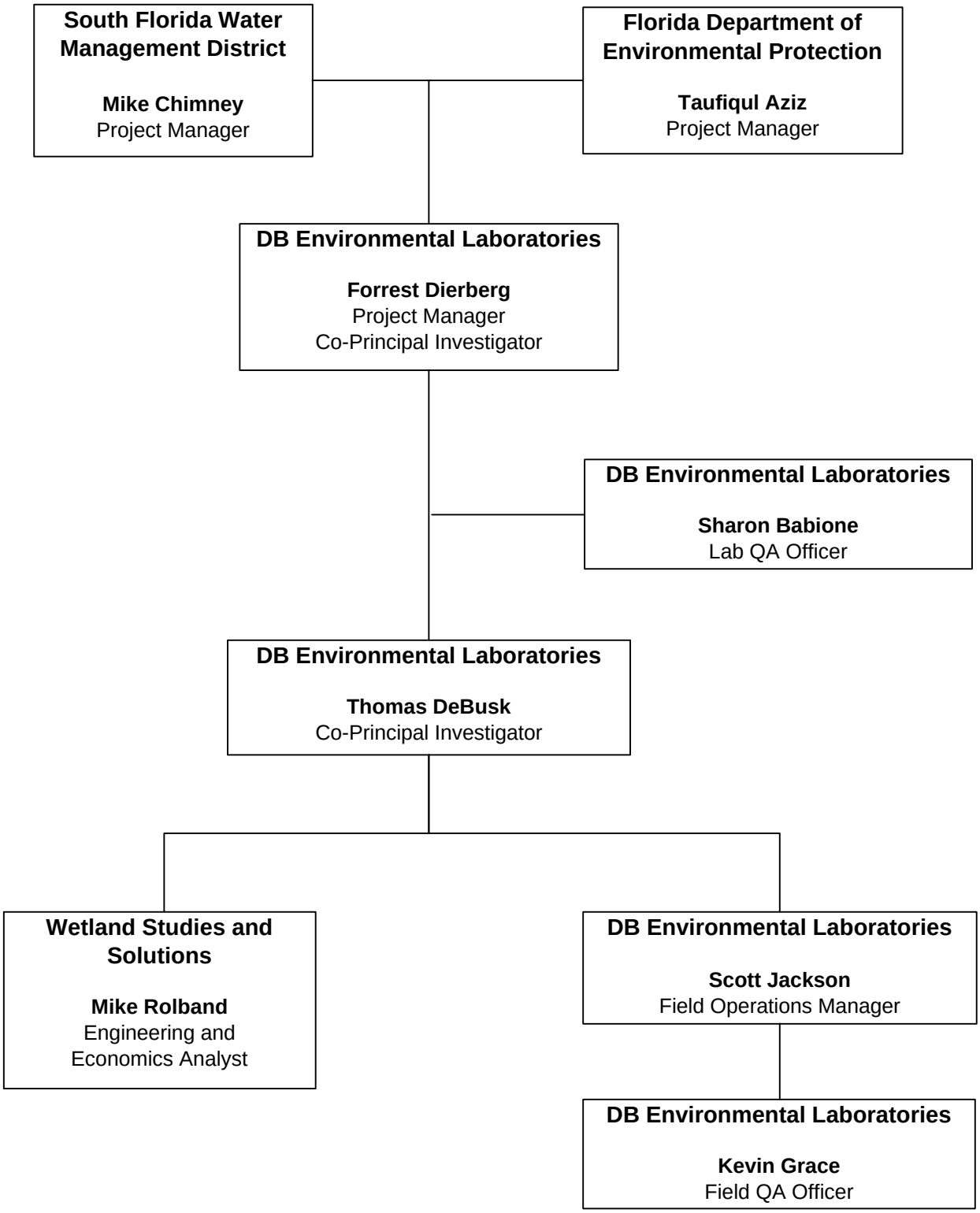

Figure 3.1 Project organization for the Submerged Aquatic Vegetation / Limerock demonstration project.

IV. Preliminary Site and Analytical Work: Subtasks 4A and 4B

Subtask 4A. Chemical Characterization of Limerock from Proposed STA Sites

Methods

On April 21, 1998, DBEL sampled limerock (LR) from eight distinct locations in South Florida, which yielded 10 samples for chemical characterization. These sites included an area adjacent to the ENR entrance; Cell 5 of STA-1W; STA 3 - 4; STA-1E; canals along SR 80 and CR 880; and a quarry on US 98 (Palm Beach Aggregates). With the exception of the quarry, limerock was found at all locations as surface or previously-excavated outcroppings. Limerock at the quarry was sampled from two depths, namely shallow caprock and deep base rock. A sample of peat from Cell 5 of STA-1W was also analyzed since it was used as the organic soil source for the SAV mesocosms in Subtask 4C.

All substrate samples were analyzed for calcium (Ca), magnesium (Mg), iron (Fe), silica (SiO_2) and P contents. Details (e.g., method numbers) for these analyses are provided in Appendix B.

Results and Discussion

Based on the results of the elemental analyses (Table 4.1), the caprock from the Palm Beach Aggregates quarry was selected as the source material for the Subtask 4C and 4D LR beds. Our criteria for limerock selection were relatively low concentrations of P, Mg and Fe, and higher levels of Ca and SiO_2. The Palm Beach Aggregate quarry caprock met these criteria, and was readily available for delivery to the study sites.

Table 4.1. Chemical composition of 10 limerock sources and one muck soil from areas within or adjacent to the Stormwater Treatment Areas in south Florida.

Location	Ca (%)	Mg (%)	Fe (%)	SiO_2** (%)	P (mg/kg)
Cell 5 of STA-1W Muck Soil	5.7	0.21	0.30	16.4	239
Cell 5 of STA-1W Limerock	24	0.43	0.35	16.9	80
Palm Beach Aggregate Caprock-Final*	26	0.24	0.19	30.8	126
Palm Beach Aggregate Caprock-First	24	0.24	0.22	29.4	142
Palm Beach Aggregate Base Rock	23	0.22	0.09	32.6	425
ENR Entrance - Limerock 1	25	0.18	0.20	20.2	104
ENR Entrance - Limerock 2	18	0.16	0.22	35.4	286
STA-1E	23	0.28	0.52	28.6	75
STA-3/4 Rockpile at Test Cells	29	0.83	0.32	2.5	73
STA-3/4 Between Test Cells	29	0.89	0.78	6.0	79
Rockpile on County Rd. 880	28	1.1	0.21	8.3	82
Rockpile on SR 80	25	3.7	0.32	3.5	155

* Represents the source rock used in the LR columns and raceways in Subtasks 4C and 4D, which came from a different area of the quarry than the first sample of caprock collected for the screening tests.

** Average of two replicate samples

Subtask 4B. Site Development Activities and Description of Experiments

Construction and Site Development

The SAV/LR experiments were conducted at two locations: the North Supplemental Technology Site (north site), at the northern end of the ENR supply canal; and the South Supplemental Technology Site (south site), adjacent to the ENR effluent pump station. Considerable site infrastructure (a graded pad, fencing, electricity, influent pumps) was available at both sites due to previous work by District and contractor personnel.

During the first quarter, DBEL and its subcontractors installed additional electrical service at the north site, as well as an influent supply pump. The existing influent pump and manifold system at the north site could not be operated at low flow rates without incurring severe pump cavitation. Pump cavitation problems were encountered at the south site as well. At this site pump cavitation was corrected by installation of a bypass line.

DBEL conducted four experiments at the north site, and one experiment at the south site. At the north site, we used nine SAV tanks (mesocosms) (4.66m L x 0.79m W x 1.0m D) with associated LR beds to investigate the effects of hydraulic residence time (HRT) and hydraulic loading rate (HLR) on effectiveness of both the SAV and LR unit processes for removing P from Post-BMP waters (Subtask 4C). An additional nine tanks (2.23m L x 0.79m W x 1.0m D for 6 tanks and 2.23m L x 0.79m W x 1.3m D for 3 tanks) were used to assess the effects of water depth on SAV performance (Subtask 4F); three tanks (2.23m L x 0.79m W x 1.0m D) were used to evaluate SAV harvesting effects (Subtask 4E); and a final SAV tank (4.66m L x 0.79m W x 1.0m D) with associated LR columns was used to assess effects of LR size and source on P removal (Subtask 4G).

For our "Post-STA" water investigations, we fabricated and delivered three types of experimental units to the south site. The first was a 1m deep mesocosm, identical in design to the HRT tanks deployed at the north site in Subtask 4C. The second experimental unit was a long (43.9 m), narrow (0.3 m) fiberglass raceway with 15-cm high side walls. An even shallower (8 cm high walls), long (43.9 m) raceway comprised the third experimental unit.

In March 1998, District construction personnel delivered ninety cubic yards of muck soil collected from Cell 5 of STA-1W to the north site for stocking into the Subtask 4C mesocosms. In late May, DBEL had 50.5 tons of caprock (limerock) from Palm Beach Aggregates delivered to the north and south sites.

Description of Experiments and Statistical Methods

A list of experiments performed at the north and south sites is provided below. Schematics and photographs of all experiments are provided in Figs. 4.1 – 4.9.

North Supplemental Technology Site (Post-BMP Waters)

- Effect of HRT (HLR) of SAV and LR unit processes on phosphorus removal efficiency (Subtask 4C) (Fig. 4.1)

- Effect of plant harvesting on SAV phosphorus removal efficiency (Subtask 4E) (Fig. 4.2)
- Effect of water depth on SAV phosphorus removal efficiency (Subtask 4F) (Fig. 4.2)
- Effect of limerock chemical composition and size on P removal efficiency (Subtask 4G) (Fig. 4.3)

South Supplemental Technology Site (Post-STA Waters)

- Performance of SAV/Limerock systems in low nutrient waters (Subtask 4D) (Fig. 4.4)

Results from all subtasks performed at the north site (4C, 4E, 4F, and 4G), using Post-BMP waters, are provided in Sections V and VII. Data from the south site experiment (4D) using Post-STA water are contained in Section VI. While most experiments were conducted using triplicate mesocosms for each treatment, for purposes of clarity we have omitted standard deviation "error bars" from many of the summary graphs. In general, however, the variation of results from replicate experimental units within each treatment was low (e.g., see Fig. 5.1). Standard deviations for the replicate experimental units on each sampling event are found in tables throughout Chapters V, VI and VII, and in Appendices C (Subtask 4C), D (Subtask 4D), and E (Subtasks 4E, 4F, and 4G).

For selected north and south site experiments (Subtasks 4C, 4D, and 4F), which included experiments on the major hydraulic and P loading variables affecting P removal efficiencies in SAV and LR components, statistical analyses were performed on TP data using SPSS version 7.5.1. The data first were tested for normality ($P<0.05$) using Kolmogorov-Smirnov and Shapiro-Wilkes tests. If the data were normally distributed, repeated measures analysis of variance (ANOVA) was used to determine if significant differences ($P<0.05$) existed between three or more treatments. The Bonferroni post hoc test was used to group the data based on significant differences. A paired t-Test was used to determine if significant differences ($P<0.05$) existed between normally distributed data for only two treatments. For non-normally distributed data from experiments with three or more treatments, we analyzed data using a Kruskal-Wallis H test to determine significant differences ($P<0.05$).

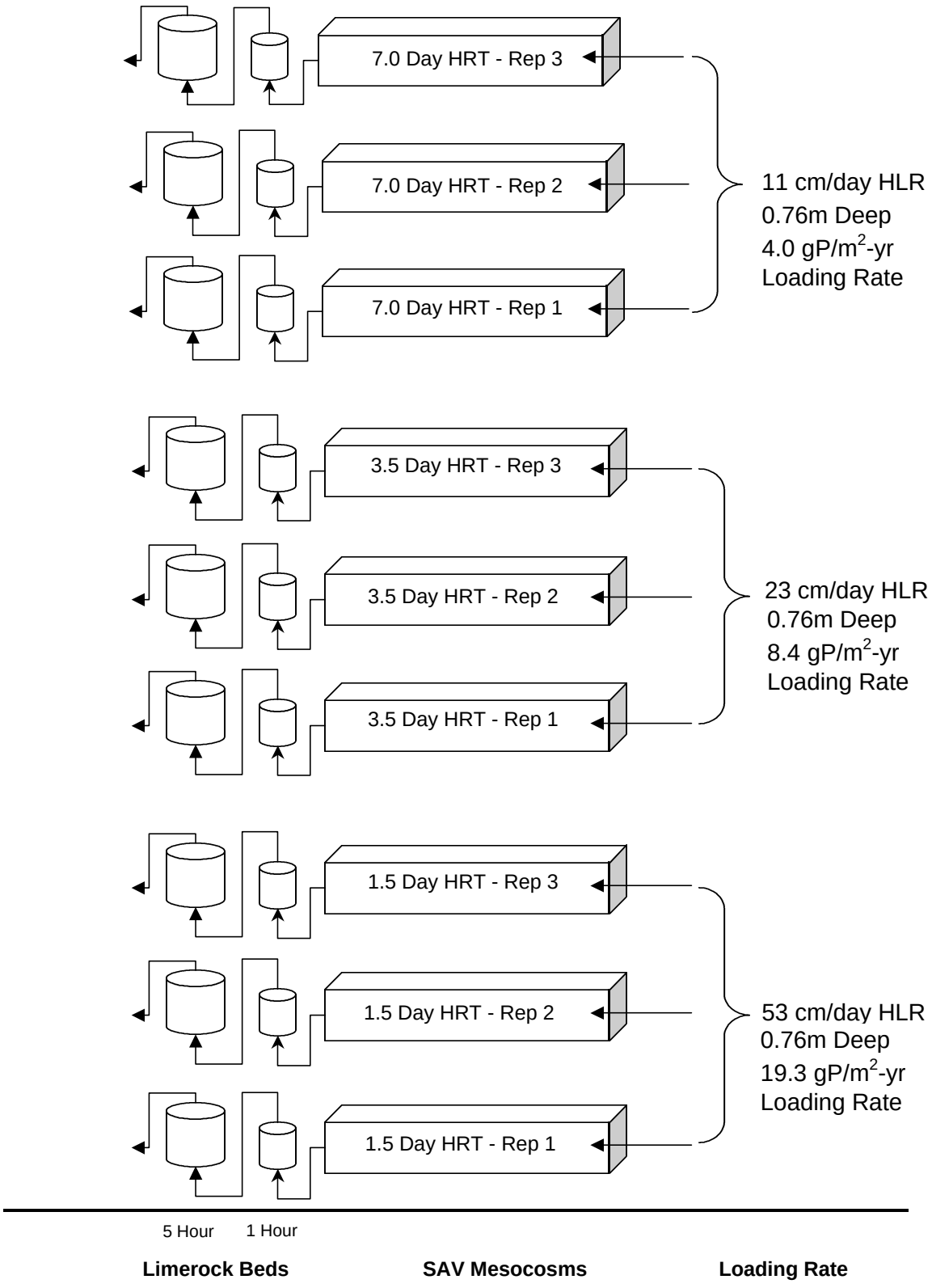

Figure 4.1 Schematic of experimental design for assessing effects of HRT, HLR and P loading rate on phosphorus removal efficiency (Subtask 4C).

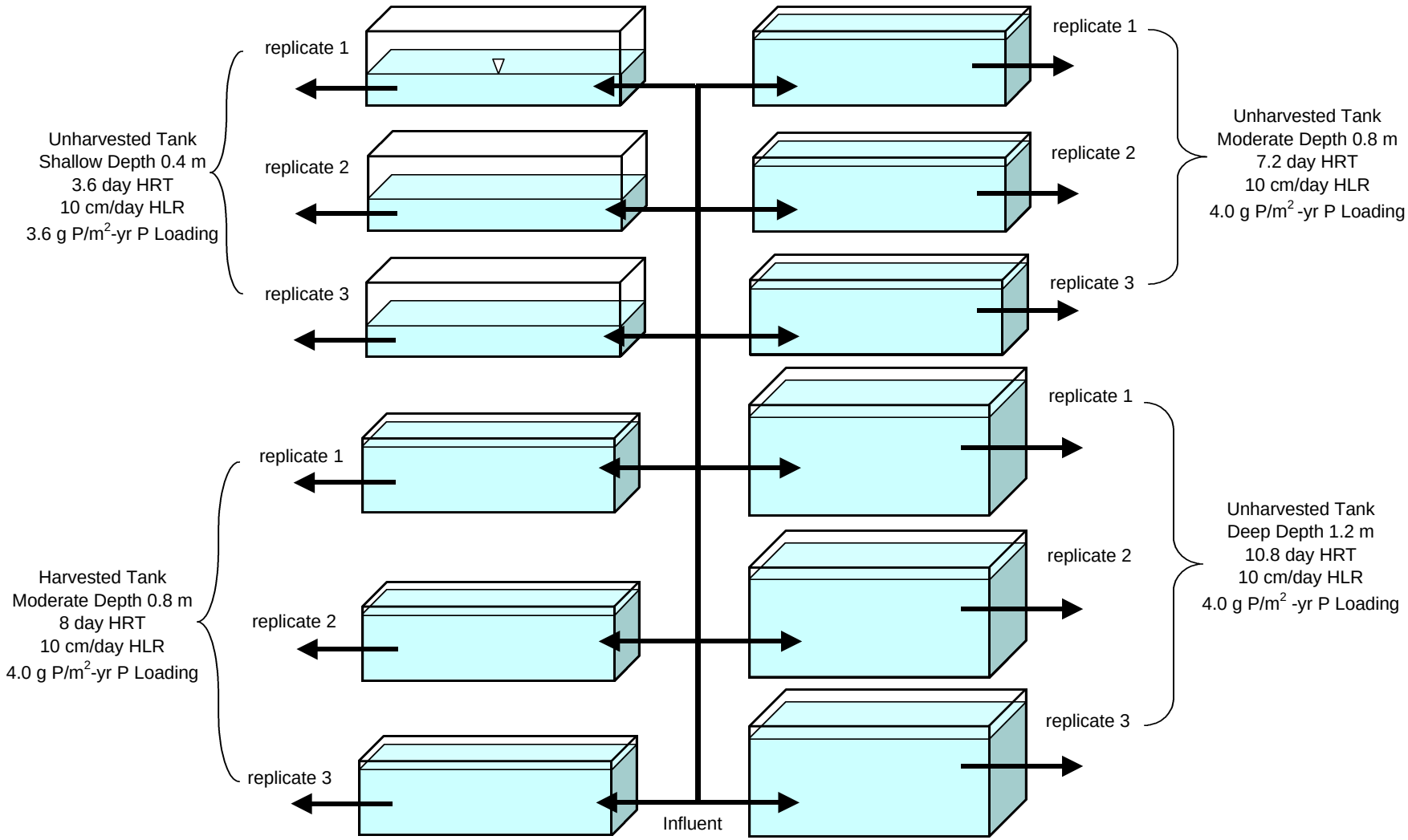

Figure 4.2 Schematic of experimental design for assessing effects of plant harvesting and water depth and HRT on SAV phosphorus removal performance (Subtasks 4E & 4F).

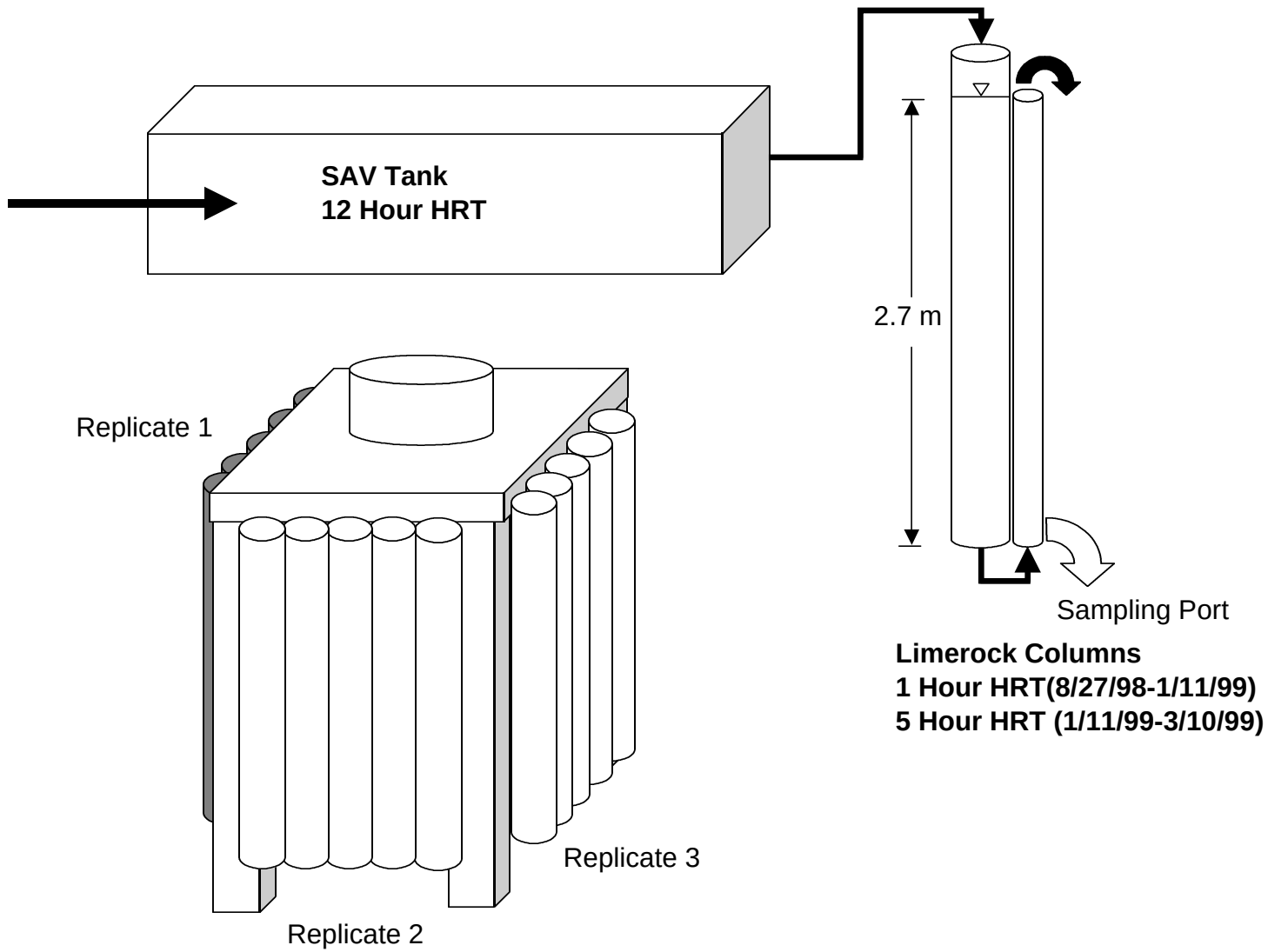

Figure 4.3 Schematic of experimental design for assessing effect of limerock chemical composition and size on P removal performance (Subtask 4G).

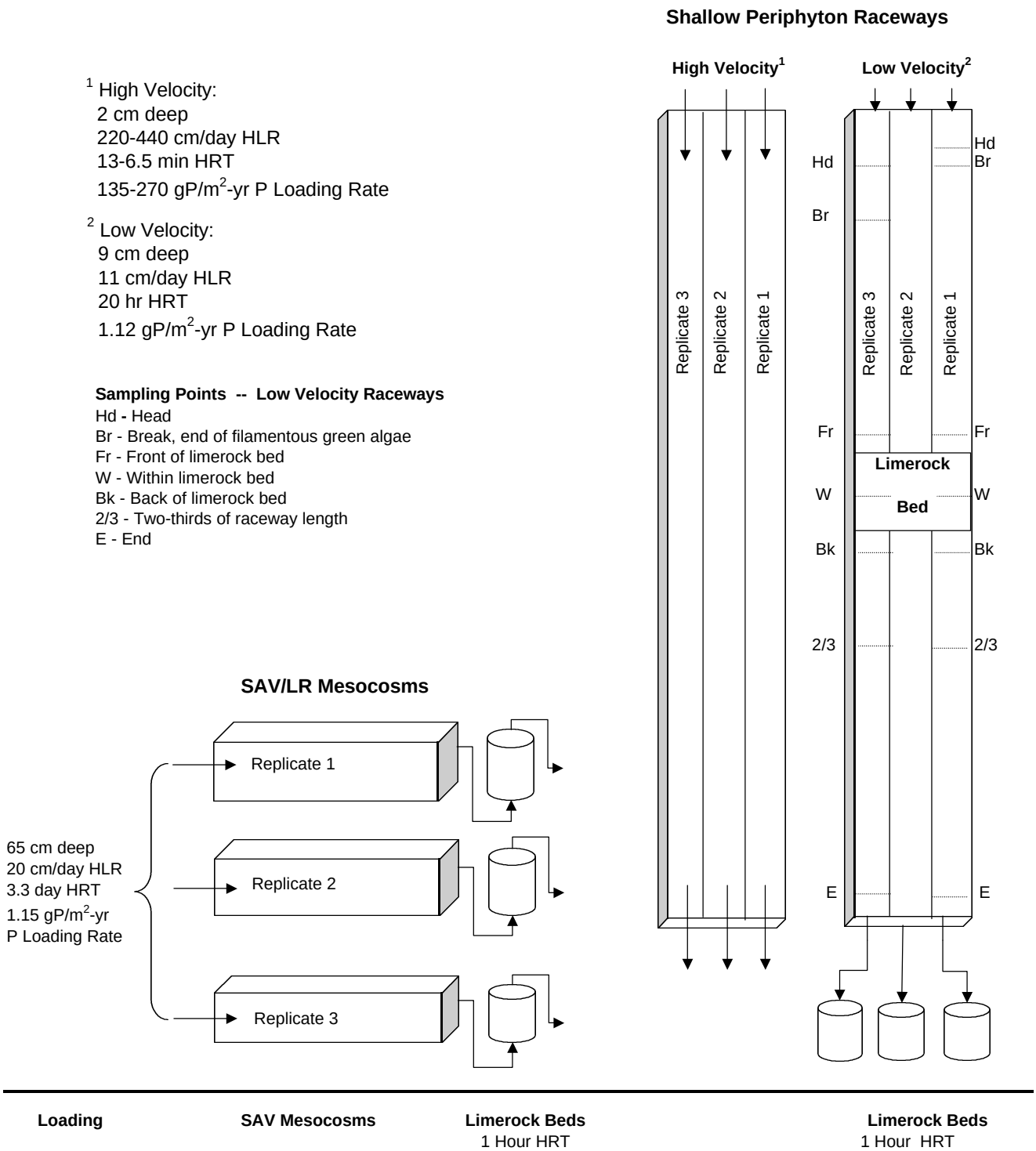

Figure 4.4 Schematic of experimental design for assessing performance of SAV/LR systems in low nutrient (Post-STA) waters (Subtask 4D). Plant, sediment and limerock sampling stations are shown for the Low Velocity raceways.

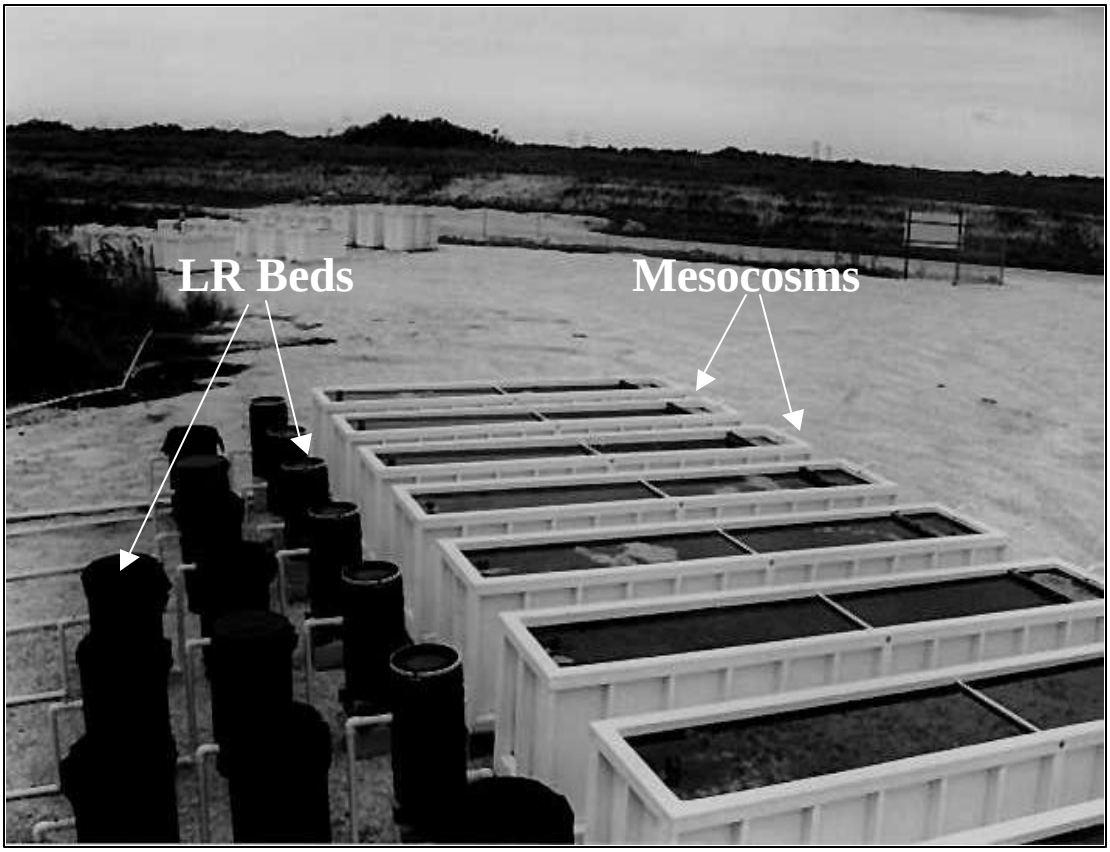

Figure 4.5. SAV mesocosms and associated upflow LR beds used for the HRT study (Subtask 4C) at the North Supplemental Technology Site.

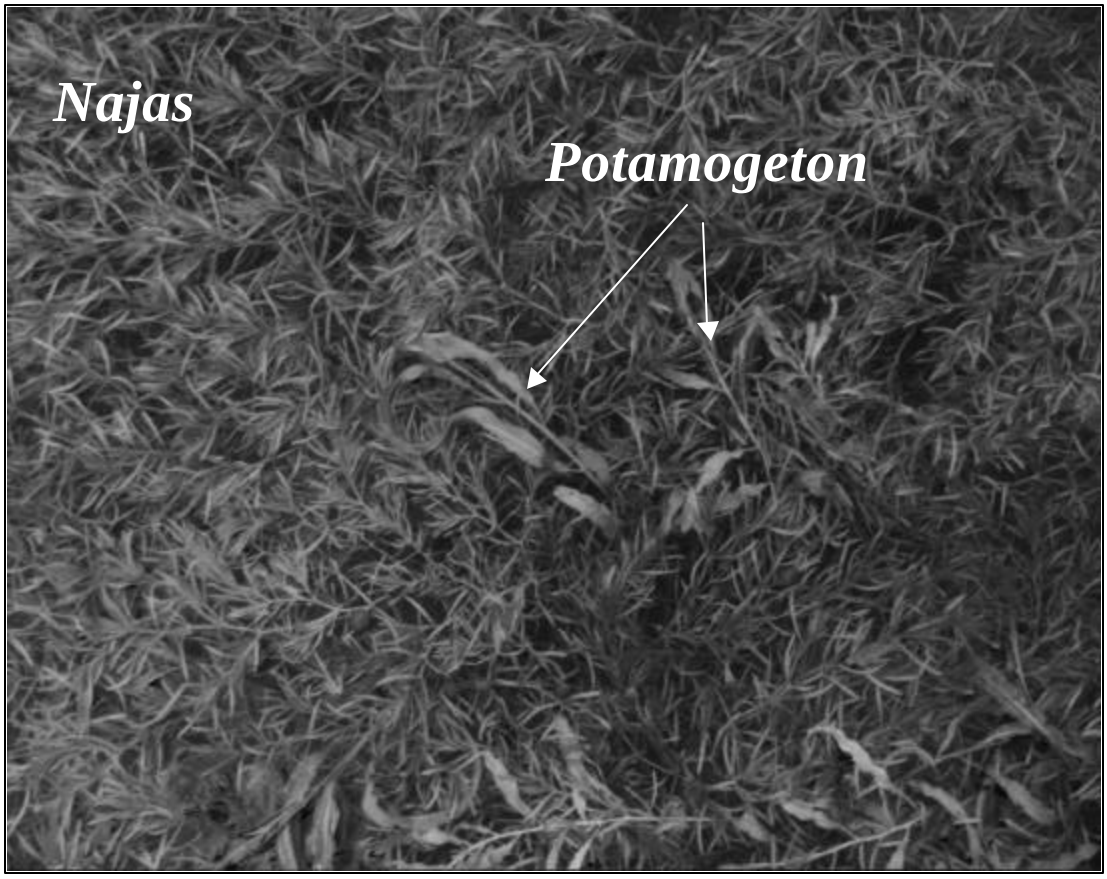

Figure 4.6 A submerged aquatic vegetation community consisting of *Najas* and *Potamogeton* .

Figure 4.7. Deep (1.2 m) and moderate depth (0.8 m) mesocosms used for the SAV depth study (Subtask 4F) at the North Supplemental Technology Site.

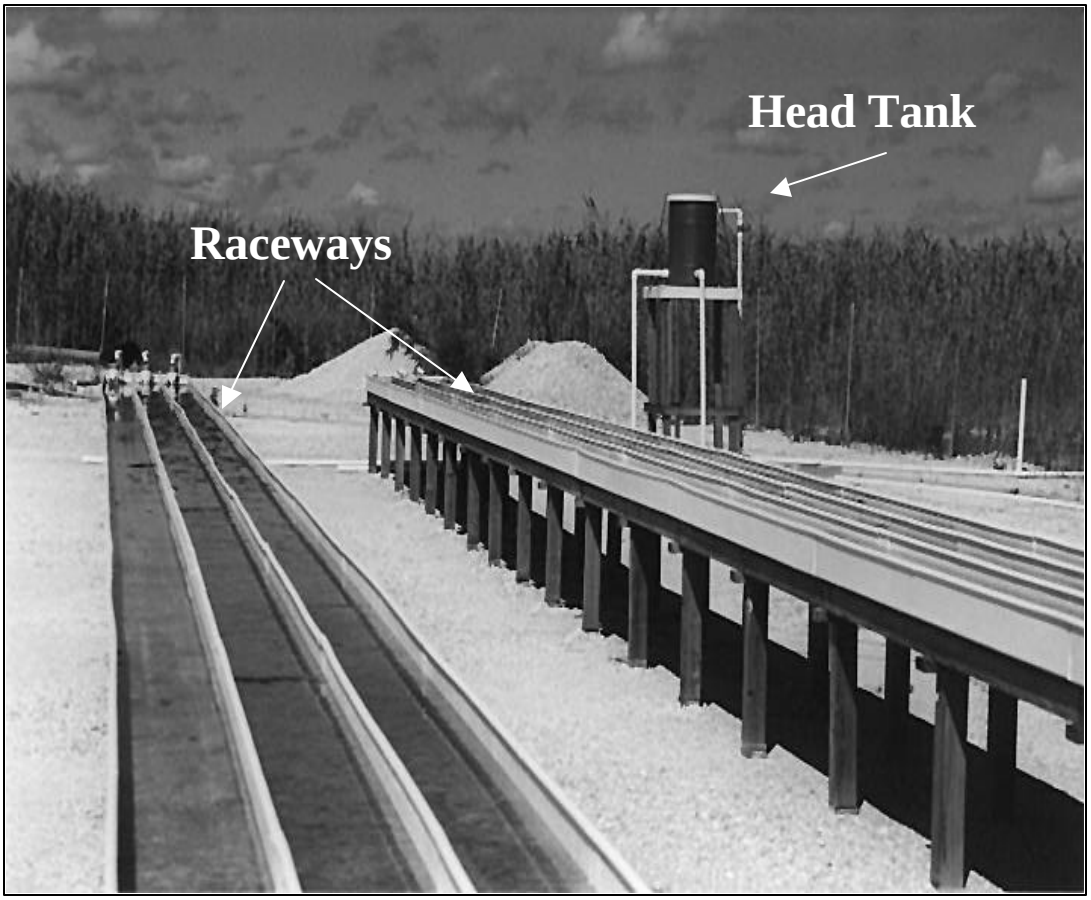

Figure 4.8 Shallow, high velocity (left) and low velocity (right) raceways used for low-level P removal (Subtask 4D). Head tank on right provided a constant gravity flow of water to all mesocosms at the South Supplemental Technology Site.

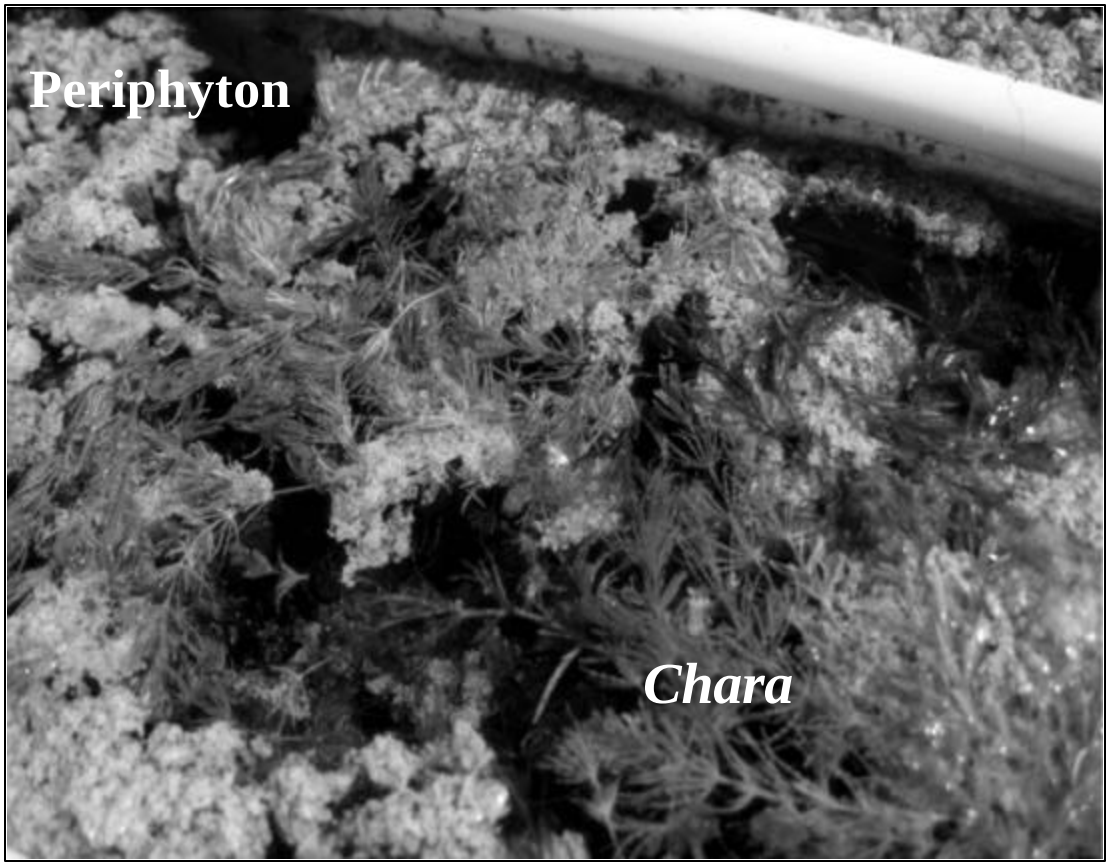

Figure 4.9. Typical macrophyte (*Chara* sp.) and periphyton assemblages found in the influent region of the shallow (9 cm), low velocity raceway at the South Supplemental Technology Site.

V. Mesocosm Experiments: Subtask 4C

Subtask 4C. Effects of Hydraulic Retention Time and Relative Unit Process Sizes on Phosphorus Removal Efficiency

For this study, we operated triplicate SAV mesocosms at HRTs of 1.5 days, 3.5 days and 7 days. Each SAV mesocosm was followed by a series of limerock beds (113 or 208 L barrels), providing retention times of 1 hr and 5 hr corresponding to sampling points along the flow path within the limerock beds (Fig. 4.1). We selected these SAV and LR HRTs based on our previous experience with the SAV/LR technology at the microcosm scale. Note that these HRTs are quite short relative to those utilized in the ENR project (i.e., 11 to 48 days). This experiment was monitored for 36 weeks, from June 1, 1998 to February 2, 1999.

Methods

Nine SAV/LR treatment systems were established at the ENR North Supplemental Technology Site. The SAV tanks (internal dimensions: 4.66m L x 0.79m W x 1.0m D) were constructed of lumber and fiberglass and then plumbed with PVC pipe. Muck was placed in the bottom of each mesocosm to a depth of 15-cm and the water depth maintained at 76 cm. Plywood baffles (56 cm deep) were installed at the influent region of each tank, about 30-cm downstream from the inflow, to minimize hydraulic short-circuiting. Source water (i.e., Post-BMP runoff) was pumped from the ENR supply canal into a headtank, and distributed to the mesocosms by gravity (Figure 4.5).

The HRT treatments of 1.5, 3.5 and 7 days were obtained by establishing daily hydraulic influent loadings of approximately 53, 23 and 11 cm. Flow rates to the mesocosms were manipulated by adjusting either aperture size of the inlet nozzle, or duration of flow on a daily basis. Flow rates into each SAV/LR system were measured and recorded five days per week (Monday through Friday).

We conducted a preliminary reconnaissance during April 1998 and found that the SAV community in ENR Cell 4 consisted of the following genera: *Ceratophyllum, Najas, Potamogeton*

and *Chara*. A mixture of these four genera therefore was added to the experimental mesocosms. For the HRT SAV tanks, *Ceratophyllum* and *Najas* were stocked at the highest density (1.2 kg wet wt/m^2), with *Chara* and *Potamogeton* stocked at a lower density (0.08 kg wet wt/m^2). Plant tissues and sediments were sampled on May 18 and May 22, respectively, for initial wet and dry biomass, and elemental (P, Ca, N and C) concentrations.

Crushed limerock was acquired from Palm Beach Aggregates Inc. (Loxahatchee, FL). The limerock was screened to achieve a nominal size range of 1.5 to 2.5 cm and placed in black plastic barrels (208 and 113 L). The barrels were opaque which inhibited algal growth. Barrels were plumbed in series after each SAV tank to serve as upflow LR beds. Sample ports were constructed within the LR beds at an intermediate point (i.e., a 1hr HRT) and the system effluent point (i.e., a 5 hr HRT).

In early February 1999, upon completion of the experiment, plant biomass in two of the three SAV mesocosms in each treatment was harvested and weighed. The composition of the two dominant species (% dry weight, P, C and N contents) was measured in the laboratory. Sediment cores were collected at the influent and effluent regions to determine sediment accumulation, bulk density, and elemental composition.

Long-Term Phosphorus Removal Performance

The first SAV mesocosm water samples for Subtask 4C were collected on June 1, and effluents from the LR beds were sampled initially on June 27, 1998 (construction of the limerock beds was not completed until three weeks after SAV sampling was initiated). Samples were collected at the influent nozzles leading to the mesocosms, the water surface adjacent to the effluent standpipe, and at the intermediate and effluent limerock sampling ports. Each weekly sample typically consisted of a composite of two grab samples, collected during the week. The final samples were collected on February 2, 1999.

Each week, water samples were analyzed for TP and SRP. Temperature and pH measurements were performed in the field at the time of water sample collection. Every other week, water samples also were analyzed for total soluble phosphorus (TSP), calcium (Ca) and alkalinity.

Continuous logging temperature probes (On-Set "Optic Stowaway") were provided by the District, and deployed at mid-depth in one SAV mesocosm for each of the HRT treatments. A

rainfall gauge was situated at the site, and rainfall measured and recorded five days per week (Monday through Friday).

Diel Water Quality Characteristics

On two dates (September 22-23 1998 and January 26-27 1999), we conducted water sampling to assess the diel variability in effluent quality from the SAV/LR systems operated at various HRTs. Water samples were collected and field measurements (temperature, pH, conductivity and dissolved oxygen [D.O.] content) were performed at approximately 6 hour intervals over a 24 hr period. All water samples were analyzed for TP, TSP and SRP, and a subset (separated by 12 hour intervals) was analyzed for Ca and alkalinity.

General Water Treatment Performance of SAV-LR Systems

During September and November 1998, we collected samples at influent, SAV effluent and LR effluent (5 hr HRT) locations from duplicate mesocosms for each HRT treatment. In addition to those parameters mentioned above these samples were analyzed for the following 16 additional water quality parameters: total suspended solids (TSS), chloride (Cl), color, dissolved aluminum (Al), dissolved iron (Fe), dissolved magnesium (Mg), turbidity, reactive silica (SiO_2), dissolved potassium (K), dissolved sodium (Na), nitrate + nitrite nitrogen (NO_x), ammonium nitrogen (NH_4-N), sulfate, total Kjeldahl nitrogen (TKN), total dissolved solids (TDS) and total organic carbon (TOC).

Chemical Characterization of Sediments

On February 10, 1999, we collected sediment cores from two of the three tanks in each HRT treatment. Five cores from the inflow half and five cores from the outflow half of each tank were composited in the field after separating the unconsolidated upper layer of sediment (representing the estimated sediment accrued since commencement of operations) from the underlying muck. All of the underlying muck was discarded except for a sample from one of the 3.5 day HRT mesocosms, which was kept for later analysis along with the newly accrued sediment. Each sample was subdivided into two parts: one to be extracted for different P fractions and the other for dry weight and bulk density measurements. We elected not to maintain anoxic conditions

during core extrusion in the field or in the lab during the NH_4Cl extractions since our diel D.O. data indicated that the bottom waters of the mesocosms do not become anoxic. This means that oxic conditions probably also prevailed in the upper sediment layers, which contained the newly deposited sediment.

The P extraction sequence (Penn et al. 1995) and the forms of P extracted in each fraction are presented in Table 5.1. For each sediment sample, ≈ 2.5 g of wet material was placed in a 50-mL polypropylene centrifuge tube. Extractant (35 mL) was then added and the centrifuge tube agitated on an oscillating shaker table @ 55 oscillations per minute for the times listed below. The samples were then centrifuged @ 22,000 rps for 15 min before filtering the supernatant through 0.45 μm polyether sulfone membrane filters. The filtrates subsequently were analyzed for SRP and TSP (for the 0.1 M NaOH extracts only). The non-SRP reactive soluble component (i.e., biogenic-P in Table 5.1) was determined by difference of the TSP and SRP in the NaOH extracts. Total P analysis was performed on an aliquot of each sediment before (initial P) and then again on the sediment following all extractions (residual P). This residual P form represents the refractory organic P and inert mineral P.

Sediment dry weights and bulk densities were determined by drying a known wet weight and volume of material at 75-80°C for 5 days.

Table 5.1 Phosphorus fractionation sequence for sediments and limerock.

Extracting Solution	**No. of Extractions**	**Duration of Extraction**	**Fraction**
1 M NH_4Cl pH=7.0	Twice	2 hr each	**$CaCO_3$-P:** porewater, loosely sorbed, and $CaCO_3$-associated P
0.1 M NaOH	Once	17 hr	**Fe & Al-P:** Fe and Al bound-P **Biogenic-P:** labile organic-P and polyphosphates
0.5 M HCl	Once	24 hr	**Calcium mineral-P**
Residual*			**Residual-P:** refractory organic-P and inert mineral-P

* Analyzed as a total P digestion

Hydraulic Characteristics of the Limerock Barrels

We performed tracer studies in this task to further our understanding of the hydraulic characteristics (e.g., flow path, detention behavior, nominal vs. actual retention times) of the and LR beds. These data will facilitate our interpretation of the P removal efficiencies of various reactor designs and also help provide insight into P removal processes (e.g., chemical precipitation and adsorption, biological uptake), which in turn are likely related to hydraulic characteristics.

On March 17, 1999, we introduced 39.0, 17.2, and 7.7 mg, respectively, of Rhodamine-WT dye into the influent of LR barrels (in duplicate) associated with the SAV 1.5, 3.5 and 7.0 day HRT treatments. Simultaneously 2.379, 1.051, and 0.470 g of LiCl were also added to these respective LR influent locations. Each tracer was applied in 100-mL volumes over a one minute time span. Samples of LR effluent were collected from the 5-hr HRT location at 0, 1, 2, 3, 4, 5, 6, 8, 10, and 12 hours after injection. Concurrent with this experiment, we injected the same tracers at the influent of the SAV tanks operated at three depths (see Section VII).

Laboratory Analyses of Tracers

Rhodamine-WT concentrations were measured on a Turner Model 112 fluorometer with excitation and emission filters of 545 and 590 nm, respectively (Wilson et al. 1986). The emission filter consisted of an orange sharp-cut filter superimposed on a blue-green band-pass filter (Wilson et al. 1986). The light source was a far-UV lamp. The standard curve was linear to 100 μg/L and the method detection limit was 0.5 μg/L. Since Rhodamine-WT fluorescence is sensitive to temperature, both standards and samples were analyzed at room temperature. Prior to analyses, all water samples were stored in amber-colored bottles.

Lithium was measured on filtered, HNO_3 preserved samples by atomic absorption spectrophotometry (P.E. 5100-ZL) in the emission mode at $\lambda = 670.8$ nm. The linear working range of the standard curve was 1-100 μg/L; the method detection limit ranged from 2-5 μg/L.

Computations for Hydraulic Retention Time (τ) and Residence Time Distribution (RTD)

The nominal HRT, τ, is the ratio of the volume of water in the treatment component (V) divided by the volumetric flow rate of water (Q):

$$\tau = V/Q \quad (1)$$

The tracer residence time, τ_a, defined as the average time that a tracer particle spends in a treatment unit (i.e., LR bed or SAV mesocosm), was calculated by dividing the first moment (M_1) (Eq. 4) of the tracer flow distribution (g·day), by the zeroth moment, M_0 (g) (Eq. 3), both of which are based on mean outflow rates and tracer concentrations (Kadlec 1994):

$$\tau_a = M_1/M_0 \quad (2)$$

$$M_0 = \int_0^{t_f} Q_e(t)\,C(t)\,dt \quad (3)$$

$$M_1 = \int_0^{t_f} tQ_e(t)\,C(t)\,dt \quad (4)$$

where C(t)=exit tracer concentration (μg/L for the LR beds and mg/m^3 for the SAV mesocosms); Q_e=flow rate (L/hr for the LR beds and m^3/day for the SAV mesocosms); t=time (hours for the LR beds and days for the SAV mesocosms); and t_f=total time span of the outflow pulse (hours for the LR beds and days for the SAV mesocosms).

The residence time distribution (RTD) represents the time various fractions of water spend in each of the treatment units. It is the contact time distribution for the system (Kadlec 1994). The RTD defines the key parameters that characterize the actual detention time. Levenspiel (1989) uses the RTD in the analysis of reactor behavior.

To find the RTD, the concentration response curve (experimental C(t) vs. t curve) is converted to an E_t curve by changing the concentration scale so that the area under the response curve is unity (Levenspiel 1989). This is done by multiplying the concentration readings by the volumetric flow rate divided by the mass (M) of injected tracer:

$$E_t = C(Q_e/M) \quad (5)$$

where E_t = RTD in reciprocal time units.

The RTD can be also expressed in terms of the dimensionless time scale by multiplying the Y-axis (i.e., the E_t function) units by τ (the nominal HRT):

$$E_\Theta = \tau E_t \quad (6)$$

where E_Θ= dimensionless RTD,

and dividing the time units of the X-axis by τ:

$$\Theta = t/\tau \quad (7)$$

where Θ = dimensionless time scale.

This changes the X and Y axes so that the area under the curve = 1 and the mean =1 (Levenspiel 1989).

Phosphorus Mass Balances

At the end of the study we calculated mass balances for sediment and vegetation using the following method. The plant standing crop of P for influent and effluent regions of each tank was estimated by multiplying the wet weight standing crop by the dry wt/wet wt ratio. Then the resulting dry matter standing crop for each SAV species was multiplied by its tissue P content (dry wt basis). These values (in units of g P/m^2) were summed for all species at the influent and effluent regions of the mesocosms. Sediment P storage was calculated from the bulk density and P content of the marl sediments that accrued above the native muck.

Sediment + SAV P storages were then compared to the mass of P removed from the water (influent flow rate) X (influent – effluent total P concentrations). We made no correction for evaporation or rainfall (i.e., effluent flows were assumed to equal influent flows), because even at our lowest flow rates the atmospheric water fluxes were not significant (e.g., a minimum of 40.2 m/yr influent water loading vs. 1.3 m/yr of evaporation and rainfall).

Results and Discussion

Initial Vegetation and Sediment Characteristics

The dominant SAV species stocked in the HRT mesocosms, *Najas* and *Ceratophyllum*, differed slightly in their elemental composition. *Ceratophyllum* had higher N, P and C contents, and *Najas* exhibited the higher Ca content (Table 5.2). We did not measure the elemental composition of the *Chara* and *Potamogeton.* These species were stocked at a 15-fold lower standing crop than the two dominant species.

The initial chemical composition of the organic soils stocked into the mesocosms was comparable among the three treatments, with low P and high N contents (Table 5.2). While the N

concentration is typical of surface muck soils in the region, the P content is 2-3 times lower (Reddy et al. 1998).

Long-Term Phosphorus Removal Performance

Influent TP concentrations of the Post-BMP drainage water fluctuated widely, from 35 to 183 μg/L during the period June 1, 1998 through February 2, 1999. Regardless of influent P concentrations ($\bar{x}$ = 100 μg/L), the SAV unit processes were remarkably effective at reducing influent TP levels. TP effluent concentrations from the 3.5 and 7.0 day HRT SAV systems were consistently low, averaging 23 and 18 μg/L, respectively (Fig. 5.1; Table 5.3). By contrast, the extremely short, 1.5 day HRT treatment periodically experienced "breakthrough" of influent TP, and exhibited a much higher effluent concentration (39 μg/L) during the study (Fig. 5.1; Table 5.3). For the entire study period effluent TP levels were significantly different ($P < 0.05$) among HRT treatments.

Further reductions in TP concentrations occurred as the water exited the SAV mesocosms and flowed through the LR beds (Fig. 5.2). We observed significant ($P < 0.05$) decreases in the TP levels between the SAV mesocosms effluents and 1 hr HRT LR sampling locations. While we detected differences between the 1 hr and 5 hr LR sampling locations, they generally were not statistically significant (Table 5.3).

Despite variations in air temperature, water temperature and solar radiation during the study, we observed no obvious seasonal effects on P removal performance by the SAV/LR systems (Figs. 5.1 and 5.2). The maximum observed mid-depth water temperature in the SAV mesocosms was 33 ^{o}C (in August 1998) and the minimum was 10.5 ^{o}C (in January 1999). The longer HRT mesocosms exhibited only slightly wider temperature extremes than those operated at a short HRT.

Diel Water Quality Characteristics

There were no discernible diel D.O. fluctuations for the Post-BMP influent water (Fig. 5.3). However, due to photosynthesis, D.O. concentrations within the SAV mesocosms varied widely. Daytime D.O. levels reached supersaturation, followed by nighttime readings <1.0 mg.L (Fig. 5.3). The 1.5 day HRT SAV mesocosm usually had lower (<1.0 mg/L) nighttime D.O. concentrations than the 3.5 and 7.0 day HRT treatments. The LR beds lowered the high daytime D.O. concentration of the SAV effluent, but also increased the low nighttime D.O. concentrations,

Table 5.2. Initial physical and chemical characteristics and standing crop biomass of the submerged vegetation (top panel) and soils (bottom panel) stocked in the HRT/HLR mesocosms (n=3).

Treatment	Dry Stocking Weight (g/m^2)	TP		TN		TC		Ca	
		(mg/kg)	(%)	(mg/kg)	(%)	(mg/kg)	(%)	(mg/kg)	(%)
1.5 day HRT									
Najas									
mean	74	1550	0.155	18,400	1.84	336,000	33.6	108,000	10.8
s.d.	7	260	0.026	2,300	0.23	30,000	3.0	36,000	3.6
Ceratophyllum									
mean	65	2910	0.291	21,000	2.10	364,000	36.4	75,000	7.5
s.d.	5	390	0.039	2,300	0.23	20,000	2.0	32,000	3.2
3.5 day HRT									
Najas									
mean	74	1860	0.186	19,600	1.96	326,000	32.6	120,000	12.0
s.d.	9	130	0.013	1,000	0.10	8,000	0.8	10,000	1.0
Ceratophyllum									
mean	72	2610	0.261	20,900	2.09	370,000	37.0	640,000	6.4
s.d.	8	430	0.043	1,900	0.19	6,000	0.6	4,000	0.4
7.0 day HRT									
Najas									
mean	68	1560	0.156	19,000	1.90	340,000	34.0	106,000	10.6
s.d.	5	60	0.006	700	0.07	12,000	1.2	22,000	2.2
Ceratophyllum									
mean	63	3060	0.306	20,800	2.08	358,000	35.8	72,000	7.2
s.d.	7	400	0.040	1,200	0.12	18,000	1.8	21,000	2.1

Treatment	Bulk Density (g/cc)	TP		TN		TC		Ca	
		(mg/kg)	(%)	(mg/kg)	(%)	(mg/kg)	(%)	(mg/kg)	(%)
1.5 day HRT									
mean	0.180	234	0.023	25,800	2.58	456,000	45.6	60,000	6.0
s.d.	0.005	13	0.001	1,500	0.15	23,000	2.3	8,000	0.8
3.5 day HRT									
mean	0.190	242	0.024	24,200	2.42	431,000	43.1	67,000	6.7
s.d.	0.210	19	0.002	1,700	0.17	24,000	2.4	8,000	0.8
7.0 day HRT									
mean	0.169	233	0.023	26,600	2.66	460,000	46.0	65,000	6.5
s.d.	0.005	28	0.003	900	0.09	23,000	2.3	10,000	1.0

Table 5.3. Total P (TP) and soluble reactive P (SRP) concentrations for the three HRT treatments in Subtask 4C. Values represent means (s.d.) of either 33 or 36 weekly measurements. Sample locations were SAV influent, SAV effluent, and 1 hr & 5 hr HRTs in the limerock (LR) bed. Within each column, means for total P with the same letters are not significantly different (P > 0.05). Within each row, means with the same number are not significantly different (P > 0.05).

	Total P (µg/L)			
Treatment	**SAV Influent**	**SAV Effluent**	**LR (1 hour HRT)**	**LR (5 hour HRT)**
1.5 day HRT				
mean	98	$39^{a,1}$ (4.5)	$32^{a,2}$ (4.4)	$32^{a,2}$ (2.4)
max.	183	76	68	75
min.	35	20	19	12
3.5 day HRT				
mean	96	$23^{b,1}$ (3.1)	$18^{b,2}$ (2.3)	$15^{b,2}$ (1.6)
max.	178	69	35	32
min.	34	9	9	9
7.0 day HRT				
mean	104	$18^{c,1}$ (2.2)	$15^{b,2}$ (1.8)	$12^{b,2}$ (1.7)
max.	182	42	45	27
min.	37	8	6	5

	SRP (µg/L)			
Treatment	**SAV Influent**	**SAV Effluent**	**LR (1 hour HRT)**	**LR (5 hour HRT)**
1.5 day HRT				
mean	60	10 (2.6)	14 (2.8)	18 (2.1)
max.	150	34	40	52
min.	24	1	2	2
3.5 day HRT				
mean	60	3 (0.9)	5 (1.4)	5 (1.0)
max.	159	16	21	12
min.	22	1	2	1
7.0 day HRT				
mean	59	3 (0.8)	3 (0.8)	3 (1.0)
max.	163	15	7	9
min.	16	1	1	1

effectively dampening the diel swings of the SAV mesocosm effluents (Fig. 5.3). At no time was the D.O. concentration undetectable at any system point, indicating that aerobic conditions were maintained within the SAV community and LR bed during the diel cycle.

Although many parameters (e.g., pH, D.O.) exhibited a diel periodicity, the overall ionic composition of the Post-BMP influent and SAV/LR effluents remained rather consistent (Fig. 5.4). There was, however, a slight increase in specific conductance during passage through the SAV mesocosms. Five hours residence time within the LR beds did not result in further consistent changes in the specific conductance.

The original research and development work with the SAV/LR technology (Dierberg and DeBusk, unpublished) demonstrated that pH plays an important role in P removal. In the SAV unit process, biological uptake of water column P is thought to be supplemented by P coprecipitation with calcium carbonate, a process that can occur under the high pH conditions that prevail during the daylight hours. In the present study, we observed a sharp decline in calcium and alkalinity as Post-BMP waters passed through the SAV unit process (Table 5.4), which supports this precipitation hypothesis. A second part of our theory suggests that as high pH water from the SAV-dominated wetland is fed into a limerock bed, the rock surface serves as a nucleating site for further P precipitation and removal. As part of this study, it was therefore critical to assess whether diel fluctuation in water column pH would influence P removal performance by the SAV/LR system components.

Our data from two diel monitoring periods demonstrate that despite the marked temporal fluctuation in water column D.O. and pH (Figs. 5.3 and 5.5) in the SAV/LR system (e.g., pH change from 7.4 at night to 10.6 during daytime), overall system P removal performance was fairly consistent on a diel basis (Fig. 5.6). For the September 1998 diel, LR effluent TP ranged for the 7 day, 3.5 day and 1.5 day HRT systems were 11-14, 13-16, and 20 - 23 μg/L, respectively (Fig. 5.6). By contrast, the SAV influent TP samples exhibited substantial diel variability (93-157 μg/L), probably due to intermittent pumping activities at the S-5A and ENR pump stations. Possible mechanisms for the consistent diel P removal performance observed in the SAV unit process are discussed in the following section.

Water Column Phosphorus Speciation Within SAV/LR Systems

As part of the Subtask 4C monitoring protocol, we measured influent and effluent TP and SRP levels weekly. Every other week we measured TSP, which enabled us to calculate the concentration of dissolved organic P (DOP=TSP-SRP) and particulate P (PP=TP-TSP). During the study, SRP was the prominent P fraction in the water from the ENR supply canal (Tables 5.3 & 5.5; Fig. 5.7). In the 7.0 and 3.5 day HRT treatments, SRP was essentially removed in the SAV mesocosms (Table 5.3; Figs. 5.8 & 5.9), while the LR bed removed smaller amounts of PP and DOP. Only in the 1.5 day HRT treatment, did SRP "break through" the entire SAV/LR process train (Table 5.3; Figs. 5.10). The slightly reduced SRP removal effectiveness at high concentrations in the 1.5 day HRT, relative to the 7.0 day HRT, is depicted in Figure 5.11. During periods of high influent TP concentrations (ca. 150 ug/L), the 1.5 day HRT mesocosms produced an effluent SRP of 20 ug/L and higher. This "residual" SRP declined to 5 ug/L during periods of low influent concentrations (Fig. 5.11).

Because phosphorus precipitation as a distinct calcium phosphate phase or as a co-precipitate is a concentration-dependent process (based on solubility equilibria) (Diaz et al. 1994), we believe that the extremely low SRP levels that were encountered limited the effectiveness of this removal mechanism in the LR beds. On a percentage basis, the LR unit process accomplished 11%, 10% and 7% of the TP removed by the 1.5 day, 3.5 day and 7.0 day HRT treatments, respectively. While the LR bed removed only a small percentage of the P relative to the SAV unit process, it removed P fractions (DOP and PP) that may be difficult or impossible to remove by biological processes within a wetland-based treatment system. In the 1.5 day HRT treatment, for example, the LR bed (5 hr HRT) exported an average of 18 μg SRP/L (Table 5.3) during the study, but removed an average of 14 μg DOP + PP/L from the SAV effluent stream (Table 5.5). Limerock berms situated within a SAV cell may therefore prove to be an effective "transformer" of somewhat recalcitrant P to a more labile form. The rapid depletion of SRP in the SAV systems probably explains the lack of diel variation in P removal as noted previously. Even though the north site SAV/LR systems received drainage waters with "moderate to high" nutrient concentrations, they appeared to quickly become P limited. The competition for P by biota in these systems probably results in little daytime or nighttime export of P.

Table 5.4. Dissolved Ca and alkalinity concentrations for the three HRT treatments in Subtask 4C. Values represent means (s.d.) of 16 biweekly measurements. Sample locations are SAV influent, SAV effluent, and 1 hr & 5 hr HRTs in the limerock (LR) bed.

	dissolved Ca (mg/L)			
Treatment	**SAV Influent**	**SAV Effluent**	**LR (1 hour HRT)**	**LR (5 hour HRT)**
1.5 day HRT				
mean	74	62 (3.3)	63 (2.4)	70 (1.9)
max.	113	104	100	105
min.	39	27	28	27
3.5 day HRT				
mean	74	59 (3.1)	57 (2.4)	62 (3.2)
max.	111	97	93	100
min.	40	23	26	26
7.0 day HRT				
mean	74	51 (5.8)	48 (3.1)	50 (3.4)
max.	110	133	82	81
min.	40	26	27	25

	alkalinity (mg$CaCO_3$/L)			
Treatment	**SAV Influent**	**SAV Effluent**	**LR (1 hour HRT)**	**LR (5 hour HRT)**
1.5 day HRT				
mean	242	207 (10.0)	204 (7.3)	234 (6.0)
max.	400	368	360	376
min.	102	91	86	106
3.5 day HRT				
mean	241	201 (8.6)	194 (7.6)	213 (4.7)
max.	408	356	360	352
min.	104	72	86	86
7.0 day HRT				
mean	241	174 (10.1)	168 (9.4)	178 (6.9)
max.	400	318	320	312
min.	100	74	72	68

Table 5.5. Particulate P (PP) and dissolved organic P (DOP) concentrations for the three HRT treatments in Subtask 4C. Values represent means (s.d.) of 16 biweekly measurements. Sample locations were SAV influent, SAV effluent, and 1 hr & 5 hr HRTs in the limerock (LR) bed.

	Particulate P (µg/L)			
Treatment	**SAV Influent**	**SAV Effluent**	**LR (1 hour HRT)**	**LR (5 hour HRT)**
1.5 day HRT				
mean	23	15 (2.5)	6 (3.1)	4 (1.7)
max.	91	29	20	12
min.	4	7	0	0
3.5 day HRT				
mean	22	11 (3.8)	5 (2.1)	4 (1.4)
max.	85	24	12	12
min.	2	1	0	0
7.0 day HRT				
mean	26	9 (2.0)	5 (2.7)	4 (1.6)
max.	84	21	26	10
min.	5	2	0	0

	DOP (µg/L)			
Treatment	**SAV Influent**	**SAV Effluent**	**LR (1 hour HRT)**	**LR (5 hour HRT)**
1.5 day HRT				
mean	14	13 (1.4)	12 (2.6)	10 (1.5)
max.	26	19	30	15
min.	2	7	0	1
3.5 day HRT				
mean	14	9 (1.9)	8 (1.2)	6 (1.5)
max.	29	22	13	12
min.	6	2	3	2
7.0 day HRT				
mean	18	7 (1.5)	8 (1.4)	6 (1.3)
max.	88	12	46	12
min.	5	1	1	0

General Water Treatment Performance of SAV/LR Systems

The bulk of our sampling and analyses for this project focused either on removal of P species, or on analytes closely associated with P cycling in the environment (e.g., Ca, alkalinity). On two dates (September 8 and November 30, 1998), we collected water samples for analysis of a suite of other constituents. Most of these "ancillary" parameters were found to be dynamic in both the SAV and LR unit processes, with most soluble constituents exhibiting a concentration reduction as the drainage water passed through the system (Figs. 5.12 – 5.15). Total dissolved solids (TDS) declined primarily in the SAV mesocosms, and this was mirrored by reductions in Cl, K, Mg, Na, Al, Fe, TKN, and sulfate. Declines in TDS and chloride were most prominent on the November sampling date. Chloride is reputed to be fairly conservative in wetlands (Dierberg and Brezonik 1983), but our data suggest that this may not be the case for SAV-dominated systems. A fluctuation in influent Cl concentrations (i.e., lower influent Cl levels during the preceding week) could also explain this apparent decline in Cl within the SAV unit process.

Reactive SiO_2 exhibited an increase in the SAV unit process on the September 8 sampling date, but declined on the November sampling date (Fig 5.15). In contrast to dissolved constituents, the SAV unit process appeared to generate suspended solids (Fig. 5.15). This increase, however, was not reflected in the turbidity measurement, which suggests that the TSS may have been comprised of larger particles that would have been less sensitive to a turbidimetric response than smaller particles. The high TSS value may also have been a sampling artifact. Inorganic N species (NO_x and NH_4-N) declined markedly in the SAV unit process, presumably due to plant uptake and/or microbial metabolism (Fig. 5.14). NO_x concentrations subsequently increased in the LR unit process, which suggests the limerock surfaces harbor nitrifying bacteria.

The HRT of the SAV/LR system influenced removal rates of many parameters. Concentration reductions for dissolved Fe and for color were markedly higher in the 7.0 day HRT SAV systems than for the shorter HRT treatments. Similarly, Cl reductions in November for the 7.0 day HRT SAV systems were greater than for either the 3.5 or 1.5 day HRT treatments.

Vegetation Characteristics

The species composition of the vegetation changed during the study, with the nutrient regime influencing relative dominance of the various SAV species. *Ceratophyllum* thrived in regions with greatest nutrient loading, such as the influent region of the 1.5 day HRT treatment.

Chara was much more prevalent in the lower nutrient regions, with highest *Chara* biomass observed at the outflow of the 7.0 day HRT treatment (Table 5.6). The rank order of tissue P content of the macrophytes was *Ceratophyllum> Najas >Chara*. For each species, tissue P levels also decreased with increasing HRT. On both a mass dry weight and mass total P basis, *Najas* was the dominant species in all treatments at the time of harvest.

Chemical Characterization of Sediments

Sediment TN varied slightly between inflow and outflow sections of the SAV mesocosms for each HRT treatment (Table 5.7). There was little variation in TN concentration among treatments, with sediment levels for the 1.5 day, 3.5 day and 7.0 day HRTs averaging 1.98, 1.95, and 1.87%, respectively. The muck had nitrogen concentrations that were *ca*. 20% higher than the newly deposited sediments.

The changes in sediment P concentrations followed the P concentration gradient in the water column, with sediment TP concentrations consistently higher in the inflow half of the mesocosms (Table 5.7). This indicates that particulate P in the source water, and/or *in situ* P removal processes (e.g., SAV detritus production, calcium carbonate-P coprecipitation) deposited disproportionately more P at the inflow than at the outflow. Differential losses/immobilization of P during decomposition of organic detritus also could explain the spatial differences in sediment P concentrations. In contrast to the trend observed for muck N levels, P concentrations of the recently deposited sediments were significantly higher than the underlying muck by 73-173% in all of the treatment tanks.

Calcium concentrations were also significantly higher (by two-fold) in the upper layer of recently deposited sediments than in the muck (Table 5.7), indicating that calcium carbonate ($CaCO_3$) precipitation was a significant process within the SAV mesocosms. There were no appreciable differences in average sediment Ca concentrations among the three HRT treatments, even though a slightly higher concentration in the inflow sections compared to the outflow sections of the 1.5 day and 7.0 day HRT treatments was observed.

Table 5.6. Standing crop biomass and tissue P storage in submerged macrophytes recovered from inflow and outflow halves of duplicate SAV mesocosms (for 3 separate HRT treatments) in February 1999. Missing values indicated plant biomass was negligible at that location.

Treatment		Dry Weight Recovered (g/m^2)		TP Concentration (mg/kg)		Mass TP (mg/m^2)	
		Inflow	Outflow	Inflow	Outflow	Inflow	Outflow
1.5 day HRT							
Najas	mean	188	327	5070	3910	878	1289
	s.d	196	86	730	290	856	432
Ceratophyllum	mean	149	106	5400	4580	804	483
	s.d	1	14	510	380	68	24
Chara	mean	-	-	-	-	-	-
	s.d	-	-	-	-	-	-
3.5 day HRT							
Najas	mean	368	748	3030	1370	1093	1025
	s.d	167	47	270	180	407	196
Ceratophyllum	mean	28	43	3230	1670	90	72
	s.d	-	-	-	-	-	-
Chara	mean	60	172	2650	1620	157	279
	s.d	-	-	-	-	-	-
7.0 day HRT							
Najas	mean	504	242	1470	840	756	197
	s.d	144	77	250	160	336	27
Ceratophyllum	mean	-	-	-	-	-	-
	s.d	-	-	-	-	-	-
Chara	mean	255	760	1250	590	323	452
	s.d	37	-	230	-	104	-

Table 5.7. Elemental composition of the original muck and the newly deposited sediment layer from inflow and outflow sections of SAV mesocosms operated at three HRTs. The single muck sample represents the underlying substrate that was added to each tank prior to start-up. Values represent means of samples collected from duplicate tanks.

Station	TN	TC	TOC	TIC	TCa	TP
	(%)	(%)	(%)	(%)	(%)	(µg/g)
1.5 day HRT Inflow	**1.91**	**32.6**	**27.8**	**4.8**	**16.3**	**667**
1.5 day HRT Outflow	**2.05**	**35.4**	**32.0**	**3.4**	**14.4**	**614**
1.5 day HRT Avg.	***1.98***	***34.0***	***29.9***	***4.1***	***15.3***	***641***
3.5 day HRT Inflow	**1.90**	**33.4**	**28.0**	**5.4**	**16.2**	**457**
3.5 day HRT Outflow	**2.01**	**34.4**	**31.2**	**3.2**	**16.0**	**359**
3.5 day HRT Avg.	***1.95***	***33.9***	***29.6***	***4.3***	***16.1***	***408***
7.0 day HRT Inflow	**1.72**	**30.5**	**23.6**	**6.9**	**20.5**	**472**
7.0 day HRT Outflow	**2.02**	**34.8**	**29.8**	**5.0**	**15.0**	**447**
7.0 day HRT Avg.	***1.87***	***32.6***	***26.7***	***6.0***	***17.7***	***460***
3.5 day HRT Original Muck	**2.47**	**41.4**	**37.9**	**3.5**	**7.9**	**236**

Total carbon concentrations were higher in the muck than the accrued sediments by approximately 33%, due to the higher organic matter and lower mineral content measured in the recently deposited sediments (Table 5.7).

For the sediment extraction sequence, the sum of the $CaCO_3$-P, Fe & Al-P, and biogenic-P fractions is considered the labile P pool, while the sum of the Ca-mineral-P and residual-P is commonly identified as the nonlabile P pool (Penn et al. 1995). Most of the accrued P was in the nonlabile P pool (fraction B: Table 5.8), with only 8-26% of the total P found in the labile P pool (fraction A: Table 5.8). We are uncertain whether this was due to the nature of the particulate P in the source water, the processes occurring within the water column and SAV community, or diagenesis within the sediment. Nevertheless, most of the P deposited onto the sediment surface is nonlabile, and is subject to remobilization under only the most severe circumstances (e.g., desiccation). Even the labile P pool, considered by most soil and sediment scientists to have the potential for mobilization, probably remains sequestered in the sediments under typical

environmental conditions. We base this observation on the consistently low effluent P levels obtained from the SAV culture tanks, and on the relatively constant SRP water column depth profiles (see Section VII), both of which demonstrated little internal P loading during the 8-month monitoring period. While internal loading of sediment P has been documented to occur under extreme environmental conditions, such as desiccation, anoxia, or acidic or low P influents, these conditions have yet to be tested for SAV sediments.

Compared to the underlying muck, which was obtained from an area under agricultural production, the sediment that accrued within the SAV mesocosms was enriched in all five P fractions (Table 5.8). This sediment enrichment was expected, considering the P loading rates and the low initial P concentrations of the muck (236 μg/g). The greatest enrichment was observed within the $CaCO_3$-P and Fe & Al-P fractions, although in absolute amounts those fractions represented smaller P increments than the Ca-mineral-P and residual-P fractions. Biogenic-P was the only P fraction measured for which sediment and underlying muck concentrations were relatively comparable.

Because higher P loadings were associated with the increased hydraulic loading, the 1.5 day HRT mesocosms had higher concentrations of sediment P for all fractions than either the 3.5 or 7.0 day HRT treatments (Table 5.8). The 1.5 day HRT mesocosms also had a higher percentage of labile P (fraction A: average of 22%) than the other HRT mesocosms (fraction A: average of 11% each).

Higher P loading rates to the 1.5 day HRT mesocosm also likely accounts for the higher percentages of the deposited P found in all the labile pools, particularly the $CaCO_3$-P pool (Table 5.8). This cannot be due to differences in the concentrations of $CaCO_3$ in the sediments, since they were similar among the HRT treatments (Table 5.7). Of the three HRT treatments, the 1.5 day mesocosms were the only SAV systems where SRP was consistently above detectable concentrations in the water column (Table 5.3). Sorption of water column SRP to the calcium carbonate precipitate could therefore have been more prevalent in the 1.5 day HRT mesocosms than in the longer HRT treatments.

We also observed differences in the concentration of the P fractions between sediments collected from the inflow and outflow sections of the SAV tanks (Table 5.8). The inflow sections of the treatment tanks, regardless of the HRT, always had higher $CaCO_3$-P, Fe & Al-P, Ca-mineral-P, and residual-P. This may indicate that particulate P in the source water, which is likely to settle

quickly, contributes significantly to these P pools. Alternatively, SAV productivity and calcium carbonate saturation indexes may be higher in the inflow section of the culture tanks, and thereby cause a higher deposition rate of calcium carbonate-, Fe-, Al-, and detrital-associated P. In contrast to the recently deposited sediments, the spatial concentration gradients for the underlying muck were slight (Table 5.8).

Phosphorus Mass Balances

We compared removal of water column phosphorus with the P stored in the vegetation and newly deposited sediments. In the original scope of work, mass balances were to be performed by completely disassembling all mesocosms, and quantitatively measuring the dry matter and P mass in the vegetation and sediment compartments. Because of the value in keeping all of the mesocosms operational, as well as some completely undisturbed, we performed plant sampling on only two of the three SAV mesocosms in each HRT treatment. Additionally, in these same mesocosms, we collected sediments by piston corer (approximately 10 cores per mesocosm), rather than by completely draining the tanks. Sediment coring was performed first, followed by the vegetation harvest.

We recovered from between 0.44 and 1.60 g P/m^2 as submerged vegetation, with the higher values occurring in the shorter HRT treatments (Table 5.9). *Najas* provided the bulk of the vegetation P storage in all treatments, with *Ceratophyllum* contributing substantial P storage in the 1.5 day HRT treatment, and *Chara* providing a moderate level of P storage in the 7.0 day HRT treatment (Table 5.9).

Due to the short duration of the study, we found only a thin layer of newly deposited sediments (0.4 to 1.1 cm deep), particularly in the longer HRT treatments. It was quite difficult to accurately quantify the thickness of this material, due not only to their shallow depths but also because of sediment disturbance caused by the rooted macrophytes. The rooted macrophytes near the sediment surface presented an impediment to retrieving an undisturbed core by becoming lodged along the edges of the coring device during penetration into the sediments. This caused the sediment surface within the core to become disturbed as the plant stems and roots were dragged along the inside wall of the core. We therefore do not have a good measure of the uncertainty in the sediment "depth" measurements provided in Table 5.9.

Table 5.8. Phosphorus fractions from the newly deposited sediment layer within inflow and outflow halves of SAV mesocosms operated at three different HRTs. Fraction A (sum of $CaCO_3$-P, Fe & Al-P, and extractable biogenic-P) represents the labile P pool; fraction B (sum of Ca mineral-P and residual-P) corresponds to the nonlabile P pool. Values represent means (s.d.) from duplicate tanks. All units are μg/g dry wt except when otherwise noted.

Fraction		1.5 day HRT		3.5 day HRT		7.0 day HRT		Muck*	
		Inflow	**Outflow**	**Inflow**	**Outflow**	**Inflow**	**Outflow**	**Inflow**	**Outflow**
A	**$CaCO_3$-P**	79 (14.6)	67 (1.0)	34 (7.8)	14 (1.2)	25 (13.6)	12 (2.4)	4	1
	Fe & Al-P	42 (9.8)	34 (0.5)	22 (4.1)	14 (2.3)	22 (6.2)	21 (8.4)	4	5
	Biogenic-P	13 (5.4)	31 (3.8)	7 (2.4)	6 (1.0)	17 (0.6)	16 (22.3)	10	4
B	**Ca-mineral-P**	154 (45.3)	108 (10.0)	102 (2.3)	91 (53.5)	107 (41.8)	94 (1.6)	42	36
	Residual-P	479 (4)	402 (51)	338 (11)	285 (7)	435 (148)	322 (40)	163	175
	Σ Fraction A	134	132	63	34	63	49	18	10
	Σ Fraction B	633	510	440	376	540	416	205	211
	Fraction A: % TP	18%	26%	13%	8%	12%	11%	9%	5%
	Fraction B: % TP	82%	74%	87%	92%	88%	89%	91%	95%

*Represents the underlying substrate that was added prior to start-up from only one of the 3.5 day HRT tanks.

Table 5.9. Vegetation P storage (top panel), P storage in newly deposited sediments (middle panel) and overall P mass balance for HRT study (bottom panel). Values represent means of samples collected from duplicate tanks.

	1.5 day HRT	3.5 day HRT	7.0 day HRT
Vegetation			
Najas			
Std crop (kg/m^2)	0.25	0.54	0.39
P conc. (mg/kg)	4483	2197	1153
P storage (g/m^2)	1.13	1.17	0.45
Ceratophyllum			
Std crop (kg/m^2)	0.16	0.02	-
P conc. (mg/ kg)	4990	2450	-
P storage (g/m^2)	0.78	0.04	-
Chara			
Std crop (kg/m^2)	-	0.07	0.32
P conc. (mg/ kg)	-	2397	1124
P storage (g/m^2)	-	0.18	0.36

	1.5 day HRT	3.5 day HRT	7.0 day HRT
Sediment			
Depth (cm)	1.0	0.6	0.5
Bulk Density (g/cc)	0.17	0.23	0.19
P conc. (mg/kg)	641	408	459
P storage (g/m^2)	1.11	0.57	0.44

	1.5 day HRT	3.5 day HRT	7.0 day HRT
	----------g P /m^2----------		
Final SAV Storage	1.91	1.37	0.75
Initial SAV Stock	0.31	0.31	0.31
Net SAV Storage	1.60	1.05	0.44
SAV + Sediment P	2.71	1.62	0.88
Water P load	8.0	4.4	2.2
% Recovered in SAV + Sediment	34	37	39

Our estimate of P accrual in the sediments for the study period of June 1998 – February 1999 ranged from 0.44 g P/m^2 in the 7.0 day HRT mesocosms, to 1.11 g P/m^2 in the 1.5 day HRT mesocosms (Table 5.9). Total P storage in the SAV systems (plant + sediments) therefore ranged from 0.88 g P/m^2 (7.0 day HRT) to 2.71 g P/m^2 (1.5 day HRT) (Table 5.9). The P storages that we assessed in the mesocosms accounted for only 34 – 39% of the observed P removed from the water column. As noted above, we believe the weakest point in this mass balance is the sediment depth measurement. For the mesocosms, this estimate can be improved by additional sampling after a longer period of operation and sediment deposition.

Hydraulic Characteristics of the Limerock Barrels

The objectives of this hydraulic assessment of the LR barrels were to:

- measure the HRTs of the LR reactors
- measure and compare the residence time distributions among treatments (normalizing the area under the concentration vs. time curves to 1)
- look for faulty flow lines (e.g., short-circuiting or stagnant areas)
- compare the stability and longevity of the tracers Rhodamine-WT and lithium

Tracer Response Curves

After a lag of approximately two hours from injection, the concentrations of both tracers increased sharply to a high of 80 μg/L for Rhodamine and 600 μg/L for Li at all flow rates before steadily decreasing to near baseline concentrations after about 12 hours (Fig. 5.16). Other than one of the duplicate LR barrels which short-circuited (16.8 L/hr flow from the 7.0 day HRT SAV tank), the concentration response curves resembled a left-skewed normal distribution, with longer tails associated with the higher flow rates (Fig. 5.16). The profiles resemble those for plug flow with dispersion (Levenspiel, 1989). The fastest flow rate (79.2 L/hr from the 1.5 day SAV HRT) produced a response curve which was closest to the ideal for plug flow (i.e., symmetrical with the peak concentration coinciding with the τ_a [=6.5 hr]). A faster flow rate is more likely to produce a classical plug flow response since advection becomes more significant compared to diffusion and dispersion. As the flow rate decreases, dispersion and diffusion become more prominent in the mixing process, which leads to a more pronounced tailing effect.

Tracer Mass Balances

Rhodamine and lithium mass balances were checked by comparing the added tracer mass to the total tracer mass recovered at the effluent. Although the monitoring period ended before the return of the tracer concentrations to background levels, a comparison of the recovered tracer mass and the amount added to each treatment unit indicated a good recovery for both tracers (Table 5.10). Rhodamine recovery was higher than the lithium, suggesting that lithium adsorption onto LR surfaces may have occurred.

Table 5.10. Comparison of recovered tracer mass with the amounts added to LR barrels operated at three different flow velocities. Values represent means (s.d.) of duplicate LR barrels.

Treatment	Mass Added (mg)		Mass Recovered (mg)		% Recovery	
	Dye	Li	Dye	Li	Dye	Li
High Flow: 79.2 L/hr	39.0	390	34.8 (0.7)	294 (3.8)	89.1	75.5
Mid Flow: 34.2 L/hr	17.2	172	15.3 (0.4)	138 (4.7)	89.2	80.3
Low Flow: 16.9 L/hr	7.7	77	7.3 (0.4)	63 (1.9)	95.3	82.2

Tracer Detention Time

Measurements using Rhodamine-WT and lithium yielded comparable HRTs (τ_a). However, these tracer detention times were from 1.1 to 1.7 hours longer than the nominal detention times (τ) (Table 5.11). Either an inaccurate estimation of the LR bed void volume and/or the truncated tracer dataset may have accounted for the difference between the "tracer" and nominal detention times. We used a void volume of 42% in the calculation of τ, which had been derived from measurements on the same size rock (1.3 - 2.5 cm diameter) as used in the LR beds. To more accurately estimate τ_a, the truncated data should be extrapolated to zero concentration via an exponential decay (Kadlec 1994). Since M_0 is sensitive to the long "tail" of the concentration response curve, excluding it may result in a somewhat longer τ_a.

Table 5.11. Comparison of nominal (τ) and measured (τ_a) detention times in LR barrels with three different flow velocities. The values represent means and standard deviations (n=2).

Treatment	τ (hr)	τ_a (hr)	
		Dye	Li
High Flow: 79.2 L/hr	4.9	6.5 (0.3)	6.5 (0.4)
Mid Flow: 34.2 L/hr	5.0	6.3 (0.3)	6.4 (0.3)
Low Flow: 16.9 L/hr	4.6	5.7 (0.9)	5.7 (0.8)

Residence Time Distribution (RTD)

The RTD represents the time various fractions of water spend in each of the treatment units. It is the contact time distribution for the system and defines the key parameters that characterize the actual detention time (Kadlec 1994). Levenspiel (1989) uses the RTD in the analysis of reactor behavior.

The dimensionless RTD curves (Fig. 5.17) assist in defining the mixing characteristics and diagnosing any irregularities in classical plug or mixed flow profiles. The fastest flowing (79.2 L/hr) LR barrels exhibited a longer lag time, closer timing of peak height (E_Θ) to Θ=1, and better symmetry (relative to their nominal retention times) than the slower flow treatments in the dimensionless analysis (Fig. 5.17). All three of the characteristics expressed by the faster flowing LR barrels are more consistent with plug flow than other types of flow regimes (e.g., mixed). The slowest flow rate LR barrels (16.8 L/hr) deviated the most from the classical "plug flow with dispersion" profile. Therefore, flow rate is an important factor in determining the hydraulic behavior of a LR bed.

In conclusion:

- Rhodamine-WT was a more inert tracer than lithium when applied to enclosed LR beds.
- the two tracers produced congruent response curves.
- LR beds behave hydraulically like a plug flow reactor with dispersion
- one of the LR beds displayed a faulty flow line by short-circuiting within one hour of injection.

- an incorrect LR bed void volume and/or the truncated tracer dataset probably explain why measured τ_a > nominal τ.
- the LR beds receiving the fastest flow rates produced response profiles which were closest to plug flow with dispersion, indicating that the relative contributions of advective and dispersive flows in the hydrodynamic model are important in determining the hydraulic characteristics of LR reactors.

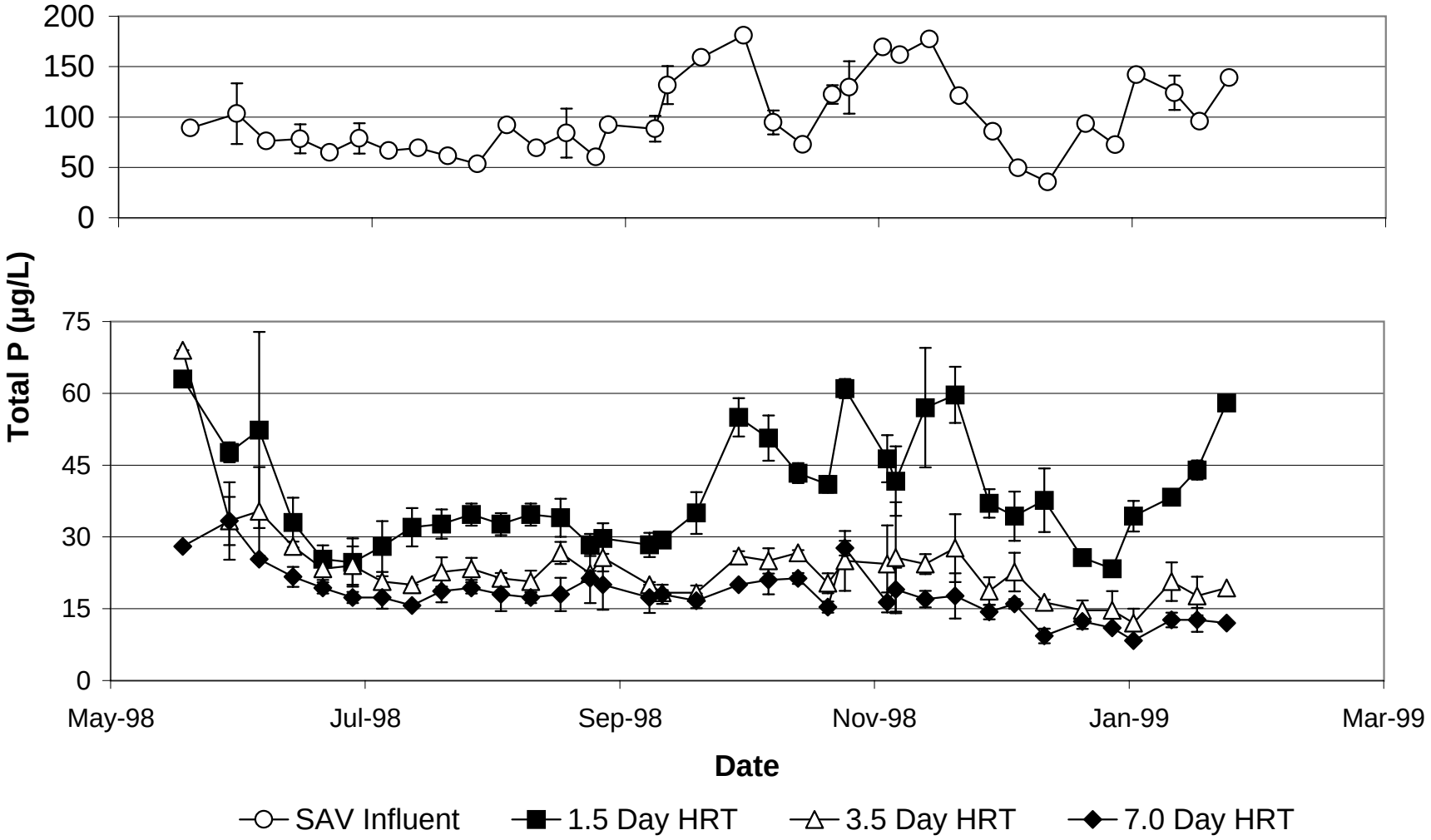

Figure 5.1 Mean total P concentrations (n=3) at SAV influent and SAV effluent locations for mesocosms operated at three hydraulic retention times. Bars represent ±1 s.d.

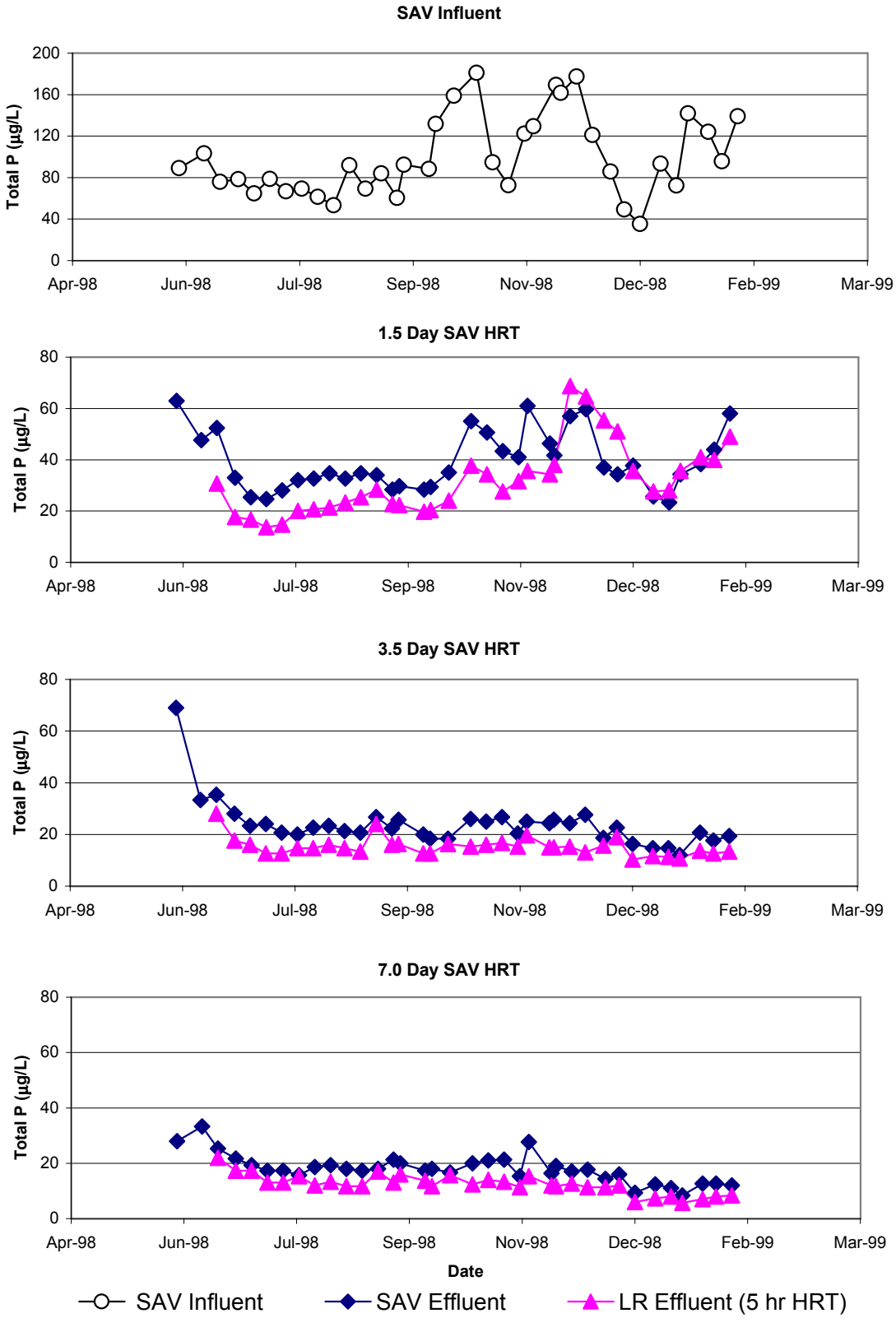

Figure 5.2 Mean total P concentrations (n=3) at three locations in the treatment train: SAV influent, SAV effluent, and LR (5 hr HRT) effluent.

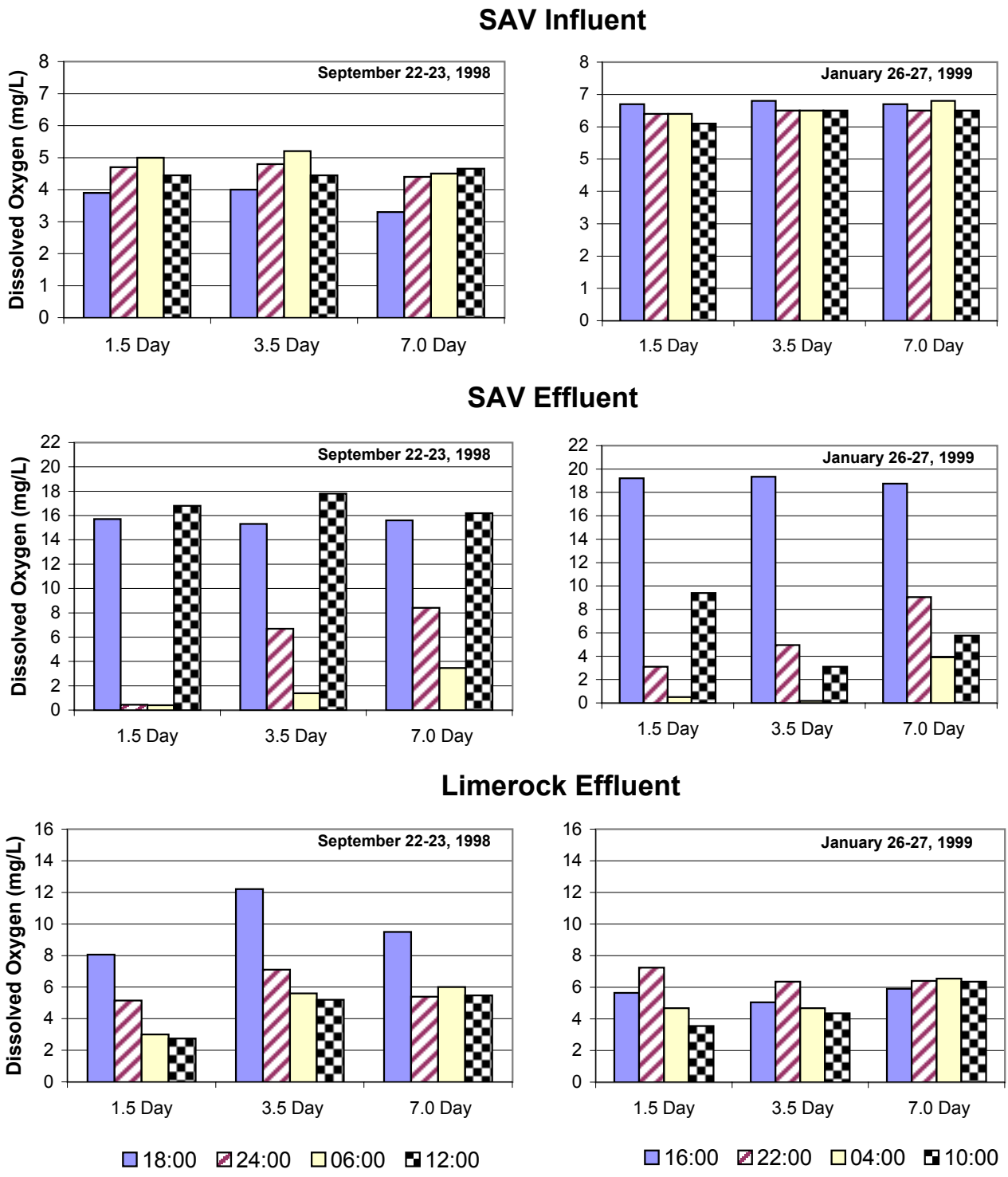

Figure 5.3 Diel dissolved oxygen concentrations at three locations in the SAV/LR treatment train on September 22-23, 1998 and January 26-27, 1999. N=1 for influent, N=2 for SAV and limerock effluents.

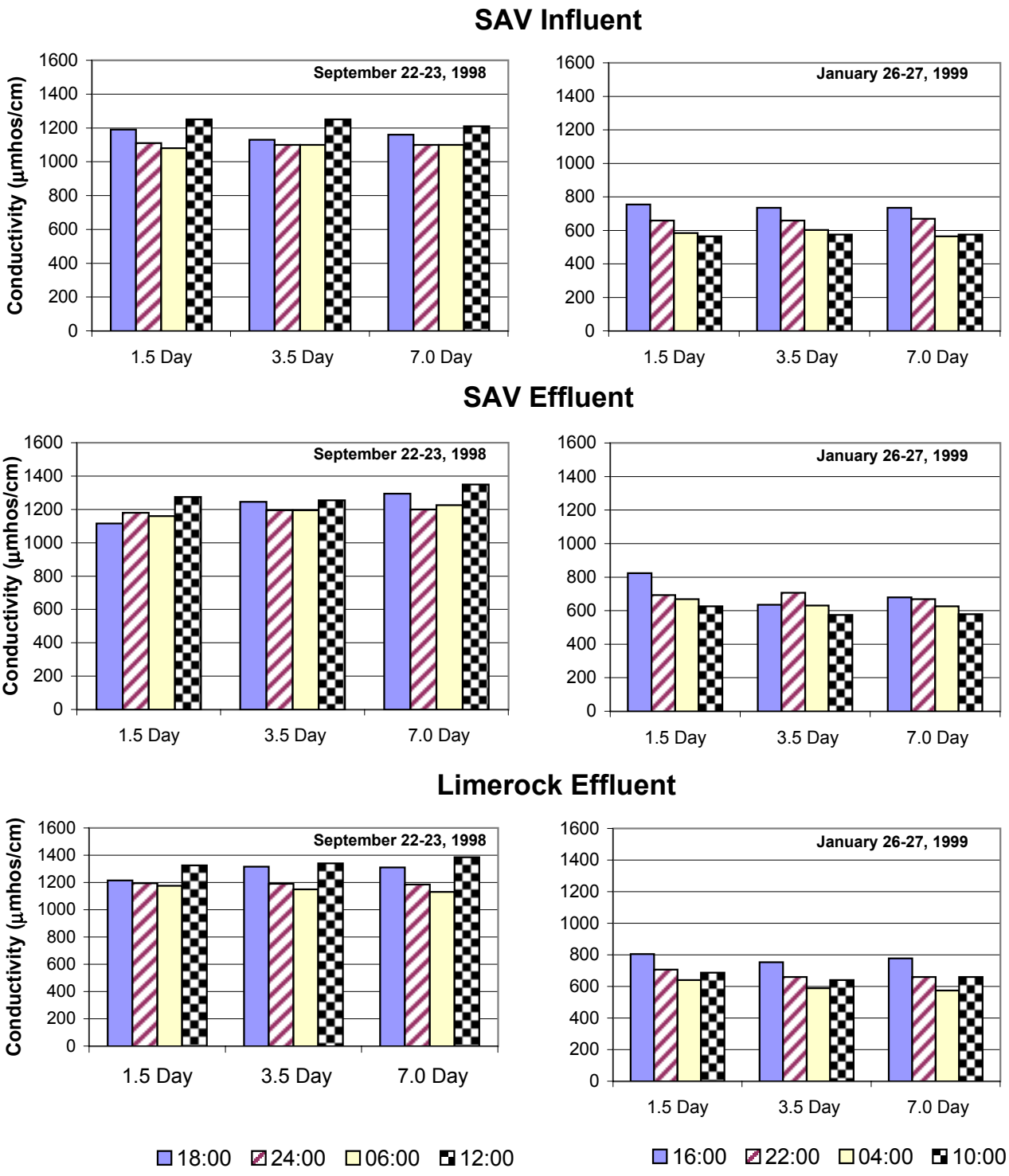

Figure 5.4 Diel conductivity levels at three locations in the SAV/LR treatment train on September 22-23, 1998 and January 26-27, 1999. N=1 for influents, N=2 for SAV and limerock effluents.

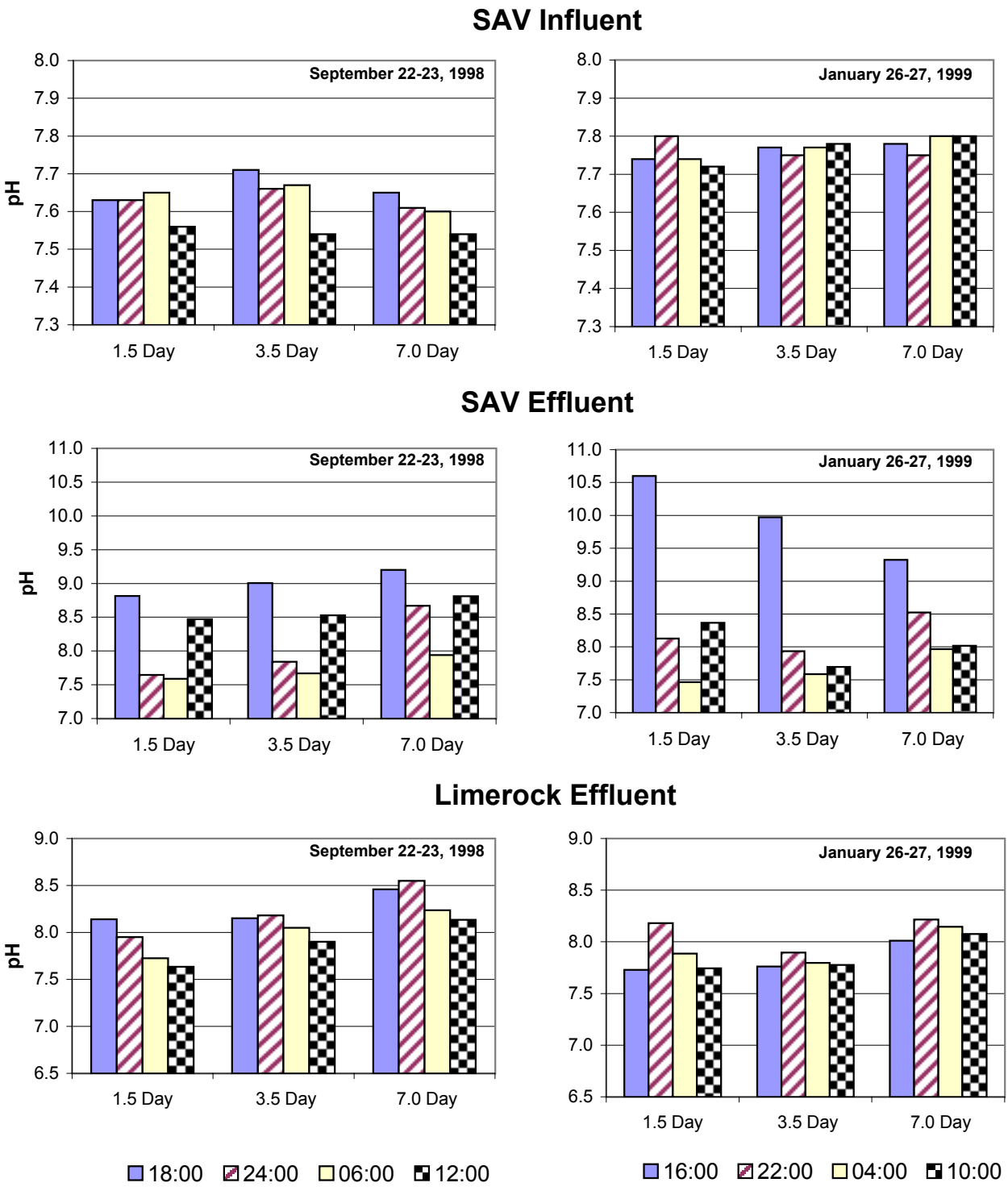

Figure 5.5 Diel pH values at three locations in the SAV/LR treatment train on September 22-23, 1998 and January 26-27, 1999. N=1 for influent, N=2 for SAV and limerock effluents.

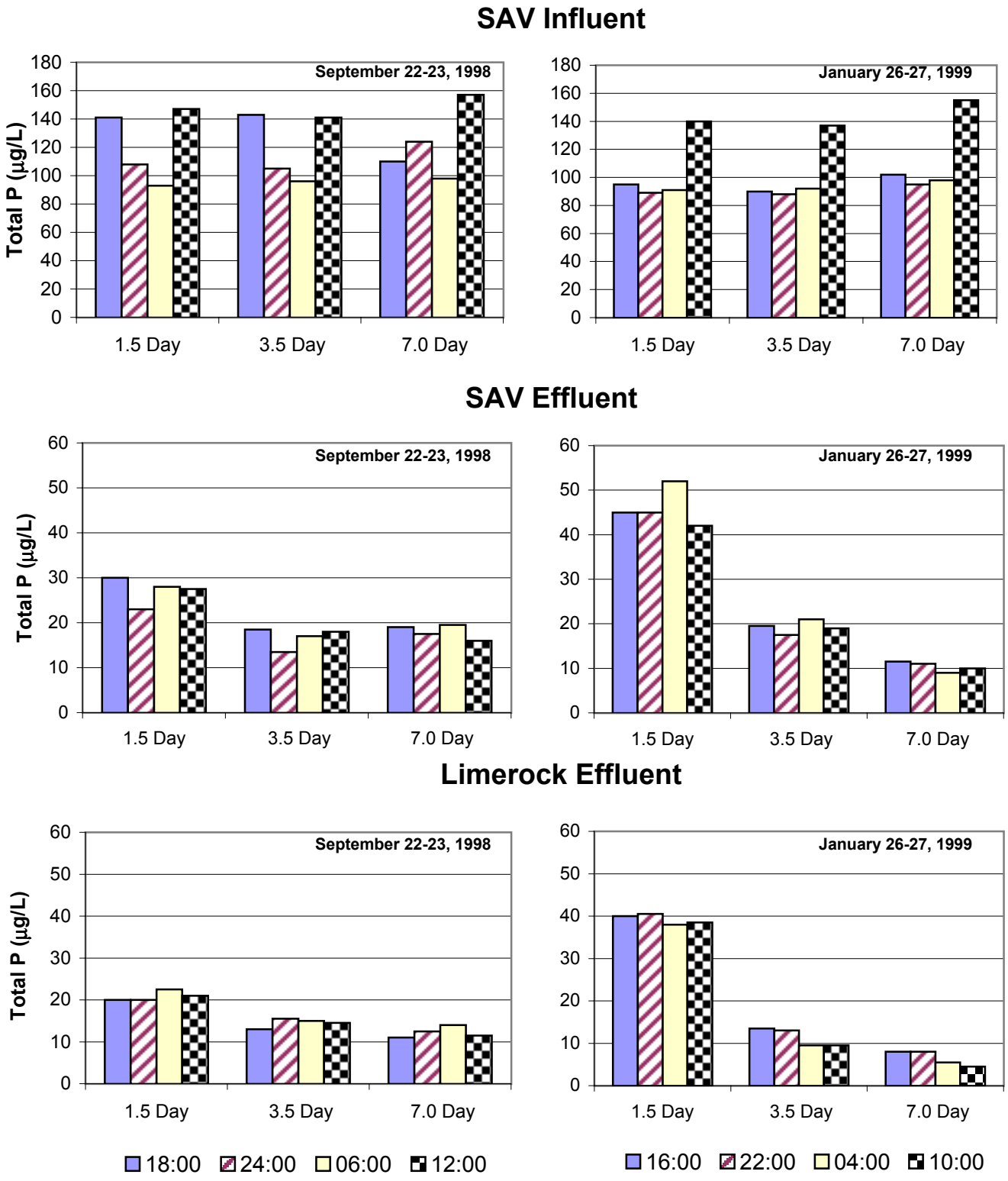

Figure 5.6 Diel total P concentrations at three locations in the SAV/LR treatment train on September 22-23, 1998 and January 26-27, 1999. N=1 for influent, N=2 for SAV a limerock effluent.

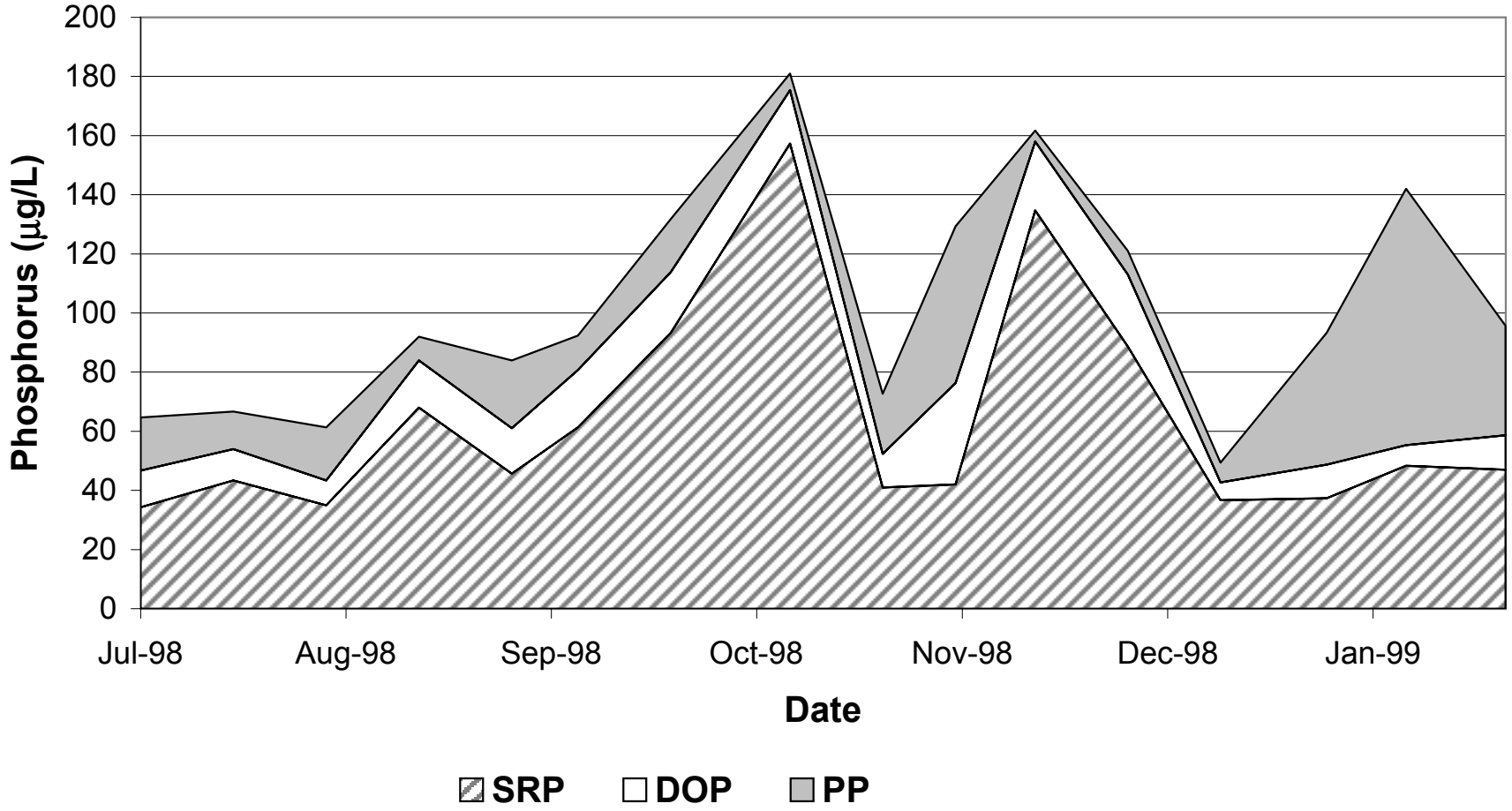

Figure 5.7 Soluble reactive P (SRP), dissolved organic P (DOP) and particulate P (PP) concentrations in the Post-BMP influent waters from the ENR supply canal.

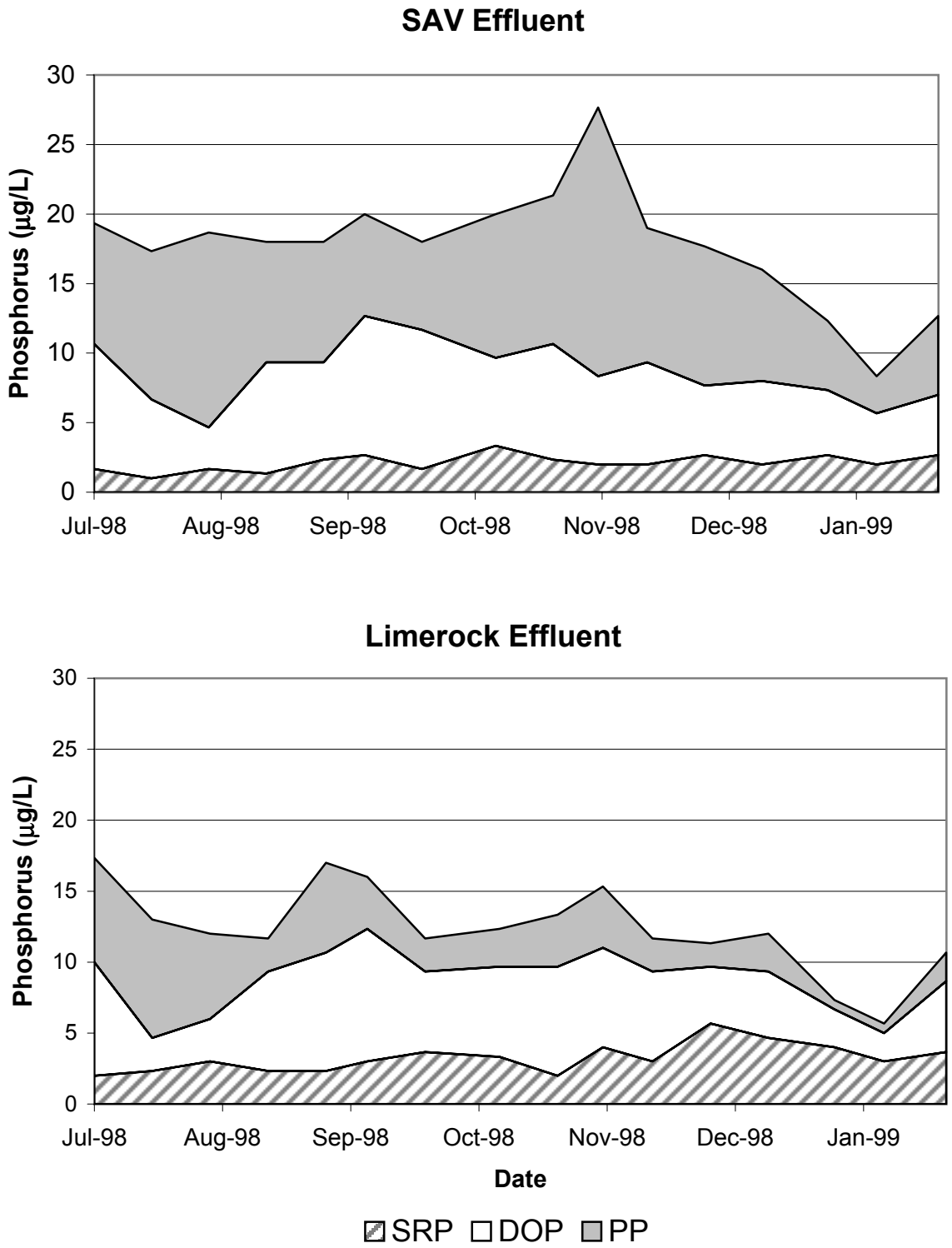

Figure 5.8 Soluble reactive P (SRP), dissolved organic P (DOP) and particulate P (PP) concentrations in the SAV mesocosm effluent (7.0 day HRT) and the effluent from its associated LR bed (5 hr HRT).

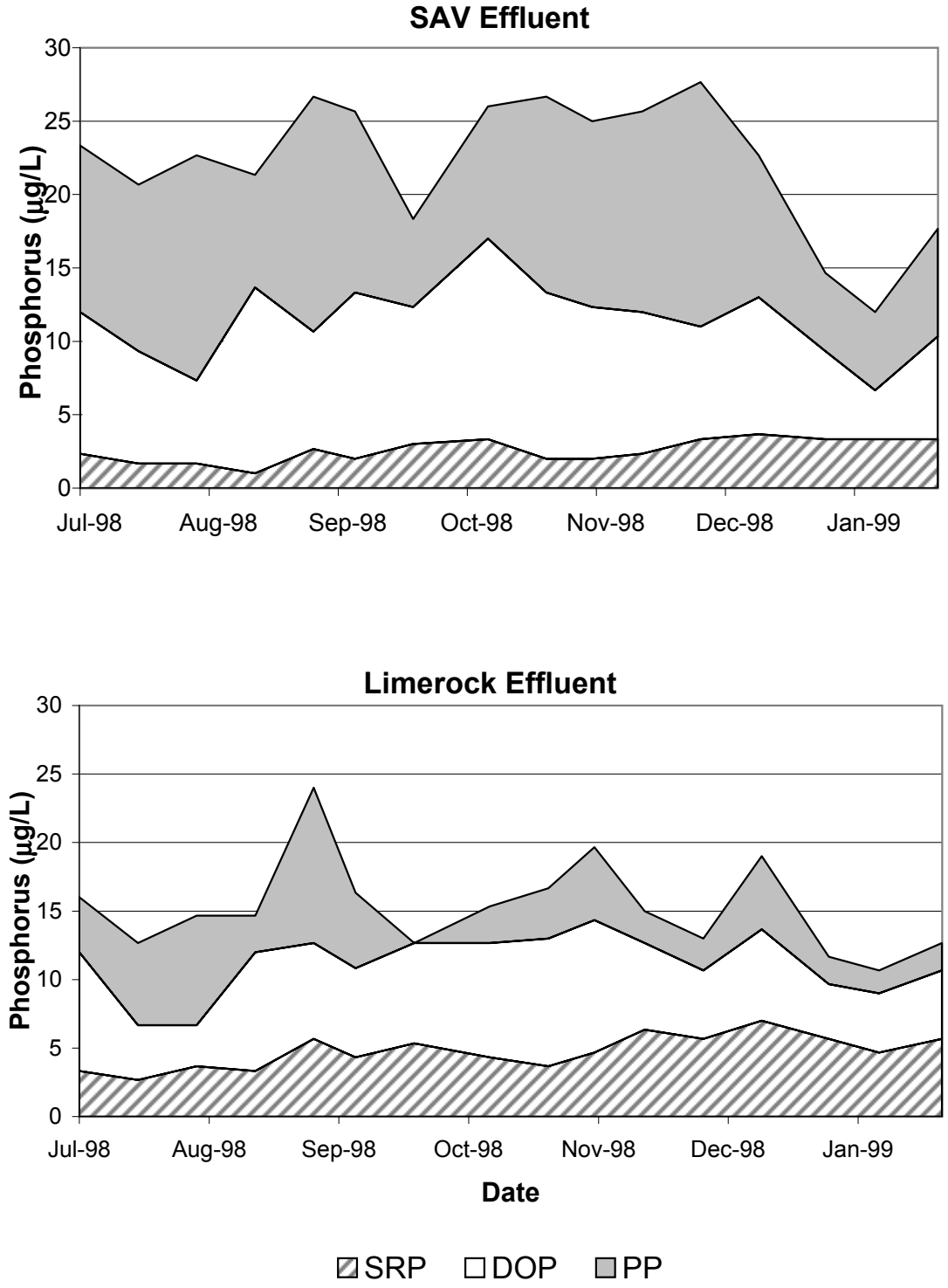

Figure 5.9 Soluble reactive P (SRP), dissolved organic P (DOP) and particulate P (PP) concentrations in the SAV mesocosm effluent (3.5 day HRT) and the effluent from its associated LR bed (5 hr HRT).

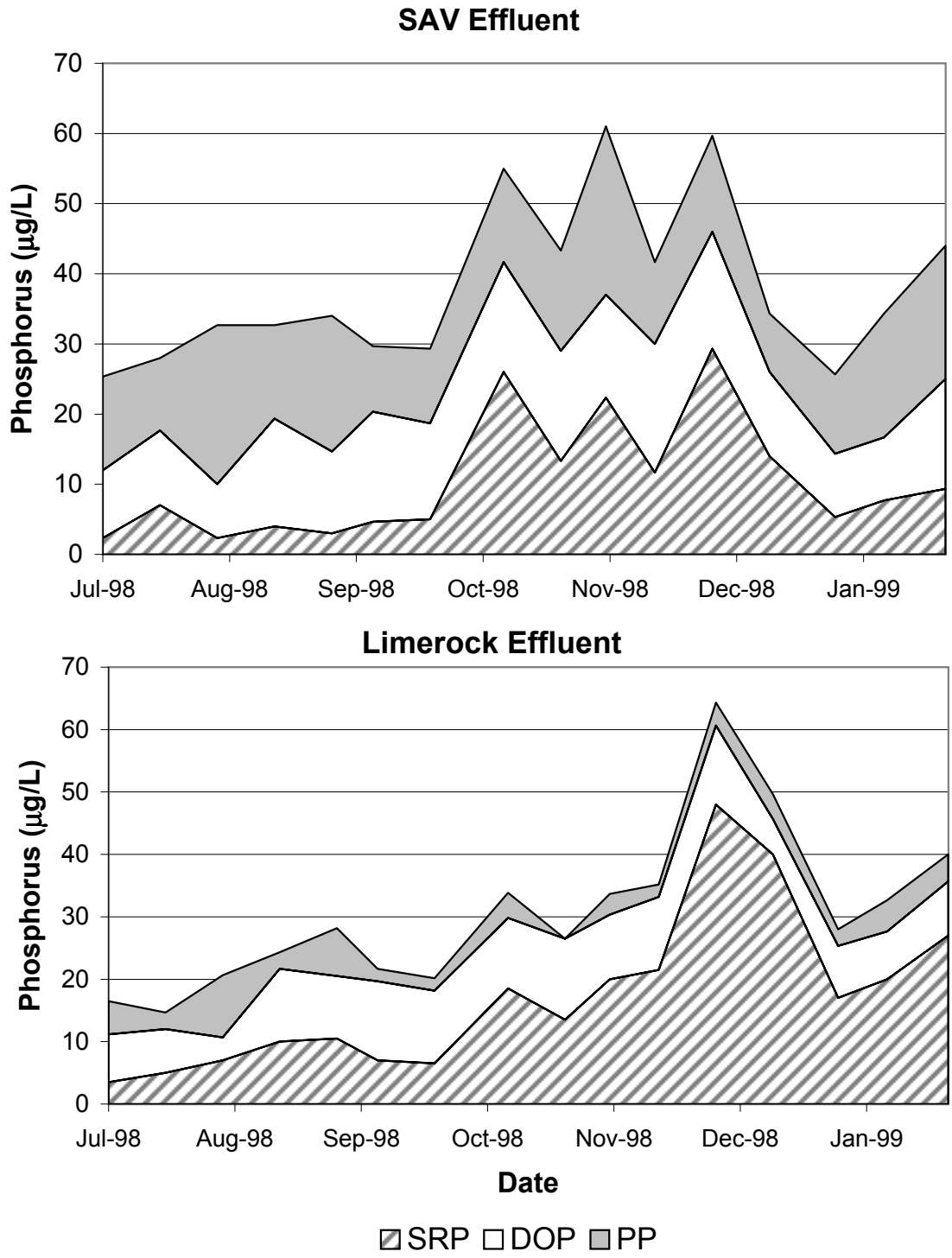

Figure 5.10 Soluble reactive P (SRP), dissolved organic P (DOP) and particulate P (PP) concentrations in the SAV mesocosm effluent (1.5 day HRT) and the effluent from its associated LR bed (5 hr HRT).

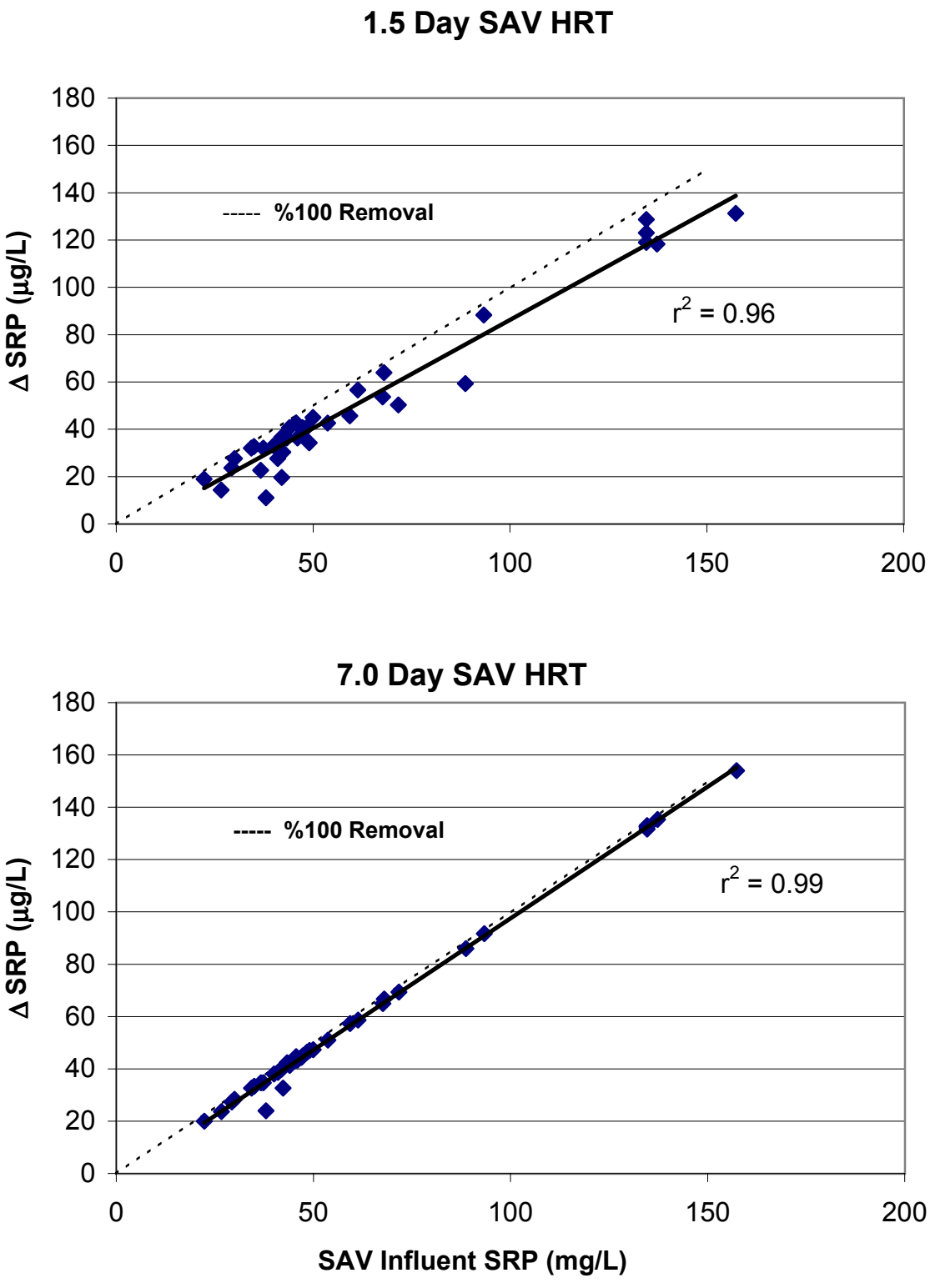

Figure 5.11 Relationship between SAV influent SRP concentration and SRP removal in the 1.5 and 7.0 day HRT SAV mesocosms.

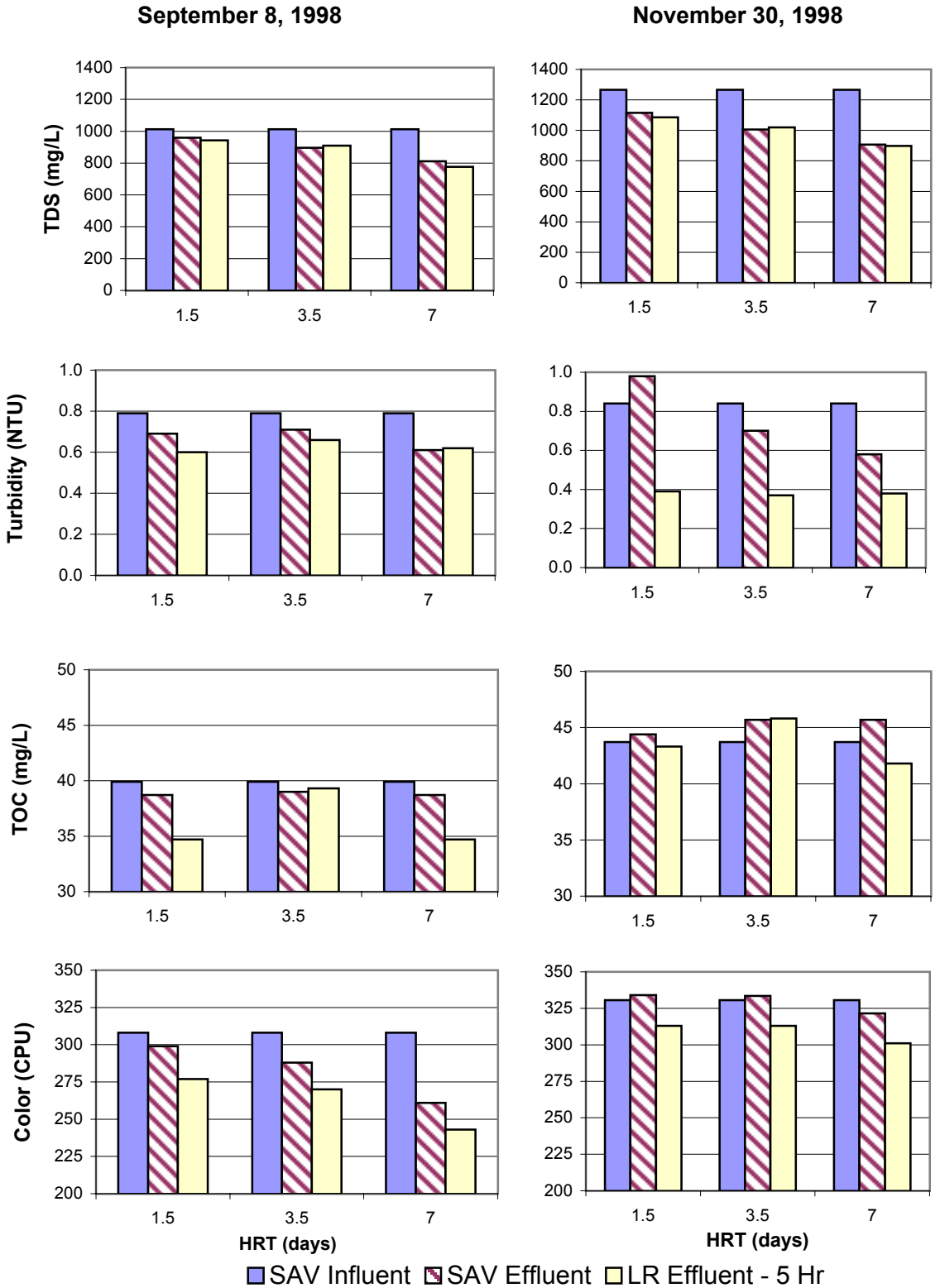

Figure 5.12 Concentrations of TDS, turbidity, TOC and color (n=2) at three locations in the SAV/LR process train on two sampling dates.

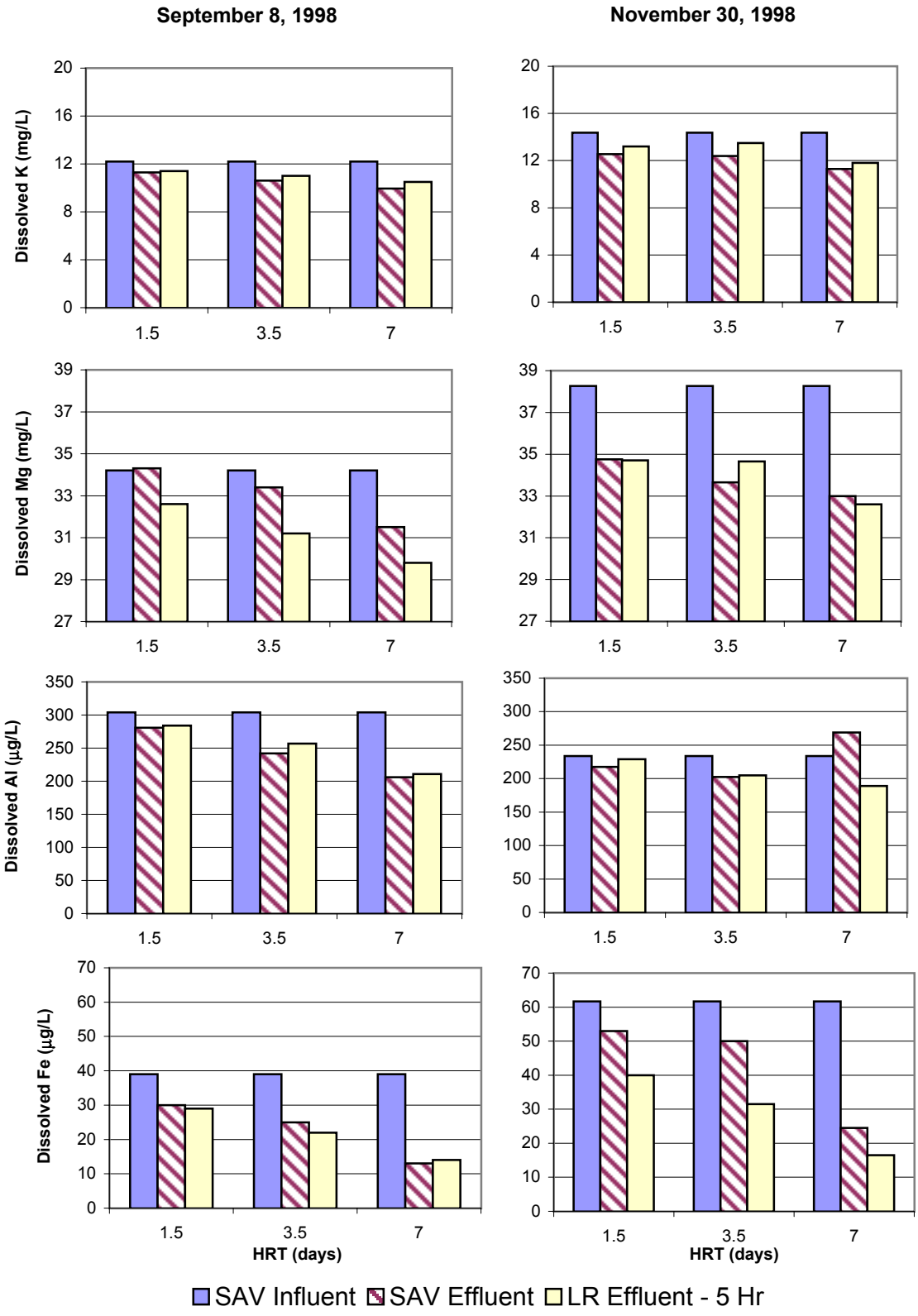

Figure 5.13 Concentrations of dissolved K, Mg, Al, and Fe (n=2) at three locations in the SAV/LR process train on two sampling dates.

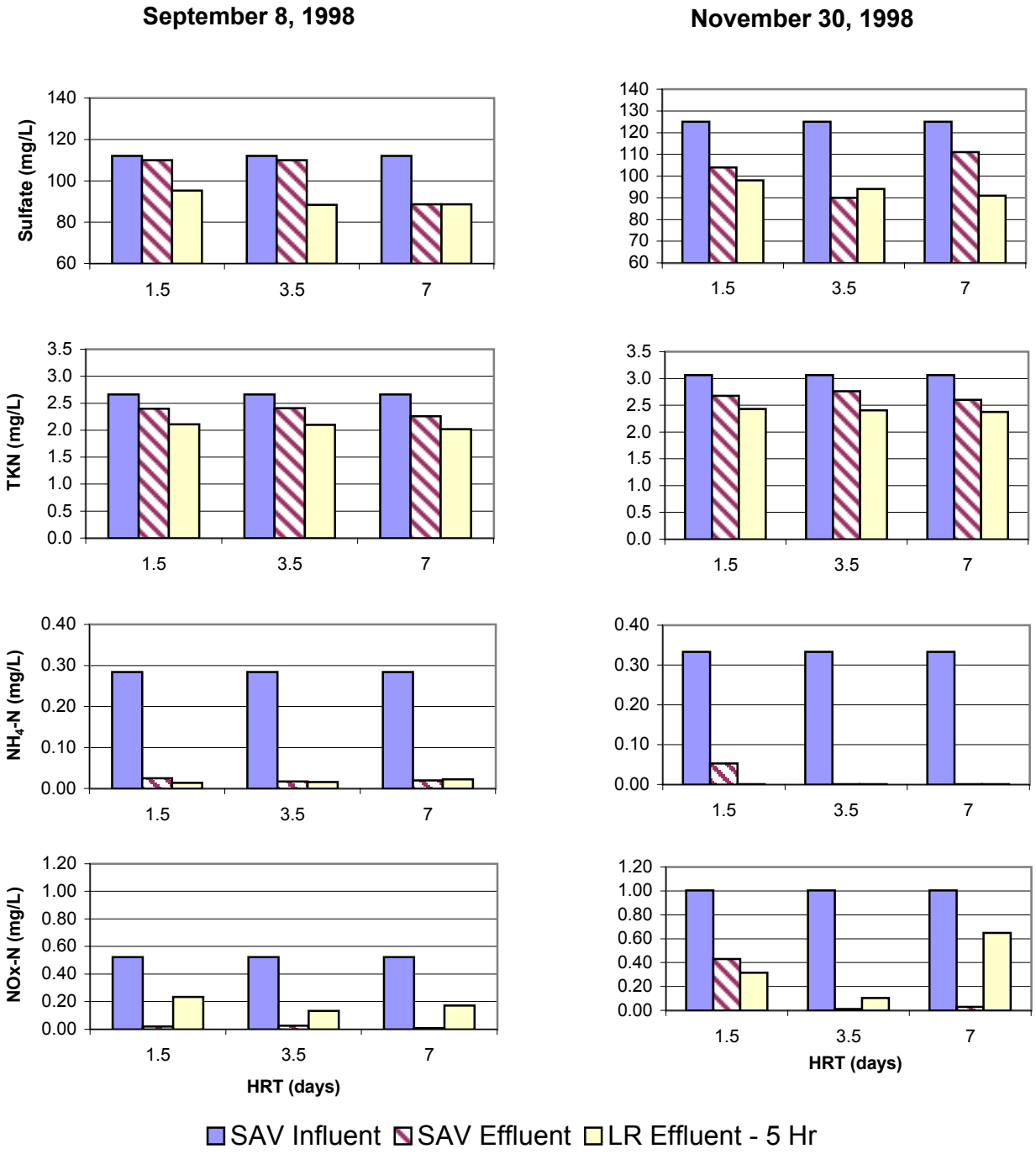

Figure 5.14 Concentrations of sulfate, TKN, NH_4-N and NOx-N (n=2) for three locations in the SAV/LR process train on two sampling dates.

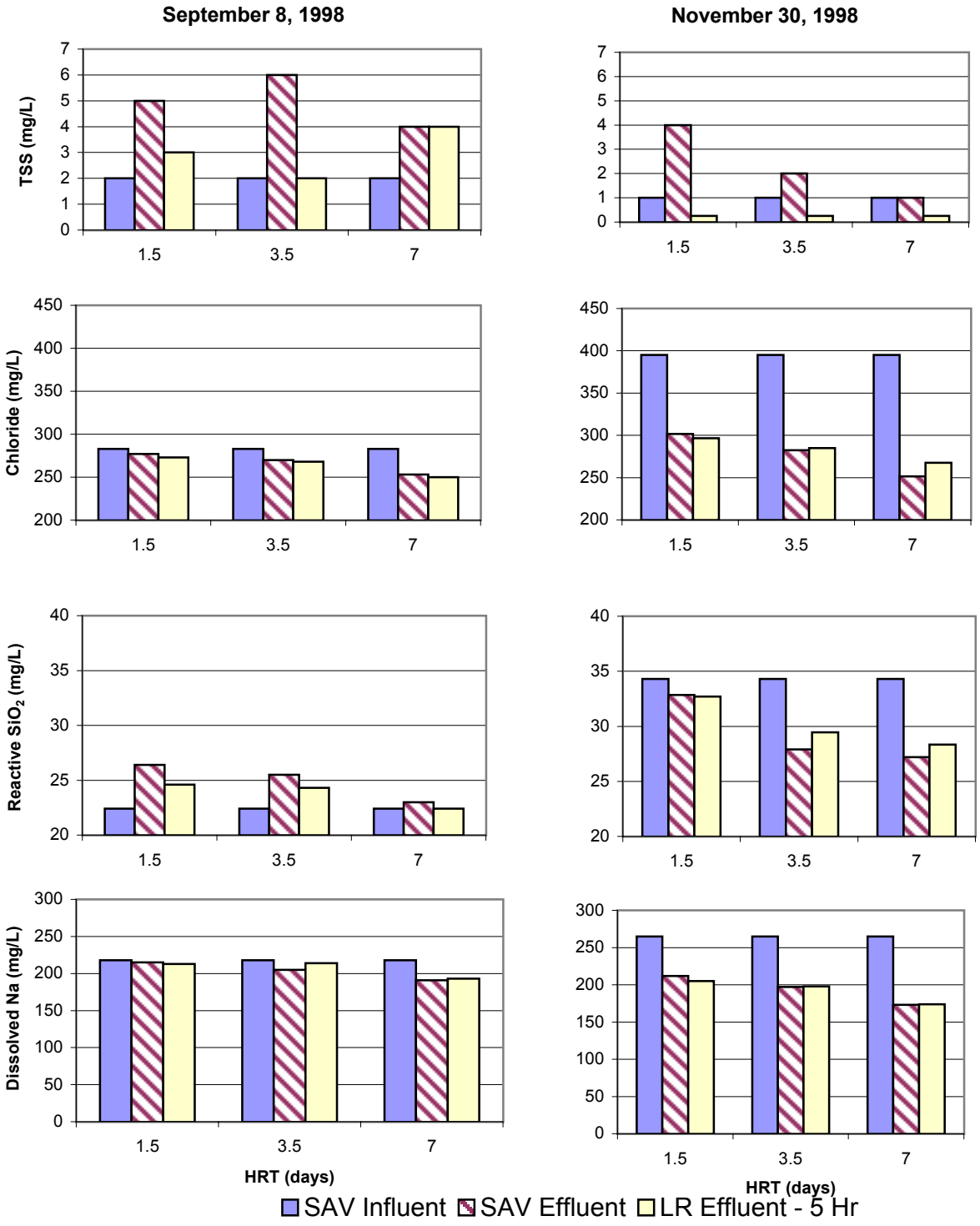

Figure 5.15 Concentrations of TSS, chloride, reactive silica and dissolved Na (n=2) at three locations in SAV/LR process train on two sampling dates.

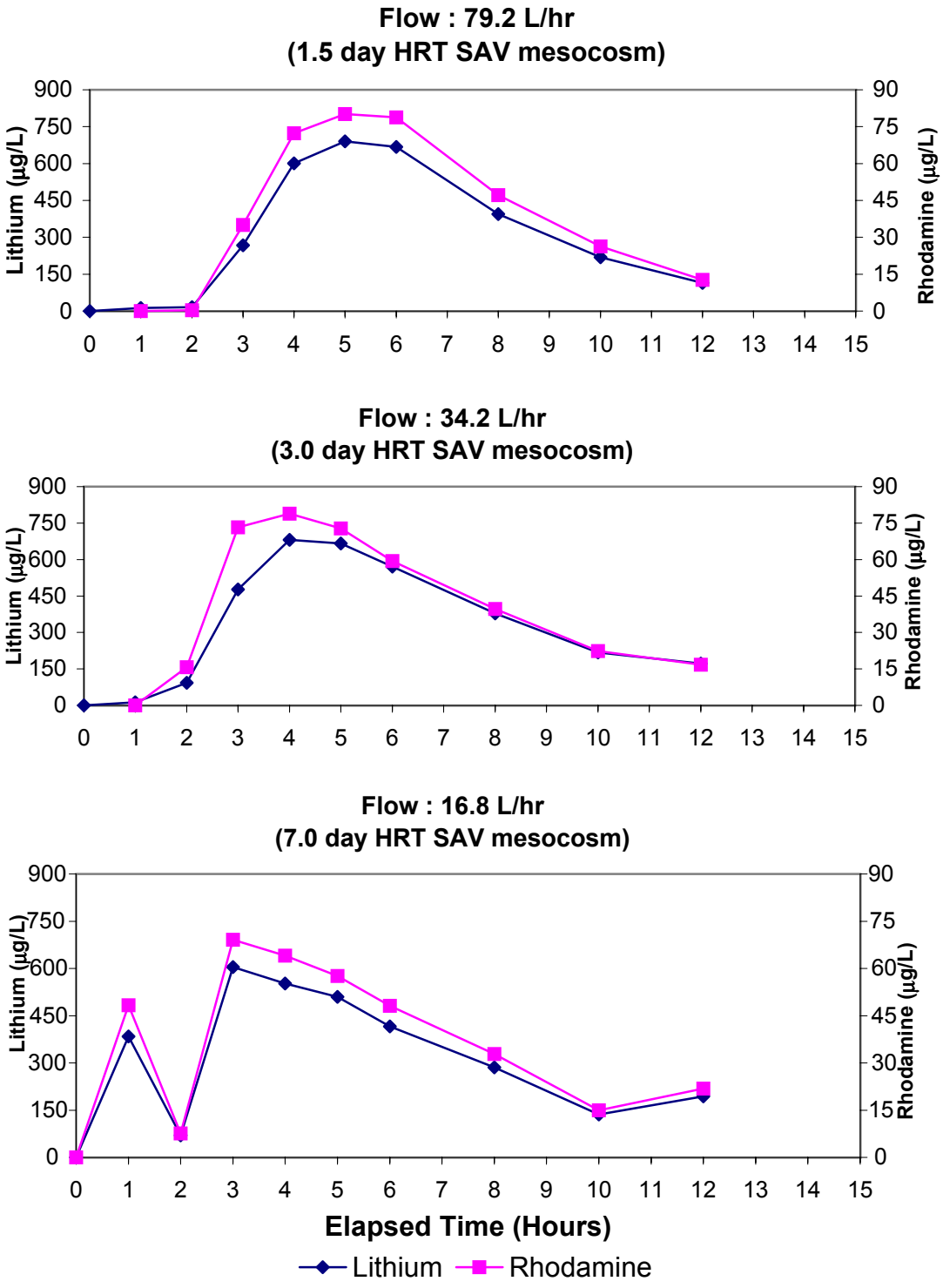

Figure 5.16 Tracer response curves for Rhodamine-WT and lithium applied to upflow limerock barrels at three flow rates. Tracer concentrations represent the means of two limerock barrels per hydraulic loading rate.

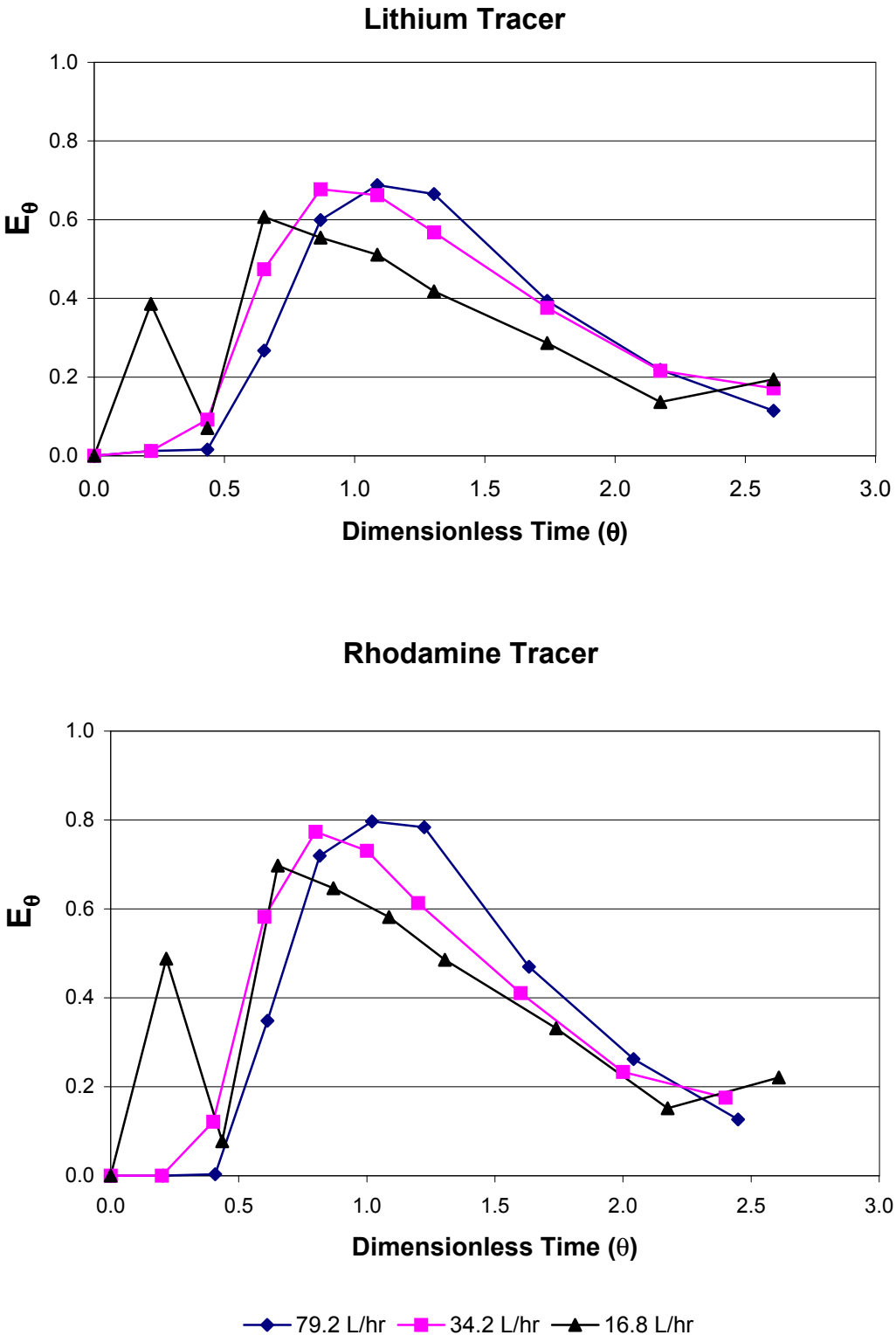

Figure 5.17 Dimensionless residence time distribution for Rhodamine-WT and lithium tracers applied to upflow limerock barrels at three flow rates.

VI. Mesocosm Experiments: Subtask 4D

Subtask 4D. SAV/Limerock Assessment in Low Phosphorus Waters

Methods

At the south site, we tested three SAV/LR configurations for their ability to remove P from the ENR effluent (Post-STA) waters. The first experimental system was a 0.65 m deep mesocosm equipped with a limerock substrate. This system was fed ENR effluent waters at a hydraulic loading rate of 20 cm/day, providing a 3.3 day HRT. This was established as a deep, low velocity system suitable for submerged macrophytes and periphyton.

The second experimental system was a raceway 9 cm deep, equipped with a limerock substrate, and operated at a 0.8 day HRT (Figure 4.8). This also was a low velocity system, but it provided a more intense solar radiation regime and wider temperature fluctuations than the 0.65 m deep mesocosms. The 9 cm deep system was equipped with a limerock bed (1 hr HRT) at the midpoint of the raceway. Effluent from both the 9 cm and 0.65 m deep systems was fed into upflow limerock reactors with a 1 hr HRT.

The final SAV configuration that we investigated was a shallow (2 cm deep), high velocity raceway (Fig. 4.8). High velocity raceways can provide an environment conducive to rapid periphyton growth, and are designed to be routinely harvested. We were interested in investigating the ability of this system to elevate the water column pH, as well as for its P removal performance. This high velocity system received a hydraulic loading of 2.2 – 4.4 m/day, providing a very short HRT (13 - 6.5 minutes). A schematic of these three Post-STA experiments is provided in Fig. 4.4.

During the last two weeks of June 1998, we stocked plants into the 0.65 m deep mesocosms and 9 cm deep raceways. The deep mesocosms (triplicate units for each treatment) received a mixture of *Ceratophyllum* and *Chara* (1.2 kg/m^2 of each species), as well as a smaller amount (0.6 kg/m^2) of *Najas*. The influent halves of the shallow raceways were stocked with *Najas* and *Chara* at 0.08 kg/m^2, and *Ceratophyllum* at 0.24 kg/m^2. The effluent half of the shallow systems received 0.08 kg/m^2 of *Ceratophyllum* and *Najas*, and 0.24 kg/m^2 of *Chara*. We also added 6 L of miscellaneous periphyton collected from WCA-2A to both the deep and shallow systems. In

contrast with the other two systems, we did not directly stock vegetation into the 2 cm deep, high velocity periphyton raceways. We instead relied on algae imported in the influent surface waters to inoculate the bottom and sides of the raceways.

Long-Term Phosphorus Removal Performance

The initial mesocosm and raceway samples for Subtask 4D were collected the first week of July 1998. For the deep mesocosms, water samples were collected at the influent nozzles leading to the tanks, the water surface adjacent to the effluent standpipe, and at the effluent limerock bed sampling port. The final samples were collected on March 2, 1999. The hydraulic loading to the mesocosms was controlled by the aperture size of the influent nozzle and the frequency of pulsed flow from the head tank. For both sets of raceways, flow was controlled solely by the aperture size of the inlet nozzles as water was delivered continuously by gravity flow from the head tank.

Each week, water samples were analyzed for TP and SRP. Temperature and pH measurements were performed in the field at the time of water collection. Every other week beginning August 26, 1998, water samples also were analyzed for TSP, Ca and alkalinity.

Continuous logging temperature probes (On-Set "Optic Stowaway") were provided by the District, and deployed at mid-depth in one deep SAV mesocosm and in the influent, mid-point and effluent regions of one low velocity raceway. A rainfall gauge situated at the site was used to measure rainfall quantity five days per week (Monday through Friday).

Diel Water Quality Characteristics

On two dates (October 1-2, 1998 and January 18-19, 1999), we conducted water sampling to assess the diel variability in effluent quality from the shallow and deep, low velocity systems. Water samples were collected and field measurements (temperature, pH, conductivity and D.O.) were performed at approximately 6 hour intervals over a 24 hour period. All water samples were analyzed for TP, TSP and SRP, and a subset was analyzed for Ca and alkalinity.

General Water Treatment Performance of SAV-LR Systems

On September 10, 1998 and December 7, 1998, we collected samples at SAV influent, SAV effluent and LR effluent stations from two of the three replicate mesocosms and low velocity raceways. These samples were analyzed for the following 16 water quality parameters: total suspended solids (TSS), chloride (Cl), color, dissolved aluminum (Al), dissolved iron (Fe), dissolved magnesium (Mg), turbidity, reactive silica (SiO_2), dissolved potassium (K), dissolved sodium (Na), nitrate + nitrite nitrogen (NO_x), ammonium nitrogen (NH_4), sulfate, total Kjeldahl nitrogen (TKN), total dissolved solids (TDS) and total organic carbon (TOC).

Chemical Characterization of Sediment and Limerock-Associated Phosphorus

Limerock, rather than muck, was used as a substrate for the mesocosms and low velocity raceways. Upon completion of the study in March 1999, we had difficulty in collecting sediments from either system. We attribute this to the low concentration of particulate matter and nutrients in the influent waters, the low standing crop of SAV in the mesocosms, and the high biomass of flocculant periphyton in the low velocity raceways. This flocculant material obscured sediment particles and made it impossible to discriminate between sediments and live periphyton.

The influent region of the shallow raceways was one location where sediments had accumulated in sufficient quantities to sample. In the first and third replicate raceways we collected sediments from adjacent locations immediately within the zone of inflow. Further down-gradient in the shallow raceways there was insufficient sediment to sample, so we elected to perform the P extraction sequence (Table 5.1) on the limerock substrate. Limerock was collected from 6 stations (labeled *head, break, front, within, back, end* in Fig. 4.4*)* along the 44 m length of each of two low velocity, shallow raceways. We also collected limerock from the inflow and outflow sections of two of the mesocosms and their corresponding LR beds.

The *head* station for the low velocity raceways represents an area within 0.3-0.4 m of the point of inflow, which was colonized by filamentous green algae dominated by *Cladophora*. The next downstream location (*break*) corresponds to a transition zone between the green algae typical of the periphyton in the influent region and the blue-green algae (e.g., *Schizothrix, Scytonema*, and *Lyngbya*) dominant in the remainder of the raceway. This point was 1.2 and 3.7 m from the point of inflow in raceways #1 and 3, respectively. The *front, within,* and *back* stations were located

immediately in front, within, and after a small, covered "in line" limerock bed half-way down each raceway. Limerock from the *end* station was collected from near the effluent ends of the 44 m long raceways.

The large size of the limerock (relative to sediment particles) created several difficulties for the extraction sequence. First, it was difficult to obtain a "representative" sample. Second, because of the low P concentrations in the influent waters, we expected to recover only small amounts of P in the extracts. For these reasons, we used larger amounts of limerock substrate and greater extraction volumes. From 7 to 10 rocks weighing ≈ 65 g in the aggregate were placed in 250-mL polyethylene bottles and extracted with 130 ml of the extracting solutions listed in Table 5.1. Other than a slightly more vigorous shaking rate (62 oscillations per minute), the extraction procedure was identical to that used for the SAV sediments in Subtask 4C with the exception that we did not perform initial or residual total P analyses on the limestone rocks. The four sediment samples collected from the influent region of the shallow raceways also were extracted using the analytical procedure described in Table 5.1.

Phosphorus Mass Balances

At the end of the study, only a small amount of sediment had accumulated in the mesocosms and shallow raceways. With the exception of the *head* station at the influent of the shallow raceways, we were unable to collect sufficient sediments for analysis. We therefore used the macrophytes and periphyton as the principal P storage compartments in calculating mass balances on Post-STA waters.

We harvested periphyton from six locations (quadrat size of 0.0465 m^2) along the length of two of the shallow raceways. These were the same locations used for the limerock sampling, except we substituted a station two-thirds down the raceway for the "*within*" station. We measured dry weight standing crop, as well as tissue P content of the harvested biomass. In the mesocosms, we sampled macrophyte biomass (quadrat size of 0.125 m^2) and P composition in influent and effluent regions of two of the mesocosms.

Management and Monitoring of High Velocity Treatment Systems

Shallow, high velocity raceways, such as the ones operated in Subtask 4D, typically

develop a dense growth of algae that attaches to the raceway's bottom and walls. With time, the periphyton attains a high standing crop and begins to "slough" particles into the current. Routine harvesting therefore is required to maintain a rapidly growing standing crop, and to minimize biomass losses due to sloughing.

We divided each high velocity raceway into four sections of equal area: an influent quarter, two mid-quarters, and an effluent quarter. At one to two week intervals, we harvested the algae from each quarter using a 55 L wet/dry vacuum. The harvested slurry was mixed, the volume measured, and a subsample of known volume was collected for analysis of solids content. Elemental composition (C, N and P) of the slurry subsamples was periodically determined. In the days following harvest, algae recolonized the culture surface from holdfasts that were not removed by harvesting.

Results and Discussion

Initial Vegetation Characteristics

Ceratophyllum and *Chara* had tissue P contents higher than that of *Najas* at the time of plant stocking. *Ceratophyllum* had the highest N content, and *Chara* the highest Ca content (Table 6.1). During June and July 1998, we observed that the macrophyte biomass in the 9 cm deep low velocity raceways steadily declined, while the biomass of the benthic and floating periphyton increased. From that time through the duration of the study, macrophytes persisted only in the influent region of these shallow raceways. By contrast, the macrophytes *Chara* and *Najas* persisted in the 0.65 m deep mesocosms, while the periphyton standing crop remained low. The high velocity raceways were not stocked with macrophytes and developed a robust growth of filamentous periphyton after several weeks of water inputs.

Long-Term Phosphorus Removal Performance

From July 1998 through February 1999, influent TP concentrations to the mesocosms ranged from 9 to 32 μg/L, exhibiting an average concentration of 16 μg/L. The mean effluent TP level during this period was slightly lower (14 μg/L) than the influent value (Table 6.2; Fig. 6.1). The limerock beds provided 60% of the overall system P removal, with an average effluent

concentration of 11 μg/L. Differences in mean TP concentration between the SAV effluent and the LR effluent were significant ($P < 0.05$).

The low velocity raceways that were dominated by periphyton proved more effective at TP removal than the mesocosms, with influent and effluent values averaging 17 and 10 μg/L, respectively (Table 6.3; Fig. 6.2). The limerock bed that followed the raceway provided a slight, but not statistically significant ($P > 0.05$) decrease, with a mean effluent concentration of 8 μg/L.

We observed wide variations in water temperatures during the study, particularly in the shallow raceways. Raceway water temperatures often exceeded 38 °C (the maximum range for our temperature probes) in the summer, and on one morning in January the water temperature dropped

Table 6.1. Initial standing crop biomass and elemental composition of submerged vegetation stocked into mesocosms and low velocity raceways.

Treatment	Dry Stocking Weight	TP		TN		TC		Ca	
	(g/m^2)	(mg/kg)	(%)	(mg/kg)	(%)	(mg/kg)	(%)	(mg/kg)	(%)
Mesocosms									
Najas									
mean	50	1240	0.124	17,300	1.73	354,000	35.4	87,000	8.7
s.d.	4	80	0.008	900	0.09	9,000	0.9	11,000	1.1
Ceratophyllum									
mean	84	1950	0.195	21,700	2.17	372,000	37.2	53,000	5.3
s.d.	7	430	0.043	4,400	0.44	16,000	1.6	26,000	2.6
Chara									
mean	128	1960	0.196	14,700	1.47	243,000	24.3	213,000	21.3
s.d.	8	510	0.051	1,500	0.15	12,000	1.2	25,000	2.5
Low Velocity									
Najas									
mean	0.7	1240	0.124	17,300	1.73	354,000	35.4	87,000	8.7
s.d.	1	80	0.008	900	0.09	9,000	0.9	11,000	1.1
Ceratophyllum									
mean	11	1950	0.195	21,700	2.17	372,000	37.2	53,000	5.3
s.d.	1	430	0.043	4,400	0.44	16,000	1.6	26,000	2.6
Chara									
mean	17	1960	0.196	14,700	1.47	243,000	24.3	213,000	21.3
s.d.	1	510	0.051	1,500	0.15	12,000	1.2	25,000	2.5

Table 6.2. Influent and effluent water quality characteristics [mean, (s.d.)] of the SAV mesocosms at the South Supplemental Technology Site. Values in the top panel are based on 35 (TP and SRP) weekly, and 16 (Part. P and DOP) and 14 (Ca and alkalinity) biweekly measurements. Means for total P superscripted with different letters are significantly different (P<0.05).

	SAV Influent	**SAV Effluent**	**Limerock Effluent**
Total P (μg/L)			
mean	16[a]	14[b] (1.4)	11[c] (1.3)
max.	32	32	22
min.	9	6	6
Ca (mg/L)			
mean	60	55 (2.0)	56 (2.6)
max.	76	76	75
min.	48	37	35
Alkalinity (mg/L)			
mean	240	223 (9.3)	222 (8.4)
max.	292	288	284
min.	172	194	160

	SAV Influent	**SAV Effluent**	**Limerock Effluent**
Particulate P (μg/L)			
mean	4	4 (1.6)	3 (1.3)
max.	10	7	5
min.	0	0	1
DOP (μg/L)			
mean	8	6 (1.5)	5 (1.1)
max.	12	14	9
min.	4	1	0
SRP (μg/L)			
mean	4	2 (0.4)	2 (1.8)
max.	7	3	3
min.	1	1	1

Table 6.3. Influent and effluent water quality characteristics [mean, (s.d.)] of the low velocity raceways at the South Supplemental Technology Site. Values in the top panel are based on 36 (total P and SRP) weekly, and 16 (Part. P and DOP) and 14 (Ca and alkalinity) biweekly measurements. Means for total P superscripted with different letters are significantly different (P<0.05).

	SAV Influent	**SAV Effluent**	**Limerock Effluent**
Total P (μg/L)			
Mean	17^{a} (1.5)	10^{b} (1.1)	8^{b} (1.2)
max.	34	26	16
min.	9	2	2
Ca (mg/L)			
Mean	60 (1.9)	56 (1.9)	53 (2.0)
max.	79	74	72
min.	46	40	28
Alkalinity (mg/L)			
Mean	239 (4.9)	226 (6.5)	222 (6.0)
max.	312	284	288
min.	172	148	152

	SAV Influent	**SAV Effluent**	**Limerock Effluent**
Particulate P (μg/L)			
Mean	5 (1.5)	2 (1.4)	2 (1.7)
max.	10	7	5
min.	0	0	0
DOP (μg/L)			
Mean	7 (0.7)	4 (0.9)	4 (0.8)
max.	12	8	8
min.	3	0	0
SRP (μg/L)			
Mean	4 (0.4)	2 (0.8)	2 (0.4)
max.	7	3	3
min.	1	1	1

to 1°C. The deep mesocosms exhibited a narrower temperature range, fluctuating from 35.5°C to 7 °C. Despite these marked seasonal temperature variations, we observed no obvious seasonal effect on P removal performance (Figs. 6.1 and 6.2).

Diel and Spatial Water Quality Characteristics

During October 1998 and January 1999, we performed periodic sampling over 24 hours to determine if the SAV/LR system P removal performance was influenced by diel variations in D.O. and pH. Dissolved oxygen concentrations in both the SAV-dominated mesocosms and the periphyton-dominated raceways exhibited a diel pattern with the highest values (9.6 and 12.1 mg/L for the SAV and periphyton effluents, respectively) occurring during the afternoon (Fig. 6.3). The lowest D.O. concentrations were in the early morning hours: 4.9 and 3.5 mg/L for the SAV and periphyton effluents, respectively (Fig. 6.3). The LR bed effluent D.O. concentrations ranged between the values reported above for the effluents of the mesocosms and raceways (Fig. 6.3). Specific conductance did not vary during the diel cycle nor with passage through the SAV and LR components of the treatment systems (Fig. 6.4).

In contrast to the SAV/LR systems operated on Post-BMP waters, the diel pH variations for these systems receiving Post-STA waters were minimal. The maximum diel pH fluctuation observed was from 7.8 to 8.5, during the October sampling in the low velocity raceways (Fig. 6.5).

The effluent from the SAV mesocosms exhibited minor variability in TP concentrations, but this did not appear related to diel solar radiation or pH changes. The LR beds were fairly effective at further reducing SAV effluent TP levels (Fig. 6.6). The shallow raceways were both more effective and more consistent with respect to diel TP performance. However, unlike the deep SAV-dominated systems, the LR beds contributed little further P removal beyond that provided by the periphyton raceway during the two diel sampling events (Fig. 6.6).

We conducted a final diel sampling on March 2-3, 1999 to better characterize variation in spatial P removal along the length of the low velocity raceways. Samples were collected at mid-afternoon, and again before dawn at six locations in two raceways. Sampling locations are depicted in Fig 6.7 and were the same as those described in the preceding methods section on *Phosphorus Mass Balances.*

During this spatial sampling, SRP concentrations declined immediately downstream of the influent region, and remained low throughout the length of the raceway (Fig. 6.7). The exception was the sampling location just downstream of the mid-point limerock bed, at which slight increases in both SRP and TP were observed at the afternoon sampling. This elevation in P was attributed to contamination from a population of frogs that inhabited the LR bed during the daytime. These frogs may have contributed P-laden wastes to the shallow water column.

We observed a decline in TP concentrations with distance along the length of the low velocity raceways. Total P levels continued to decline past the LR bed at the mid-point of the raceways during both afternoon and pre-dawn samplings, with final effluent concentrations reaching 30 – 44% of influent values (Fig. 6.7).

Phosphorus Speciation During Passage Through SAV/LR Mesocosms and Low Velocity, Periphyton/LR Raceways

Dissolved organic P was the most prominent P fraction in the influent waters fed to the mesocosms and low velocity raceways (Tables 6.2 and 6.3). The SAV mesocosms slightly reduced the DOP and SRP fractions, and the LR bed further reduced PP and DOP (Table 6.2; Fig. 6.8). The low velocity raceway was effective at reducing DOP, SRP and PP fractions. During the latter part of the study when we measured all P fractions, the downstream LR bed provided no additional P removal (Table 6.3; Figs. 6.2 and 6.9).

General Water Quality Characteristics in SAV/LR Mesocosms and Low Velocity, Periphyton/LR Raceways

We sampled a suite of water quality parameters on two occasions to assess their concentration trends with passage through the mesocosms and low velocity raceways (Figs. 6.10 – 6.13). Both color and TOC exhibited a decrease in concentrations during passage through the periphyton raceways and SAV mesocosms (Fig. 6.10). There was a slight increase in Mg in the shallow periphyton raceways on both sampling dates, and dissolved Fe levels slightly increased in both the SAV mesocosms and low velocity, periphyton raceways (Fig. 6.11). Nitrogen also was fairly dynamic: inorganic N species typically declined in both systems, and on December 7, there

was a decline in NH_4-N in the mesocosms that was accompanied by an increase in NO_x-N (Fig. 6.12). Passage through the treatment trains *did not* result in substantial alterations in water quality that were outside the range of values observed in the Post-STA influent waters during the same period of record.

Characterization of Sediment and Limerock-Associated Phosphorus

The P fractionation sequence with which we characterized the newly-deposited sediments at the north, Post-BMP site was only of a limited value with the south site sediments and limerock. This was due to heterogeneity of the collected sediments and low P concentrations in the material associated with the limerock.

The first sediment sample, closest to the point of inflow in one of the low velocity raceways (replicate 1), had a cohesive, clay-like consistency, with a gray-bluish color. The second sample, immediately downstream and adjacent to the first sample location, consisted of unconsolidated particles darker in color. The clay-like zone present in replicate 1 raceway was not observed in the other (replicate 3) low velocity raceway, where only the unconsolidated, darker sediments were found.

The clay-like sediments recovered from one of the raceways had higher concentrations of labile P than the other, darker sediments (Table 6.4). The cohesive material was either produced *in situ*, a result of precipitation of iron oxides and aluminum silicates, possibly under anoxic conditions, or deposited from particle-laden source water resulting from SAV maintenance dredging in the ENR effluent canals. The concentrations of Fe and Al in these sediments resulted in a higher P concentration in this fraction than in the other two unconsolidated sediment samples subjected to P fractionation (Table 6.4). These unconsolidated sediments immediately downstream of the clay-like sediments probably consisted of detrital particles from periphyton senescence, which were deposited under the mat.

Although there was considerable variation in the P fractions among the three sediment samples (Table 6.4), there was some commonality when these values are compared to the sediment fractions from the Post-BMP site (Table 5.8). The Post-STA sediments from the raceways generally had a higher labile P pool, particularly the biogenic and Fe & Al fractions, than the sediments collected from the SAV mesocosms at the north site (Tables 5.8 and 6.4). On a

Table 6.4. Phosphorus fractions for sediment collected near the inflow (*head*) of shallow, low velocity raceways that received Post-STA waters. Fraction A (sum of $CaCO_3$-P, Fe & Al-P, and extractable biogenic-P) represents the labile P pool; fraction B (Ca mineral-P) corresponds to the nonlabile P pool. See text for description of station locations. All units are μg/g dry wt except where otherwise noted.

Fraction		**Low Velocity Raceways**		
		Rep. 1 Head	**Rep. 1 Head (Clay)**	**Rep. 3 Head**
A	**$CaCO_3$-P**	9	414	112
	Fe & Al-P	11	593	142
	Biogenic-P	52	437	336
B	**Ca-mineral-P**	123	524	476
	Residual-P	288	1180	949
	Σ Fraction A	72	1444	590
	Σ Fraction B	411	1704	1425
	Fraction A: % Initial TP	15%	46%	29%
	Fraction B: % Initial TP	85%	54%	71%

percentage basis, the labile P pool for the south site sediments (15-46%) was higher than those collected from the SAV mesocosms at the north site (8-26%).

We hypothesize that most of the particles in the influent region of the shallow raceways were probably produced *in situ* since they were found under the dense periphyton mats. Particulate P concentrations in the influent stream were quite low (Fig. 6.9), and the turbulence of the flow within the influent section of the raceway likely kept any influent-borne particles in suspension long enough to be transported further down the raceway.

Phosphorus fractionations performed on the LR from the raceways and mesocosms were often below analytical detection limits (Table 6.5). Moreover, many of the analyses indicated P concentration that were lower than those of the initial LR, which had not been exposed to the Post-STA influent water. Only the head station (immediately adjacent to the inflow nozzle) of the shallow system exhibited P pools in concentrations consistently greater than those associated with the initial (control) LR.

The Ca-mineral-P was the only P fraction that had concentrations higher than the initial (control) LR for most of the stations (Table 6.5), suggesting that the LR may have some limited irreversible sorptive properties. However, the quantities of P removed within the LR Ca-mineral-P fraction were minute when compared to levels of this fraction in the sediment substrate (Table 6.4).

These data demonstrate that the limerock substrate was not serving as a prominent P sink in the SAV and periphyton systems that received Post-STA waters. This was almost certainly due to the low phosphorus concentrations in the inflow waters to these systems. Additionally, in the shallow raceways, the periphyton at times completely covered the top of the limerock, thereby shielding the underlying substrate from particulate or dissolved P inputs.

Phosphorus Mass Balances

Despite the shallow water depth, the dry weight standing crop of periphyton in the low velocity raceways was substantially higher (area-weighted mean of 867 g/m^2) than that of the macrophytes in the mesocosms (54, 21 and 116 g/m^2 for *Najas, Ceratophyllum* and *Chara,* respectively) (Table 6.6). The periphyton collected at the 'head" of the shallow raceways contained a high tissue P content, but tissue P levels decreased dramatically at the "break" location and remained low for the length of the raceway (Table 6.6). We obtained close agreement between the

Table 6.5 . Phosphorus fractions for limerock collected from low velocity raceways and SAV/LR mesocosms that received Post-STA waters. Fraction A (sum of $CaCO_3$-P, Fe & Al-P, and extractable biogenic-P) represents the labile P pool; fraction B (Ca mineral-P and residual-P) corresponds to the nonlabile P pool. See text for description of station locations. Initial LR = 'unexposed' limerock which originated from the same batch that was stocked into the treatment systems. All units are μg/g dry wt except where otherwise noted. n.d. = not determined. "T" signifies the value is less than the MDL.

Fraction		Low Velocity Raceways						SAV/LR Mesocosms			Initial LR
		Head	Break	Front	Within Bed	Back	End	In	Out	LR Barrel	
A	**$CaCO_3$-P**	0.15	0.02	0.06	0.10	0.06	0.04	0.06	0.08	0.07	0.07
	Fe & Al-P	0.05	0.02	0.01T	0.01T	0.04	0.01T	0.02	0.01T	0.01T	0.01T
	Biogenic-P	0.25	0.08	0.02T	0.02T	0.22	0.02T	0.37	0.32	0.02T	0.02T
B	**Ca-mineral-P**	0.72	1.1	0.81	1.9	0.60	0.89	0.99	2.0	1.3	0.79
	Residual-P	n.d.	n.d.	n.d.	n.d.	n.d.	n.d.	n.d.	n.d.	n.d.	n.d.
	Σ Fraction A	0.45	0.12	0.09	0.13	0.32	0.07	0.45	0.41	0.10	0.10
	Σ Fraction B	0.72	1.1	0.81	1.9	0.60	0.89	0.99	2.0	1.3	0.79
	Fraction A: % TP	38%	10%	10%	6%	35%	7%	31%	17%	7%	11%
	Fraction B: % TP	62%	90%	90%	94%	65%	93%	69%	83%	93%	89%

Table 6.6. Dry weight standing crop biomass and P composition for macrophytes from mesocosms and periphyton from the low velocity raceways.

Treatment	Dry Weight (g/m^2)				TP Concentration (mg/kg)				Mass TP (mg/m^2)			
	Rep 1	Rep 2	Mean	s.d.	Rep 1	Rep 2	Mean	s.d.	Rep 1	Rep 2	Mean	s.d.
SAV Mesocosms												
Chara In	144	98	121	32.5	391	768	579	266.6	56.3	75.3	65.8	13.4
Out	67	154	110	61.5	369	707	538	239.0	24.7	108.9	66.8	59.5
Mean	106	126	**116**		380	738	**559**		**40.5**	**92.1**	**65.3**	
Najas In	24	93	58	48.8	549	648	599	70.0	13.2	60.3	36.7	33.3
Out	43	57	50	9.9	519	870	695	248.2	22.3	49.6	35.9	19.3
Mean	34	75	**54**		534	759	**647**		**17.7**	**54.9**	**36.3**	
Utricularia Out	1.6		0.8		703				1.1			
Ceratophyllum In		42	21			857	**429**			36.0	**18.0**	
Out		45	23			618	**309**			27.8	**13.9**	
Mean		43	**21**			738	**369**			31.9	**15.9**	
Low Velocity Raceways												
Head	675	551	613	87.7	720	1470	1095	530.3	486	810	648	229.1
Break	1557	1260	1409	210.0	600	362	481	168.3	934	456	695	338.0
Front LR Bed	632	985	809	249.6	308	222	265	60.8	195	219	207	17.0
Back LR Bed	763	708	735	38.9	212	285	249	51.6	162	202	182	28.3
Two-thirds	913	785	849	90.5	196	165	181	21.9	179	130	155	34.6
End	1366	1022	1194	243.2	242	175	209	47.4	331	179	255	107.5
Mean	984	885	**935**		380	447	**413**		381	333	**357**	

two replicate low velocity raceways in periphyton standing crops, tissue P concentrations, and mass P storages (Table 6.6).

Due both to higher standing crop biomass and tissue P levels, the mass of P stored in the plant tissues was higher in the third than the first SAV mesocosm (Table 6.6). Biomass and TP concentrations differences between the inflow and outflow halves of the mesocosms exhibited no clear pattern (Table 6.6). Of the three dominant macrophytes, *Ceratophyllum* had the highest tissue P content, followed by *Najas* and *Chara*. Although *Utricularia* had been inoculated into the SAV mesocosms, only a minute amount persisted until the end of the study.

For the mesocosms, we found a net reduction in P storage in the macrophyte community during the study, since the final P standing crop was lower than that of the initial mass of vegetation stocked (Table 6.7). By contrast, on an inflow – outflow basis, we found a net removal of 87 mg P/m^2 from the water in the deep mesocosms during this period. We feel that the "missing" P clearly is bound to sediment particles that have settled between and on the limerock substrate. However, we had no means of sampling this material without completely disassembling the tank.

Table 6.7. Mass balance comparing the P stored in the SAV and periphyton biomass in the mesocosms and low velocity raceways, respectively, with the P removal from the Post-STA inflows. All units are mg P/m^2 unless otherwise noted.

	SAV Mesocosms			**Low Velocity Raceways**		
	Rep 1	Rep 2	Mean (s.d.)	Rep 1	Rep 2	Mean (s.d.)
Final Plant Storage	58	179	119 (85.6)	222	237	229 (10.6)
Initial Plant Stock	478	478	478	64	64	64
Net Plant Storage	-420	-299	-359	158	173	165
Input-Output (water)	87	87	87	171	171	171
% Recovered in biomass	0	0	0	92	101	97

The mass balance for the shallow, periphyton-dominated raceway was more successful. We observed an average accumulation of 165 mg P/m^2 in the periphyton community (after subtracting the P in the vegetation originally stocked). On an inflow – outflow basis, we observed that 171 mg

P/m^2 was removed from the water during the study. The periphyton storage therefore accounted for a mean of 97% of the observed P removal from the water (Table 6.7).

We ignored atmospheric P inputs for the mass balances performed at the north and south project sites. Estimates for rainfall + dryfall P input rates vary widely, but other investigators have used values in the range of 50 mg P/m^2 –yr (Walker, 1995). The low mass P storages and removal rates at the south site suggest that atmospheric P inputs may need to be addressed for rigorous mass balance purposes.

Performance of High-Velocity Periphyton Systems

The high velocity raceways reduced TP concentrations from an average of 17 to only 14 μg/L (Fig. 6.14). Although small, this difference was statistically significant ($P < 0.05$). During passage through the raceway, the daytime pH of the water was elevated from an average of 7.80 (range of 7.55 – 8.06) to 8.35 (range of 7.78 – 8.81).

We have established and monitored several other high-velocity periphyton systems during the past five years, and it has been our experience that routine water quality monitoring techniques may not adequately characterize P removal performance. One problem is the rapid flow rate, which in the present study resulted in a HRT of only 6.5 – 13 minutes. At this high hydraulic loading (2.2 – 4.4 m/day), we observed only minimal P concentration reductions. A second problem is intermittent algal sloughing, which results in a semi-continuous release of organic particulate matter. Collection of grab samples that accurately represents the average effluent quality therefore is difficult. Water sampling of the high velocity systems is useful, however, in that it can pinpoint potential growth limiting nutrients (e.g., SRP) to the plant standing crop.

For purposes of defining total P mass removal performance, we prefer using direct measurements of periphyton standing crop. Like water sampling, periphyton sampling is subject to the errors created by periodic algal sloughing, but based on our prior experience with high velocity systems, we believe P accrual in recoverable biomass provides the most accurate metric of overall system mass P removal.

Despite the high hydraulic and P loadings (2.2 m/day and 37 mg P/m^2-day) there was a prominent gradient in periphyton growth on the raceway bottom and side walls, with highest biomass production occurring in the influent region (Fig. 6.15). Dry matter productivity averaged

3.8 g/m^2-day for the entire length of the raceways, but ranged from 5.9 g/m^2-day in the first quarter of the raceways, to 2.4 g/m^2-day in the effluent regions. Periodic measurements of nutrient content also demonstrated a marked tissue P concentration gradient for the periphyton, from a high of 1201 mg/kg in the first quarter to 764 mg/kg in the effluent quarter (Fig. 6.15). The N gradient down the length of the culture surface was less pronounced, ranging from 17,300 to 13,200 mg/kg.

The P removal performance of our high velocity system was markedly poorer than that of a high velocity periphyton system previously tested on a sugar cane farm near Belle Glade (Adey et al, 1993). The "Belle Glade" system received canal waters with mean TP and SRP contents of 53 and 18 μg/L, respectively. The periphyton raceway produced effluent TP and SRP levels of 44 and 1 μg/L, respectively, and provided a P mass removal rate (based on algal uptake) of 45 g P/m^2-yr. Mass P removal performance of our system at the south site, based on biomass P recovery, was 1.4 g P/m^2-yr, or only 3% of the rate achieved by the Belle Glade system on higher nutrient sugar cane canal water.

The overall low productivity of the periphyton in our high velocity system, coupled with the decline in growth rates and P content down the length of the culture surface, suggests that SRP levels in the influent waters are the master factor that controls productivity and P removal performance. Indeed, based on influent and effluent data, the Belle Glade periphyton system appeared to strip all of the SRP from the canal water, and exported either particulate P or DOP. Despite an obvious P limitation of growth, our high velocity system removed P at a rate four times higher (on a mass per unit area basis) than the low velocity system. For a full-scale periphyton-based treatment system, this increase in mass removal performance would need to be balanced by the costs and benefits of routine biomass management.

Performance Comparison of Three Treatment Systems for Post-STA Waters

No investigations on wetland treatment of Post-STA waters had been conducted prior to this study. One goal of our work at the South Supplemental Technology Site therefore was to assess how a diverse array of treatment configurations would perform with respect to removing TP and elevating the water column pH. In two of the three configurations, we also tested the effectiveness of an upflow limerock bed as a final polishing step.

Among the three biological treatment systems, the low velocity periphyton system provided the best P removal performance with respect to effluent quality, although the mass P removal rate was not overly high (Table 6.8). In terms of both final effluent TP concentration and mass P removal rate, the SAV was not as effective as the periphyton (Table 6.8). In contrast with the periphyton, which thrived on the limerock used as a bottom substrate, SAV growth on the limerock in the mesocosms was poor, presumably because of inadequate nutrition. The high velocity (routinely harvested) periphyton provided the highest mass P removal rate, but at the high HLRs used in this system it was not effective at providing low effluent TP concentrations (Table 6.8).

Daytime pH elevations in the biological systems at this site were not as pronounced as those observed at the North Supplemental Technology Site, probably because of the reduced photosynthetic activity in the Post-STA waters. Despite the absence of SRP in the feedwaters to the final limerock beds, these unit processes did provide some P removal, primarily acting as a physical filter for particulate P.

Table 6.8 A comparison of the P removal performance of the SAV mesocosms and the low and high velocity periphyton raceways at the South Supplemental Technology Site. Within column means for TP followed by the same letter are not significantly different (P > 0.05).

Treatment	HLR (cm/d)	HRT	Depth (m)	Total Phosphorus (µg/L)			Mass Removal Rate ($g/m^2 \cdot yr$)
				Influent	SAV/ Periphyton Effluent	Limerock Effluent	
SAV	20	3.3 d	0.65	16	14[a]	11	0.15
Periphyton, Low Velocity	11	0.8 d	0.09	17	10[b]	8	0.29
Periphyton, High Velocity	220 - 440	6.5 - 13 min	0.02	17	14[a]	-	1.4[1]

1 - mass removal rate based on biomass accumulation and harvest

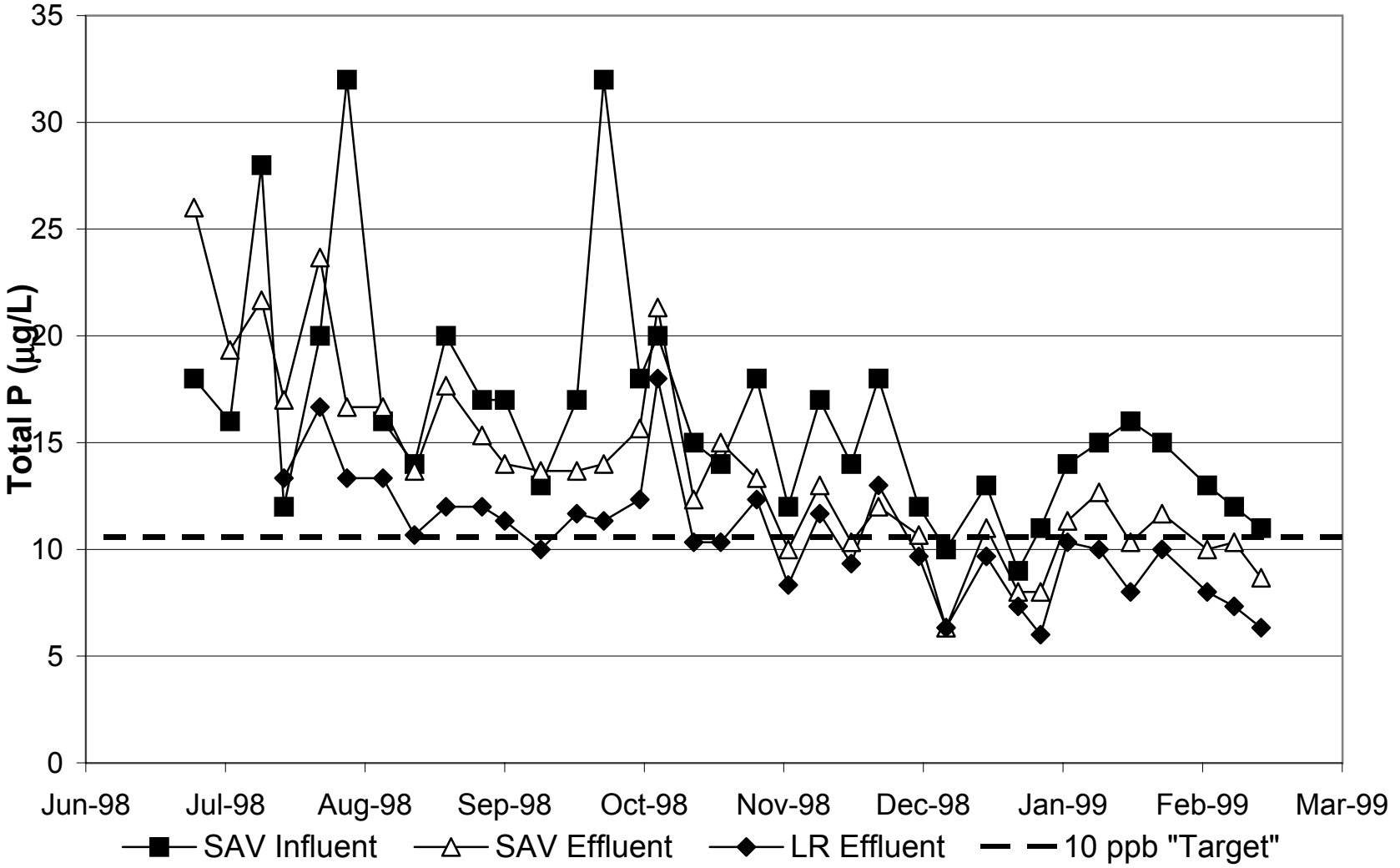

Figure 6.1 Mean total P concentrations (n=3) for three locations in the SAV mesocosm-LR process train. The 10 ppb "target" represents the tentative effluent target (i.e., "threshold level") for protection of the Everglades.

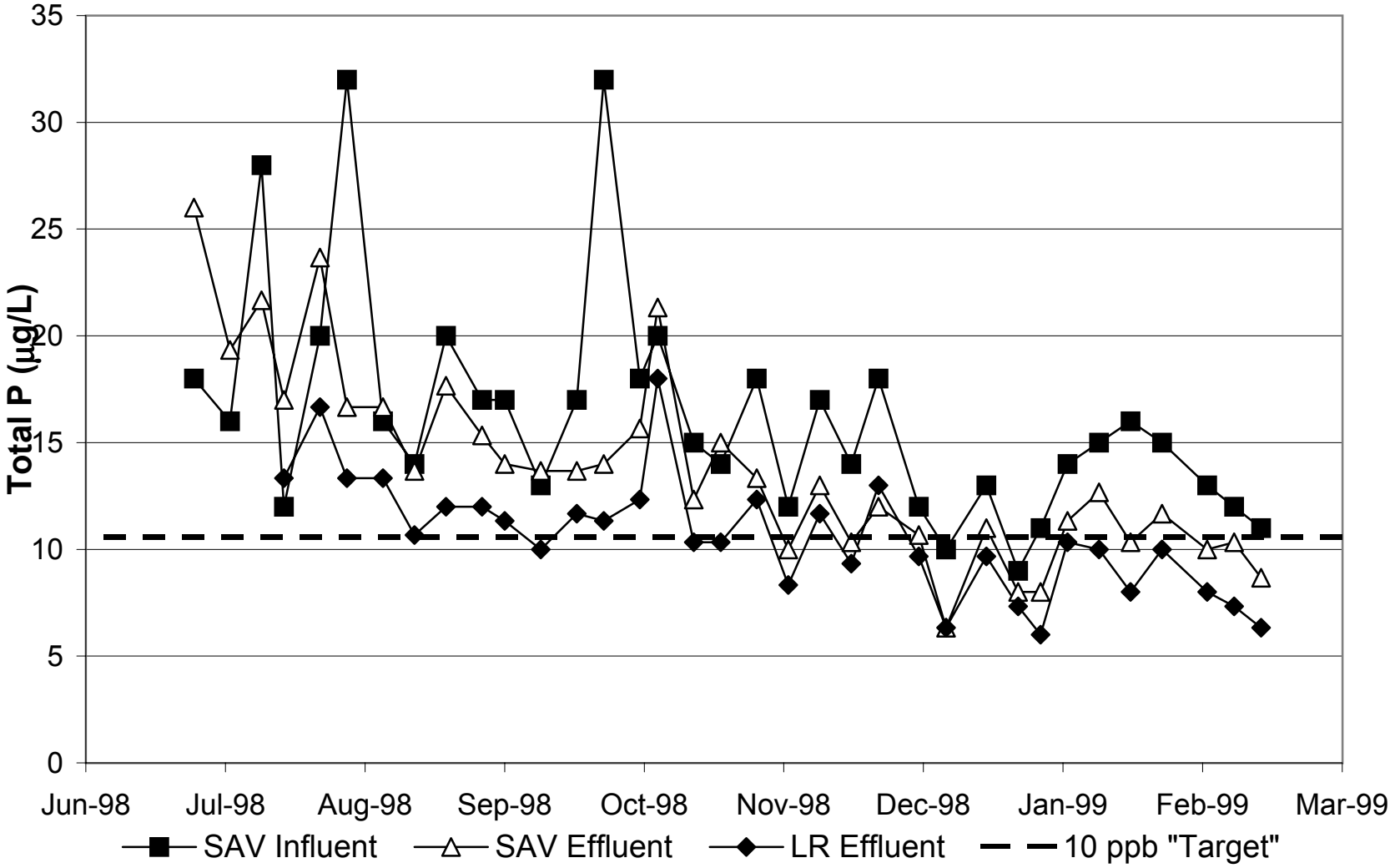

Figure 6.1 Mean total P concentrations (n=3) for three locations in the SAV mesocosm-LR process train. The 10 ppb "target" represents the tentative effluent target (i.e., "threshold level") for protection of the Everglades.

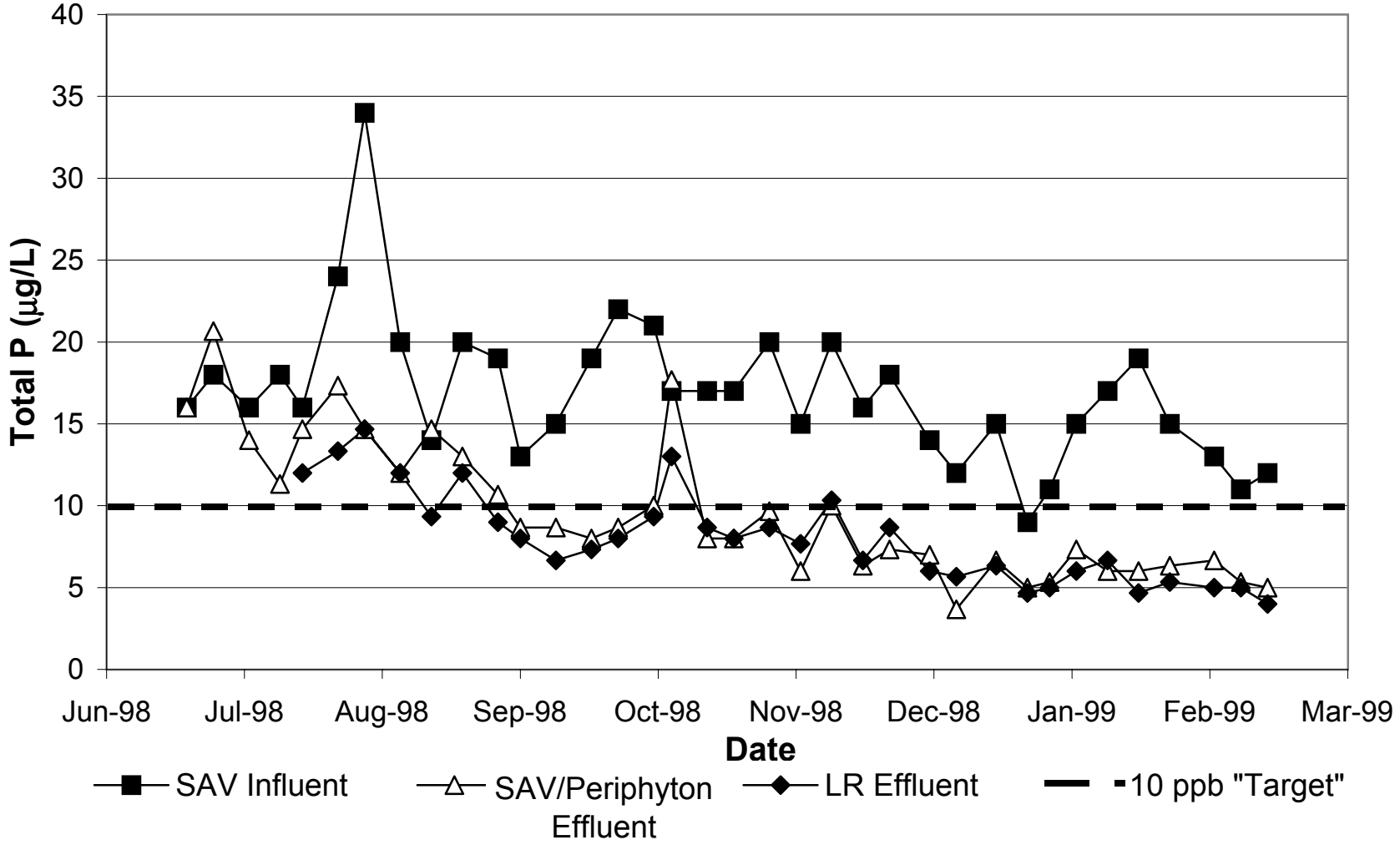

Figure 6.2 Total P concentrations (n=3) for three locations in the low velocity raceways. The 10 ppb "Target" represents the tentative effluent target (i.e., "threshold level") for protection of the Everglades.

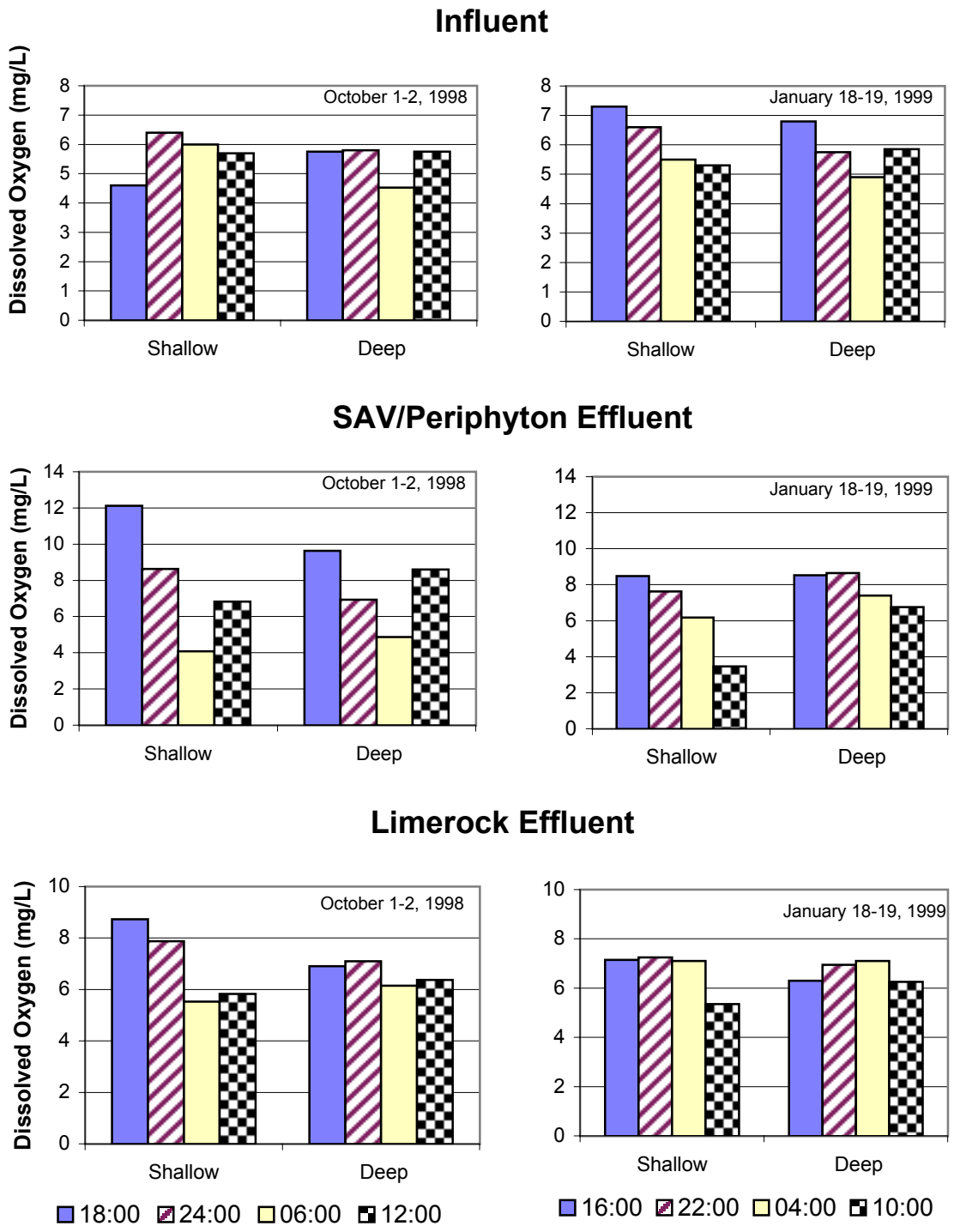

Figure 6.3 Diel dissolved oxygen concentrations at three locations in the low velocity shallow raceways (0.8 day HRT) and the deep SAV mesocosms (3.3 day HRT) on October 1-2, 1998 and January 18-19, 1999.

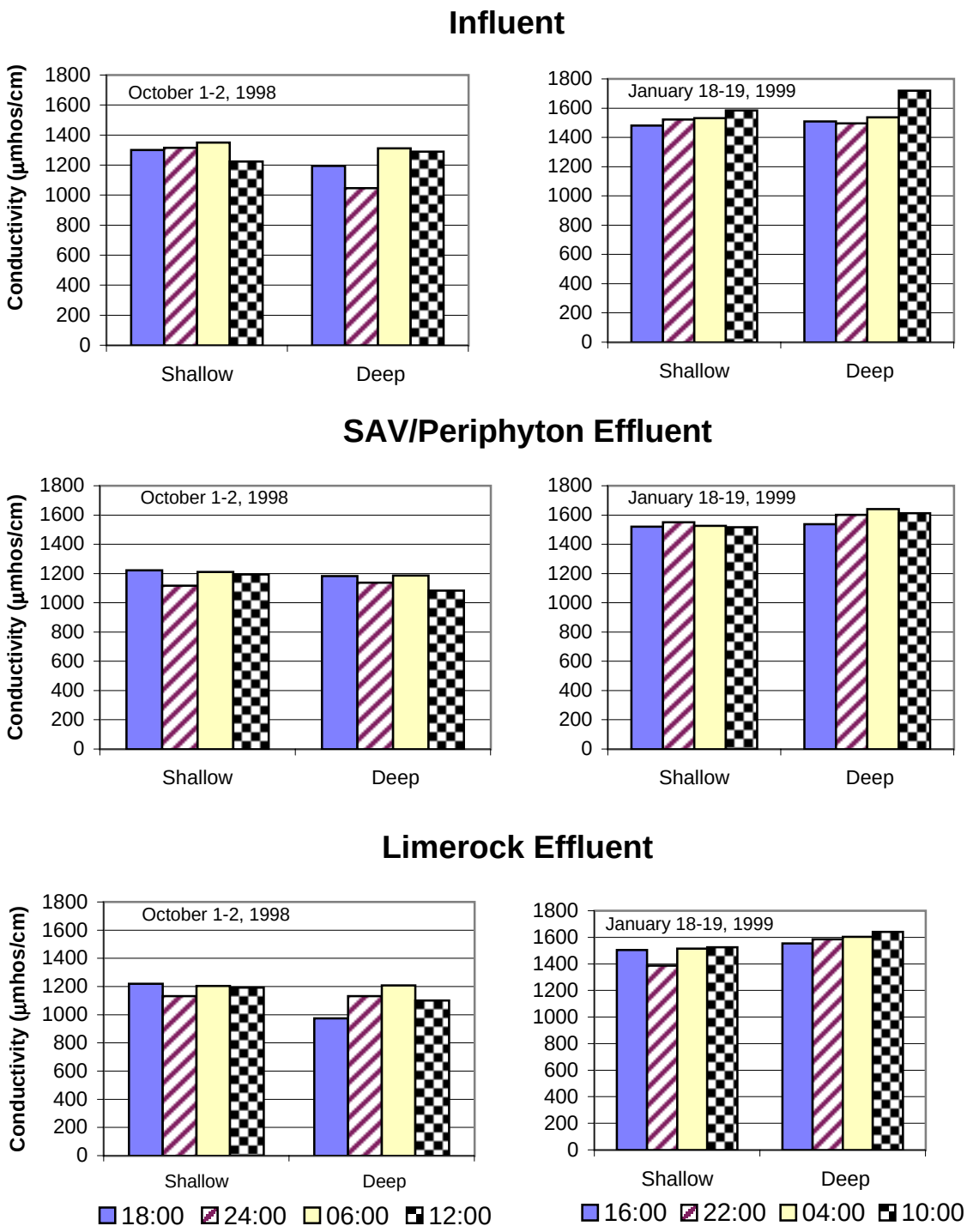

Figure 6.4 Diel conductivity levels at three locations in the low velocity shallow raceways (0.8 day HRT) and the deep SAV mesocosms (3.3 day HRT) on October 1-2, 1998 and January 18-19, 1999.

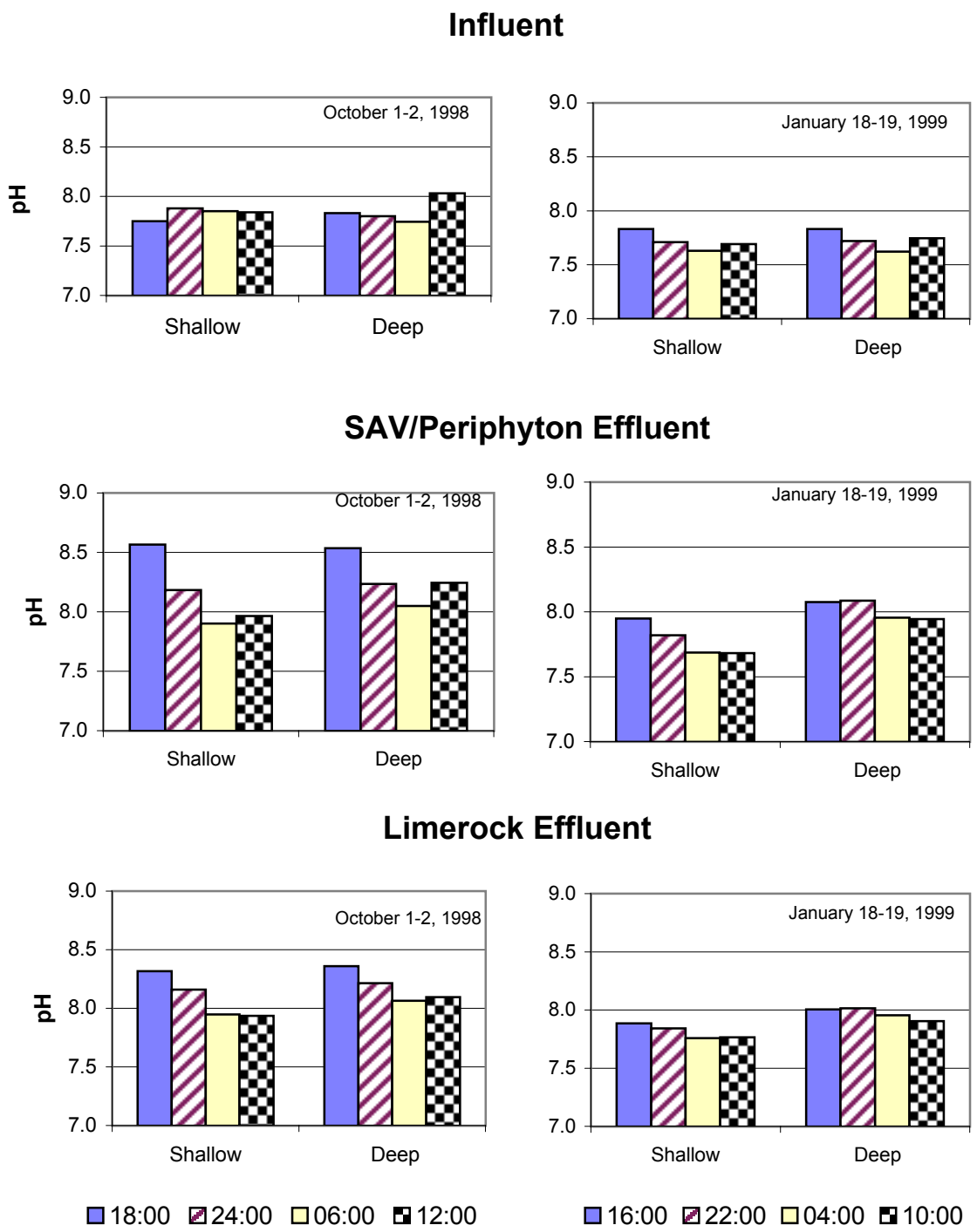

Figure 6.5 Diel pH levels at three locations in the low velocity shallow raceways (0.8 day HRT) and the deep SAV mesocosms (3.3 day HRT) on October 1-2, 1998 and January 18-19, 1999.

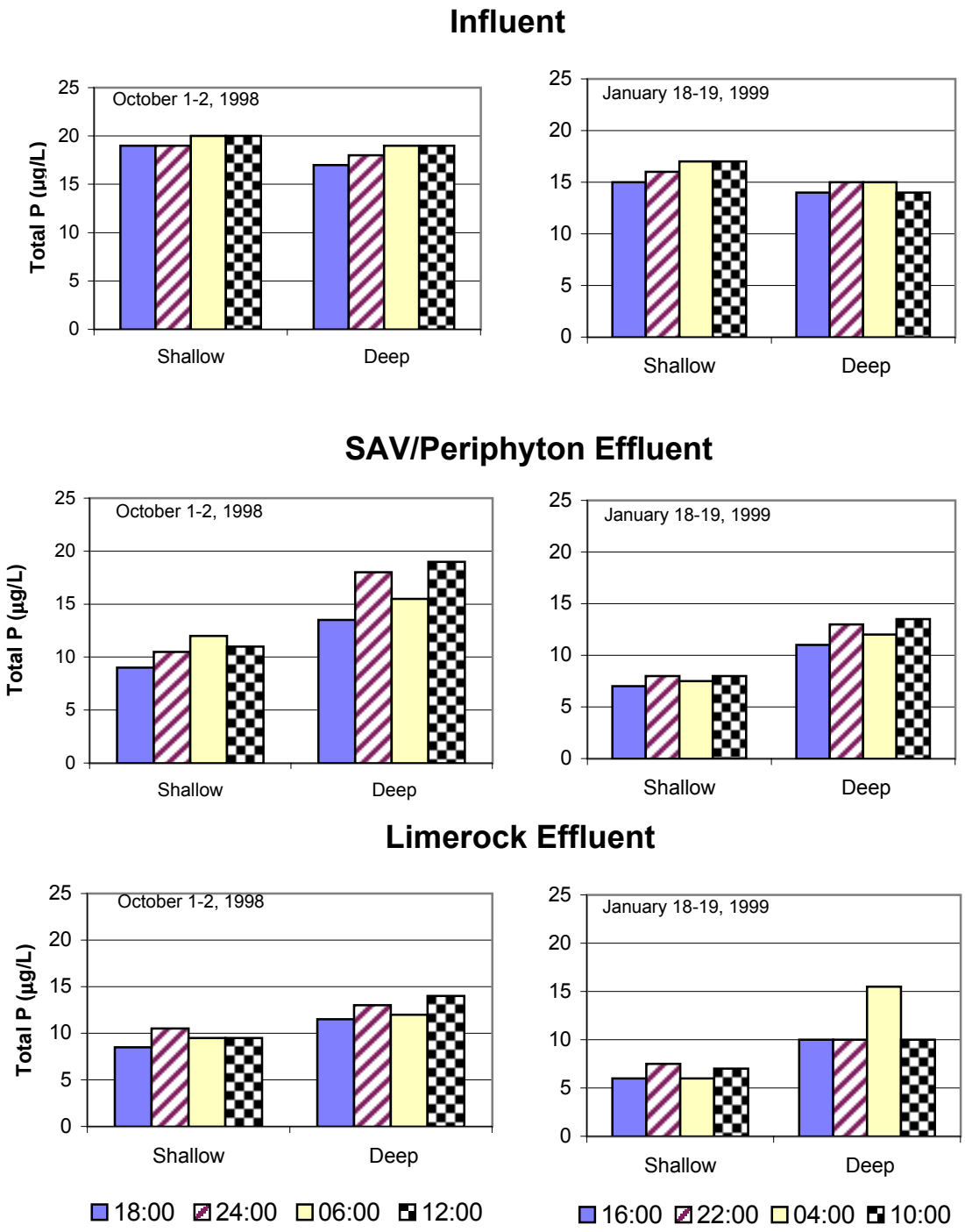

Figure 6.6 Diel total P concentrations at three locations in the low velocity shallow raceways (0.8 day HRT) and the deep SAV mesocosms (3.3 day HRT) on October 1-2, 1998 and January 18-19, 1999.

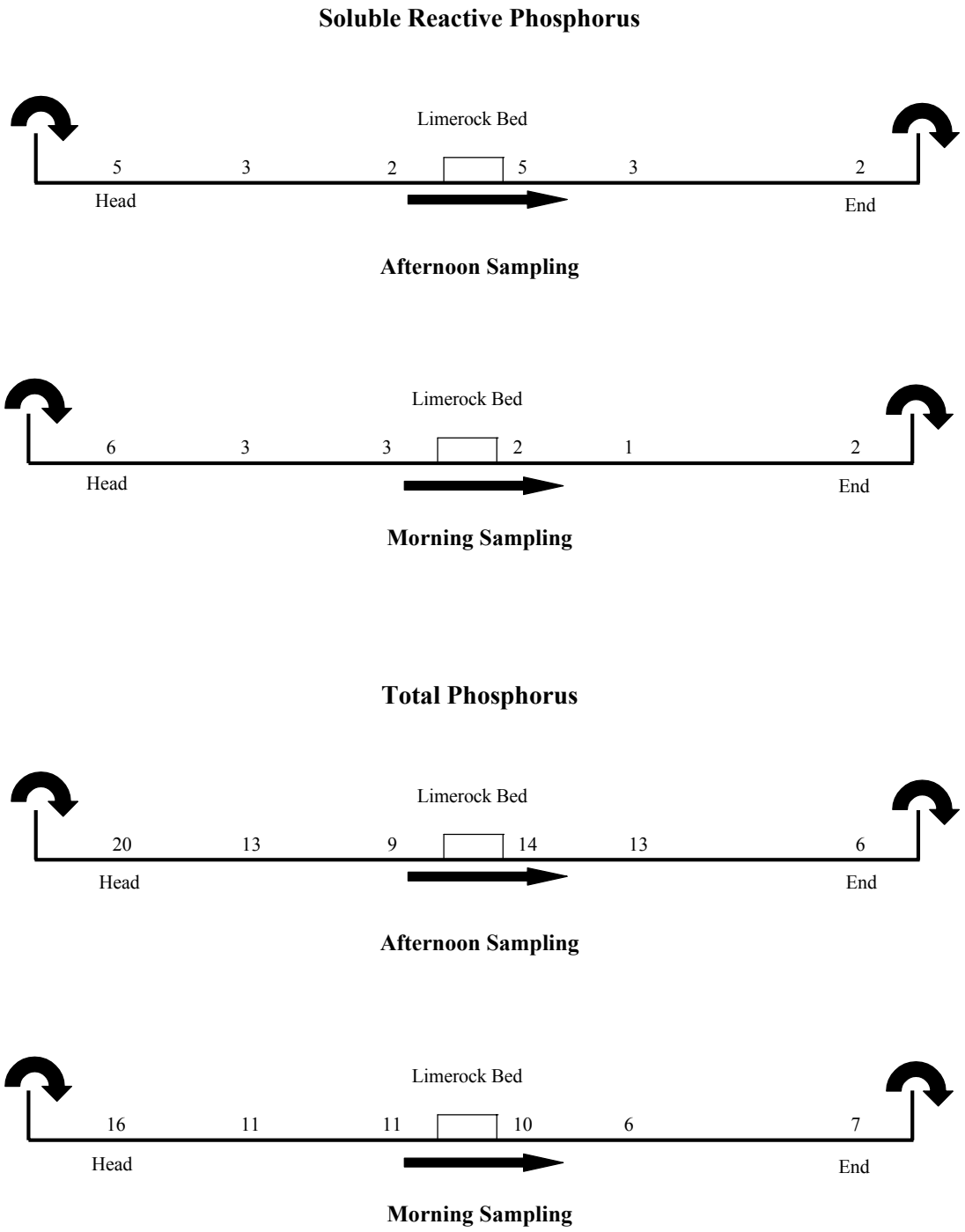

Figure 6.7 Spatial characteristics of SRP and total P concentrations (µg/L) in the low velocity raceways. Afternoon samples were collected between 13:00 and 16:50. Morning samples were collected before dawn. Values represent means from duplicate raceways. Arrows indicate direction of flow. See Fig. 4.4 for exact locations of sampling points.

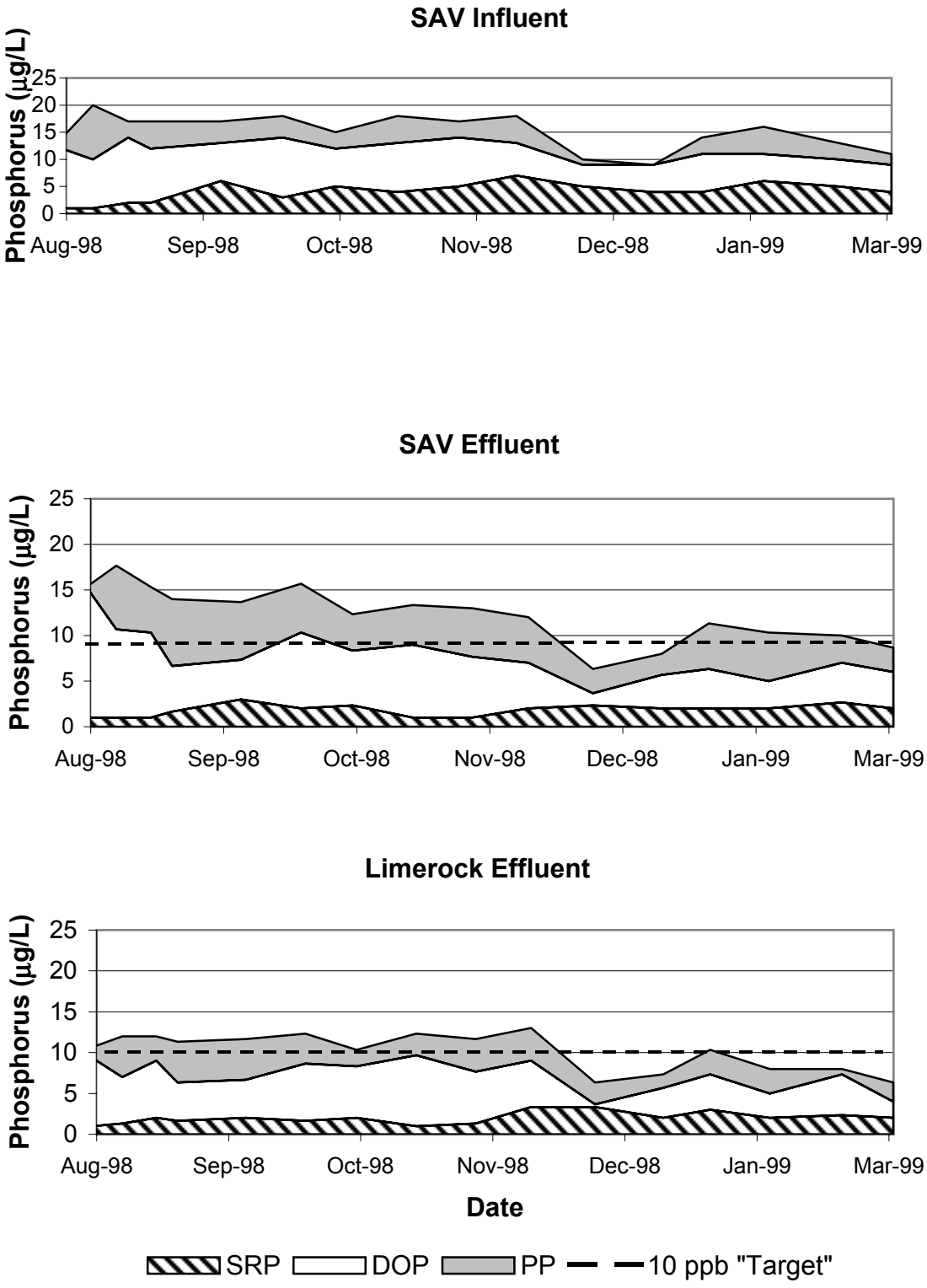

Figure 6.8 Soluble reactive P (SRP), dissolved organic P (DOP) and particulate P (PP) concentrations at three locations in the SAV mesocosm/LR process train.

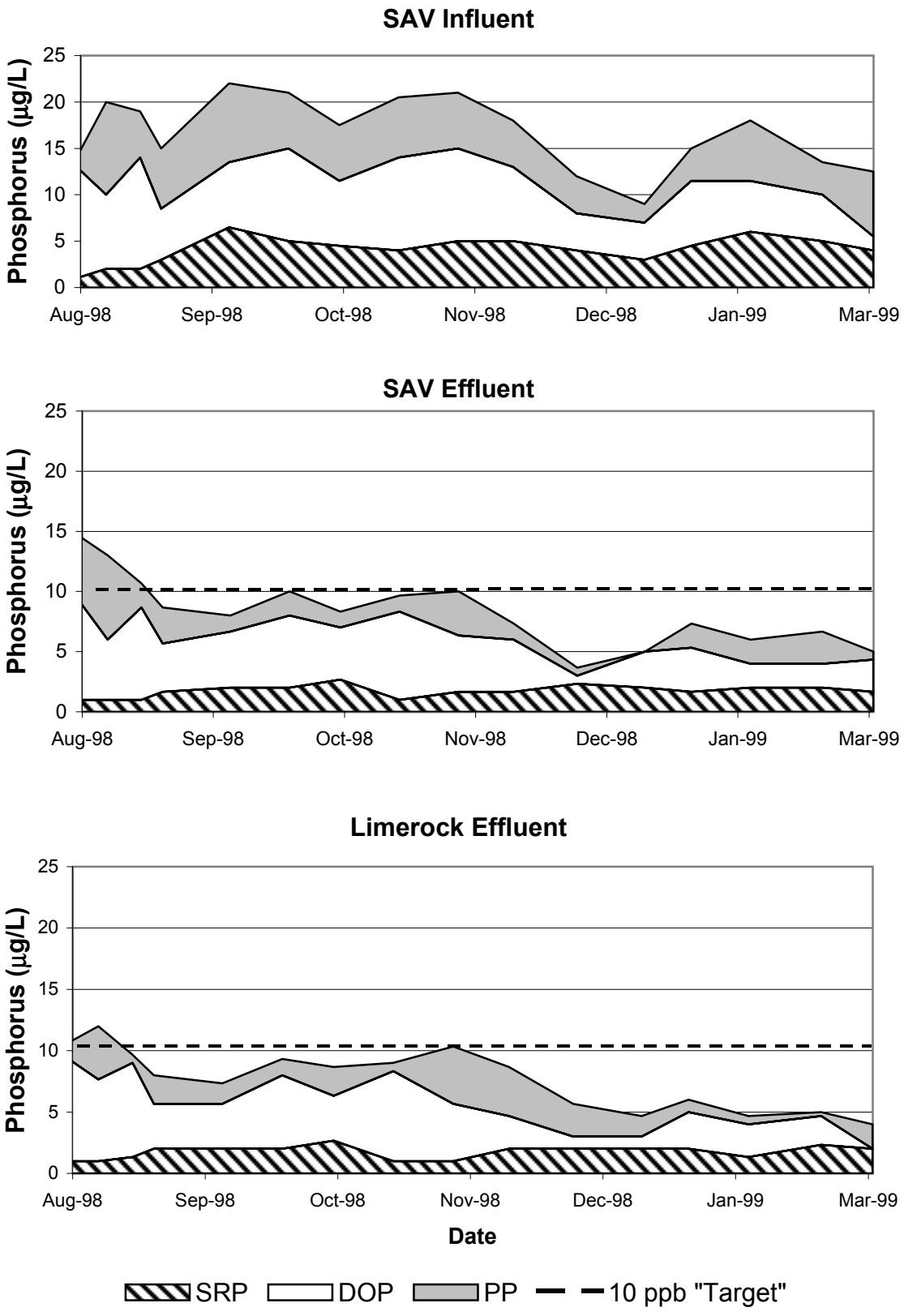

Figure 6.9 Soluble reactive P (SRP), dissolved organic P (DOP) and particulate P (PP) concentrations at three locations in the low velocity raceway/LR process train.

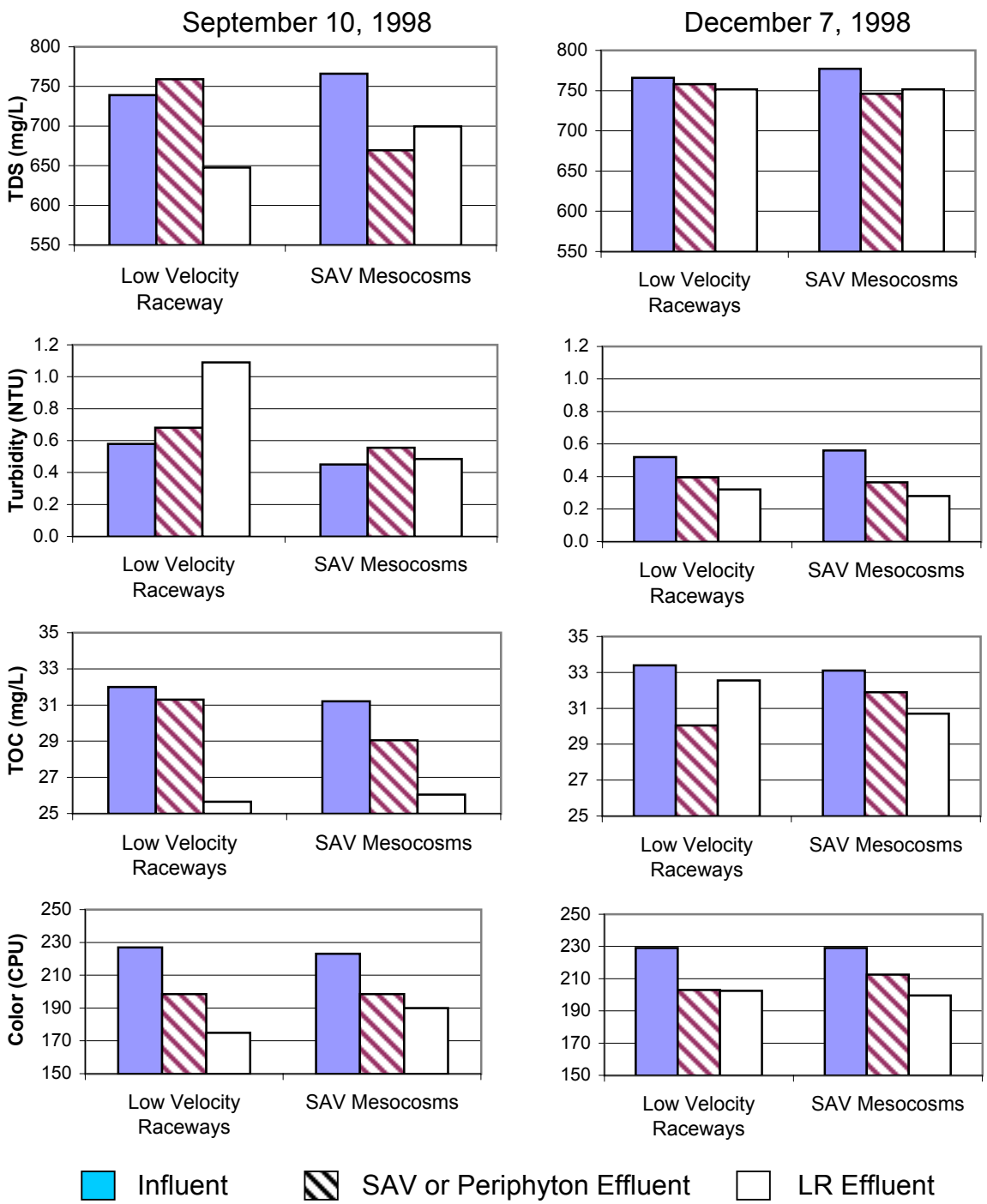

Figure 6.10 Concentrations of TDS, turbidity, TOC and color (n=2) at three locations in the deep and shallow, low velocity process trains on two sampling dates.

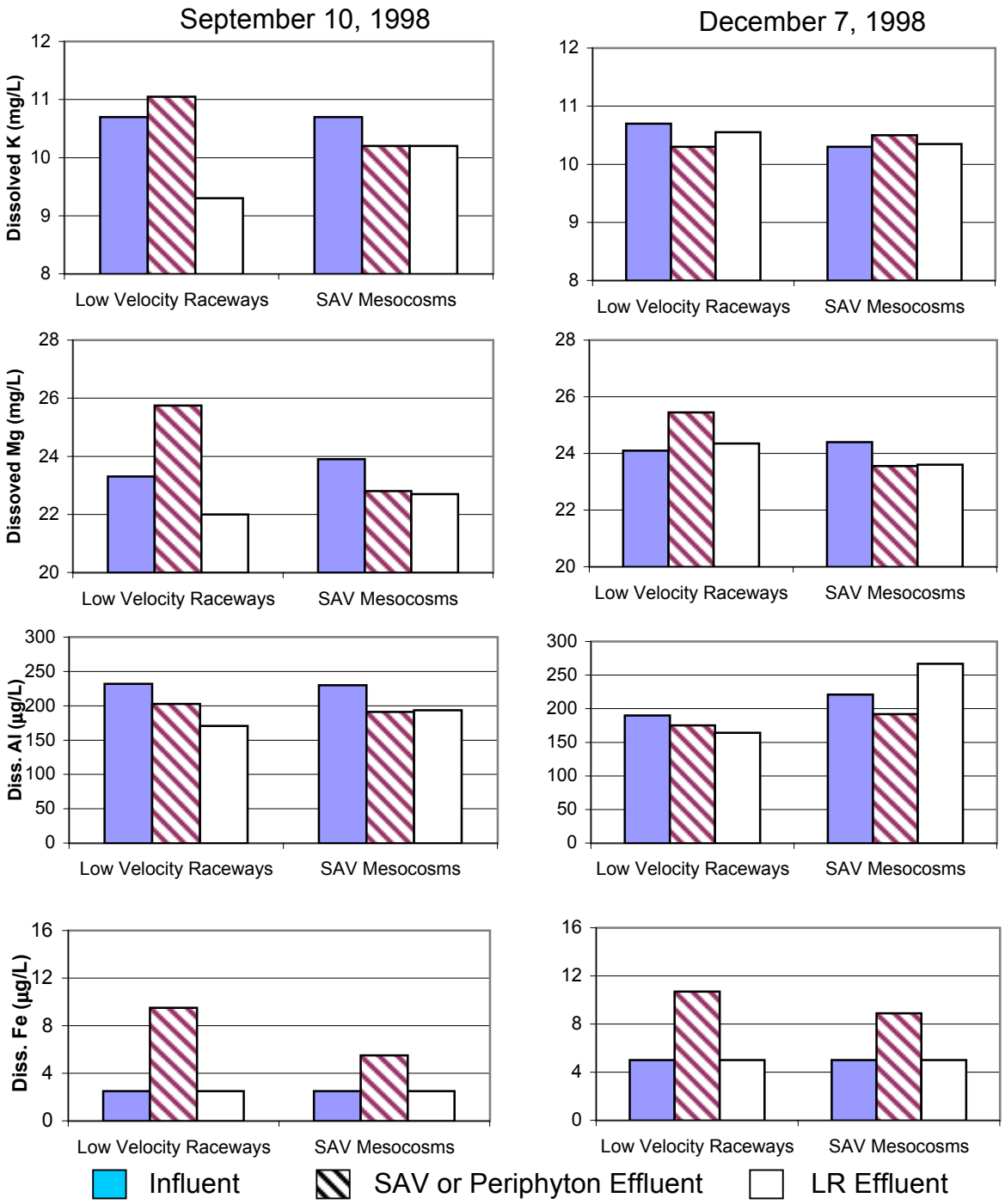

Figure 6.11 Concentrations of K, Mg and dissolved Al and Fe (n=2) at three locations in the deep and shallow, low velocity process trains on two sampling dates.

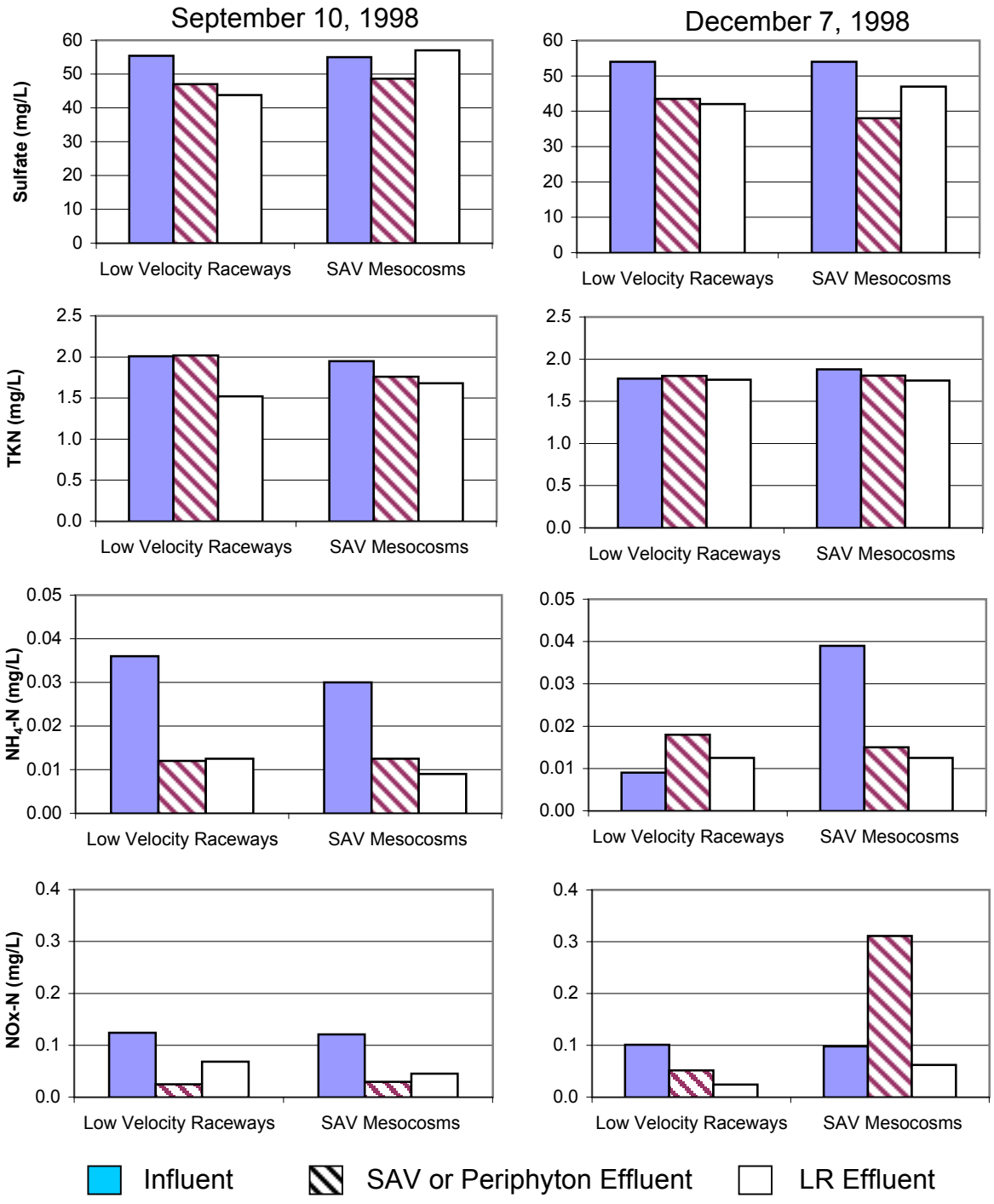

Figure 6.12 Concentrations of sulfate, TKN, NH4-N and NOx-N (n=2) at three locations in the deep and shallow low velocity process trains on two sampling dates.

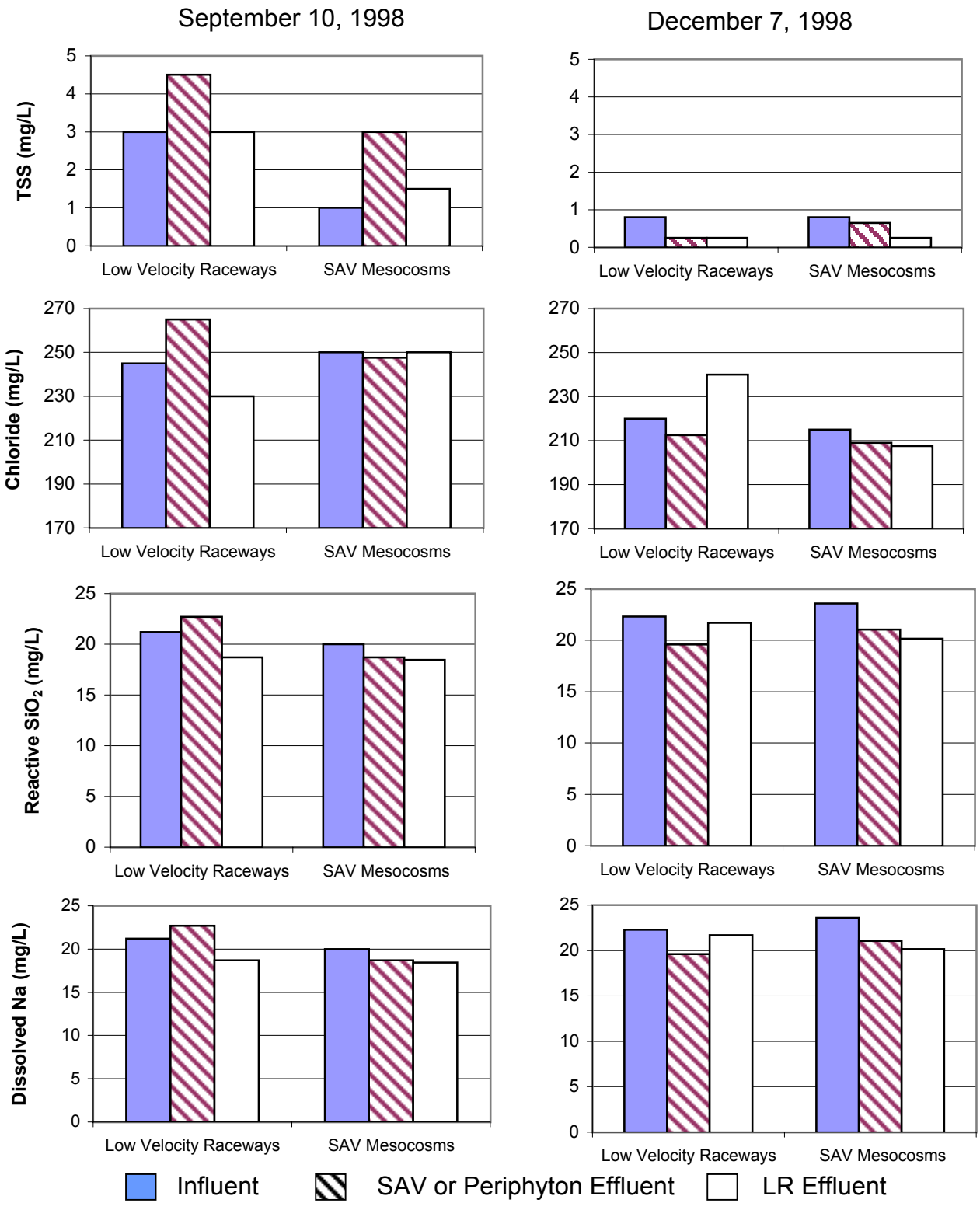

Figure 6.13 Concentrations of TSS, chloride, reactive silica and dissolved sodium (n=2) at three locations in the deep and shallow low velocity process trains on two sampling dates.

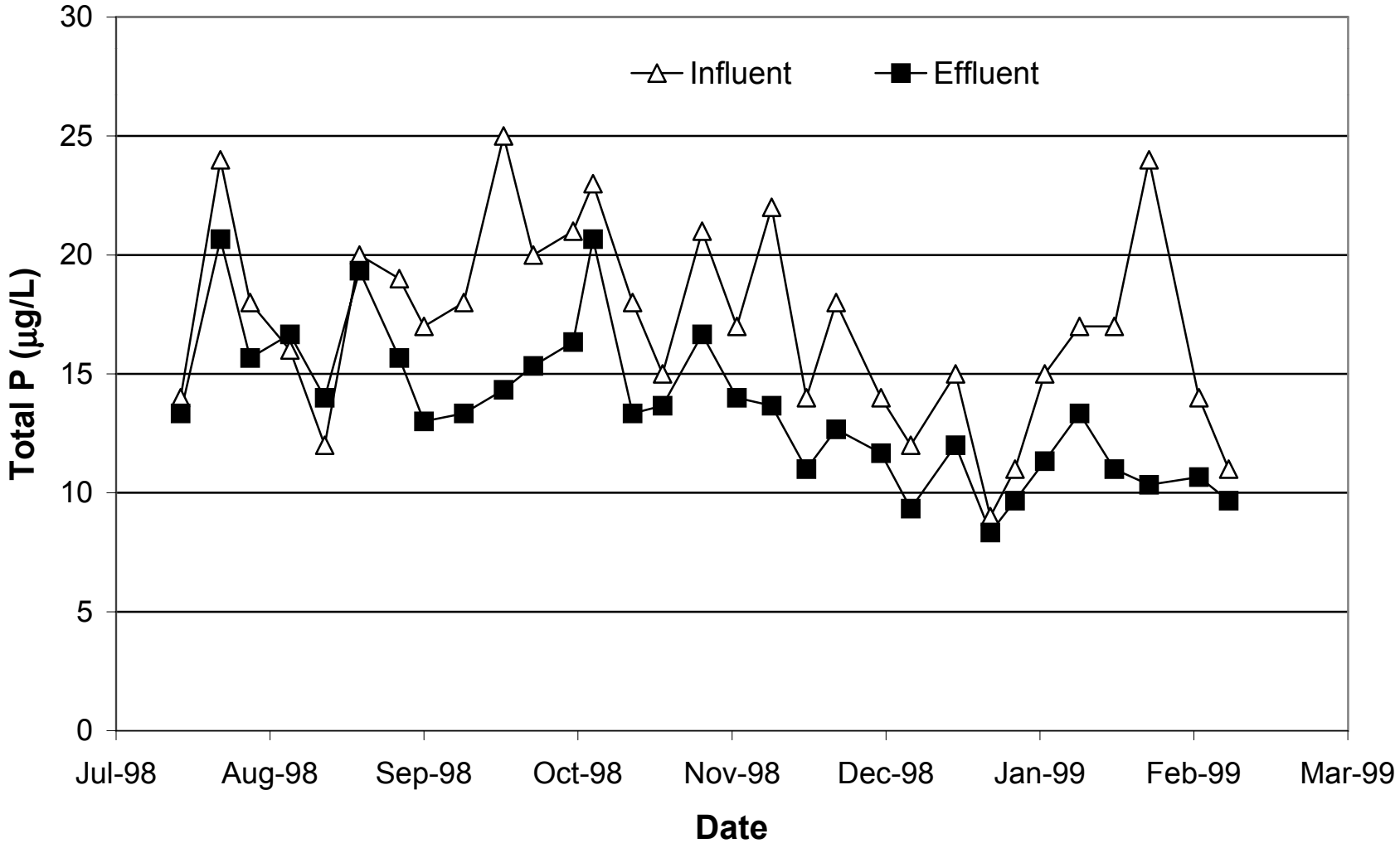

Figure 6.14 Mean influent and effluent total P concentrations (n=3) for the high velocity raceways.

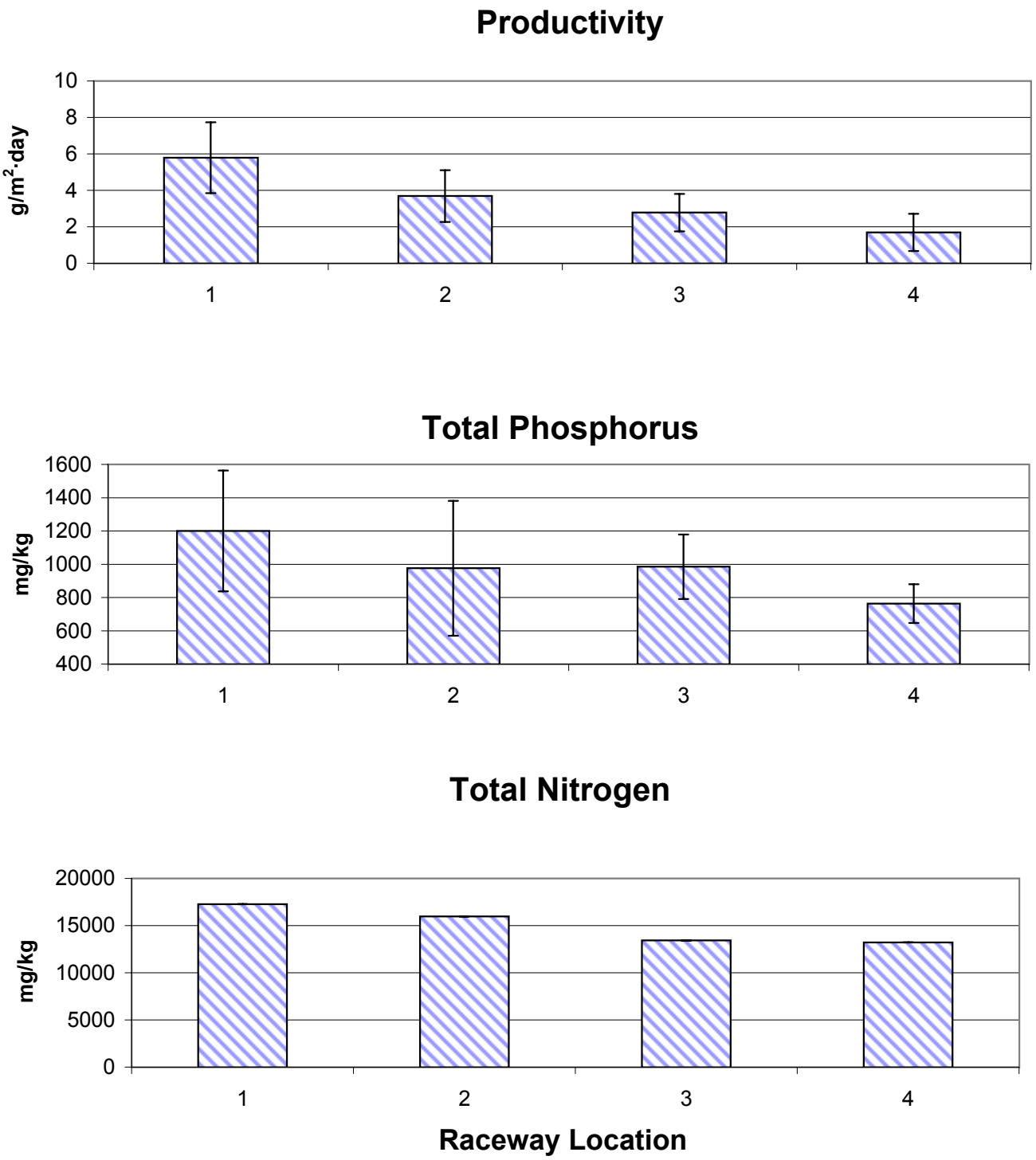

Figure 6.15 Mean productivity (based on 10 – 14 day harvest intervals) and tissue N and P content of periphyton in the high-velocity raceways (n=3, 1 s.d.). Biomass was collected from the four quarters of each raceway, ranging from influent region (1) to effluent region (4). Data collection period was August 1998 through February 1999.

VII. Mesocosm Experiments: Subtasks 4E, 4F and 4G

Subtask 4E. Effect of Plant Harvesting on SAV/Limerock Performance

Methods

To evaluate the effects of plant harvest on total P removal, we fabricated six SAV mesocosms (2.2 m L x 0.79 m W x 1.0 m D) of wood and fiberglass. These mesocosms were situated at the north site and plumbed with PVC pipe to receive a semi-continuous flow of Post-BMP waters. Three tanks were designated for periodic plant harvest, and three tanks were maintained as controls, with no plant harvest performed (Fig. 4.2). The same water source, distribution method, and influent baffles were used for these systems as for the mesocosms in Subtask 4C. A 15-cm layer of muck was placed in the bottom of each tank. Water column depths were set at 80 cm. An influent hydraulic loading of 10 cm/day was established, providing a HRT of 8 days.

Macrophytes were stocked into the mesocosms during July 1998. Submerged macrophytes were collected from ENR Cell 4, subsampled for analyses of dry matter content and elemental composition, and stocked into each tank. *Najas* and *Ceratophyllum* were stocked at 1.3 kg wet wt/m^2 each and *Chara* and *Potamogeton* were stocked at 0.17 kg wet wt/m^2 each.

Sediment samples were collected initially to determine the characteristics of the muck substrate. After macrophyte stocking, the mesocosms were allowed to stabilize for one month prior to water sampling. Water quality samples were then collected weekly at influent and effluent stations in the system. Temperature and pH were measured in the field at the time of sample collection. Water samples were analyzed for TP and SRP.

After eight weeks, the SAV in the "experimental" tanks was harvested, separated by species, subsampled for chemical and dry weight analyses, and weighed (i.e., wet weight after allowing the plants to drip-dry). After harvesting, the SAV was placed back into the respective system at close to the original stocking densities. Water sampling and field measurements were continued weekly for the remainder of the study.

Results and Discussion

Due to its high dry matter content, *Najas* had a higher dry wt. standing crop than *Ceratophyllum* at the time of stocking even though both were stocked at the same wet weight. *Ceratophyllum*, on the other hand, had the higher tissue P content (Table 7.1). The muck soils stocked in the "harvested" mesocosms prior to the beginning of the study had a slightly higher bulk density and P content than that in the control (unharvested) mesocosms (Table 7.2).

At the time of initial macrophyte stocking, the plants were placed into the water column, but none were directly rooted. Between July and September 1998 the submerged macrophyte community in the mesocosms changed in two respects: first, most of the plants became rooted; and second, there was a dramatic shift towards dominance by one species, *Najas*. The *Najas* standing crop increased to 2.0 kg wet wt/m^2 (200 dry g/m^2), and the biomass of *Ceratophyllum* and *Chara* declined sharply: the former from a standing crop of 1.3 to 0.6 kg wet wt/m^2, and the latter from 0.17 to 0.045 kg wet wt/m^2.

Our vegetation harvesting protocol had an adverse impact on water quality. Even though the *Najas* was firmly rooted by the harvest date, we chose to remove all of the macrophyte biomass from the tanks. This method was selected over just "mowing" the top of the vegetation, since this latter approach would not provide quantitative biomass data. Although there appeared to be enhanced growth of *Potamogeton* after harvesting, *Najas* remained the dominant species. There was no noticeable increase in periphyton biomass during the post-harvest period.

Removal of the SAV community disrupted the surficial sediments and likely stressed the plants themselves (note that a portion of the removed biomass was restocked). As a consequence, TP removal for about two months after the harvest date was much poorer than in the "non-harvested" treatment. At times, effluent TP levels from the harvested systems were almost double those of the control tanks (Table 7.3; Fig. 7.1). Once the macrophyte standing crop stabilized, however, performance among the treatments was again comparable. For the entire study, effluent TP concentrations in the harvested mesocosms averaged 22 µg/L, and those in the "control" mesocosms averaged 17 µg/L.

Visually, the SAV standing crop in the harvested mesocosms appeared to recover about two months after harvest. Even though our experimental protocol specified to harvest vegetation every 7 to 8 weeks, we chose to postpone any additional harvests until late spring or summer 1999, when the SAV species would be more productive and recover more readily from the trauma of harvesting.

Based on data collected to date, the harvested mesocosms performed no better after they recovered than did the unharvested systems. On the short term, it does not appear that harvesting improves performance, but longer-term operations with additional harvests are needed to determine the value of this management practice.

Table 7.1. Standing crop biomass and total P content of SAV species stocked in the vegetation harvest and depth study mesocosms (n=3 replicates per treatment).

Treatment	Stocking Dry Weight (g/m^2)	TP (mg/kg)
0.8m deep, harvested		
Najas		
mean	86	1210
s.d.	12	222
Ceratophyllum		
mean	58	1920
s.d.	8	210
0.8m deep, unharvested		
Najas		
mean	72	1380
s.d.	21	200
Ceratophyllum		
mean	46	2160
s.d.	7	494
0.4m deep, unharvested		
Najas		
mean	84	1440
s.d.	5	219
Ceratophyllum		
mean	67	1870
s.d.	11	285
1.2m deep, unharvested		
Najas		
mean	85	1560
s.d.	12	173
Ceratophyllum		
mean	64	1950
s.d.	14	89

Table 7.2. Bulk density and total P content of muck soils stocked in the vegetation harvest and depth study mesocosms (n=3 replicates per treatment).

Treatment	Bulk Density (g/cc)	TP (mg/kg)
0.8m deep, harvested		
mean	0.207	206
s.d.	0.025	18
0.8m deep, unharvested		
mean	0.175	181
s.d.	0.016	33
0.4m deep, unharvested		
mean	0.194	262
s.d.	0.021	69
1.2m deep, unharvested		
mean	0.192	198
s.d.	0.022	7

Table 7.3. Phosphorus removal performance of the 0.8 m deep harvested and non-harvested SAV mesocosms at the North Supplemental Technology Site. Mean (s.d.) values are based on 33 weekly measurements (n=3 replicates per treatment).

	"Harvested" Influent	"Harvested" Effluent	"Non-Harv." Influent	"Non-Harv." Effluent
Total P (µg/L)				
mean	105	22 (3.8)	108	17 (3.0)
max.	189	63	178	39
min.	32	9	37	7
SRP (µg/L)				
mean	61	3 (0.9)	66	3 (1.1)
max.	157	8	154	16
min.	20	1	26	1

Subtask 4F. Effect of Water Depth on SAV/Limerock Performance

Methods

In the "depth" study, nine tanks were established to provide three treatments (in triplicate) of shallow (0.4 m), moderate (0.8 m), and deep (1.2 m) water columns. The mesocosms all received a similar hydraulic loading of 10 cm/day, creating HRTs of 3.6, 7.2, and 10.8 days for the shallow, moderate and deep systems, respectively (Fig. 4.2). These systems were configured similar to those in Subtask 4E, with 15 cm of muck substrate. Submerged aquatic vegetation was collected from ENR Cell 4 and was stocked at the densities described in Subtask 4E.

Sediment samples were collected to determine initial characteristics of the muck substrate. After macrophyte stocking, the mesocosms were allowed to stabilize one month prior to sampling. Water samples were collected weekly at influent and effluent regions of each system, and analyzed for TP and SRP. We initiated sampling of TSP in these mesocosms on November 24, 1998, which enabled us to characterize the various P forms in the influent and effluent waters over the 13 weeks until termination of the study on March 5, 1999.

Temporal and Spatial Water Column Characteristics

In February 1999, we performed a more rigorous spatial and temporal sampling of the water column in the various mesocosms. Water samples were collected, and field measurements (pH, D.O. and temperature) performed, at several depths (3 and 30 cm for shallow mesocosms; 3, 30 and 60 cm for moderate depth mesocosms; and 3, 30, 60, and 90 cm for deep mesocosms) at both the influent and effluent regions of the mesocosms. These measurements were performed during both afternoon (13:00-16:50) and early morning (03:00-06:00). Water samples were returned to the laboratory and analyzed for the following parameters: Ca, alkalinity, SRP and TSP. TP was measured only on surface samples (3 cm) due to the difficulty of collecting undisturbed samples at subsurface depths. Alkalinity and Ca analyses were performed on only the shallowest and deepest stations.

Hydraulic Characteristics of the SAV Mesocosms

In February and March 1999 we performed a tracer study to assess hydraulic characteristics of the mesocosms operated at different water depths. Rhodamine-WT and LiCl were added to the baffled influent end of two of the three replicate SAV tanks for each of three depth treatments. The injection date and time was 23:45, March 16, 1999. The mass of Rhodamine-WT applied to the shallow, moderate, and deep SAV tanks was 71, 142, and 212 mg, respectively; LiCl was added at 4.337, 8.674, and 12.95 grams, respectively. All of the tracer concentrates were applied in volumes of 106 ml. Grab samples of mesocosm effluents were collected at times 0 (background), every 6 hrs for the first 42 hours, then days 2.25, 2.75, 3.5, 4.4, 5.4, 6.6, 8.6, 11.7 and 14.5. In addition, effluents from moderate and deep mesocosms were sampled on days 18.5, 21.4, 25.5, 28.4, and 32.5, and due to their long HRTs, the deep mesocosms were sampled again on days 36.6 and 43.3.

Results and Discussion

There were slight between-treatment differences in the initial dry weight standing crops of the SAV species, as well as in the TP content and bulk density of the muck soils placed in the mesocosms (Tables 7.1 and 7.2). However, during the initial five weeks of the study (July 22 – August 19), all depth treatments produced effluent TP concentrations that were similar (Fig. 7.2). Following this startup period, effluent TP concentrations among the different treatments began to diverge, with the shallow mesocosms (0.4 m depth) producing the lowest effluent TP levels (i.e., best P removal performance), and the deep mesocosms (1.2 m) providing the highest (Fig. 7.2). The mean effluent total P concentration of 13 µg/L in the shallow system was significantly different ($P < 0.05$) than the effluent from the moderate and deep systems (17 and 19 µg/L, respectively). This trend in P removal is particularly interesting since the HRT of the shallow mesocosms (3.6 days) was one-third that of the deep systems (10.8 days).

From November 1998 – March 1999, the mean SRP, PP and DOP influent concentrations for all systems averaged 56, 37 and 7 µg/L, respectively. For unknown reasons, the deep system received a higher mean PP concentration (45 µg/L) than the other two systems (34 and 33 µg/L; Table 7.4). The effluent from the mesocosms had the same mean levels of DOP (5 µg/L), although the shallow system appeared to be superior at removing PP and SRP (Table 7.4 and Fig. 7.3).

Temporal and Spatial Water Column Characteristics

To assess whether the enhanced performance of the shallow systems (despite their short HRT), was due to a more favorable pH, temperature, and/or D.O. regime than the moderate and deep mesocosms, we performed sampling within the mesocosms on February 17-18 to document internal water chemistry profiles. Mean characteristics of the influent Post-BMP waters during this sampling event were: 97 µg TP/L, 51 µg SRP/L, 5 µg DOP/L, 41 µg PP/L, 36 mg Ca/L and 99 mg alkalinity (as $CaCO_3$)/L.

Table 7.4. Influent and effluent concentrations [mean, (s.d.)] of TP and individual P species for SAV mesocosms operated at three different depths at the North Supplemental Technology Site. Values are based on 13 weekly measurements (n=3 replicates per treatment) collected from the last four months of the depth study. Means with same letters are not significantly different (P> 0.05).

	Deep Influent	**Deep Effluent**	**Moderate Influent**	**Moderate Effluent**	**Shallow Influent**	**Shallow Effluent**
TP (µg/L)						
mean	111	17[b] (1.6)	100	16[b] (4.0)	98	12[a] (1.3)
max.	34	10	37	7	35	4
min.	172	69	163	39	154	17
SRP (µg/L)						
mean	59	4 (1.4)	59	3 (0.8)	58	2 (0.5)
max.	149	10	141	5	138	5
min.	26	2	26	1	25	1
DOP (µg/L)						
mean	7	5 (1.3)	7	5 (0.9)	7	5 (0.8)
max.	20	12	25	14	17	10
min.	0	1	-5	1	0	-1
PP (µg/L)						
mean	45	8 (2.7)	34	8 (3.5)	33	5 (1.2)
max.	106	23	88	31	88	9
min.	3	3	-3	2	-1	0

We found it impossible to collect subsurface waters within SAV beds without dislodging fine particles, which subsequently were swept into the sample bottle. For this reason, we collected water samples for TP analyses only at the surface (3 cm depth). Nevertheless, we still obtained one particle-laden sample, at the effluent region of the 1.2 m deep mesocosm, in the early morning hours. Interestingly, upon examination of this water sample we found that the

particles were zooplankton, which at this time were migrating vertically within the water column. With the exception of this one sample, there was a distinct horizontal inflow – outflow TP gradient in all the depth study mesocosms (Fig. 7.4).

Considering that the TP inflow averaged 97 μg/L during the afternoon sample collection period, substantial TP removal occurred even at the influent region of the mesocosms. Soluble reactive P exhibited a similar horizontal gradient, and concentrations of this analyte also varied with depth (Fig. 7.5). At the effluent regions, SRP concentrations tended to be slightly higher in the 60 and 90 cm water depths of the moderate and deep tanks. Diel changes in SRP concentrations were minimal (Fig. 7.5). Unlike SRP, DOP did not display consistent spatial or temporal gradients (Fig. 7.6). During the afternoon sampling, dramatic vertical water column gradients were found for pH, dissolved oxygen (D.O.) and temperature (Figs. 7.7-7.9). These gradients were absent in the morning. The deeper regions of the water column consistently exhibited higher concentrations of Ca and alkalinity (Figs. 7.10 and 7.11). Additionally, during early morning hours there was an influent – effluent decline in Ca and alkalinity at the surface (3 cm).

These spatial and temporal water column samples revealed that the SAV communities, in particular the community in the shallow, short HRT systems, were remarkably efficient at sequestering the SRP component of the influent feedwater. Despite pronounced vertical gradients (e.g., pH, D.O.) that arise and dissipate on a diel cycle, vertical gradients in DOP and SRP did not occur in the effluent regions of the shallow mesocosms (Figs. 7.5 and 7.6). This suggests that under the environmental conditions that prevail in the shallow SAV communities, dissolved P species were not remobilized from the deposited sediments. However, SRP data from the medium and deep tanks did show some concentration increases near the bottom, which may indicate remobilization from the sediments. It may be that in the shallow tanks the base of the water column was within the metabolically active portion of the SAV bed, while in the deeper tanks the base of the water column was in a region devoid of SAV activity.

Hydraulic Characteristics of the SAV Mesocosms

Tracer Response Curves

The concentration response curves for the SAV mesocosms represented left skewed normal distributions (Fig. 7.12), with tracer appearing at the effluent regions sooner than the nominal hydraulic retention times. We observed a lag of 1.75-2.25 days for the shallow mesocosms and 2.25 days for the moderate and deep mesocosms before the peak tracer concentration reached the effluent region of the tank. Nevertheless, with the exception of a lag after tracer injection, the profiles of these curves are characteristic of mixed flow conditions, where there is an initial rapid increase in the concentration, which is then followed by exponential decay.

Tracer Mass Balances

The Rhodamine-WT and lithium mass balances were calculated by comparing the added tracer mass to the tracer mass found at the effluent. The total mass of tracer exiting the SAV tanks is given by Eq. 3 (Section V). A comparison of the recovered tracer mass and the amount added to each mesocosm demonstrate a good recovery for Rhodamine-WT in the shallow and mid-depth tanks (Table 7.5). Rhodamine-WT and lithium appeared to perform equally well as tracers in this study (Fig. 7.13).

Table 7.5. Comparison of recovered tracer mass with the tracer amounts added to mesocosms operated at three different water depths. Values represent means (s.d.) from duplicate mesocosms.

Treatment	**Mass Added (mg)**		**Mass Recovered (mg)**		**% Recovery**	
	Dye	Li	Dye	Li	Dye	Li
Deep: 1.2 m	212	2120	183 (2.8)	2,031 (32)	86.2	95.8
Moderate: 0.8 m	142	1420	143 (5.1)	1,283 (10)	100.7	90.4
Shallow: 0.4 m	71	710	68.2 (1.5)	532 (34)	96.0	75.0

Tracer Detention Time

Our data show that τ_a was slightly longer than the nominal detention time (τ) in the shallow depth mesocosms (τ_a=4.45 days vs. τ=3.6 days). For the moderate depth and deep mesocosms, τ_a was closer in agreement to τ but still longer: τ_a=7.8 days vs τ= 7.2 days for the moderate depth mesocosms and τ_a = 11 days vs. τ= 10.8 days for the deep mesocosms.

This is an apparent violation of the materials balance, so there may have been some inaccuracies associated with the flow, mass, or volume measurements. However, given the nearly 100% recovery of the dye, and the careful measurements of injection mass, flow, and tank volume, other reasons may account for the disparity between the measured and nominal HRTs. Examples of factors that complicate interpretation of tracer response curves include: excluded zones, internal recirculation, physical blockage created by the uneven SAV biomass distribution, and the presence of the inflow baffle.

Residence Time Distribution (RTD)

The dimensionless RTD curves (Fig. 7.14) assist in defining the mixing characteristics and diagnosing any irregularities in classical plug or mixed flow profiles. For the SAV mesocosm data, the dimensionless RTD curves had the following attributes that are characteristic of mixed flow reactors:

- the response curve exhibited an exponential decay from a peak concentration that occurred close to the time when the tracer was injected.
- the dimensionless concentration (E_Θ) values never exceeded 1.0, but did come close. Plug flow conditions yield E_Θ values that are greater than one, whereas E_Θ equals 1.0 at Θ=0 and decreases exponentially thereafter under classical mixed flow conditions (Levenspiel 1989).
- at dimensionless time Θ=1, the corresponding E_Θ value equals 0.37 under mixed conditions and >1.0 for plug flow. Although the E_Θ values for the shallow and moderate depth tanks were higher than 0.37 (i.e., 0.50), the E_Θ value for the deep SAV tanks was 0.37 (Fig. 7.14).

While the tracer curves did have attributes similar to completely mixed reactors, the lag time (the period following injection, but before appearance of the dye in the effluent region) is an important diagnostic feature of the curves. The 0.8 and 1.2 m deep mesocosms, despite having long theoretical HRTs (7.2 and 10.8 days, respectively), exhibited dye breakthrough (appearance at the effluent) sooner than the short HRT, shallow mesocosms.

There are two factors that probably contributed to this more rapid short-circuiting through the 0.8 m and 1.2 m deep tanks. The first factor is the distribution of the SAV, which undoubtedly affects the arrival time and concentration of the tracer. Once the tracer plume clears the injection

area by flowing underneath the baffle, it will follow the flow paths that offer the least resistance. Those flow lines would be in zones that have the lowest SAV density, such as at the water surface (assuming neither SAV nor associated periphyton are "topped out") and adjacent to the mesocosm bottom, where SAV densities typically are lower. The water columns of the 0.4 m deep mesocosms are entirely within the light compensation point for most SAV species, and therefore would be expected to have the least amount of "free water" devoid of SAV.

The other factor that likely influences the tracer response curve is thermal stratification of the water column (Fig. 7.9). Under stratified conditions during the day, part of the tracer plume can become isolated (i.e., no vertical mixing) in either a surface or bottom layer. If this layer lies within a higher flow rate field, then a "frontal edge" of the plume could reach the effluent sampling station within the first six hours after injection, as we observed in this study. Under this short-circuiting scenario, the remaining mass of tracer would gradually arrive in ever-increasing concentrations until it peaked. The subsequent decline in tracer concentration would represent the slower moving fluid particles that had been dispersed and detained within more hydrodynamically isolated pockets of the water column. Shallow water columns that support a dense SAV community therefore may offer fewer density gradient-related or "free-water" zones that facilitate hydraulic short-circuiting.

In addition to a greater lag time before the appearance of the dye in the effluent region, the shallow tanks had a longer tail (i.e., shallower slope) on their dimensionless response curves (Fig. 7-14). This indicates that there is better mixing occurring in the shallower tanks, probably because of the higher degree of contact of fluid particles with SAV. The more prolonged lag time and the longer tail associated with the shallow depth tanks mean that on a relative basis, fluid particles are generally more dispersed and remain within the mesocosm for longer time compared to the deeper tanks. This hydraulic differentiation may partially explain the higher P removal efficiencies in the 0.4 m deep SAV systems.

In conclusion:

- in our mesocosms, Rhodamine-WT and lithium were both conservative, and thus appear to be effective tracers under the environmental conditions that prevail in SAV systems
- variability of tracer response curves between duplicate SAV mesocosms was negligible
- following a lag period, the tracer response curves show that SAV mesocosms behave like completely mixed reactors

- free water zones alternating with SAV zones, along with temperature-related density gradients in the water column, probably account for the short-circuiting that results in appearance of the tracer much sooner than the calculated retention time
- the hydraulic attributes of the shallow tanks were more “ideal” (e.g., slightly reduced short-circuiting) than the deeper tanks, which may in part account for their superior P removal performance

Subtask 4G. Effect of Limerock Chemical Composition and Size on Phosphorus Removal Performance

Methods

We selected three different limerock sources to examine the effect of compositional differences on P removal. The first was caprock mined from the Palm Beach Aggregates quarry near the ENR study site, which represented a "high quality" substrate. This is the same substrate that was stocked in the limerock beds in Subtasks 4C at the north site and 4D at the south site. The other two rocks represented "poorer quality" substrates: one originated from the baserock mined at the Palm Beach Aggregates quarry and the second was excavated material from a holding pond along SR 80. The Palm Beach Aggregates baserock was selected as a “poor” quality rock because of its high native P content, and the SR 80 rock was selected as a poor substrate because of its high Mg and low Si contents. We included a measure of structural strength (i.e., Si concentration) of the LR in our consideration of "high quality" LR substrate because it represents a measure of the resistance of the LR to chemical (dissolution) and physical (ablation) degradation. Chemical characteristics of the various limerocks are provided in Table 4.1. With respect to gross physical characteristics, the baserock contained considerable shell material, and the SR 80 rock had lower structural strength (as measured by Si concentration - see Table 4.1) than the high quality caprock.

We crushed and screened the rock materials, providing a nominal diameter of between 1.3 and 2.5 cm for each of the three limerock types in the LR "quality" comparison. To examine the effect of rock size on phosphorus removal efficiency, we screened three sizes of the “high quality” caprock from the Palm Beach Aggregate quarry, providing nominal sizes of 0.6 - 1.3 cm, 1.3 - 2.5 cm, and 2.5 - 3.5 cm.

Rock from each of the five LR categories (i.e., "high quality" caprock at three different size ranges and two "low quality" limerock sources at the 1.3 - 2.5 cm diameter size) were packed into

triplicate 3 m L x 10 cm diameter LR columns (total of 15 columns) (Fig. 4.3). Hydraulic conductivity measurements (i.e., the time it takes to drain a predetermined volume of water through each column) were performed before influent and effluent plumbing was attached.

The columns were oriented vertically, and plumbed to receive effluent from a large SAV mesocosm operated at a short HRT (0.5 days). The effluent was fed into the top of each column, and a constant water level was maintained by means of an external standpipe. The approximate HRT within the columns was 1 hour. After 4 months the HRT was increased to 5 hours, to increase exposure time in the columns. Total P and SRP analyses were performed on samples collected weekly from the column influents and effluents. Column hydraulic conductivities were measured at the end of the study in order to assess the potential plugging (by inorganic particles) and/or biological fouling. Limerock within the reactors was visually inspected for slime growth, accumulation of fines, and structural integrity at the termination of the project.

Results and Discussion

The initial four months of this study demonstrated that neither limerock size nor composition had much effect on P removal efficiency in the columns. During this period the LR columns typically removed a small amount of TP (mean of 7 µg/L in some treatments), but essentially no SRP was removed (Table 7.6, Figs. 7.15 and 7.16). The nominal 1.3 and 2.5 cm caprock sizes performed slightly better than the larger (5.0 cm) rock. Moreover, the "high quality" PBA caprock outperformed the PBA baserock and SR 80 rock, although the differences were slight. During this period, the LR columns appeared to be acting as a physical filter that trapped PP, similar to what we observed in the Post-BMP HRT study.

Table 7.6. Phosphorus removal performance of three limerock (caprock) size fractions (top) and three types of 2.5 cm nominal diameter limerock (bottom). Values represent 19 weekly measurements from August 27 – December 29, 1998 (n = three replicates per limerock size and type).

	Influent	**1.3 cm**	**2.5 cm**	**5.0 cm**
Total P (µg/L)				
mean	83 (1.7)	74 (5.5)	77 (5.0)	77 (3.1)
max.	187	165	180	169
min.	31	27	30	29
SRP (µg/L)				
mean	56 (1.5)	53 (2.3)	55 (4.5)	58 (2.5)
max.	151	130	138	133
min.	9	5	7	5

	Influent	**PBA Caprock**	**PBA Baserock**	**SR 80 Rock**
Total P (µg/L)				
mean	83 (1.5)	77 (5.0)	78 (7.5)	75 (7.2)
max.	187	180	167	169
min.	31	30	32	29
SRP (µg/L)				
mean	56 (1.3)	55 (4.5)	54 (3.5)	53 (4.7)
max.	151	138	136	130
min.	9	7	5	6

During the final seven weeks of the study, performance of the columns changed dramatically, and several of the columns began exporting enormous amounts of soluble and particulate P (Fig. 7.15 and 7.16). This was unexpected, because we had operated LR columns in our laboratory for over 20 months on a similar inflow stream and had not observed this type of degradation in performance.

Upon termination of the study, we drained the columns and found that all contained particulate-laden water. Upon inspection of the columns, we believe that the particle generation and export was caused by light penetration into the columns. These were fabricated of PVC pipe and wrapped with shade cloth, but it appears that enough light penetrated into the columns to promote

internal algae growth. This normally would not be a problem in a larger LR bed, but our vertically oriented, narrow (10 cm diameter) columns had a high surface area to volume ratio, and the peripheral light penetration therefore impacted almost the entire column. The algal populations therefore built up during the study, and their growth was probably further accelerated in the last weeks of the study when we increased the column HRT from 1 to 5 hours.

In summary, we believe that the data from September – December 1998, which demonstrate little impact of LR size or composition on P removal, accurately reflect the performance of various types of LR in these systems (Table 7.6). The dramatic export of particulate and soluble P in February 1999 is almost certainly an artifact of our LR column design, since we have not found particle laden waters in any other LR beds, many of which have been operated for a longer period of time, and under high nutrient loadings, than those in this subtask.

Another important observation during the September – December operational period is that removal of SRP by heterogeneous nucleation onto LR surfaces did not meet our expectations in this subtask. We believe that the lack of a steady-state detention time may have accounted for the limited SRP removal. The columns were plumbed in a fashion where the inflow water was pulse-fed. In reviewing characteristics of our water delivery system, it appears that the duration and timing of pulses may have been such that while mean column detention time (over a day's time) was 1 hr, the actual detention time at the time of sample collection may have varied from 10 minutes to several hours. The kinetics of calcium phosphate nucleation and crystal growth can be slow and variable, depending on solution composition and transport rate. Transport in reactive flow systems is coupled to the reaction rate. If the precipitation reactions are slow relative to the transport of water through the LR bed, then local disequilibrium will result (Steefel and Lasaga, 1990). It may be that the LR column HRTs were insufficient to allow nucleation and crystal growth.

Although these data do not support P removal by heterogeneous nucleation of metastable calcium phosphate compounds for SAV-treated Post-BMP waters, the LR still appears to serve as a prominent substrate for P removal by other physical and chemical processes. Particulate P filtration by the LR beds in Subtask 4C (Section V) has proven to be important in reducing TP concentrations in the final effluent stream.

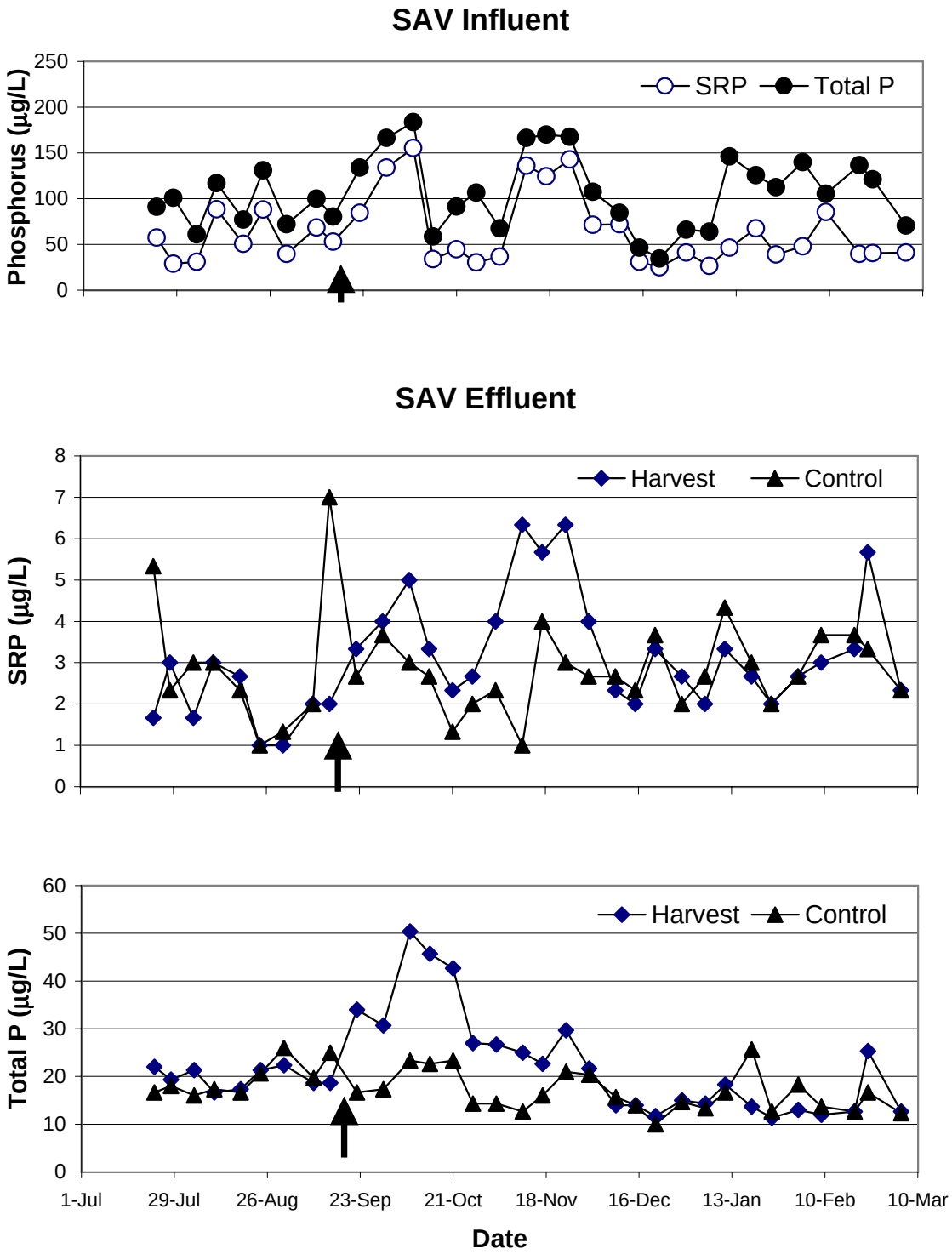

Figure 7.1 Mean influent and effluent total P and soluble reactive P concentrations (n=3) in the 0.8m deep harvested and control (non-harvested) SAV mesocosms. A vegetation harvest was performed on September 14 (as indicated by the arrow).

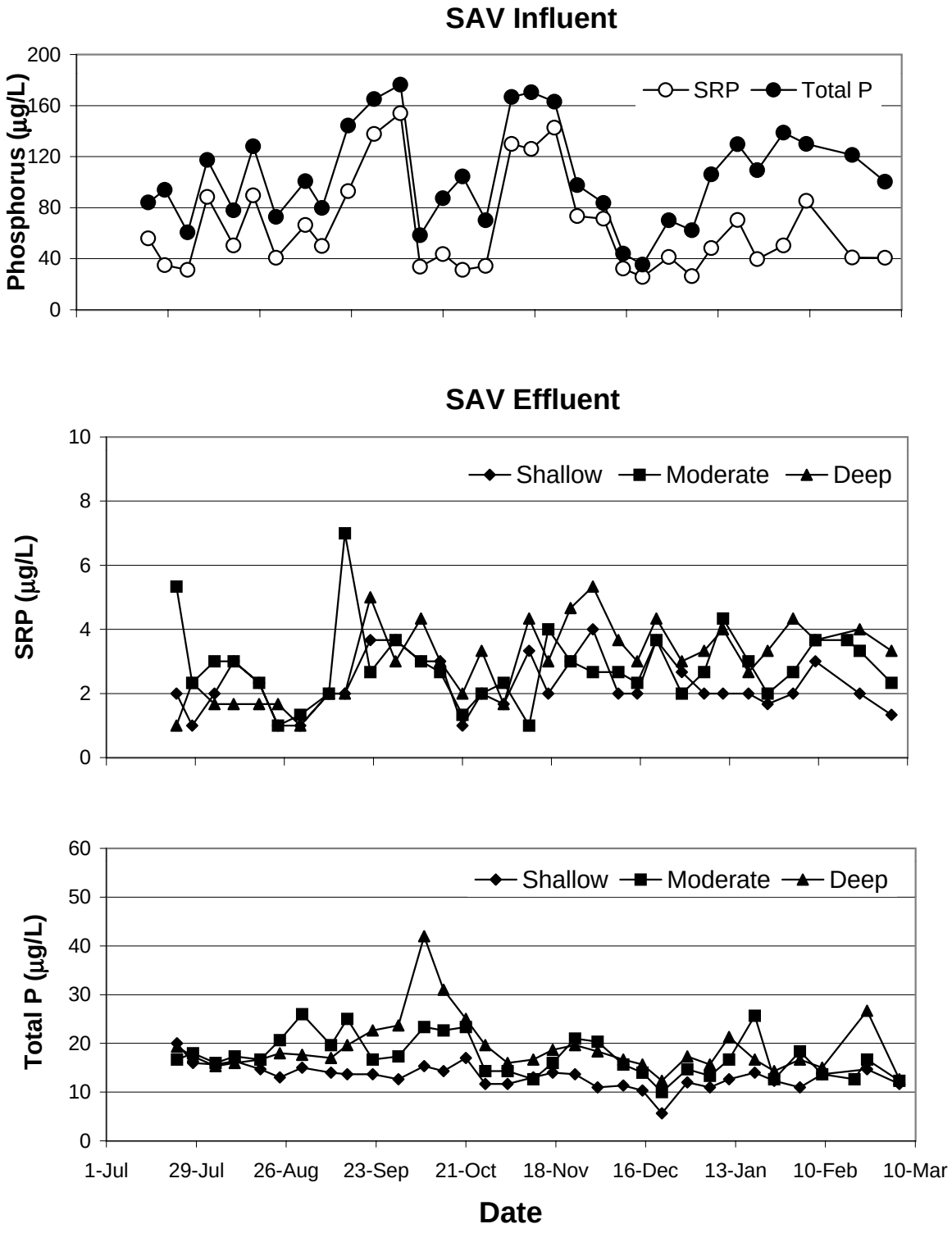

Figure 7.2 Mean influent and effluent total P and soluble reactive P concentrations (n=3) in SAV mesocosms operated at shallow (0.4 m), moderate (0.8 m) and deep (1.2 m) depths.

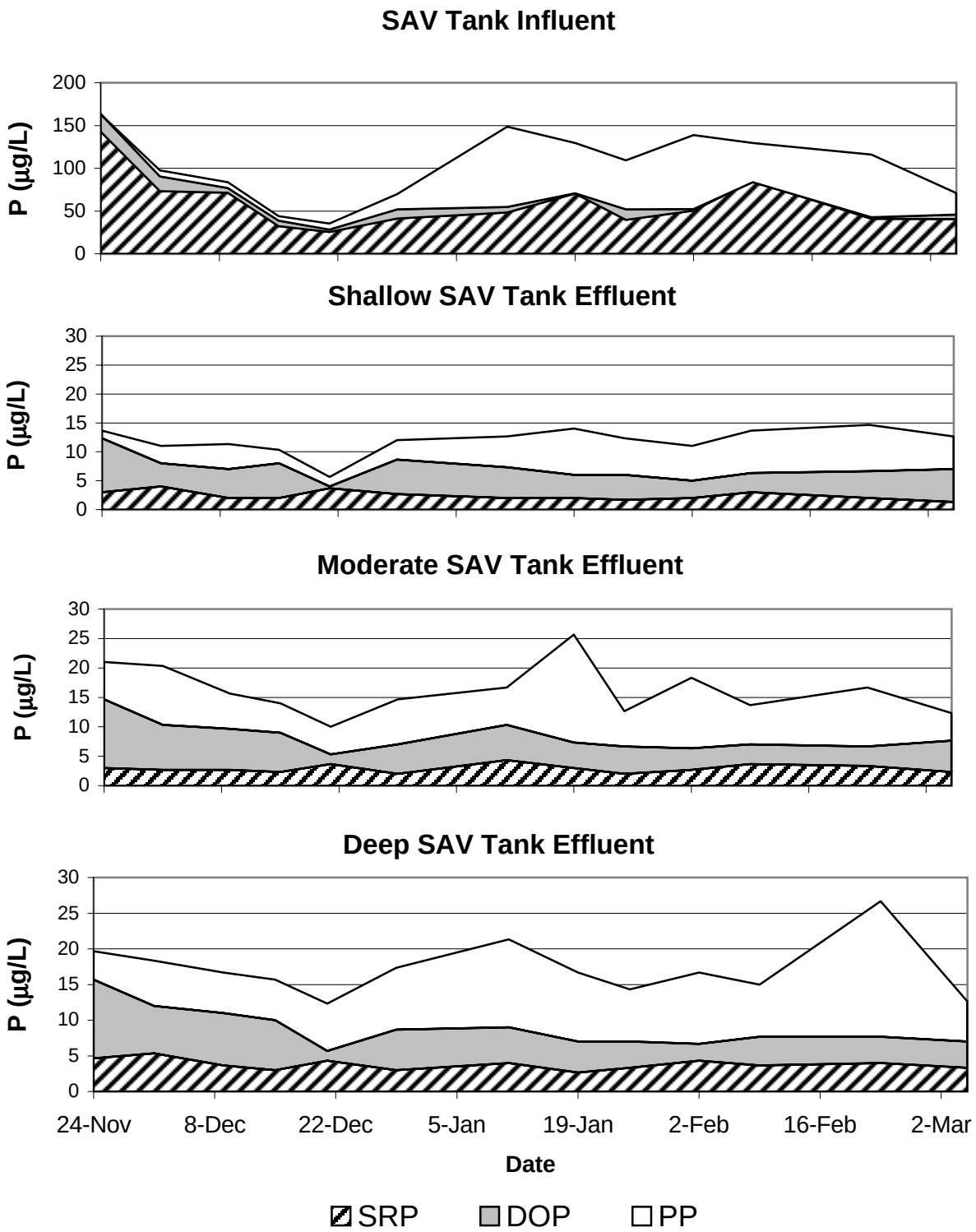

Figure 7.3 Soluble reactive P (SRP), dissolved organic P (DOP) and particulate P (PP) concentrations in the influent and effluent of SAV mesocosms operated at three depths (0.4 m, 0.8 m, and 1.2 m deep).

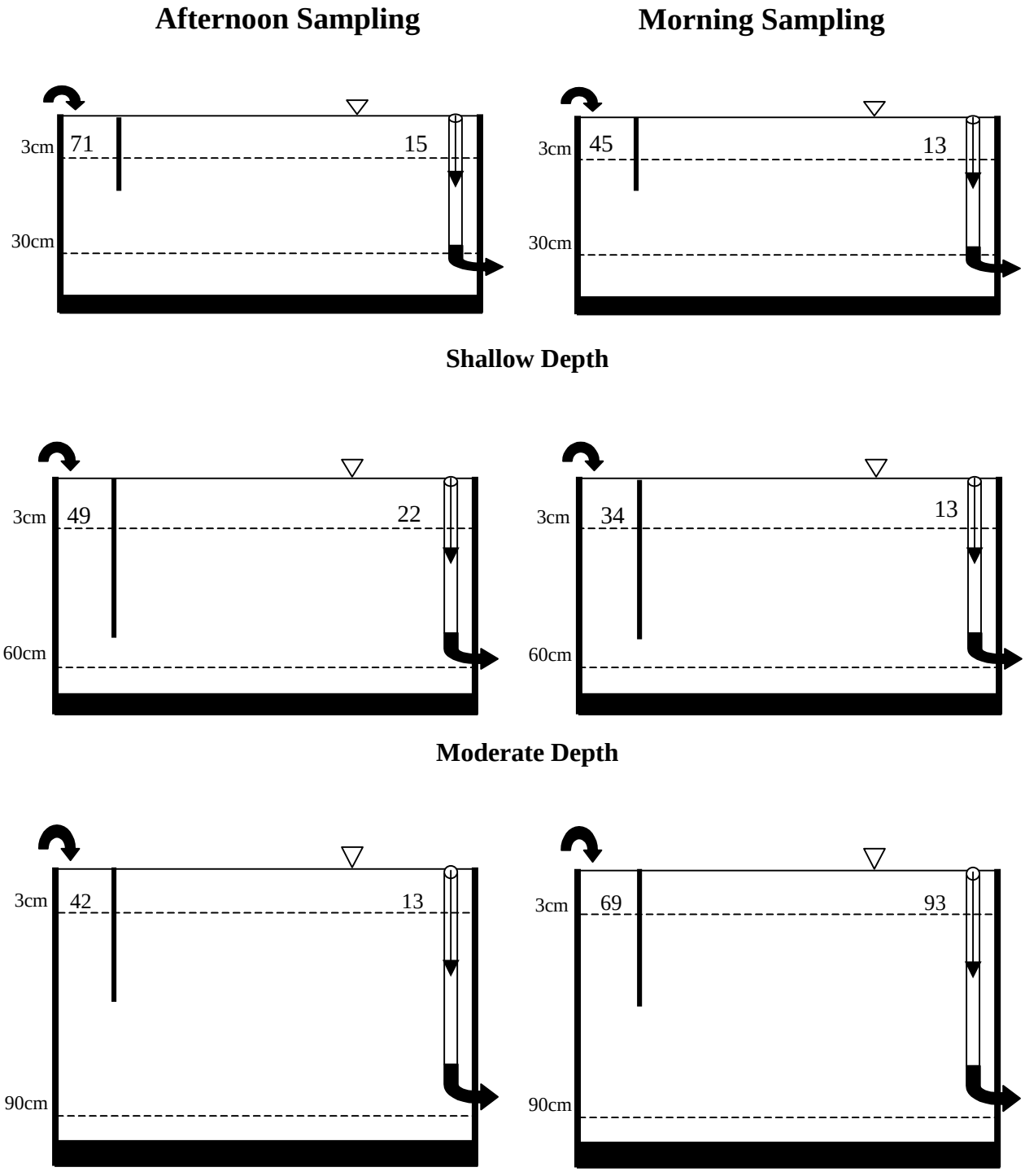

Figure 7.4 Spatial water column characteristics of total P (µg/L) in the influent and effluent regions of SAV mesocosms operated at three depths. Afternoon sampling was performed from 13:00-16:50 on February 18, and morning sampling was performed before dawn on February 19. Arrows indicate direction of flow.

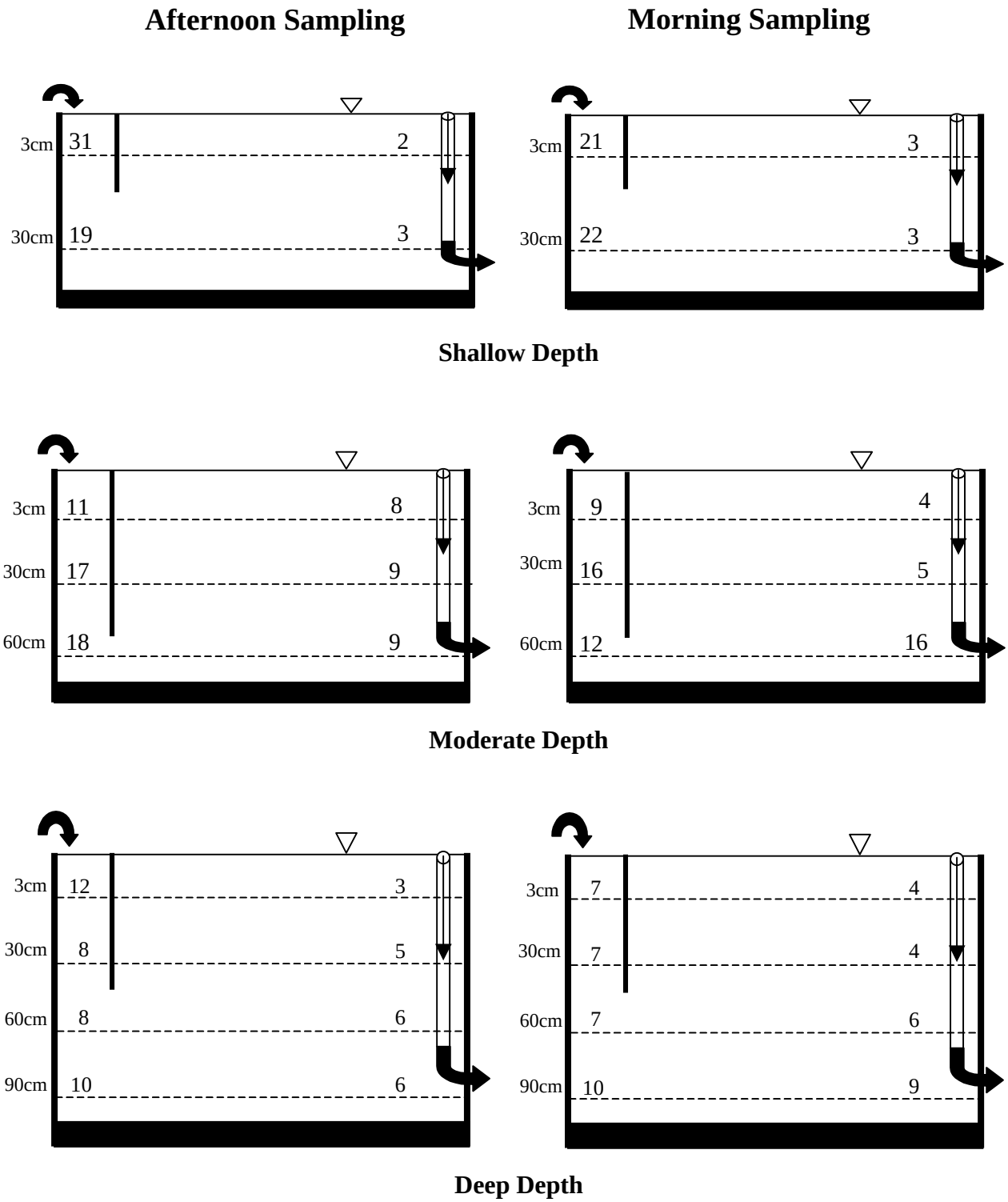

Figure 7.5 Spatial water column characteristics of soluble reactive P (µg/L) in the influent and effluent regions of SAV mesocosms operated at three depths. Afternoon sampling was performed from 13:00-16:50 on February 18, and morning sampling was performed before dawn on February 19. Arrows indicate direction of flow.

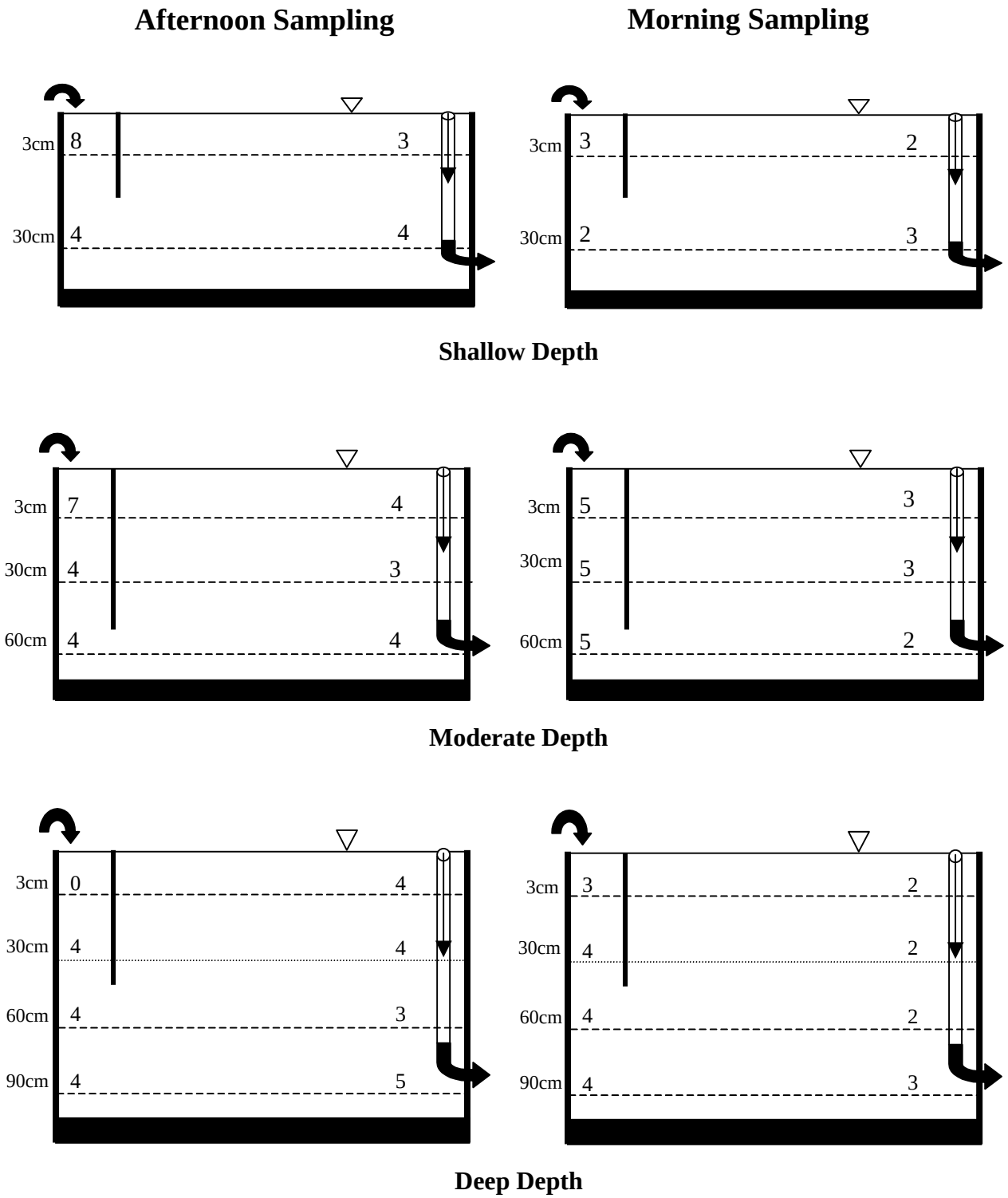

Figure 7.6 Spatial water column characteristics of dissolved organic P (μg/L) in the influent and effluent regions of SAV mesocosms operated at three depths. Afternoon sampling was performed from 13:00-16:50 on February 18, and morning sampling was performed before dawn on February 19. Arrows indicate direction of flow.

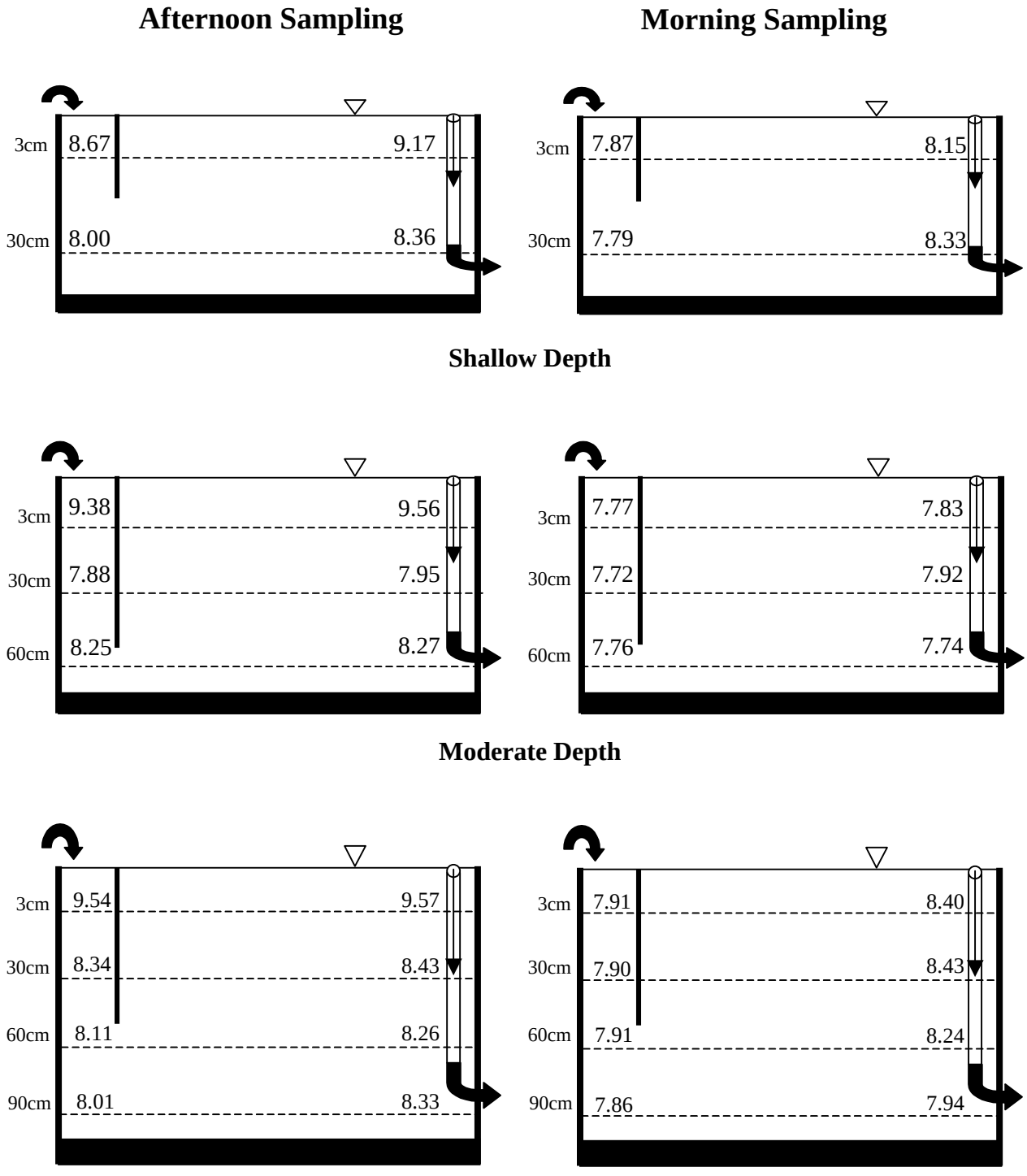

Figure 7.7 Spatial water column characteristics of pH in the influent and effluent regions of SAV mesocosms operated at three depths. Afternoon sampling was performed 13:00-16:50 on February 18, and morning sampling was performed before dawn on Febraury 19. Arrows indicate direction of flow.

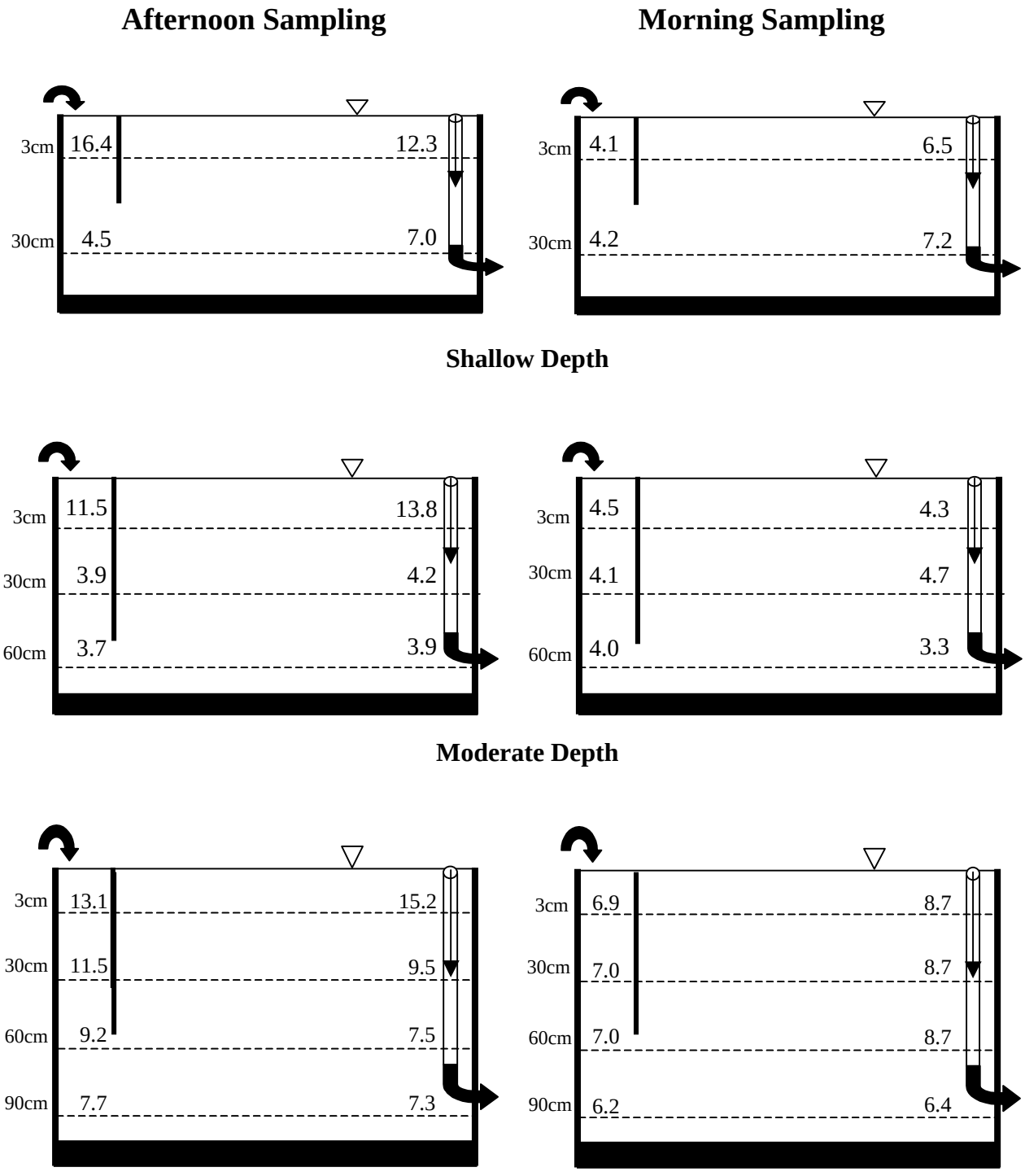

Figure 7.8 Spatial water column characteristics of dissolved oxygen (mg/L) in the influent and effluent regions of SAV mesocosms operated at three depths. Afternoon sampling was performed 13:00-16:50 on February 18, and morning sampling was performed before dawn on February 19. Arrows indicate direction of flow.

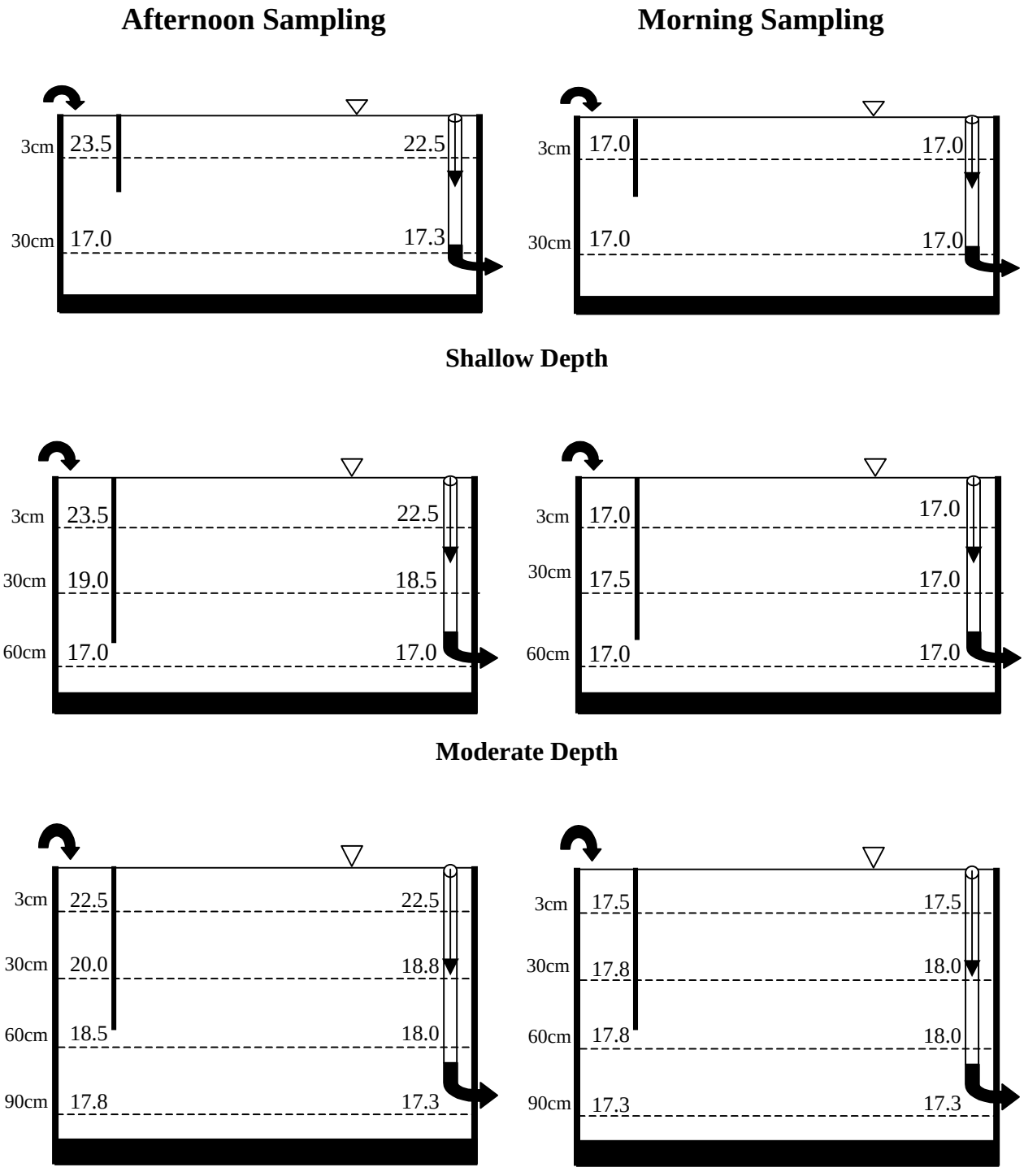

Figure 7.9 Spatial water column characteristics of temperature (° C) in the influent and effluent regions of SAV mesocosms operated at three depths. Afternoon sampling was performed 13:00-16:50 on February 18, and morning sampling was performed before dawn on February 19. Arrows indicate direction of flow.

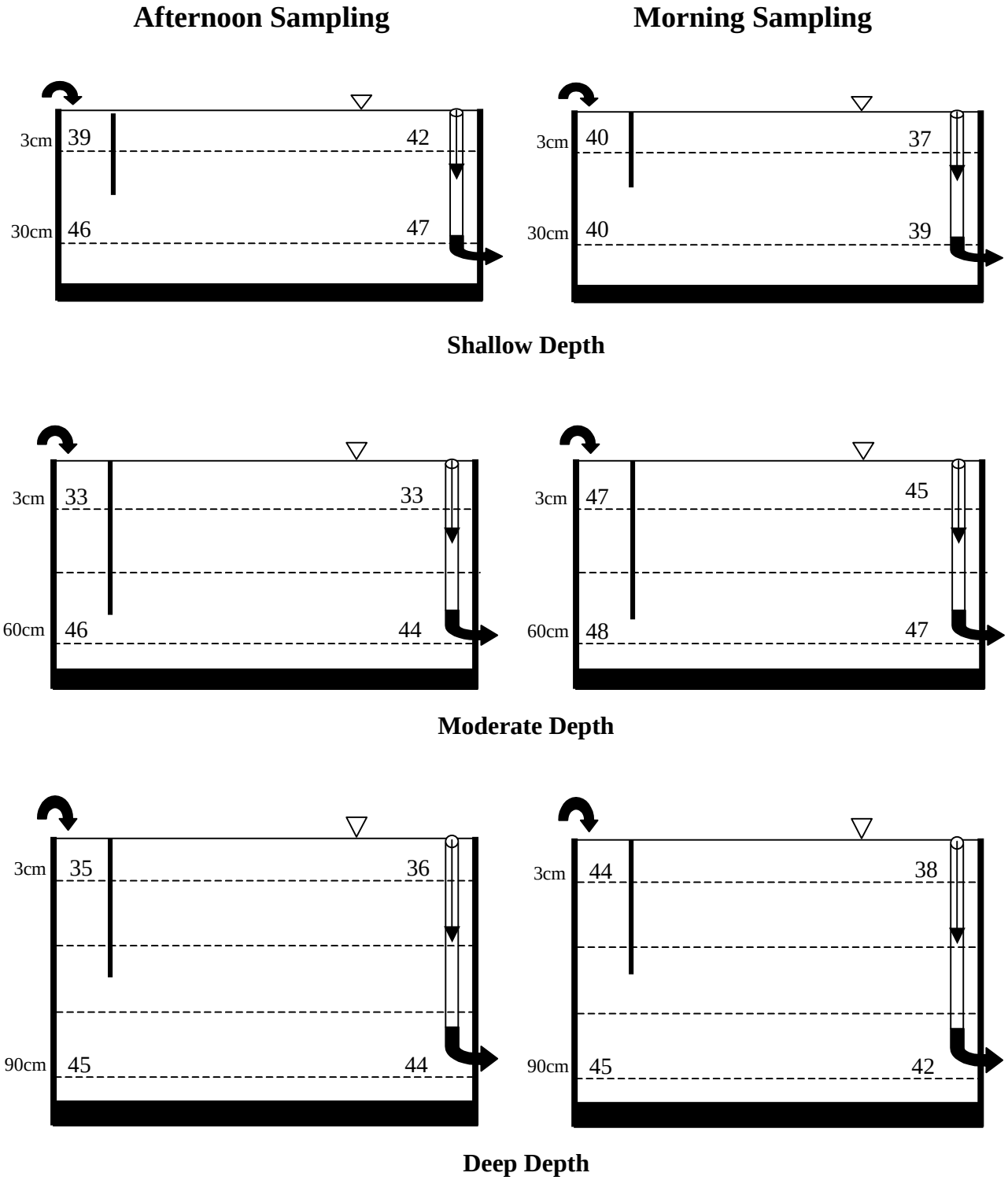

Figure 7.10 Spatial water column characteristics of dissolved calcium (mg/L) in the influent and effluent regions of SAV mesocosms operated at three depths. Afternoon sampling was performed 13:00-16:50 on February 18, and morning sampling was performed before dawn on February 19. Arrows indicate direction of flow.

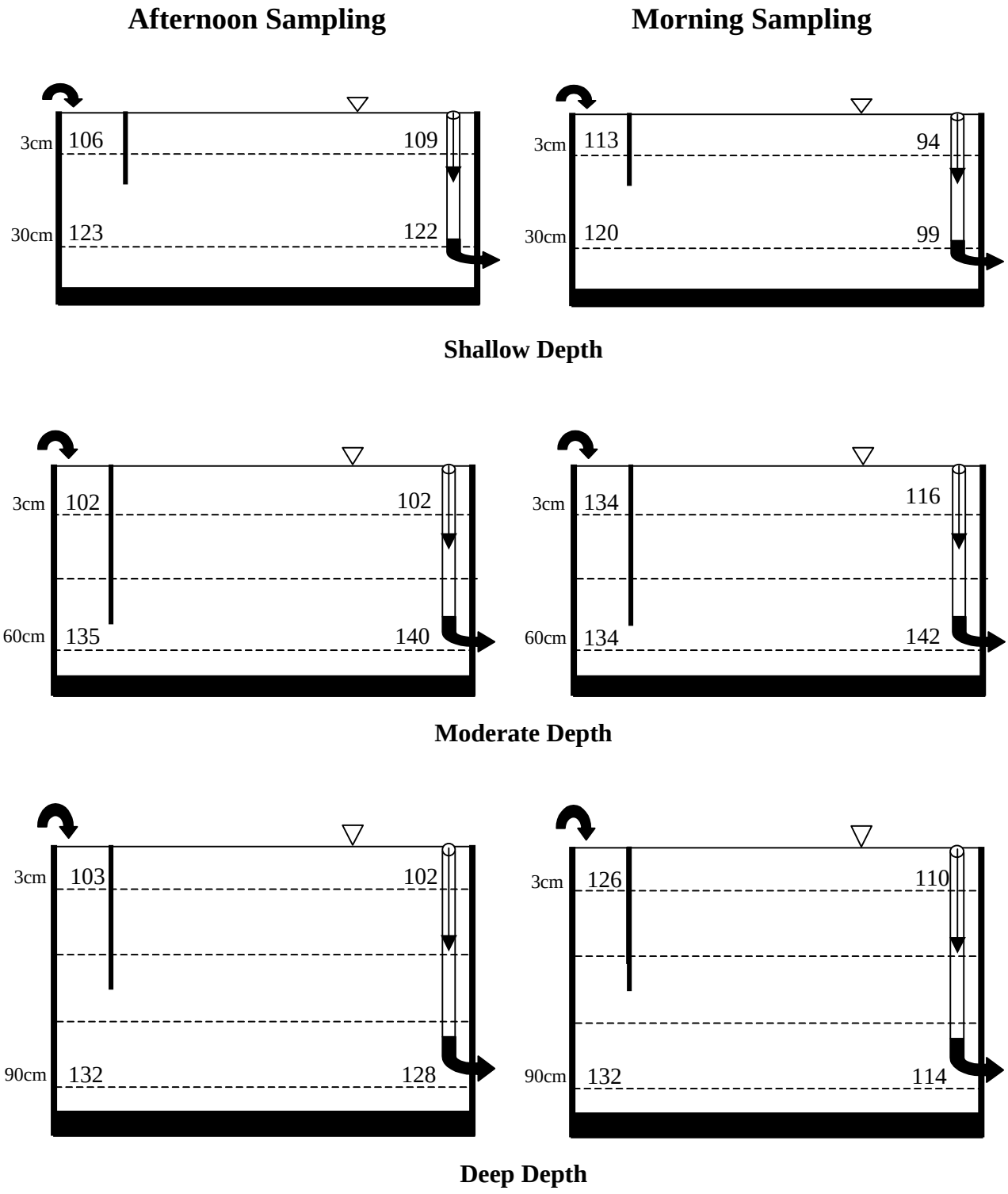

Figure 7.11 Spatial water column characteristics of alkalinity (mg $CaCO_3$/L) in the influent and effluent regions of SAV mesocosms operated at three depths. Afternoon sampling was performed 13:00-16:50 on February 18, and morning sampling was performed before dawn on February 19. Arrows indicate direction of flow.

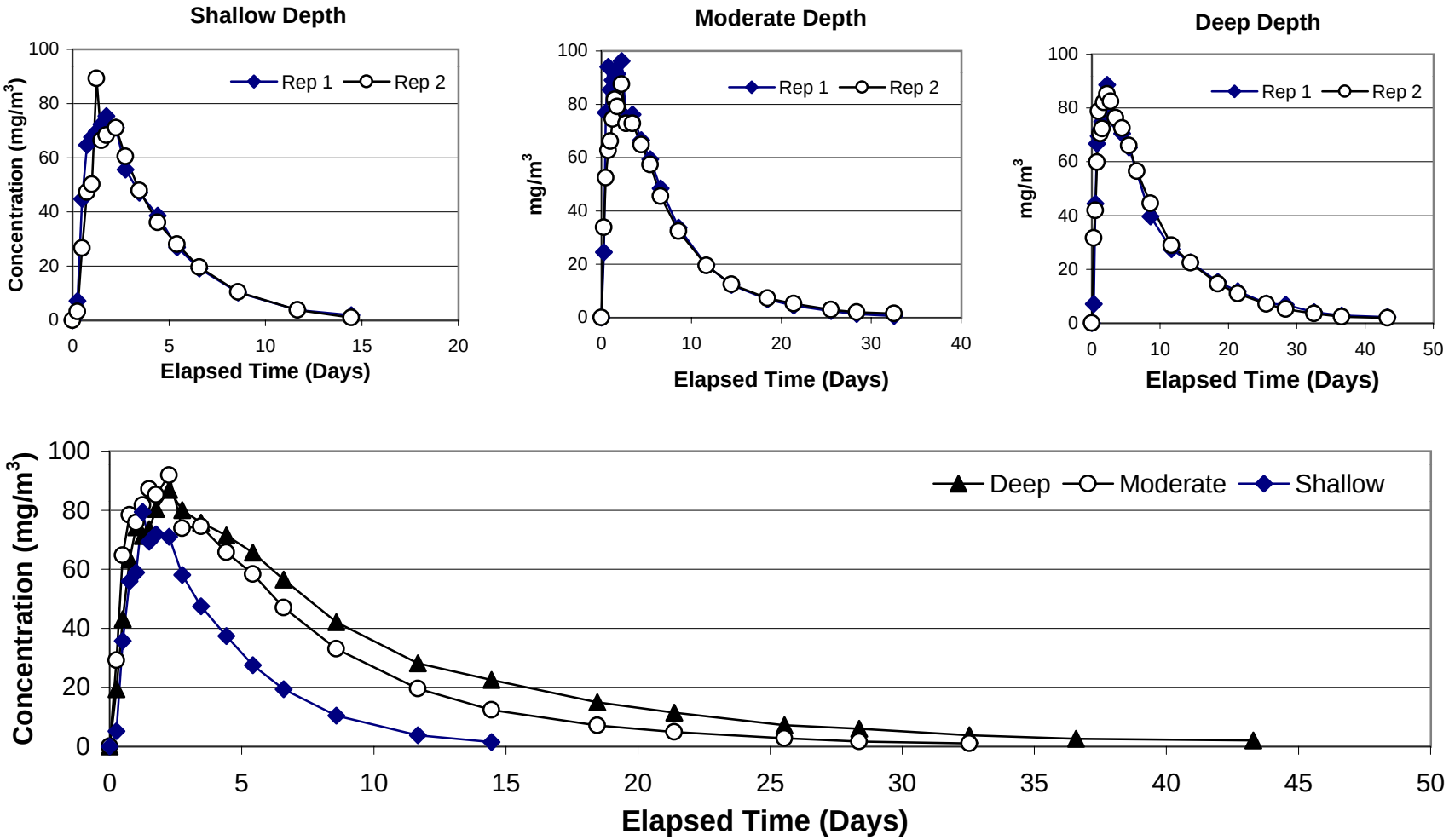

Figure 7.12 Tracer response curves for the fluorescent dye Rhodamine-WT applied to shallow (0.4 m), moderate (0.8 m), and deep (1.2 m) SAV mesocosms. Top figures depict tracer performance for the duplicate mesocosms in each treatment. Bottom figure compares mean tracer performance of the three depths.

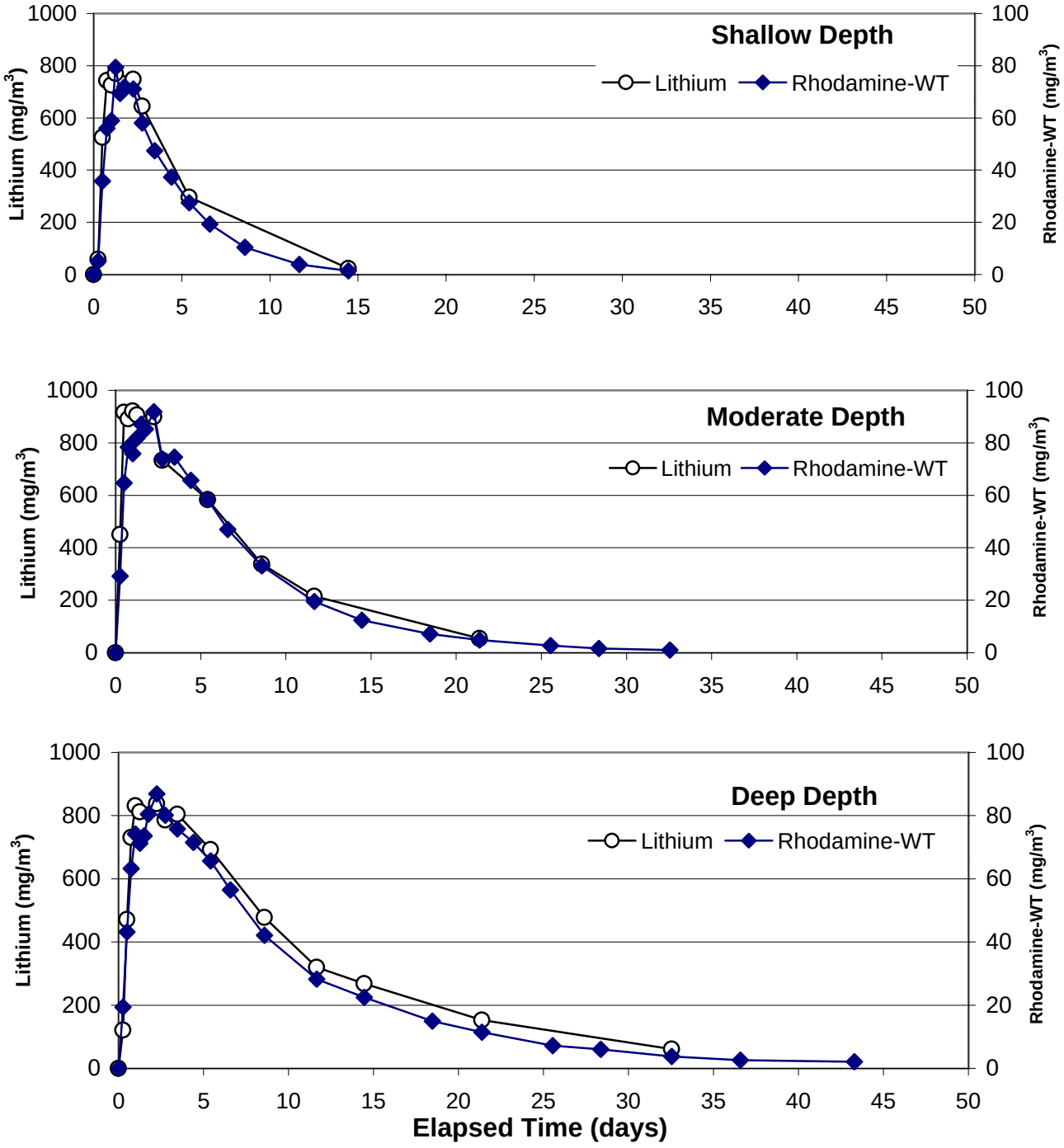

Figure 7.13 Tracer response curve for lithium and Rhodamine-WT applied to the shallow (Z=0.4 m, HRT=3.6 days), moderate (Z=0.8 m, HRT=7.2 days) and deep (Z=1.2 m, HRT=10.8 days) SAV mesocosms.

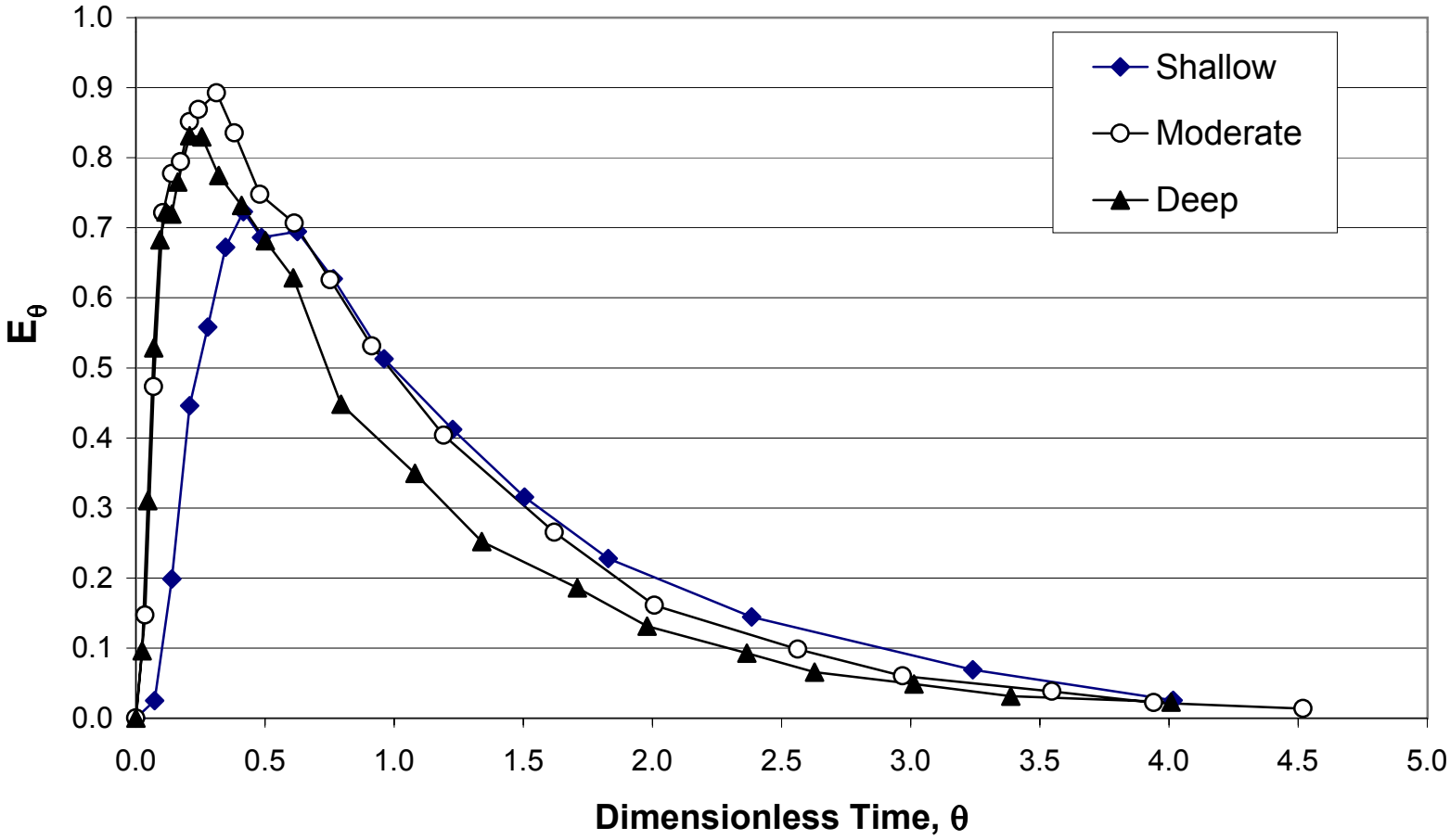

Figure 7.14 Dimensionless residence time distribution (RTD) curves for Rhodamine-WT applied to SAV mesocosms operated at three depths.

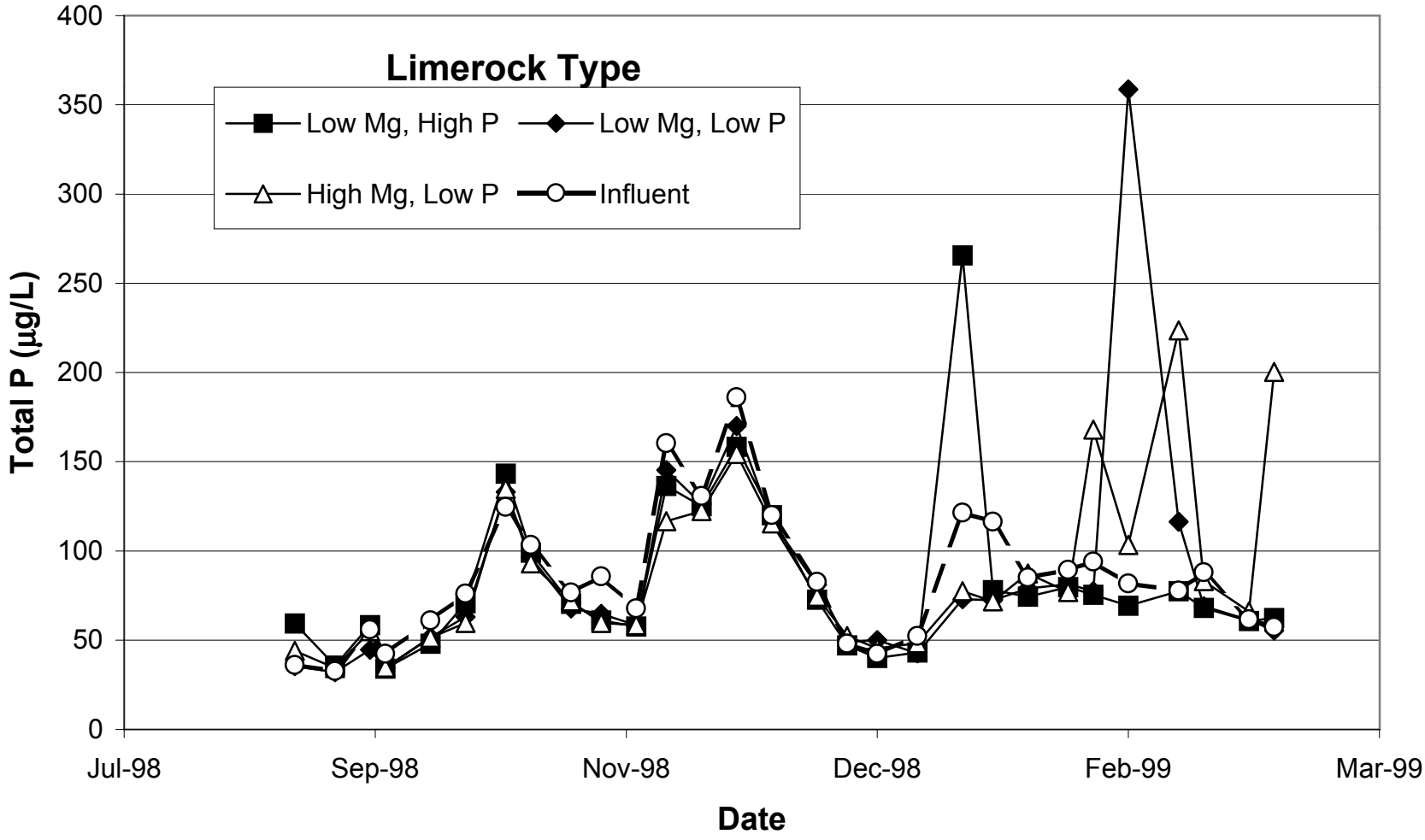

Figure 7.15 Mean influent and effluent total P concentrations (n=3) for LR columns containing three types of limerock. The LR types are described in the text.

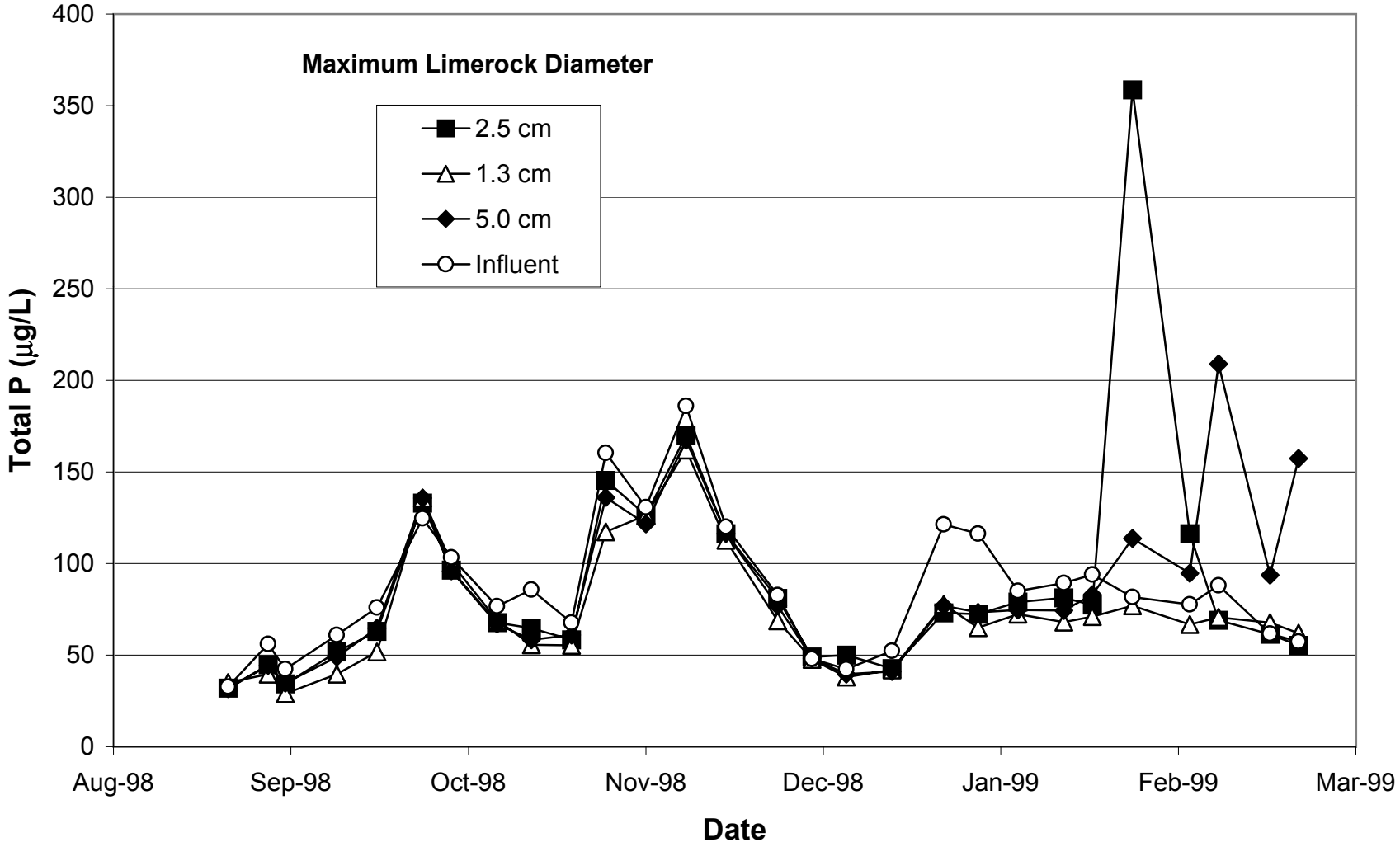

Figure 7.16 Mean influent and effluent total P concentrations (n=3) for LR columns containing three sizes of limerock (PBA caprock).

VIII. Technology Assessment: Subtasks 5A and 5B

Subtask 5A: Field Observations of Different SAV Communities in the ENR Project

Methods

This subtask entailed field observations of different SAV communities in the ENR Project. We performed a brief evaluation of SAV populations in ENR Cells 1 and 4 during late April 1998. This work was conducted to assess which SAV species should be stocked into our experimental mesocosms and to obtain a preliminary assessment of water quality profiles in the SAV-populated regions of the ENR. On April 30 and May 1, 1998, we measured TP, SRP, temperature, pH, conductivity, and dissolved oxygen profiles at six stations in Cell 4 and at two stations in Cell 1 of the ENR. The station locations followed a north-south transect and were selected based on SAV community characteristics, and on their proximity to major inflows and outflows of the cells. All measurements and grab samples were performed between 10:40 and 15:25. Water column depths ranged from 0.7 to 0.9 m in both cells, with 0.2 - 0.4 m of free water observed above the SAV beds (except for the *Ceratophyllum* bed in cell 4). TP was not sampled at the bottom stations in Cell 4 because of particle resuspension during the sampling process.

On December 19 and 20, 1998, we performed more rigorous sampling in these same ENR Cells. In Cell 4, we collected four sediment cores from the influent region, and three sediment cores from the effluent region. These cores were sectioned into three depth fractions (0 - 4 cm, 4 - 10 cm, and 10 - 20 cm), and transported to the lab for bulk density, Ca, TP, and total C and N analyses. Samples of SAV were also collected from these sites and analyzed for dry weight standing crop and the above-listed elements. Water samples were collected in Cell 4 during the daytime (12:15 - 16:05) at the influent, effluent, and along two transects (both perpendicular to flow) situated across the middle of the cell. These samples were analyzed for TP, TSP and SRP, dissolved Ca and alkalinity.

In Cell 1, we established three transects, running from influent to effluent regions. The western and central transects each had five sampling stations, and the easternmost transect had

three sampling locations. In order to characterize diel variations in water quality, we sampled the five westernmost transect stations during both night (03:00 - 06:00) and daytime (11:00 - 17:00) hours. The remaining Cell 1 sample locations were sampled only during the daytime (11:00 - 17:00).

At each site, field measurements were performed (D.O., temperature and pH) and water samples were collected from two depths (10 cm below surface and 10 cm above bottom). The water samples were field-filtered and transported to the lab for analyses of TSP and SRP.

Results and Discussion

Characterization of ENR Cells 1 and 4 in April 1998

In April 1998 we found ENR Cell 4 to be dominated exclusively by SAV species, primarily *Najas*, with some *Ceratophyllum*, *Potamogeton*, and *Chara*. By contrast, Cell 1 contained dense cattail stands along its eastern edge, as well as near the influent and effluent regions of the Cell. The middle of Cell 1, largely open water, was populated with sparse SAV beds containing the above mentioned species as well as *Hydrilla*.

Cells 1 and 4 both exhibited a decline in water column TP concentrations from inflow to outflow regions (Table 8.1). The Cell 1 water column had slightly higher TP concentrations than Cell 4. This is presumably due to the higher constituent concentrations of waters flowing into Cell 1, which receives drainage water directly from the buffer cell. Outflow region TP levels also were higher for Cell 1 than for Cell 4. Water column pH and temperature levels were comparable in the SAV communities in the two cells.

In Cell 4, characteristics of the SAV communities appeared to influence the water chemistry within the beds. The dense, topped out *Ceratophyllum* bed depressed the D.O. concentrations and pH values, probably because of shading effects (Table 8.1). Phosphorus concentrations were high near the *Ceratophyllum* beds, likely because of their close proximity to the Cell 4 inflow culverts. Immediately "downstream" of the inflow region of Cell 4, the P concentrations within the SAV beds were rather uniform, and similar to the outflow concentrations.

In Cell 4, most water quality constituents exhibited little variation with depth. Environmental conditions 0.1 m below the water surface, at mid-depth in the water column (frequently within or just above the SAV bed), and 0.1 m above the sediment were quite similar

Table 8.1. Mean water quality characteristics along longitudinal transects from inflow to outflow at two stations in ENR Project Cell 1 and six stations in ENR Project Cell 4. Each station represents the average of either two or three depths from which measurements were conducted on April 30 and May 1, 1998. For dissolved oxygen concentrations, the range is provided in addition to the mean.

	ENR Cell 1						
Distance from Inflow (as % of cell length)	**Dominant SAV**	**Temp (°C)**	**DO (mg/L)**	**pH**	**Cond (µmho/cm)**	**SRP (µg/L)**	**TP (µg/L)**
31%	*Najas*	28.0	7.8	8.02	480	13	59
97%	*Ceratophyllum*	28.3	8.9	7.95	500	4	33

	ENR Cell 4						
Distance from Inflow (as % of cell length)	**Dominant SAV**	**Temp (°C)**	**DO (mg/L)**	**pH**	**Cond (µmho/cm)**	**SRP (µg/L)**	**TP (µg/L)**
6%	*Ceratophyllum*	25.5	4.5 (1.6-6.0)	7.58	600	19	47
14%	*Najas*	27.3	7.9 (0.4-11.9)	8.50	610	4	25
24%	Mixed	27.4	8.9 (0.4-12.3)	8.14	600	13	38
86%	*Najas*	26.1	6.3 (0.9-9.8)	7.93	520	6	24
Field Duplicate 86%	*Najas*	27.8	6.8 (0.7-10.0)	8.26	530	4	23
96%	*Potamogeton*	26.6	7.7 (6.3-8.5)	8.09	600	4	21
100% (outflow)	None	26.4	8.3 (7.9-8.5)	8.03	600	6	18

Table 8.2. Mean and range of water chemistry depth profile measurements for two stations in Cell 1 and six stations in Cell 4 on April 30 and May 1, 1998.

	ENR Cell 1					
Depth (m)	**Temp (°C)**	**DO (mg/L)**	**pH**	**Cond (µmho/cm)**	**SRP (µg/L)**	**TP (µg/L)**
0.1	28.4 (28.4-28.5)	7.9 (7.4-8.3)	8.01 (7.99-8.03)	500 (500-500)	9 (4-14)	46 (32-61)
0.1 (from bottom)	27.7 (27.4-28.1)	8.8 (8.1-9.5)	7.96 (7.86-8.05)	480 (450-500)	8 (4-12)	46 (35-57)

	ENR Cell 4					
Depth (m)	**Temp (°C)**	**DO (mg/L)**	**pH**	**Cond (µmho/cm)**	**SRP (µg/L)**	**TP (µg/L)**
0.1	26.1 (24.8-27.3)	9.1 (6.0-11.9)	8.02 (7.52-8.44)	580 (510-610)	6 (3-17)	26 (18-47)
0.4	27.0 (25.9-28.2)	9.6 (6.0-12.3)	8.16 (7.63-8.56)	580 (520-610)	8 (4-17)	30 (20-55)
0.1 (from bottom)	27.1 (25.8-28.3)	2.6 (0.4-7.9)	8.07 (7.59-8.54)	570 (480-610)	9 (4-24)	

(Table 8.2). The notable exception was D.O. Of the five SAV-dominated stations sampled in Cell 4, the most consistent water quality with depth was found in the outflow region *Potamogeton* bed, probably due to the low density of plants. The more dense *Najas* and *Ceratophyllum* beds reduced D.O. levels in the underlying waters, but not to the point of anoxia.

One of the six stations sampled in Cell 4 included the outflow, which was characterized by a discernible advective flow and no SAV. Bottom dissolved oxygen at that station was 7.9 mg/L.

We had anticipated finding high pH levels in the mid-depth stations since they were frequently located within or just above the SAV beds. Our lower than expected pH readings were more a function of "microenvironmental" effects than to a lack of a photosynthetically-induced pH rise. When the pH was measured with the electrode positioned immediately within the interfacial zone separating the top of the SAV bed and the water column, higher pH values (8.5-8.8) were routinely observed.

Unlike Cell 4 where the SAV occurs in high densities, the SAV in Cell 1, where it exists, appeared to occur at a low standing crop biomass. As a consequence, light penetrated to the bottom of the water column. The dissolved oxygen at the bottom was generally higher (by up to 1 mg/L) than in the surface waters.

Characterization of ENR Cells1 and 4 in December 1998

Water Column Characteristics of Cells 1 and 4

Our water column transect sampling of *Typha* and SAV in Cell 1 revealed dramatic differences between the two communities. SAV sampling locations exhibited very high daytime D.O.s (mean of 11.0 mg/L), and low concentrations of SRP (5 µg/L) and DOP (4 µg/L). These values reflect the mean of both surface and bottom sampling stations. *Typha* beds, by contrast, had low daytime D.O. (0.4 mg/L), and high concentrations of SRP (50 µg/L) and DOP (9 µg/L) (Fig. 8.1). The conditions under which we sampled probably represented a "best" case for the characterizing water column conditions of the two communities, because inflow to the ENR had been curtailed for the preceding four days due to construction activities, and there was no "free water" situated above the SAV beds.

We sampled the westernmost transect of Cell 1 during both daytime and nighttime hours to characterize diel variability in the above parameters. Even at night, there were marked differences for D.O. (4.8 mg/L for SAV; 0.6 mg/L for *Typha*), SRP (8 µg/L for SAV; 55 µg/L for *Typha*) and

DOP (5 µg/L for SAV; 9 µg/L for *Typha)* between plant communities (Fig. 8.2). The fairly consistent SRP levels over a diel period in Cell 1 complements our previous mesocosm observations, where we observed little diel variability in P species in the system effluents.

Our transect sampling across Cell 4, perpendicular to flow, revealed several channels that likely cause short-circuiting. We collected water samples both within the SAV beds and in the channels, to determine whether the channel locations had higher constituent concentrations. Cell 4 influent waters at the time of sampling had the following chemical characteristics: 26 µg TP/L; 11 µg SRP/L; 97 mg Ca/L and 352 mg alkalinity (as $CaCO_3$)/L. The large channel that runs along the eastern (powerline) berm of Cell 4 appeared to create a prominent short circuit through the northern half of Cell 4. We collected a water sample from this channel about one-third down the length of the cell, and it was remarkably similar in composition to the influent waters. Channel constituent concentrations were: 32 µg TP/L; 16 µg SRP/L; 107 mg Ca/L and 340 mg alkalinity (as $CaCO_3$)/L. For Cell 4 in general, TP, SRP, Ca and alkalinity levels were lower in the SAV beds than in nearby channel locations (Appendix F).

Sediment Characteristics of Cell 4

Our Cell 4 core sampling was intended to provide an assessment of physical and chemical characteristics of the sediments that originated from the SAV community. We observed a transition in many of the cores at approximately 4 cm, from a gray, marl sediment to a darker, denser sediment. Assuming that the marl sediment was material newly accreted since the flooding of the ENR Project and the denser sediment represented the original agricultural soil, we selected 0 – 4 cm as the depth of our first core section at all locations. This should not be construed, however, as the total accreted sediment depth since the beginning of operations in Cell 4, since we did not attempt to carefully scrutinize this transition at all coring locations. A second core section was collected between the 4 cm and 10 cm sediment depths, while the last sediment interval consisted of the 10 cm depth to the end of the core, which was usually 20-30 cm. The last two core sections (4-10 cm and 10-20 cm or 30 cm) served the purpose of determining whether muck characteristics varied during the period when agricultural activities were occurring.

Surficial sediments (0 – 4 cm) from four locations near the ENR Cell 4 influent contained higher TP, TC and TN levels than sediments collected from three effluent locations (Fig. 8.3). By contrast, the Cell 4 effluent surficial sediments contained more Ca and had a higher bulk density

(0.12 vs. 0.05 g/cm^3) than influent region sediments. The ENR Cell 4 influent region sediments had a substantially higher P content than the sediments that accrued in the influent region of our experimental mesocosms (1353 vs. 532 mg/kg), although P content at effluent region locations was comparable (574 mg/kg for Cell 4; 473 mg/kg for mesocosms). Mean Ca concentrations in Cell 4 sediments were slightly higher than average Ca levels found in the mesocosm sediments (184 vs. 164 g/kg).

Relative to the underlying muck, the fresh sediment was enriched with respect to both Ca and P (Fig. 8.3), indicating the deposition of a more "marl–like" material. However, relative to the surface sediments, the much higher bulk density of the subsurface muck layers (up to 0.28 g/cm^3) resulted in an increase in most constituents with core depth on a mass per volume basis. For example, the native muck soil (e.g., core depths of 10 to approx. 30 cm) at both influent and effluent regions of ENR Cell 4 contained higher N and P contents than the more recently deposited sediments (Fig. 8.3).

Vegetation Characteristics of Cell 4

Vegetation sampling at the seven Cell 4 locations revealed *Najas* beds at five sites (two influent, three effluent) and *Ceratophyllum* beds at the other two influent locations. At the influent region, the *Ceratophyllum* occurred at a higher standing crop than the *Najas* (1.77 vs. 0.73 kg dry/m^2), and also exhibited higher tissue P and Ca contents (Fig. 8.4). The *Najas* standing crop biomass at the influent region was similar to that of effluent region plants (0.70 kg dry/m^2), although tissue N, C and P contents of effluent region plants were lower (Fig. 8.4).

The standing crop biomass observed for *Ceratophyllum* near the influent of Cell 4 is dramatically higher than that obtained after 8 months growth in the 1.5 day HRT mesocosms (0.15 kg dry/m^2), the only experimental treatment where this species competed well with the other SAV species. The maximum tissue P content of the mesocosm *Ceratophyllum*, however, was much greater than that of plants in Cell 4 (5760 vs. 2290 mg/kg). Unlike *Ceratophyllum*, the maximum standing crop attained by *Najas* in the mesocosms (0.78 kg dry/m^2 at effluent of 3.5 day HRT system) was comparable to that observed for this species in Cell 4. The Cell 4 influent and effluent *Najas* was similar in tissue P content (Fig. 8.4) to the *Najas* in the 7.0 day HRT mesocosms (1470 and 840 mg/kg for influent and effluent, respectively).

In our mesocosms and in ENR Cell 4, *Ceratophyllum* had the highest tissue P content of the SAV species evaluated. Other investigators have noted the high P content of this species: in a hardwater lake with extensive SAV communities, tissue P levels in *Ceratophyllum* (4980 mg/kg) were at least two-fold higher than that of seven other SAV species (Krolikowska 1997).

Subtask 5B: Technology and Environmental Assessments

Because this demonstration project was a mesocosm-scale study, we did not rigorously conform to the Standard of Comparison document upon which all of the Supplemental Technologies ultimately will be based. We do, however, address critical technical, environmental and economic issues in this subsection.

Observations on SAV/LR Systems For Treating Post-BMP Waters, and a Model System for Scale-Up

This study has revealed several key findings related to the use of SAV/LR systems for treating Post-BMP waters. First, our data suggest that SAV-based wetlands would be very effective at removing P. At our longest HRT of 7.0 days, the SAV mesocosms provide effluent water quality comparable to that of the ENR project (Table 8.3). To date, the average settling coefficient (k) for the 7.0 day HRT system was 3.6 times higher than that of the ENR, which suggests that an SAV-dominated STA could be substantially smaller than an emergent macrophyte-dominated STA while meeting the same effluent quality targets. While the exceptional performance of the SAV mesocosms certainly could be related to their small scale or the short duration of the study, our data correlate well with a recent (1996) phosphorus balance, which reported k values of 8, 22 and 21 for ENR emergent plant-based Cells 1, 2 and 3 (W. Walker, April 1997 ETAC presentation). ENR Cell 4, which is an SAV-dominated wetland, had a substantially higher settling coefficient of 50.

Table 8.3. Phosphorus removal performance comparison of the Everglades Nutrient Removal (ENR) project with SAV mesocosms (without limerock beds) operated at two flow rates.

	ENR (full-scale)	**SAV (7.0 day HRT)**	**SAV (3.5 day HRT)**
Depth (m)	varies	0.76	0.76
Inflow (cm/day)	3.1 on average	11	23
HRT (days)	11 to 48	7.0	3.5
Influent [P] (µg/L)	110 (57 - 201)	104 (37-182)	96 (34-178)
Effluent [P] (µg/L)	22 (9 - 39)	18 (8-42)	23 (9-69)
P loading (g/m^2-yr)	1.25	4.0	8.4
P MRR* (g/m^2-yr)	1.03	3.3	6.5
% P load reduction	82	83	77
P settling rate, k (m/yr)	19	69	123

* MRR = mass removal rate

A second important finding is that the SAV unit process appears fairy robust. In this study, diel effects on treatment performance were minimal for both Post-BMP and Post-STA treatment configurations. Similarly, we did not observe any obvious seasonal influence on either SAV effluent concentrations (Fig. 5.2) or P settling rates (Fig. 8.5).

A third key finding is that there appears to exist a P concentration threshold, in the range of 10 - 15 µg/L, below which the moderate depth (0.8 m) SAV unit process cannot remove P at a short (< 7 days) HRT. At this concentration, the SAV effluent P typically is comprised entirely of PP and DOP. The limerock beds situated at the effluent of the SAV mesocosms were effective at removing small increments (5 - 10 µg/L) of this more recalcitrant P. Assuming good performance of the SAV unit process, this incremental P removal by the LR bed may be enough to achieve the 10 µg/L Supplemental Technology target default concentration specified in the Everglades Forever Act. However, the long-term effectiveness of such physical filtration and adsorption processes within a LR bed is unknown.

Shallower water column depths also appear to promote lower effluent TP levels. The water column of shallow SAV systems did not exhibit vertical P concentration gradients, and it is likely that they contained fewer non-vegetated "dead spaces".

In order to test a "model" SAV/LR system that can reduce Post-BMP TP levels down to 10 µg/L, we established a sequential system that consisted of a deep SAV (0.8 m deep) mesocosm with a 3.6 day HRT, followed by shallow SAV (0.4 m deep) mesocosm with a 1.8 day HRT. A LR bed with a 1 hr retention time served as the final unit process. From mid-November 1998 through February 1999, this system produced a mean effluent TP of 9 µg/L (Fig. 8.6) at a HLR of 400 L/day (23 cm/day). Influent TP levels during this period averaged 130 µg/L, and intermediate location TP values were 24 µg/L (effluent from deep SAV) and 11 µg/L (effluent from shallow SAV). Cost calculations for an operational-scale deep - shallow SAV/LR configuration are provided in Section IX.

Efficiency of Nutrient Concentration and Load Reduction

We assessed the efficiency of concentration and load reduction by SAV/LR systems for both north site and south site experiments. This section contains a synopsis of concentration reductions and mass and percentage removal rates for TP in key experiments.

North Site, Post-BMP Waters

Hydraulic Retention Time Study (June 1, 1998 – February 2, 1999)

- For the shortest SAV HRT assessed (1.5 days) the mean influent TP of 98 µg/L was reduced to 39 µg/L. The mass P removal rate was 11.8 g/m^2-yr, with 61% of the TP load removed (mass basis). The LR bed further reduced effluent TP levels to 32 µg/L, primarily by filtering PP.

- For the 3.5 day SAV HRT treatment, the mean influent TP of 96 µg/L was reduced to 23 µg/L. The mass P removal rate was 6.5 g/m^2-yr, with 77% of the TP load removed (mass basis). The LR bed further reduced effluent TP levels to 15 µg/L, primarily by filtering PP.

- For the 7.0 day SAV HRT treatment, the mean influent TP of 104 µg/L was reduced to 18 µg/L. The mass P removal rate was 3.3 g/m^2-yr, with 83% of the TP load removed (mass basis). The LR bed further reduced effluent TP levels to 12 µg/L.

Depth Study (July 23, 1998 – March 5, 1999)

- For the deepest (1.2 m) SAV mesocosm, the mean influent TP of 109 µg/L was reduced to 19 µg/L. The mass P removal rate was 3.3 g/m^2-yr, with 83% of the TP load removed (mass basis).

- For the 0.8 m deep SAV mesocosm, the mean influent TP of 108 µg/L was reduced to 17 µg/L. The mass P removal rate was 3.4 g/m^2-yr, with 85% of the TP load removed (mass basis).

- For the 0.4 m deep SAV mesocosm, the mean influent TP of 99 µg/L was reduced to 13 µg/L. The mass P removal rate was 3.2 g/m^2-yr, with 89% of the TP load removed (mass basis).

Sequential System (November 18, 1998 – March 5, 1999)

This system consisted of three components: a deep SAV system, a shallow SAV system, and a limerock bed.

- For the deep (0.8 m) SAV mesocosm, the mean influent TP of 130 µg/L was reduced to 24 µg/L. The mass P removal rate was 8.6 g/m^2-yr, with 82% of the TP load removed (mass basis).

- For the shallow (0.4 m) SAV mesocosm, the mean influent total P of 24 µg/L was reduced to 11 µg/L. The mass P removal rate was 1.1 g/m^2-yr, with 54% of the TP load removed (mass basis).

- For the combined DSAV and SSAV process train, the mean influent TP of 130 µg/L was reduced to 11 µg/L. The mass P removal rate was 4.8 g/m^2-yr, with 92% of the TP load removed (mass basis). The LR bed further reduced effluent TP levels to 9 µg/L.

South Site, Post-STA Waters

Shallow, Low Velocity Raceway (July 2, 1998 – March 2, 1999)

For this shallow, periphyton-dominated system, the mean influent TP of 17 µg/L was reduced to 10 µg/L. The mass P removal rate was 0.29 g/m^2-yr, with 26% of the TP load removed (mass basis). The LR bed further reduced effluent TP levels to 8 µg/L.

Deep, Low Velocity Mesocosm (July 8, 1998 – March 2, 1999)

For this deep, macrophyte-dominated system, the mean influent TP of 16 µg/L was reduced to 14 µg/L. The mass P removal rate was 0.15 g/m^2-yr, with 13% of the TP load removed (mass basis). The LR bed further reduced effluent TP levels to 11 µg/L.

Interrelationships Among HLR, HRT, Phosphorus Loading and Water Depth

At the North Supplemental Technology Site, we conducted two studies that provided treatments with varying HRTs. In the HLR study (Subtask 4C), the mesocosms were operated at a constant depth (0.8 m), so the varying HLRs (from 11 to 53 cm/day) resulted in HRTs ranging from 1.5 to 7.0 days. Mass P removal rates were higher at the higher HLRs (and shorter HRTs), whereas the longer HRTs (and lower HLRs) were required to achieve SAV effluent concentrations below 20 µg/L (Table 8.4). In the second study (Subtask 4F), we established SAV mesocosms at three water depths (0.4, 0.8 and 1.2 m deep) and provided Post-BMP inflow water at a constant HLR (10 cm/day). The differing depths provided HRTs that ranged from 3.6 to 10.8 days. In general, effluent quality was comparable (slightly better for the shallowest treatment) and mass P removal rates were almost identical for all treatments in the depth study (Table 8.4).

A confounding factor to these studies is that because all mesocosms were fed source water (Post-BMP runoff) with similar TP concentrations, the P loading always increased with increasing HLR. To separate P loading effects from HLR effects would require a separate experiment, where these two factors are kept independent by varying inflow P concentration among treatments. Our data from the North Supplemental Technology Site suggest that HLR (and/or P loading), not HRT, is a master factor in controlling mass P removal and effluent P concentrations in SAV wetlands (note, too, that the 4C and 4F mesocosms operated at similar HLRs provided comparable mass P removal rates and effluent TP concentrations) (Table 8.4). Due to the exemplary performance of the shallow SAV mesocosms (4F and sequential systems), water depth seems to be a second prominent factor that controls performance.

Table 8.4. Comparison of TP removal performance (Post-BMP feedwater) of various mesocosm treatments at the North Supplemental Technology Site.

Treatment	HLR (cm/d)	HRT (days)	Depth (m)	Total Phosphorus (µg/L)			P Mass Removal Rate ($g/m^2 \cdot yr$)
				Influent	SAV Effluent	Limerock Effluent	
Subtask 4C	55	1.5	0.8	98	39	32	11.8
	23	3.5	0.8	96	23	15	6.5
	11	7.0	0.8	104	18	12	3.3
Subtask 4F	10	3.6	0.4	99	13	-	3.2
	10	7.2	0.8	108	17	-	3.4
	10	10.8	1.2	109	19	-	3.3
Subtask 4E	10	8	0.8	105	22[1]	-	3.1
Sequential	11	3.6/1.8[2]	0.8/0.4[2]	130	24/11[2]	9	4.8

1 – plants harvested once during study

2 – data from sequential system: 1st value represents deep SAV system, 2nd value is shallow system

Schedule for Timely Implementation and Constructability

SAV/LR Technology has several attributes that should facilitate rapid deployment. Because the District technical and operations staff have successfully developed ENR Cell 4 as a SAV system over the past four years, this serves as immutable "proof of concept" of the constructability of a full-scale SAV unit process. Moreover, the performance of Cell 4 at this large scale (365 acres) has been quite good, which further substantiates the promising findings of DBEL's demonstration study.

The widespread implementation of SAV/LR will be dictated by a number of factors, including additional research on the water column P removal mechanisms as well as the stability of accreted P in the SAV and LR unit processes. The design and construction schedules of the existing STAs also will influence opportunities for SAV/LR deployment. The SAV and LR processes appear compatible with existing STA designs, which should facilitate accelerated implementation of this technology.

Long-Term System Performance, Reliability and Sustainability

Our experimental findings have demonstrated reliable performance of the SAV/LR systems over an eight-month period. Data from ENR Cell 4, which has been operational since 1993, demonstrates that a SAV system can provide high rates of P removal for four years. No such long-term data exist, however, for the LR component.

There are two critical aspects of long-term reliability and sustainability. The first relates to the actual contaminant removal mechanisms that occur in the water column. The second is the stability of the P in the accreted sediments (SAV) and entrained dissolved and organic constituents (LR bed). These can only be addressed through further long-term process-related research.

Because of the enormous scale of operational SAV/LR systems, intensive management of the vegetation will be impractical. Environmental master factors that sculpt the vegetative community therefore must be better understood. It is our contention, based both on our research in mesocosms and observations of ENR Cell 4, that an SAV community can thrive at P concentrations from 150 µg P/L down to 10 µg P/L. This concentration range is critical to providing treatment of Post-BMP waters. Additional ecological research will be required to define the most cost-effective management practices for sustaining a full-scale SAV/LR system. At a minimum, a certain amount of water level and emergent macrophyte control will be required to ensure long-term viability of the SAV-based treatment system.

Compatibility with Existing BMPs and STAs

The SAV/LR system is a wetland-based technology, and therefore is very compatible with the existing STAs. As noted above, we believe the SAV community will thrive and provide treatment for TP concentrations from 150 to 10 µg P/L. Further implementation of farm BMPs, which could result in lower TP concentrations and reduced discharge hydraulic peaks, would be beneficial to the overall performance of an SAV/LR system.

Compliance with Existing State Water Quality Standards and Marsh Readiness of the Effluent

During the conduct of this project, we obtained three indicators of general quality of the effluent from a SAV/LR system.

Chemical Characterization of SAV/LR Waters

The suite of parameters analyzed during September and November demonstrates that most aqueous constituents are either unaffected, or reduced in concentration during passage through a SAV/LR system (Figs. 5.12 – 5.15). Even pH, which during the daytime can get quite high in the SAV component, is reduced markedly by the LR bed at the effluent region of the system (Fig. 5.5).

Bioassays with SAV/LR Waters

The FDEP performed bioassays on the north and south site SAV/LR systems during October and November 1998. DBEL personnel collected water samples from the HRT study (north site) and the 0.65 m deep SAV/LR system (south site) several times weekly, and shipped these to the FDEP laboratory. FDEP personnel established chronic fish (*Cyprinella leedsi)*, zooplankton (*Ceriodaphnia dubia*) and algal (*Selenastrum capricornutum*) bioassay tests using these waters, and also analyzed them for a suite of inorganic and organic constituents (FDEP, 1999). Algal growth potential tests were also performed by FDEP.

None of the waters (SAV influent, SAV effluent and LR effluent) tested at the south site caused adverse effects to the organisms. By contrast, a SAV effluent sample from the north site slightly reduced fish survival (by 12.5% relative to the control water). Although the FDEP investigators concluded this reduction was statistically significant, they did not consider it "biologically" significant because acceptability criteria for the fish test allows up to 20% mortality in the control replicates (FDEP, 1999). Adverse impacts to water fleas also were found with the north site LR effluent sample. The investigators found a 50% mortality, and concluded that this effect was biologically significant. However, no obvious toxic constituents were detected in the water sample used for this test.

We have no good explanation for the adverse impacts to the water fleas from the north site LR effluent sample. The SAV effluent sample, which was the feedwater to the LR bed, caused no

adverse effects to the water fleas. This suggests that perhaps the limerock itself released toxic constituents. However, the limerock used for the north site experiments was similar (collected from same strata and location in the quarry) to the limerock used in the south site, where the LR effluent waters created no adverse effects. Another possible source of toxicity may have been the individual plastic barrel that contained the limerock, although these containers were all purchased new, and had been subjected to a continuous water flow for four months prior to collection of the bioassay waters. With no conclusive reason for the observed water flea toxicity, we suggest additional bioassays be performed during the Phase II research program with this technology.

The nutrient removal capacity of the SAV/LR treatment system is demonstrated by the algal growth potential tests. For the north site, the algal growth of the influent was reduced 15-fold in the SAV effluent and 5-fold in the LR effluent. Because of the low influent nutrient concentrations, the degree of the reduction in the algal growth potential by the treatment train at the south site was not as pronounced as it was for the north site. Nevertheless, the influent water algal growth potential was reduced 3 to 4-fold after the influent water passed through the SAV mesocosm and LR bed (FDEP 1999).

Mercury Sampling of SAV/LR Systems

During November 1998, District personnel performed mercury (Hg) sampling at the north and south SAV/LR facilities, and sent these samples to the FDEP laboratory for analyses. At the south site, little change in total Hg concentrations were observed with passage through the systems, with influent levels ranging from 0.25 – 0.65 ng/L, and effluent samples in the range of 0.51 – 0.70 ng/L. Influent methyl-Hg values at this site were 0.020 – 0.044 ng/L, and effluent values ranged from 0.030 to 0.17 ng/L (Fink, 1999).

Mercury concentrations in the Post-BMP waters (influent to the north facility) were higher than those in the Post-STA waters. Influent values for total Hg were 1.4 – 2.3 ng/L, and SAV/LR effluent values typically were lower, at 0.77 – 1.5 ng/L. Methyl-Hg levels in the influent waters (0.44 – 0.51 ng/L) generally were reduced (to 0.064 – 0.18 ng/L) with passage through the SAV/LR systems (Fink, 1999).

Two additional sets of water samples were collected by the District during the winter for Hg analyses, but these data are not yet available.

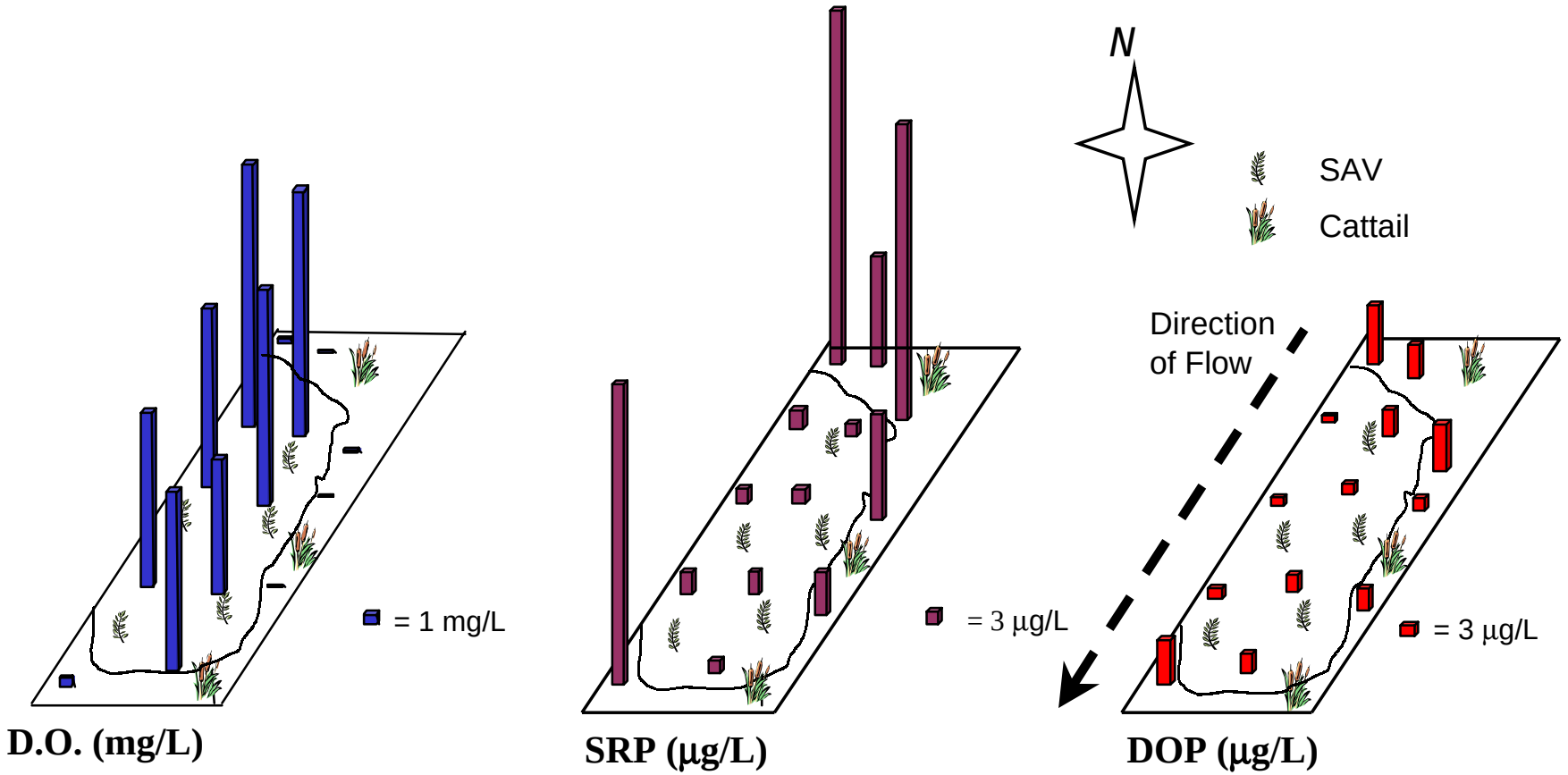

Figure 8.1 Schematic of ENR Cell 1 showing cattail zones (influent, effluent and eastern edge) and SAV zones. Depicted are daytime dissolved oxygen (D.O.), soluble reactive P (SRP) and dissolved organic P (DOP) water column concentrations along three transects running through the two plant communities on December 20, 1998.

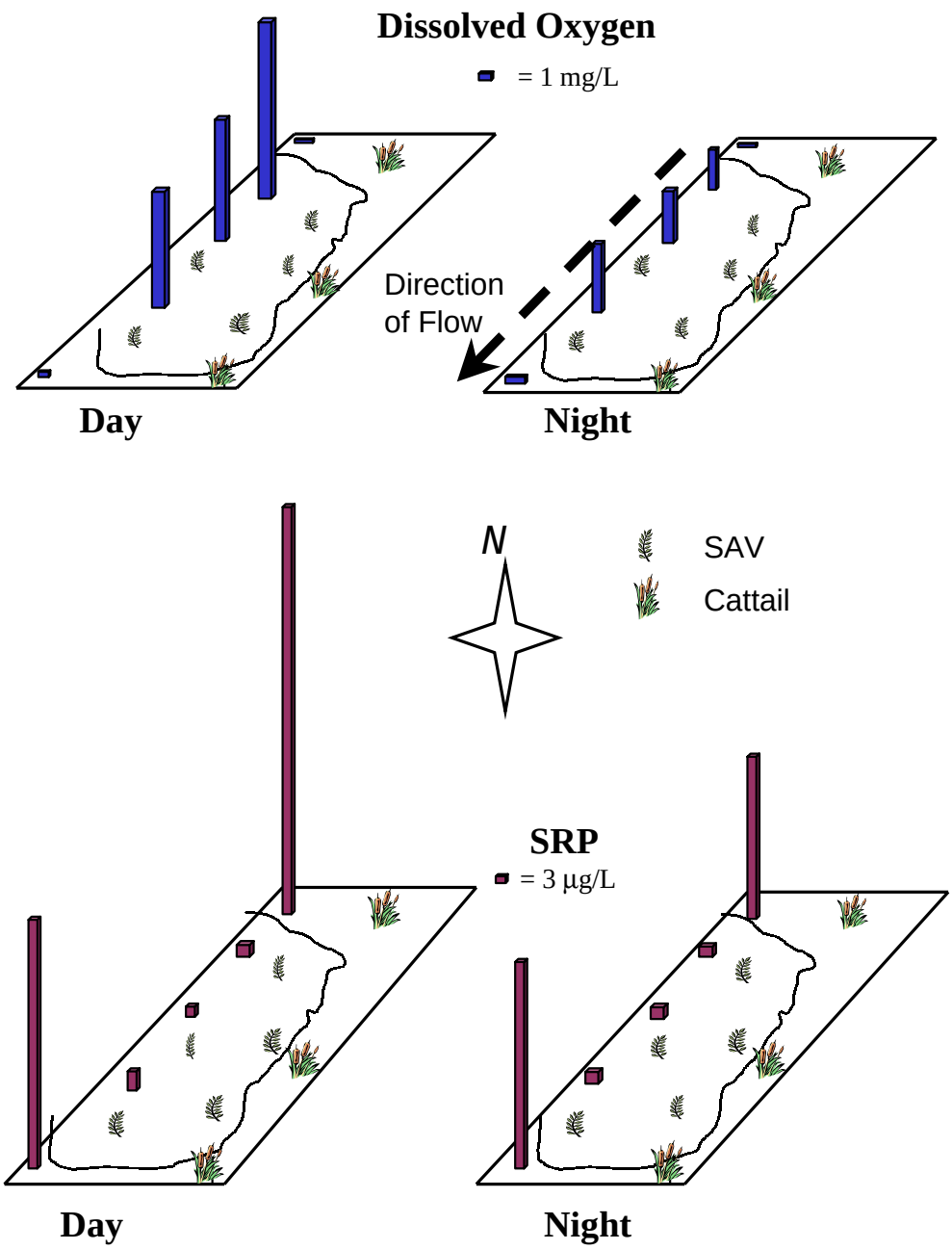

Figure 8.2 Schematic of ENR Cell 1 showing day and night (December 20, 1998) dissolved oxygen (D.O.) and soluble reactive P (SRP) water column concentrations along a single transect that extended through cattail and SAV communities.

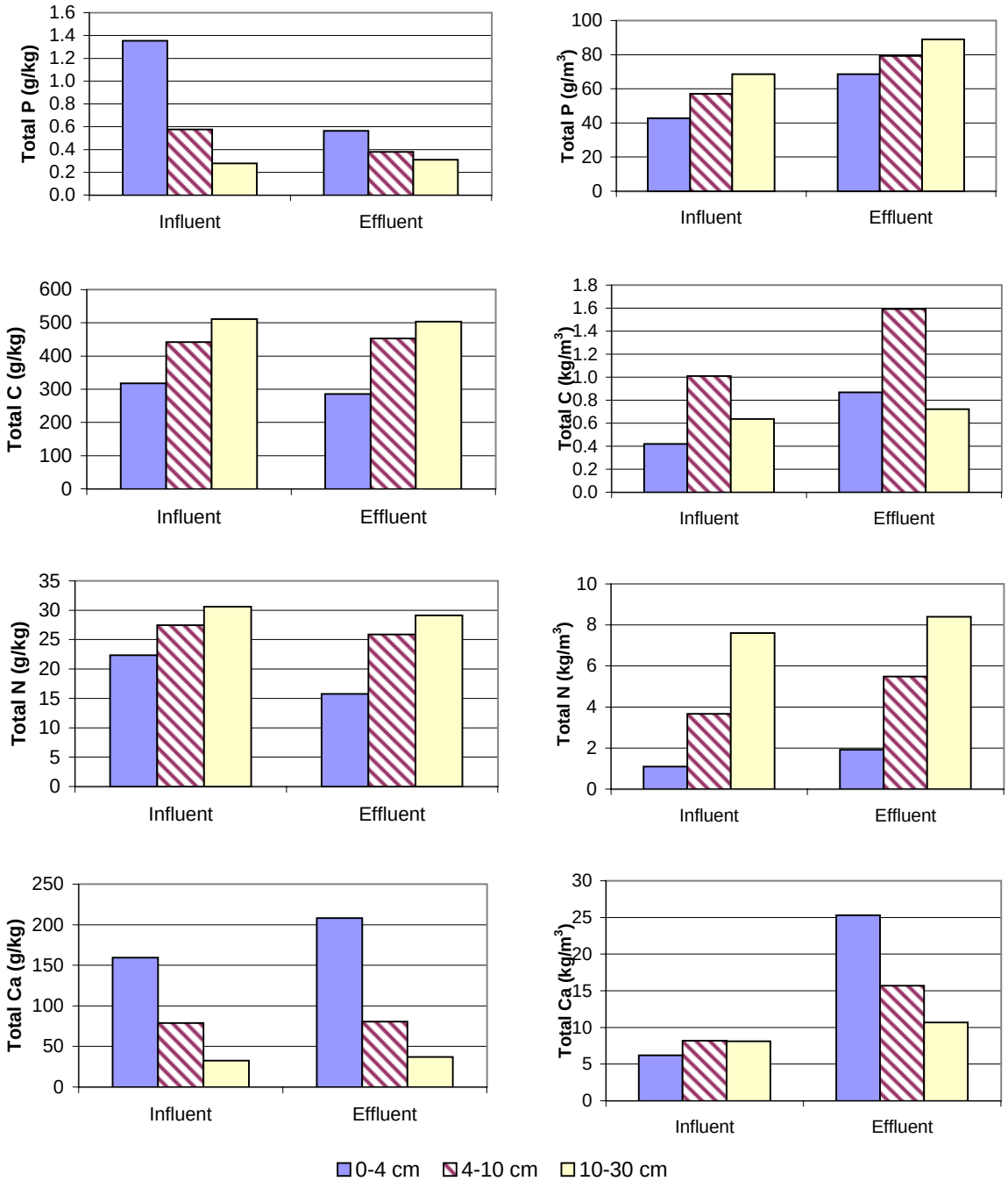

Figure 8.3 Sediment characteristics for the influent and effluent regions of ENR Cell 4. Elemental composition values are expressed in a mass per mass and mass per volume basis. Values represent the mean of four and three cores collected at the influent and effluent regions, respectively.

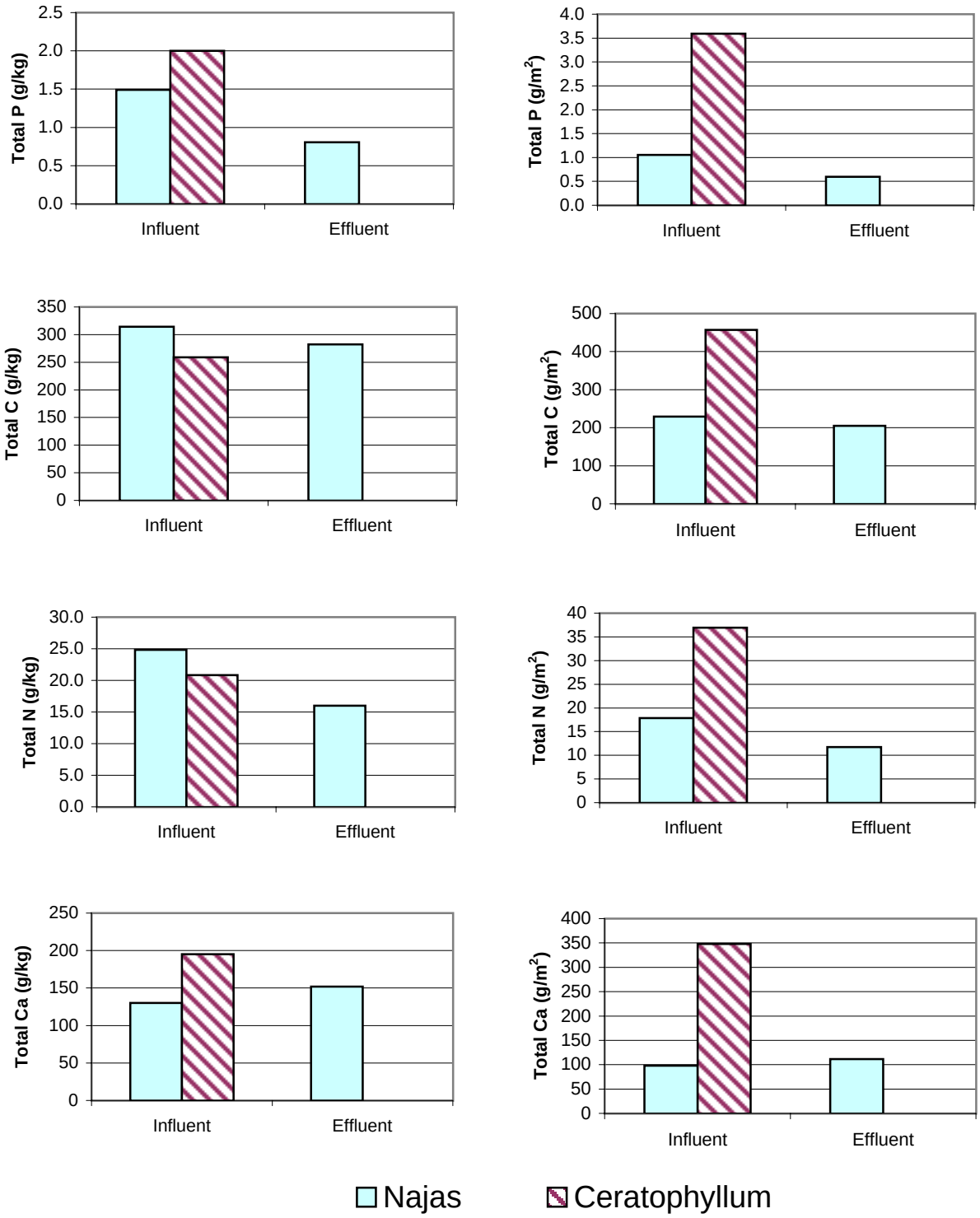

Figure 8.4 Elemental composition of dominant SAV species in the influent and effluent regions of ENR Cell 4. Values represent means of two (influent) and three (effluent) samples.

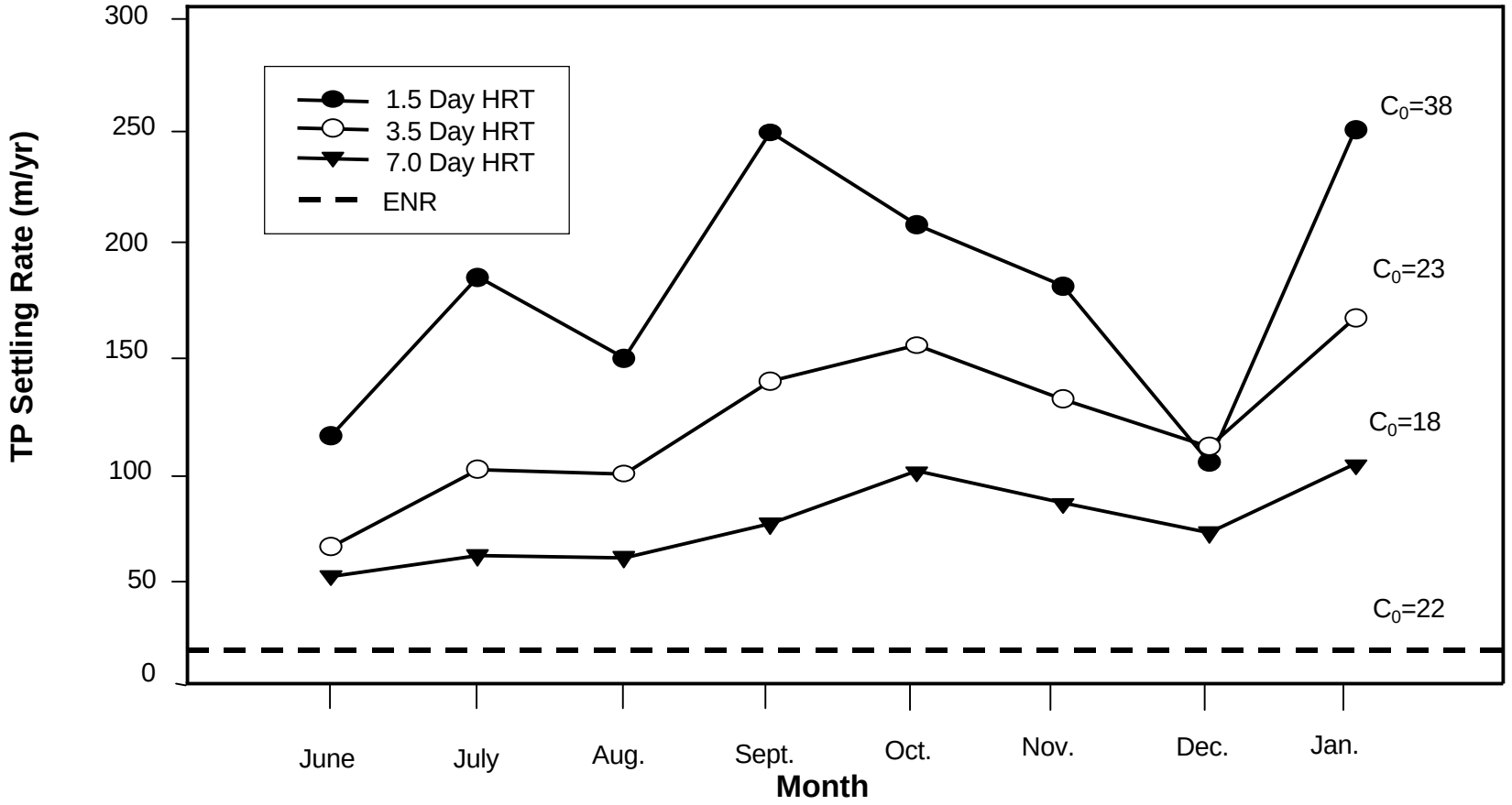

Figure 8.5 Monthly total P settling rates for the SAV mesocosms operated at three hydraulic retention times on Post-BMP waters. The mean annual settling rate for the ENR also is shown. Mean effluent concentration values (C_0 in µg/L) are provided for the SAV system and the ENR.

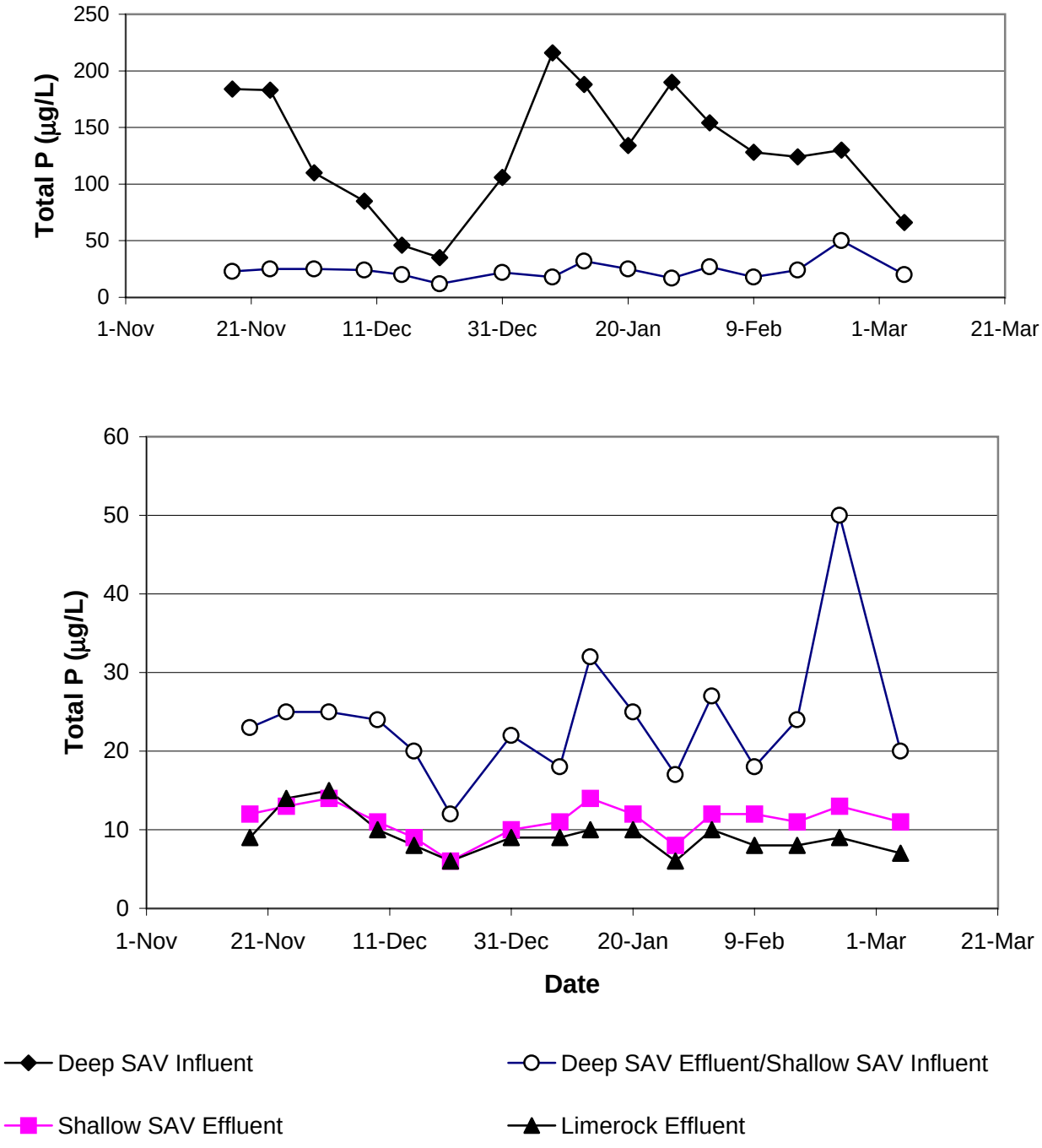

Figure 8.6 Total P removal performance of a sequential SAV/LR system that received Post-BMP waters. The system consists of a deep (0.8 m) SAV mesocosm, a shallow (0.4 m) SAV mesocosm, and a limerock bed. Note that the deep SAV effluent (top graph) is the shallow SAV influent (bottom graph). Values represent means of duplicate process trains.

IX. Economic Analysis: Subtask 5C

DBEL's engineering subconsultant, Wetland Studies and Solutions, Inc. (WSSI) prepared a conceptual cost estimate, based upon mesocosm testing and a schematic system layout, for a full-scale SAV/LR treatment system for removing phosphorus from Everglades Agricultural Area (EAA) runoff assuming Post-BMP inflows. The project team selected a Post-BMP scenario for conceptual design because of the exceptional P removal performance of the SAV/LR system on these waters, and because fairly accurate design and cost data are available for STAs, an existing Post-BMP treatment technology.

This conceptual analysis includes information on the basis of design, water and TP mass balances and cost estimates. The basis for the development of the conceptual design was two data sets, provided by the District, identifying daily flows and TP concentrations into and out of the proposed Stormwater Treatment Area 2 (STA-2) over a 9.75-year period of record. The 50-year present worth costs were estimated using cost data primarily from PEER, Brown, and Caldwell (1996) for the operation of a full-scale treatment facility.

The SAV/LR treatment system conceptual design consisted of three unit processes: (1) a flow equalization basin (FEB), (2) a submerged macrophyte wetland system with two cells of differing depths, and (3) a limerock berm contact process. We modeled this system after the sequential mesocosm experiment we established during the latter portions of the study (Fig. 8.6).

Due to the dramatic pulse hydraulic loadings of the Post-BMP runoff, a flow equalization basin is required to maintain consistent depths in the SAV unit processes. We used somewhat "shallow" depths for the deep SAV and shallow SAV systems (0.6 m and 0.2m, respectively). It is likely that both compartments can be deeper, but we chose these shallow systems for initial, conservative modeling purposes. We also looked at various degrees of bypass of the hydraulic peaks, and we investigated the sensitivity of performance to increasing the area of the treatment system. This initial conceptual model should be considered simply a "range-finding" exercise to determine the sensitivity of SAV/LR system performance to master design factors (flow equalization, bypass, land availability, pumping rates), and not an endorsement of any particular design approach. Indeed, DBEL and WSSI personnel have already formulated several design changes that will be an improvement to the model provided herein.

A. Process Description

Post-BMP agricultural flows are pumped into the FEB to stabilize and store water to achieve a constant water depth through the SAV/LR system. Stored water in the FEB will be released through a water control structure into a deep SAV (DSAV). The DSAV was designed to treat 0.6 m of water for a hydraulic residence time (HRT) of 3 days. Flow from the DSAV will pass through a LR berm (nominal HRT of 1.0 hr) equipped with an internal weir that will decrease the downstream water elevation to 0.2 m, thereby creating a shallow SAV (SSAV). The SSAV was designed to treat the water for a HRT of 1 day. Flow from the SSAV will pass through an additional LR berm (nominal HRT of 0.5 hr) prior to being pumped out. Mesocosm test data to date suggests that this process train layout and HRT can achieve effluent with TP levels as low as 10 ppb. We utilized slightly shorter HRTs for the DSAV and SSAV in this model (relative to our experimental system) because we assume some P removal will occur in the FEB. Depending on how the FEB is managed hydraulically (depth vs. duration), the vegetation may consist of floating, emergent or submerged macrophyte species. The SAV/LR schematic layout is provided in Fig. 9.1.

Note that this is a very preliminary analysis, and does not address site-specific issues (e.g., ground elevations, etc.) that could facilitate or impair construction of a system of this nature.

Sizing Scenario Methods

A. Design Goal

The design goals in sizing the SAVs were to maintain their constant SAV water elevations to:

(1) prevent drawdown and *Typha sp*. growth -

Avoiding drawdown is the most effective way in which to prevent emergent (primarily *Typha sp*.) from establishment and thus obtain the desired SAV dominance.

(2) prevent short-circuiting of flow over the SAV biomass -

Maintaining flows though the SAV by preventing flow above the SAV (i.e., depth-related short-circuiting) will assure maximum contact between the water and the SAV.

The FEB was used to control fluctuating runoff events and store water in order to achieve a constant water elevation in the SAV cells.

B. Optimize Project Sizing

Twenty-two design scenarios (A-V) were analyzed for the SAV/LR treatment technology for removing P from Post –BMP waters. The 9.75 year data set of inflows and outflows from the Stormwater Treatment Area 2 (STA-2) were provided by the District and are the basis of all design sizing and flow rates. Phosphorus removal rates were based on a SAV/LR system effluent P concentration of 10 ug/L.

In each design scenario, continuous pumping occurred if there was at least 2 ft of water in the FEB, otherwise the pumps shut off ($Q_{out} = 0$) until the FEB accumulated over 2 ft of water. Parameters that vary between scenarios were the outflow rates, bypass rates, FEB maximum heights, and the FEB area size. The SAV areas are a function of outflow rates in order to maintain depth and HRT and therefore increase as pumping rates increase. The design parameters for each scenario are provided in Table 9.1. The entire 9.75-year record of analysis for each scenario is provided in the "Supplemental" Appendix. The following design scenario groups describe each method of analysis.

Scenarios A – C. These initial scenarios were established to determine the range of bypass flow (Q_{bypass}) that would be required with varying FEB heights (4.5, 8, and 12 ft), if the total footprint remained constant at 6,430 ac and the pumping rate was equal to the average daily outflow (Q_{ave}= 430.52 ac-ft/day).

Scenarios D – F. These scenarios were established to determine the footprint size range required for varying FEB heights (4.5, 8, and 12 ft) with no bypass flow and a pumping rate equal to the average daily flow (430.52 ac-ft/day).

Scenarios G – I. The bypass flows were determined for constant FEB heights of 4.5 ft and footprint areas of 6,430 ac as the outflow pump rates were increased to 750, 1,000, and 1,500 ac-ft/day. Scenario A also fits into this grouping with a pumping rate of 430.52 ac-ft/day.

Scenarios J – L. The bypass flows were determined for constant FEB heights of 8 ft and footprint areas of 6,430 ac as the outflow pump rates were increased to 750, 1,000, and 1,500 ac-ft/day. Scenario B also fits into this grouping with a pumping rate of 430.52 ac-ft/day.

Scenarios M – Q. The bypass flows for these scenarios were determined for constant FEB heights of 4.5 ft with increasing footprint areas as the outflow pump rates were increased from 430.52 ac-ft/day to 750, 1000, 1,500, and 3,130 ac-ft/day. The footprints were increased such that footprint equaled 6,430 ac plus the SAV areas. The 3,130 ac-ft/day pump rate associated with scenario Q was the pump rate that achieved zero bypass flow.

Scenarios R – V. The bypass flows for these scenarios were determined as in M – Q, but for constant FEB heights of 8 ft with increasing footprint areas as the outflow pump rates were increased. The footprints were increased such that footprint equaled 6,430ac plus the SAV areas. The 1,837 ac-ft/day pump rate from scenario V was the pump rate that achieved zero bypass flow.

Cost Analysis

Cost estimates were based upon the guidelines provided by the PEER, Brown and Caldwell (1996) Desktop Evaluation of Alternative Technologies Final Report. These cost estimates were increased by an annual inflation rate of 3% to convert 1996 costs to 1999 dollars (PEER, Brown and Caldwell, 1996). A 3% inflation for three years

equaled a multiplication factor of 1.0927. A cost analysis spreadsheet, evaluating each design scenario, is provided in Appendix H

A. Capital costs

Pumping Stations. Base construction costs for low head pump stations (associated with Stormwater Treatment Area 2 (STA-2)) were estimated by Prescott Follett & Associates and Brown and Caldwell in April 1996 for Pumping Station G-335 for STA-2 as $16.7 million, exclusive of construction contingencies, engineering, and land purchase. This estimate was assumed to be representative on a unit basis for large pumping stations pumping into and out of STAs. Base construction costs for other capacity pumping stations were assumed to vary on a flow proportional basis. The base construction costs for the medium head and high head pumping stations were estimated to be 10 percent and 25 percent higher than the base construction cost of low head pumping stations for the same flow capacities (PEER, Brown and Caldwell, 1996, pg. 3-6).

Influent pumping stations with FEBs operating at depths up to 4.5 feet were consistent with STA water depths, and therefore were estimated at $16.7 million times an annual 3% inflation rate for three years or $18.2 million. The influent pump station cost estimate was increased by 10% ($20.1) and 25% ($22.8) for medium and high head pump stations associated with 8 ft and 12 ft FEBs, respectively (PEER, Brown and Caldwell, 1996, pg. 3-6).

To be conservative and consistent with PEER, Brown and Caldwell (1996), we used the same cost estimate for the effluent pumping station as was used for the influent pumping station. However, refinement of those cost estimates is expected to realize lower costs for effluent pumping since the peak flow rates are much lower. Therefore, base construction costs for the SAV effluent pump station were determined based on the STA-2 pump station estimates of $16.7 million due to lower heads associated with the SAVs. Thus, the effluent pump station was $16.7 million times 3% interest for 3 years or $18.2 million.

Seepage Pumping Stations. Prescott Follett & Associates and Brown and Caldwell indicated the base construction cost for seepage pump stations to be approximately $680,000 on a unit basis for STAs. Other base construction cost estimates for seepage pumping stations were assumed to

be proportional based on the STA acreage. Therefore, the unit cost for seepage pumping stations including 4.5 ft FEBs were estimated as $0.68 million divided by the area of STA-2 (6,430 ac) times the inflation rate or $116/acre.

The unit cost for medium head seepage pumping stations associated with FEBs up to 8 ft were estimated to be 2 times the base construction cost of STA seepage pumping stations with the same area to overcome the higher heads (PEER, Brown and Caldwell, 1996, pg. 3-6). Seepage pump stations including 12 ft FEBs were assumed to be 2 times the base construction cost of 8 ft FEB seepage pumping stations or $462/acre. The total costs are the unit costs multiplied by the FEB plus SAV areas (which vary between scenarios).

Flow Equalization Basin (FEB). STA-2 construction costs were estimated at $4,583 per acre (PEER, Brown and Caldwell, 1996, pg. 3-7). Cost estimates for FEBs with water depths up to 4.5 ft were consistent with STA-2 construction estimates, and therefore were estimated at $4,583 times the inflation rate or $5,008 per acre. An 80% increase in the STA-2 cost ($8,250 per acre) was estimated for FEB construction up to 8 ft, or $9,015 with 3% inflation for three years (PEER, Brown and Caldwell, 1996, pg. 3-7). Construction costs for 12 ft FEBs were assumed twice the base cost of 8 ft FEBs ($16,500) or 18,030 with inflation rates.

Submerged Aquatic Vegetation Basins (SAV). A construction cost of $5,008 per acre was used for all SAV construction based on STA-2 construction estimates and inflation rates (PEER, Brown and Caldwell, 1996, pg. 3-6).

Limerock Placement Cost. A unit cost of $2 per yard was assumed for the placement of limerock (LR). Linear feet of LR was calculated based on the assumption that the shallow SAV area is square and two sides of the square require LR berms (i.e., LR berms would be located between the deep SAV and shallow SAV areas and at the effluent side of the shallow SAV). Therefore, for example, two sides of a 656 ac SAV are 3,564 yd.

Limerock Freight Cost. A unit cost of $4.45 per ton was assumed for LR freight costs. The amount of LR (tons) required was estimated based on the volume of the LR berms times the density of LR to determine the tons of LR required for the above linear feet of LR berms.

The cross sectional dimensions of the LR berm located between the deep and shallow SAV area were 3 ft high, 30 ft wide base, and 3:1 slopes. The LR berm located at the effluent end of the shallow SAV area was 2 ft high and 24' wide at the base with 3:1 slopes. The cross sectional areas were 63 and 36 sf, respectively. For the above example, the berm volume for 3,564 yd is:

(3,564 yd)(63 + 36 sf) / (9 sf/sy) = 39,204 cy

Therefore, using a density of 2.65 g/cm^3 and 40% void space, the tons of LR can be calculated as:

(39,204 cy)(0.6)(2.65 g/cm^3)(764555 cm^3/cy)(1 lb/454 g) (1 ton/2000 lb) = 52,486 tons

SAV Plant Establishment and Maintenance. During the initial startup phase of a wetlands system, management of water regime (flood quickly and deep, avoid drawdown) is the most effective way in which to prevent emergent species (primarily *Typha sp*.) from establishment and thus obtain the desired SAV dominance. Coupled with this is a need to immediately eradicate *Typha sp*. incursions with herbicides and/or mechanical removal to give SAV the ability to become established and outcompete *Typha sp*. as it has been done in Cell 4 of the Everglades Nutrient Removal (ENR). Initial discussions with SFWMD staff indicate that Cell 4 actually took "little to moderate effort" to kill off *Typha sp.* and confirmed our experience that water regime control is the best way to minimize this cost. During the test cell stage we will need SFWMD staff to review historic records to more accurately determine this cost. For this mesocosm test stage we assume the following costs to eradicate *Typha sp*. and allow SAV to dominate the STA.

$100/ac – Initial Capital Cost

$24/ac/yr – Operating Costs

Construction Contingencies. Construction contingency costs were assumed to total 20 percent of the aggregate base construction cost for all construction components in each treatment train (PEER, Brown and Caldwell, 1996, pg. 3-8).

Engineering, Permitting and Construction Management. Engineering, permitting, and construction management costs were assumed to total 15 percent of construction costs, including construction contingency costs (PEER, Brown and Caldwell, 1996, pg. 3-8).

Land Acquisition Costs. Land acquisition costs for FEBs and SAVs were calculated at $3,500 per acre or $3,825 with inflation costs. It was assumed that 10 percent more land is needed to allow for additional facilities, access roads, and construction and buffer zones where required (PEER, Brown and Caldwell, 1996, pg. 3-8). Therefore, all FEB and SAV areas (which vary by scenario) were increased by 10% to account for these additions.

B. Operation and Maintenance Costs

Pumping Stations. PEER, Brown and Caldwell (1996) estimated annual O&M costs for low-head pumping stations delivering average daily flows of 77 mgd, 114 mgd, and 160 mgd to be $0.46 million, $0.64 million, and $0.71 million, respectively. Annual O&M costs for low-head pumping stations with other average daily flows over the 9.75-year period of record were assumed to vary from these estimates on a flow proportional basis (PEER, Brown and Caldwell, 1996, pg. 3-9). In addition, to avoid duplication of labor costs it was assumed that if both an influent and effluent pumping station were included in a treatment train, the annual O&M cost at each station would be reduced by one third (33 %) to reflect sharing of operations staff between the two (PEER, Brown and Caldwell, 1996, pg. 3-10).

Therefore, costs for influent pumping stations with a 4.5 ft FEB and SAV effluent pumping stations were based on these estimates. A second degree polynomial fit ($r^2 = 1$) was applied to the above flows and costs in the form of:

$$\text{Cost \$} = (-0.2682) + (0.01256)(\text{mgd}) - (0.00004)(\text{mgd})^2$$

The average inflow of 498 ac-ft/day (162 mgd) was calculated as approximately $ 0.72 million. This average inflow cost was multiplied by inflation costs and reduced by one third to reflect sharing costs between influent and effluent pump stations. The resulting cost was approximately $ 0.52 million for low head pumping stations. Medium and high head pumping stations, for 8 ft and 12 ft FEBs, were estimated to be 10 and 20 percent higher ($ 0.58 and $ 0.63 million), respectively (PEER, Brown and Caldwell, 1996, pg. 3-9).

The average outflow of 431 ac-ft/day (140 mgd) was calculated as approximately $ 0.52 million (including inflation costs and sharing savings) for low head pumping stations associated with SAVs. Outflows greater than 431 ac-ft/day were calculated on a flow proportional basis, i.e., for example, an out flow rate of 750 ac-ft/day was 1.7 times (750/498) the average inflow cost estimate (1.7 X $ 0.52 million), or approximately $ 0.90 million.

Seepage Pumping Stations. O&M costs for seepage pumping stations in STA-2 were $110,000 per year. Annual O&M cost for other seepage pumping station were assumed to be proportional to this estimate on the basis of the STA treatment area served (PEER, Brown and Caldwell, 1996, pg. 3-10). Therefore, the unit cost for seepage pump stations for FEB (4.5 ft) and SAVs were calculated as $110,000 divided by the STA area (6,430 ac) times inflation rates, or $19 per acre. The total cost was the unit cost ($19) times the FEB and SAV total areas.

The unit O&M cost for seepage pumping stations from FEBs up to 8 ft will be greater than STAs due to higher water depths and therefore will be 1.5 times the annual O&M costs for STAs, or $28 per acre (PEER, Brown and Caldwell, 1996, pg. 3-10). It was assumed that FEBs up to 12 ft will be 3 times the annual O&M costs for STAs, or $56 per acre.

Flow Equalization Basins (FEB). Annual O&M costs for STAs were estimated as $30 per acre in 1996 (PEER, Brown and Caldwell, 1996, pg. 3-11). The costs for 4.5 ft FEBs were consistent with STA costs and were estimated as $30 per acre times three years inflation at 3%, or $33 per acre.

FEBs up to 8 ft were assumed to be twice the STA cost estimates, or $60 per acre due to higher levees and greater seepage (PEER, Brown and Caldwell, 1996, pg. 3-11). With inflation, the unit cost was $66 per acre. It was assumed that FEBs up to 12 ft were 2 times the cost of 8 ft FEBs, or $131 per acre.

Submerged Aquatic Vegetation (SAV). Annual O&M costs for SAVs were assumed to be equal to the cost estimated for STAs, or $33 per acre (PEER, Brown and Caldwell, 1996, pg. 3-10).

Sampling and monitoring. The total O&M costs for STA sampling and monitoring was estimated to be $300,000 per year (PEER, Brown and Caldwell, 1996, pg. 3-10). Adjusted to 1999 dollars, the O&M cost was $327,818.

SAV Plant Maintenance. As described under Capital Cost, in the SAV Plant Establishment and Maintenance category above, O&M costs were assumed at $24/ac/yr.

Present Worth. The present worth for the O&M costs was calculated using a uniform-series present worth factor (P/A,4%,50yr = 21.4822) times the estimated annual O&M costs. A net interest rate of 4% determined the present worth factor (PEER, Brown and Caldwell, 1996, pg. 3-15; Lindeburg, 1989).

C. *Replacement Costs*

Pumping Stations. Replacement costs were estimated as 25 percent of the construction capital cost estimates for pumping stations with a major rebuild and refurbishment of the equipment. These estimates were multiplied by the present worth factor (P/F, 4%,25yr = 0.3751) based on the equipment being replaced once at the mid-point of the 50-year study period (PEER, Brown and Caldwell, 1996, pg. 3-12; Lindeburg, 1989).

Seepage Pumping Stations. Estimates by Prescott Follett and Associates and Brown and Caldwell indicate that pumping equipment can be expected to account for 50 percent of the total seepage pumping station construction capital costs. Fifty percent of capital unit cost estimates were multiplied by the present worth factor (P/F,4%,25yr = 0.3751) based on the equipment being replaced once at the mid-point of the 50-year study period. Seepage pump station total costs were calculated as the unit cost times the acreage that the pump station serves (PEER, Brown and Caldwell, 1996, pg. 3-13; Lindeburg, 1989).

D. Salvage Value

Demolition Costs. Demolition costs for all components were estimated at 20 percent of the original construction cost (PEER, Brown, and Caldwell, 1996, pg. 3-14).

Restoration Costs. Brown and Caldwell assigned restoration costs to FEBs and STAs for levee demolition. Only perimeter levees were considered. Demolition costs for the STA levees were $300,000 per mile of levee ($327,818 with inflation) based on information provided by the U.S. Army Corps of Engineers. For this analysis, SAV and 4.5 ft FEB levees were assumed comparable to STA levees. The perimeter length of the levees was estimated as the square root of the FEB and SAV areas on the assumption that the areas were square.

FEB levees (with water depths up to 8 ft) were estimated at $400,000 per mile of levee ($437,091 with inflation) based upon a material volume comparison between STAs and FEBs (PEER, Brown and Caldwell, 1996, pg. 3-15). It was assumed that FEB levees (with water depths up to 12 ft) were $500,000 per mile of levee ($546,364 with inflation).

Land Value. The present worth values assumed land salvage value equal to purchase price, or $3,825 per acre (PEER, Brown and Caldwell, 1996, pg.3-15).

E. 50-Yr Present Worth

Present Worth. Present worth of the salvage values was determined as the net salvage value times the present worth factor (P/F,4%,50yr = 0.1407) at the end of the 50 years. (PEER, Brown and Caldwell, 1996, pg. 3-15; Lindeburg, 1989).

Present Worth, $/million gallons treated with bypass. Calculated as the present worth divided by the total inflow of water (bypass + outflow treated) for 50 years.

Present Worth, $/million gallons treated with out bypass. Calculated as the present worth divided by the total outflow of water (treated) for 50 years.

Present Worth, $/pound phosphorus removed. Calculated as the present worth divided by the total phosphorus removed from outflow (treated) for 50 years.

Results and Discussion

The parameters of all design scenarios and their associated cost per lb P removed are summarized in Table 9.1. The results and apparent trends between design scenarios are illustrated in Figures 9.2 – 9.4.

Figure 9.2 shows the relationship between footprint size and bypass percentages for each FEB height at a constant pumping rate. The graph shows that as the footprint is increased the percent flow bypassed is decreased. This trend is apparent regardless of the FEB height. The graph also illustrates that bypass decreases as FEB height increases.

Figure 9.3 shows the relationship between outflow pumping rates and percent bypass flows for 4.5 and 8 ft FEB heights with a constant footprint area. The graph shows that as the outflow pumping rate increases the percent of flow bypassed decreases for both FEB heights. The graph also illustrates that higher FEB height has lower bypass rates for the same area.

Figure 9.4 shows the relationship between footprint size and percent bypass for each FEB height. In this illustration, the flow rate is also increased with footprint size to maintain the design HRT in the SAV/LR as outflow pumping rates are increased. The graph shows that as footprint sizes increase, and therefore as flow rates increase, the percent bypass decreases. This trend is also apparent when the flow rates remain constant as is illustrated by the first two points of both line graphs in Fig. 9.4, although to a lesser degree than when both flow rates and footprints are increasing. This graph also shows that increasing FEB height decreases bypass flows.

Figure 9.5 illustrates the least to most expensive design scenario for P removal and the associated percent of water treated. The graph differentiates which design scenario treats the most water for the least price. The graph shows that scenario K is the most cost effective design. Scenario D is the most expensive per lb P removed due to the extremely large FEB area required to store runoff flows with no bypass and a low FEB height of 4.5 feet.

Conclusions

A. Using the STA-2 footprint for the FEB and SAV areas, the lowest cost per lb of P removed is $83/lb. This is achieved in scenario K where 89% of the inflow is treated. This scenario has a maximum pumping rate of 1000 ac-ft/day, which is 2.3 times the average outflow rate (430.52 ac-ft/day). At this maximum rate, the FEB (sized to store up to 8 ft of water) is reduced to 53% of the STA-2 area. Lowering the FEB storage height to 4.5 feet (scenario H) increases the cost to $85/lb, but only 79% of the inflow could be treated due to the lower storage volume. Although these are optimal costs, the design may not be ecologically optimal because a percentage of the inflow is bypassed and not treated by the SAV with the given STA-2 footprint size and maximum FEB heights of 4.5 and 8 ft. These scenarios (K and H) bypass 11.00% and 21.24% of the inflows with P removal rates of 82 and 69 %, respectively.

B. The lowest cost/lb with no bypass (100% water treated) is $113. This is achieved in scenario V, with a maximum pumping rate of 1,837 ac-ft/day, which is 4.3 times the average outflow rate (430.52 ac-ft/day). At this maximum rate and an 8 ft FEB, the total footprint increases 1.9 times the STA-2 area. Lowering the FEB storage height to 4.5 feet (scenario Q) increases the cost to $125 per lb and increases the total footprint to 2.5 times the STA-2 area. Although the P removal rate is 93% for both scenarios, and treatment costs are still in the average "reasonable " range, these scenarios require a substantial increase in footprint area.

C. This analysis should be considered preliminary, since it doesn't address many potential engineering and site-specific constraints (e.g., is it possible to build and maintain a large, STA cell that is only 0.2m deep?). Moreover, because of specific assumptions used for this analysis, we cannot directly compare the unit P removal costs of SAV/LR treatment with costing data promulgated for the emergent plant-based STAs. Our analysis is useful, however, in that it shows the cost sensitivity of a SAV/LR system to major design variables, such as flow equalization, flow bypass and STA footprint.

Table 9.1. Summary table for submerged aquatic vegetation treatment design scenarios for the Everglades Agricultural Area runoff waters.

Scenario	A	B	C	D	E	F	G	H	I	J	K
Q_{out}	430.52	430.52	430.52	430.52	430.52	430.52	750	1000	1500	750	1000
Footprint	6,430	6,430	6,430	68,320	29,265	18,080	6,430	6,430	6,430	6,430	6,430
$SSAV_{area}$	656	656	656	656	656	656	1,143	1,524	2,286	1,143	1,524
$DSAV_{area}$	656	656	656	656	656	656	1,143	1,524	2,286	1,143	1,524
FEB_{area}	5,118	5,118	5,118	67,008	27,953	16,768	4,144	3,382	1,858	4,144	3,382
FEB_{Hmax}	4.5	8.0	12.0	4.5	8.0	12.0	4.5	4.5	4.5	8.0	8.0
Q_{bypass}%	35.59	22.83	15.44	0	0	0	25.73	21.24	18.4	14.32	11.00
%time	10.03	6.91	5.17	0.00	0.00	0.00	6.82	5.78	5.08	4.24	3.40
P_{bypass}%	37.73	21.26	12.38	0	0	0	29.43	25.64	23.53	14.45	11.78
$P_{removed}$%	58.16	73.67	82.04	94.21	93.85	93.75	65.62	69.03	70.82	79.7	82.06
$P_{removed}$/yr	35,145	44,516	49,574	56,926	56,709	56,647	39,654	41,709	42,796	48,159	49,584
Present Worth											
$/million gallons treated w/ bypass	63	78	111	349	243	262	67	70	75	79	80
$/million gallons treated w/o bypass	108	106	135	349	243	262	95	92	95	95	92
$/pound P removed	92	90	114	314	219	237	86	85	90	84	83

Scenario	L	M	N	O	P	Q	R	S	T	U	V
Q_{out}	1500	430.52	750	1000	1500	3130	430.52	750	1000	1500	1837
Footprint	6,430	7,742	8,716	9,478	11,002	15,970	7,742	8,716	9,478	11,002	12,029
$SSAV_{area}$	2,286	656	1,143	1,524	2,286	4,770	656	1,143	1,524	2,286	2,799
$DSAV_{area}$	2,286	656	1,143	1,524	2,286	4,770	656	1,143	1,524	2,286	2,799
FEB_{area}	1,858	6,430	6,430	6,430	6,430	6,430	6,430	6,430	6,430	6,430	6,430
FEB_{Hmax}	8.0	4.5	4.5	4.5	4.5	4.5	8.0	8.0	8.0	8.0	8.0
Q_{bypass}%	9.83	32.34	20.26	13.78	5.94	0.00	19.12	8.63	3.99	0.60	0.00
%time	2.86	8.90	5.25	3.93	1.83	0.00	6.21	2.70	1.38	0.28	0.00
P_{bypass}%	12.83	33.54	22.12	15.38	6.56	0.00	16.66	7.52	3.36	0.46	0.00
$P_{removed}$%	80.83	62.12	72.53	78.73	86.91	92.97	78.02	86.26	90.01	92.58	92.98
$P_{removed}$/yr	48,842	37,534	43,826	47,573	52,513	56,181	47,144	52,122	54,387	55,942	56,185
Present Worth											
$/million gallons treated w/ bypass	82	69	77	84	96	137	88	96	102	115	124
$/million gallons treated w/o bypass	93	111	101	100	103	137	113	107	107	116	124
$/pound P removed	86	95	90	90	94	125	95	94	96	105	113

Descriptions		Units
Q_{out}	= Daily outflow discharged from flow equalization basin (FEB) - variable in different design scenarios	ac-ft/day
Footprint	= Area of Stormwater Treatment Area 2 (STA-2)	ac-ft
$SSAV_{area}$	= Area of Shallow Submerged Aquatic Vegetation (SSAV)	ac-ft
$DSAV_{area}$	= Area of Deep Submerged Aquatic Vegetation (DSAV)	ac-ft
FEB_{area}	= Flow Equalization Basin (FEB) Area	ac-ft
FEB_{Hmax}	= Maximum FEB Height	ft
Q_{bypass}%	= Percent of flow bypassed from FEB	%
%time	= Percent of time period bypass occurs	day
P_{bypass}%	= The amount of P in bypassed flow	%
$P_{removed}$%	= Percent of total P removed	%
$P_{removed}$/yr	= Yearly removal rate of P	lbs/yr

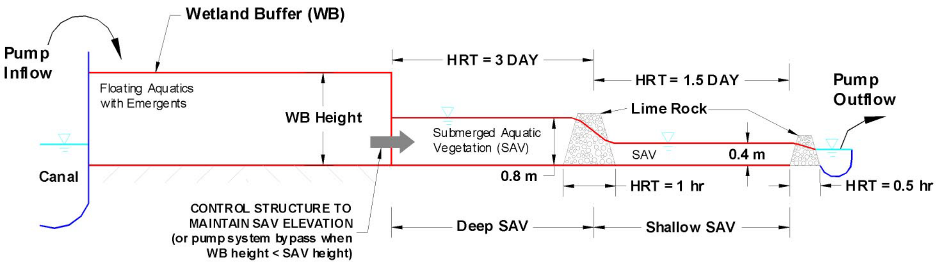

Computer File Name: k:/cadd/4775/sketch.dwg		
Design	Draft	Approved
NF	NF	MSR
sheet # 1 of 1		
SCALE: NOT TO SCALE		
DATE: March 30, 1999		

Attachment 1
SAV/LR SCHEMATIC LAYOUT

Prepared For: South Florida Water Management District

SAV/LR
EVERGLADES NUTRIENT REMOVAL (ENR) PROJECT, SOUTH FL

Wetland Studies and Solutions Inc.
14088-M Sullyfield Circle, Chantilly, Virginia 20151
Phone 703.631.5800 Fax 703.631.5804

Figure 9-2. STA Footprint Vs. Qbypass% at varying FEB heights and at constant Qout = Qave

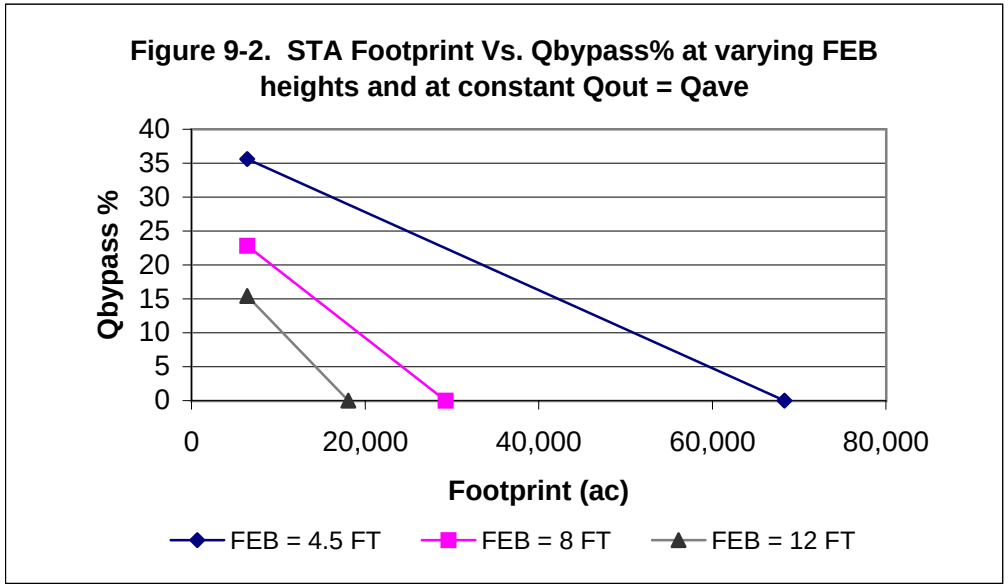

	FEB = 4.5 FT		FEB = 8 FT		FEB = 12 FT	
Scenario	**A**	**D**	**B**	**E**	**C**	**F**
Q_{out}	**430.52**	**430.52**	**430.52**	**430.52**	**430.52**	**430.52**
Footprint	6,430	68,320	6,430	29,265	6,430	18,080
Q_{bypass}%	35.59	0	22.83	0	15.44	0

Figure 9-3. Pumping Rate Vs. Qbypass% at varying FEB heights and Constant STA Footprint = 6,430 ac

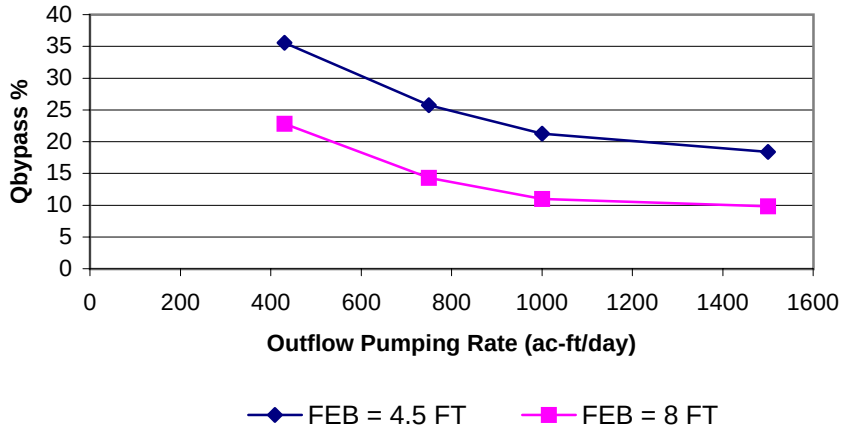

	FEB = 4.5 FT				FEB = 8 FT			
Scenario	**A**	**G**	**H**	**I**	**B**	**J**	**K**	**L**
Qout	430.52	750	1000	1500	430.52	750	1000	1500
Qbypass%	35.59	25.73	21.24	18.4	22.83	14.32	11	9.83

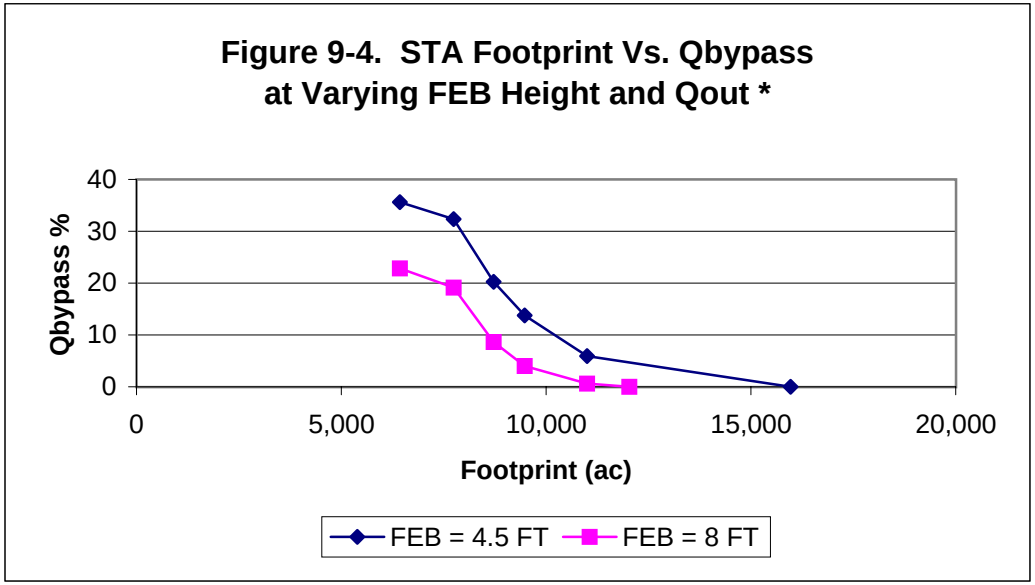

* with footprints varying to maintain design HRT in SAV/LR as outflow pumping rates (Q_{out}) are increased

	FEB = 4.5 FT						FEB = 8 FT					
Scenario	**A**	**M**	**N**	**O**	**P**	**Q**	**B**	**R**	**S**	**T**	**U**	**V**
Qout	430.52	430.52	750	1000	1500	3130	430.52	430.52	750	1000	1500	1837
Footprint	6,430	7,742	8,716	9,478	11,002	15,970	6,430	7,742	8,716	9,478	11,002	12,029
Qbypass%	35.59	32.34	20.26	13.78	5.94	0.00	22.83	19.12	8.63	3.99	0.60	0.00

Figure 9-5. Cost per lb Phosphorus Removed and %Water Treated

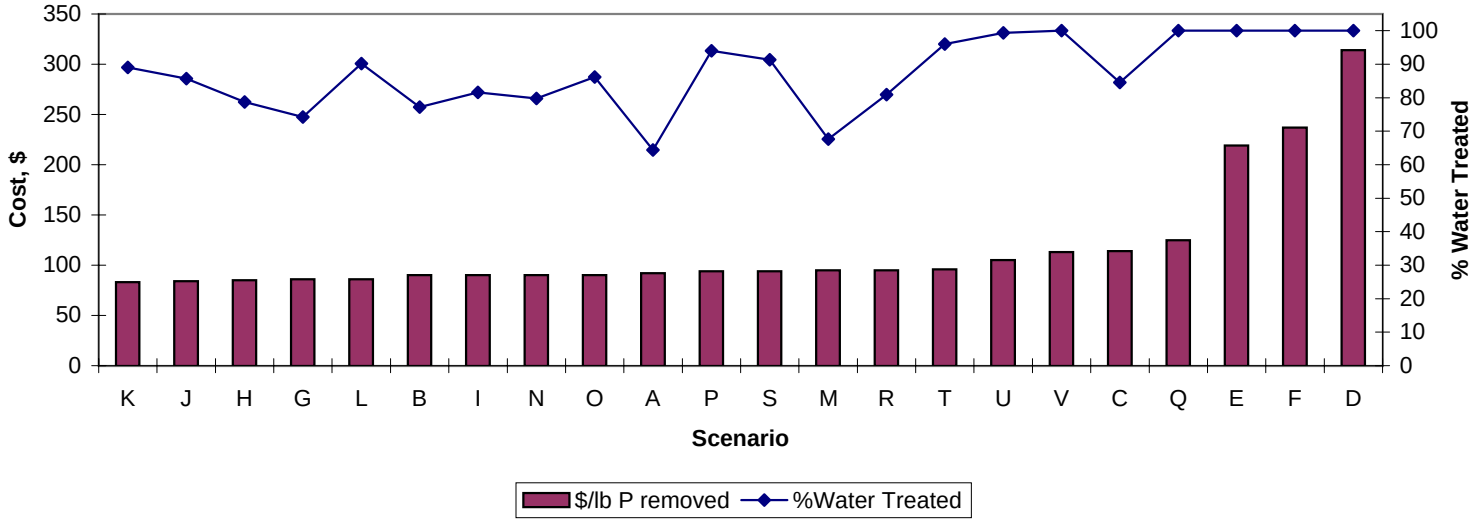

Scenario	A	B	C	D	E	F	G	H	I	J	K
$/lb P removed	92	90	114	314	219	237	86	85	90	84	83
%Water Treated	64	77	85	100	100	100	74	79	82	86	89
Scenario	**L**	**M**	**N**	**O**	**P**	**Q**	**R**	**S**	**T**	**U**	**V**
$/lb P removed	86	95	90	90	94	125	95	94	96	105	113
%Water Treated	90	68	80	86	94	100	81	91	96	99	100

X. Project Reporting and Close-Out: Tasks 6 - 9

Task 6: Project Progress Reports and Review Meetings

- Project quarterly reports were submitted on the following dates: May 28, 1998, September 4, 1998 and November 24, 1998.
- Monthly progress reports were submitted on: July 2, 1998, July 30, 1998, September 28, 1998, October 26, 1998, December 28, 1998 and January 25, 1999.
- Project review meetings were held with DBEL, District and FDEP scientists on the following dates: August 6, 1998, September 29, 1998 and November 18, 1998.

Task 7: Final Work Products

This report is one of two final work products for this demonstration project. The second is a publication on the project's findings.

Task 8: Chemical/Residue/Process Byproduct Handling, Storage and Disposal

There were no anthropogenic chemicals used or stored at either of the Supplemental Technology Sites during this study.

Task 9: Equipment Disassembly and Site Restoration

Experiments are still underway at both sites, so no disassembly has been performed. Once the study is complete, all tanks and piping will be removed. Any excess limerock will be disposed of at the site (we will use it for filling in erosion gulleys on the existing limerock pads).

XI. References

Adey, W., Luckett, C. and K. Jensen. 1993. Phosphorus removal from natural waters using controlled algal production. Restoration Ecol. 1: 29-39.

DB Environmental Laboratories, Inc. 1998. A Demonstration of Submerged Aquatic Vegetation/Limerock Treatment System Technology for Removing Phosphorus From Everglades Agricultural Area Waters. Second Qtr. Report submitted to the South Florida Water Management District. West Palm Beach, FL.

DeBusk, T.A., Peterson, J.E., Reddy, K.R., Graetz, D.A. and K.S. Clough. 1989. Optimization of the vegetative uptake of phosphorus from dairy wastewater. Final Report, Contract No. 88-009-0625, South Florida Water Management District, West Palm Beach, FL., 250 pp.

Diaz. O.A., K..R. Reddy and P.A. Moore, Jr. 1994. Solubility of inorganic phosphorus in stream water as influenced by pH and calcium concentration. Water Res. 8: 1755-1763.

Dierberg, F.E. and P.L. Brezonik. 1983. Tertiary treatment of municipal wastewater by cypress domes. Water Res. 17: 1027-1040.

Fink, L. 1999. Personal communication (fax of data set to F.E. Dierberg of DBEL). South Florida Water Management District.

FDEP, 1999. Bioassay Results for the Everglades Submerged Aquatic Vegetation/Limerock Technology Water Samples Collected Between 10/25/98 and 11/5/98. Report from Florida Department of Environmental Protection Biology Section, Tallahassee, FL.

Kadlec, R.H. 1994. Detention and mixing in free water wetlands. Ecol. Engineering 3:345-380.

Kadlec, R. and R. Knight. 1996. Treatment Wetlands. Lewis Publishers, Chelsea, Michigan.

Krolikowska, J. 1997. Eutrophication processes in a shallow, macrophyte-dominated lake- species differentiation, biomass and the distribution of submerged macrophytes in Lake Luknajno (Poland). Hydrobiologia, 342/343: 411-416.

Levenspiel, O. 1989. The Chemical Reactor Omnibook. Oregon State University Book Stores, Corvallis, Oregon 97339.

Lindeburg, M. R., 1989. Civil Engineering Reference Manual, Fifth Edition. Professional Publications, Inc., Belmont, CA, pp. 2.1-2.36.

PEER Consultants, P.C./Brown and Caldwell, Joint Venture, August 1996. South Florida Water Management District, Desktop Evaluation of Alternative Technologies Final Report, pp. 2.1 – 3.18.

Penn, M.R., M.T. Auer, E.L. Van Orman, and J.J. Korienek. 1995 Phosphorus diagenesis in lake sediments: Investigations using fractionation techniques. Mar. Freshwater Res. 46:89-99.

Reddy, K.R., J.C. Tucker, and W.F. DeBusk. 1987. The role of egeria in removing nitrogen and phosphorus from nutrient-enriched waters. J. Aquat. Plant Manage. 25:14-19.

Reddy, K.R., Y. Wang, W.F. DeBusk, M.M. Fisher and S. Newman. 1998. Forms of soil phosphorus in selected hydrologic units of the Florida Everglades. Soil Sci. Soc. Am. J. 62: 1134-1147.

Steffel, C. I., and A.C. Lasaga. 1990. Evolution of dissolution patterns: Permeability change due to coupled flow and reaction, pp. 212-225. *In:* D.C. Melchior and R.L. Bassett, Eds., Chemical modeling in Aqueous Systems II. ACS Symp. Ser. 416.

Walker, W.W. 1995. Design basis for Everglades Stormwater Treatment Areas. Wat. Res. Bull., 31:671-685.

Wilson, Jr., J.F., E.D. Cobb, and F.A. Kilpatrick. 1986. Fluorometric Procedures for Dye Tracing. U.S. Geological Survey Techniques of Water-Resources Investigations, Book 3, Chapt. A12, 34 p.